University of Alberta

Petrogenesis of Middle Jurassic to Miocene magmatism within the Nechako plateau, central British Columbia: Insight from petrography, geochemistry, geochronology and tracer isotope studies

by

Nancy Grainger ©

A thesis submitted to the Faculty of Graduate Studies and Research in partial fulfillment of the requirements for the degree of Master of Science

Department of Earth and Atmospheric Sciences

Edmonton, Alberta

Winter 2000

National Library
of Canada

Acquisitions and
Bibliographic Services

395 Wellington Street
Ottawa ON K1A 0N4
Canada

Bibliothèque nationale
du Canada

Acquisitions et
services bibliographiques

395, rue Wellington
Ottawa ON K1A 0N4
Canada

Your file Votre référence

Our file Notre référence

The author has granted a non-exclusive licence allowing the National Library of Canada to reproduce, loan, distribute or sell copies of this thesis in microform, paper or electronic formats.

The author retains ownership of the copyright in this thesis. Neither the thesis nor substantial extracts from it may be printed or otherwise reproduced without the author's permission.

L'auteur a accordé une licence non exclusive permettant à la Bibliothèque nationale du Canada de reproduire, prêter, distribuer ou vendre des copies de cette thèse sous la forme de microfiche/film, de reproduction sur papier ou sur format électronique.

L'auteur conserve la propriété du droit d'auteur qui protège cette thèse. Ni la thèse ni des extraits substantiels de celle-ci ne doivent être imprimés ou autrement reproduits sans son autorisation.

0-612-60123-4

Canadä

University of Alberta

Library Release Form

Name of Author: Nancy Grainger

Title of Thesis: **Petrogenesis of Middle Jurassic to Miocene magmatism within the Nechako plateau, central British Columbia: Insight from petrography, geochemistry, geochronology and tracer isotope studies**

Degree: Master of Science

Year this Degree was Granted: 2000

Permission is hereby granted to the University of Alberta Library to reproduce single copies of this thesis and to lend or sell such copies for private, scholarly or scientific research purposes only.

The author reserves all other publication and other rights in association with the copyright in the thesis, and except as herein before provided, neither the thesis nor any substantial portion thereof may be printed or otherwise reproduced in any material form whatever without the author's prior written permission.

N. Grainger

105-10883 Saskatchewan Dr
Edmonton, AB
T6E 4S6

Date: January 30, 2000

University of Alberta

Faculty of Graduate Studies and Research

The undersigned certify that they have read, and recommend to the Faculty of Graduate Studies and Research for acceptance, a thesis entitled **Petrogenesis of Middle Jurassic to Miocene magmatism within the Nechako plateau, central British Columbia: Insight from petrography, geochemistry, geochronology and tracer isotope studies** submitted by Nancy Grainger in partial fulfillment of the requirements for the degree of Master of Science.

Larry Heam

Dr. L. M. Heaman

Dr. R. A. Creaser

Philippe Erdm

Dr. P.E. Erdmer

Dr. A. Meldrum

Date January 27, 2000

ABSTRACT

Igneous rocks of the Middle Jurassic, Cretaceous, Eocene and Miocene periods dominate the geology of the Nechako plateau in central British Columbia. Study of the geochemistry and tracer isotope values of these rocks provides insight into their different magmatic origins and tectonic settings.

Middle Jurassic plutonism is isotopically primitive and supports emplacement above an active continental arc. Eocene volcanism was regionally continuous between 53 and 47 Ma with episodic related plutonism between 55 and 47 Ma. Eocene volcanism is isotopically primitive ($^{87}Sr/^{86}Sr_i$ = 0.7040-0.7045; εNdi = +0.9 to +4.6) and is interpreted as derived from an enriched upper mantle source. Magmas were variably modified by fractionation and contamination and erupted in a distal arc setting. Parental magmas of isotopically primitive Oligo-Miocene Chilcotin Group basalts are asthenosphere derived. Isotopic results from spinel lherzolite xenoliths entrained in Oligo-Miocene lavas indicate enriched components within the upper mantle.

DEDICATION

To the glory of God
with whom all things are possible

ACKNOWLEDGMENTS

As with any such body of work there are innumerable people who have contributed to this project and without whom this work would not have been successfully completed. I want to begin by thanking the two people who are primarily responsible for the inspiration, guidance and support of this work; Dr. Larry Heaman (University of Alberta) and Mike Villeneuve (GSC Ottawa). Mike got me hooked on geochronology and suggested the project to me. He arranged the financial support for much of the analytical work, let me use his Ar/Ar lab in Ottawa and was always on hand to offer advice if I needed it. Larry welcomed me into his lab at the University of Alberta and taught me most of what I know about U-Pb geochronology. He financially supported both this project and myself, as needed, over the past two years. His advice on every aspect of this project has proven invaluable. I greatly appreciate the time he spent carefully and critically reading every line of this thesis. I am very fortunate to have had the opportunity to work with him.

I am indebted to all of those I worked with in the field during the summers of 1997 and 1998. Lori Synder (senior mapper), whose guidance and enthusiasm for geology was much appreciated. Jonah Resnick who always kept me on my toes and persisted in calling me the 'Ootsa Queen'. I hope someday we have another opportunity to work together and argue about the geological problems you're so passionate about. Tina Pint who never complained about the bush I dragged her through and always made sure I was wide awake and ready to start the day. Steve Sellwood who always gave me a hug when I needed it. Elspeth Barnes who had no end of good humour and common sense to share. Amber McCoy who was present for the second, successful, attempt on Dayeezcha Mountain and who was a good friend when things went awry. The Alpha crew; Karen Fallas, Mike Hrudey, Crystal Huscroft, Marianne Quat, Seleena Billesberger and Kelly Franz, some of whom kept me company occasionally on traverse, others who made sure I was aware of interesting Ootsa locales and good sample sites. Also two assistants from the 1997 crew; Angelique Justason and Andy Blair. Angie and I found we shared a liking for testing the limits as well as our birthday. Andy who kept us all in stitches with his deadpan humour.

Missing from the above list are three very important people; Bert Struik (GSC Pacific), Bob Anderson (GSC Pacific) and Don MacIntyre (BCGS). I owe a great debt to Bert and Bob, from whom I learned much of what I know about field methods and techniques. Both Bob and Bert provided superb leadership and organization in the field camps I was part of. All three of these people took time out from a hectic field season to bring me to sites and help me sample in areas they were familiar with. Outside the field seasons, they provided support and engaged in discussion about the Eocene stratigraphy and other aspects of this study. Bob provided financial support for the Endako tracer isotope analyses from his research budget and supplied me with innumerable written and digital resources.

I am also indebted to Rob Creaser, who let me work in his tracer isotope lab. He taught me Rb-Sr and Sm-Nd chemistry and helped enormously in problem solving when things got tricky. I am grateful that I was given the opportunity to do the tracer isotope work in this project, as it became an increasingly important component of this project.

There is a small army of people who have helped me in laboratories at the GSC in Ottawa and the University of Alberta. I would like to thank Barbara Böhm for teaching me some of the crushing and mineral seperation techniques I needed and, more importantly, how to do them better. I greatly appreciate the help of Chris Böhm and Kim Toope who taught me a lot about U/Pb chemistry. Chris always carefully answered my questions regarding techniques and helped improve my lab practices. Thanks to Stacey Hagen for all her help in the mass spectrometry lab and work in analyzing a number of the tracer isotope samples. I need to thank Fred Quigg at the GSC for all his help in the Ar/Ar lab and his patient hard work processing all the data. Thanks to Peter Belanger and the analytical chemistry group who processed my geochemistry samples at the GSC. Thanks also to Anthony Bond who digitized my detailed maps at the GSC Vancouver.

I am privileged to have had the opportunity to study at the University of Alberta and I appreciate the financial support given to me by the Department of Earth and Atmospheric Sciences. There are many people in the department who have helped make my time at the U of A memorable and I would like to thank everyone part of this department for making it the great place to study that it is. Particular thanks to those friends who encouraged and distracted me when I needed it and generally helped me to stay sane; Dave, George, Kathy, Elspeth, Karen and, particularly, Steph and Andrea. Thanks to Rachel, Sonya and Doug, friends outside of the University in Edmonton who helped me feel like I lived here, not just studied here. Thanks to all my friends who stayed in touch from a distance and kept encouraging me; Tash, Joscelyn, Andrew, Jennifer, Crystal, Sue, Ray, Janet, Jenn, Geoff, Rachel and Jeff. Finally, thanks to my family who have always encouraged and supported me, no matter how far away my pursuits take me.

TABLE OF CONTENTS

CHAPTER 1 – Introduction 1

References 2

CHAPTER 2 – Geochronology and geochemistry of Late Tertiary, Late Cretaceous and Middle Jurassic igneous rocks in the Nechako plateau, central British Columbia 4

Introduction 4

Regional Geology 4

Previous Work 7

Oligocene - Micoene 7

Cretaceous 8

Jurassic 8

Major and Trace Element Geochemistry 9

Analytical Methods 9

Results 9

U-Pb Geochronology 14

Analytical Methods 14

Sample Descriptions and Results 14

^{40}Ar/^{39}Ar Geochronology 17

Analytical Methods 17

Results 18

Sr and Nd isotope geochemistry 23

Analytical Methods 23

Results 23

Discussion 26

Timing of Magmatism 26

Magmatic and Tectonic Evolution 29

Conclusions 31

References 31

Appendix I – Sample Locations 40
Appendix II – Analytical results of geochemical analyses 41
Appendix III – Analytical results of laser $^{40}Ar/^{39}Ar$ analyses 42
CHAPTER 3 - Timing and origin of the Ootsa Lake Group, Fort Fraser and Nechako Map areas, central British Columbia 44
Introduction 44
Geological Setting 44
Eocene Stratigraphy 48
Previous Work 48
Local Geology of the Ootsa Lake Group 52
Major and Trace Element Geochemistry 52
  Analytical Methods 52
  Results 52
U-Pb Geochronology 63
  Analytical Methods 63
  Sample Descriptions and Results 65
$^{40}Ar/^{39}Ar$ Geochronology 68
  Analytical Methods 68
  Sample Descriptions and Results 69
Sr and Nd isotope geochemistry 75
  Analytical Methods 75
  Results 75
Discussion 78
  Geochronology 78
  Petrogenesis 83
  Tectonic Setting 87
  Stratigraphy 88
Conclusions 90

References 91

Appendix I – Compilation of published age dates for the Endako Group, Ootsa Lake Group, Babine Igneous Suite and correlative rocks 99

Appendix II – Sample Locations 102

Appendix III – Analytical results of geochemical analyses 104

Appendix IV – Analytical results of laser $^{40}Ar/^{39}Ar$ analyses 107

Appendix V – Geology of the Eocene Ootsa Lake Group in northern Nechako River and southern Fort Fraser map areas, central British Columbia (Grainger and Anderson 1999) 110

CHAPTER 4 – Conclusions 120

References 121

APPENDIX I – Tracer isotope and U-Pb analytical Methods 123

LIST OF TABLES

CHAPTER 2

Table 2-1. Analytical results from U-Pb zircon analyses 15

Table 2-2. Analytical results from trace isotope analyses of Middle Jurassic Stag Lake monzogranite pluton, Chilcotin basalts and mantle xenoliths. 24

CHAPTER 3

Table 3-1. Analytical results from U-Pb zircon analyses 64

Table 3-2. Analytical results of tracer isotope analyses of Newman volcanics, Endako and Ootsa Lake Groups 76

Table 3-3. Revised stratigraphy of the Ootsa Lake Group. 90

LIST OF FIGURES

CHAPTER 2

Figure 2-1. Terrane setting of study area showing $^{87}Sr/^{86}Sr_i$ isopleths. 5

Figure 2-2. General geological map of study area showing sample locations and previous K/Ar age determinations for the Chilcotin Group. 6

Figure 2-3. AFM classification scheme for the Cretaceous volcanics. 10

Figure 2-4. Alkalies versus silica volcanic classification scheme with alkaline-subalkaline subdivision for the Cretaceous volcanics. 10

Figure 2-5. K_2O vs SiO_2 (wt %) with potassic classification schemes for the Cretaceous volcanics. 11

Figure 2-6. Chondrite normalized rare earth element variation diagram for Cretaceous volcanic, Jura-Cretaceous and Middle Jurassic Stag Lake plutonic samples. 12

Figure 2-7. Primitive mantle normalized element variation diagram for Cretaceous volcanic, Jura-Cretaceous and Middle Jurassic Stag Lake plutonic samples. 12

Figure 2-8. Mid-ocean ridge basalt normalized mixed element variation diagram for the Cretaceous volcanics. 13

Figure 2-9. Hf/3-Th-Ta tectonic discrimination diagram for the Cretaceous volcanics. 13

Figure 2-10. Concordia diagrams for the Savoury Hill dacite and Hallett Lake monzogranite. 16

Figure 2-11. Ar/Ar gas release spectra and inverse isochron plots for Chilcotin basalts. 19

Figure 2-12. εNdi versus $^{87}Sr/^{86}Sr_i$ plot of Chilcotin Group basalts and Middle Jurassic Stag Lake monzogranite. 25

Figure 2-13. Histogram of regional K/Ar ages compilation for the Chilcotin Group including new Ar/Ar age dates. 28

CHAPTER 3

Figure 3-1. Terrane setting of study area. 45

Figure 3-2. General geological map of study area. 46

Figure 3-3. Stratigraphy of the Endako Group, Ootsa Lake Group and correlated units within the Whitesail, Nechako River, Fort Fraser and Smithers map sheets (NTS 93E, 93F, 93K and 93L) 49

Figure 3-4. Compilation of published K-Ar and $^{40}Ar/^{39}Ar$ age dates for Eocene units within the Whitesail, Nechako River, Fort Fraser and Smithers map sheets. 50

Figure 3-5. Photographs of an andesite flow within the Newman volcanics and representative units within the Ootsa Lake Group at hand sample and outcrop scale. 53

Figure 3-6. Alkalies versus silica plot with alkaline-subalkaline division for the Ootsa Lake Group and Babine Igneous Suite. 54

Figure 3-7. AFM classification scheme for the Ootsa Lake Group and Babine Igneous Suite. 54

Figure 3-8. K_2O vs SiO_2 (wt %) with potassic classification schemes for the Ootsa Lake Group and Babine Igneous Suite. 56

Figure 3-9. Harker diagrams for the Ootsa Lake Group and Babine Igneous Suite. 57

Figure 3-10. Chondrite normalized rare earth element variation diagram for the Ootsa Lake Group and Babine Igneous Suite. 59

Figure 3-11. Primitive mantle normalized element variation diagram for the Ootsa Lake Group and Babine Igneous Suite. 60

Figure 3-12. Mid-ocean ridge basalt normalized mixed element variation diagram for the Ootsa Lake Group and Babine Igneous Suite. 61

Figure 3-13. Hf/3-Ta-Th tectonic discrimination diagram for the Ootsa Lake Group Babine Igneous Suite. 62

Figure 3-14. Concordia diagrams for the Ootsa Lake Group samples analyzed. 66

Figure 3-15. $^{40}Ar/^{39}Ar$ cumulative gas release plots for the Ootsa Lake Group samples analyzed. 70

Figure 3-16. εNd_i versus $^{87}Sr/^{86}Sr_i$ plot of the Babine Igenous Suite, Endako and Ootsa Lake Groups. 77

Figure 3-17. Summary of U-Pb and $^{40}Ar/^{39}Ar$ age dates determined in this study for the Nechako River and Fort Fraser map areas. 81

Figure 3-18. Composite variation diagram using the CIPW norm. 86

Figure 3-19. Tectonic discrimination diagrams 89

CHAPTER 1

Introduction

Located in central British Columbia, the Nechako plateau is dominated by Middle Jurassic to Tertiary igneous rocks. Erupted or intruded under different tectonic regimes, the geochemical composition of these rocks reflects their magmatic origin and records the geological history of the Stikine terrane. An integrated study of these rocks provides an understanding of the composition and evolution of both the continental crust and the subsurface along a convergent margin. A better understanding these processes further improves our general concepts of global magmatism and plate tectonics (Lipman and Glazner 1991).

This study was conceived to focus primarily on the timing and origin of Eocene igneous rocks within the Nechako plateau and expand on the work being conducted as part of the Nechako project. The Nechako project is a geoscientific program initiated by the Geological Survey of Canada (GSC) and British Columbia Geological Survey (BCGS) in 1995 to study the bedrock and surficial geology of the Nechako plateau. Funded in part by the GSC National Mapping Program (NATMAP), this project was established in recognition of the poor pre-existing geological database within this area of recognized economic importance (Struik and McMillan 1996). After four seasons of field mapping, the bedrock and surficial geology has been mapped over an area of more than 30 000 km^2 (Struik and MacIntyre 1999). In addition, local studies of mineral deposits, structure of the Vanderhoof Metamorphic Complex, regional and local geophysics and other studies have been completed as part of this project (e.g. L'Heureux 1997; Wetherup 1997; Lowe 1998). As a result, the distribution, lithologies, stratigraphy and structure of the geology throughout the Nechako plateau is relatively well known providing an excellent framework for this study.

This study presents new geochronological, geochemical and tracer isotope results for igneous rocks from the Middle Jurassic, Late Cretaceous, Eocene and Oligo-Miocene. Placing these results in the context of their structural and tectonic setting, as determined by local and regional studies, insight can be obtained into the magmatic origin of these rocks and the tectonic evolution of the Stikine terrane.

In Chapter 2, geochronological and tracer isotope results are presented from analyses of the Middle Jurassic Stag Lake suite, Cretaceous Tip Top Hill volcanics and Oligo-Miocene Chilcotin Group basalts and entrained spinel lherzolite xenoliths. The extent of the Chilcotin Group has been significantly expanded within the Nechako plateau by recent mapping (Anderson et al., 1998; Resnick et al., 1999). New $^{40}Ar/^{39}Ar$ data reported here are the first dates reported within the Nechako River map sheet (NTS 93F) for these rocks. These data augment the existing database of a few reported K-Ar dates from correlated rocks in adjacent areas. Sr and Nd analyses from the basalt lavas and lherzolite xenoliths are also the first reported for the Nechako River map area and provide fundamental information about the isotopic nature of the subsurface of the Nechako plateau during the Miocene. These data are compared with published results from Chilcotin Group basalts and xenoliths from the Chilcotin plateau to the south.

Geochronological results from the Middle Jurassic Stag Lake suite and Cretaceous Tip Top Hill volcanics, both originally, but incorrectly correlated with the Eocene Ootsa Lake Group, are indicative of mapping difficulties due to lithological similarities of these units within the Nechako plateau. Geochemical and tracer isotope results for these suites are contrasted with the Eocene igneous rocks to facilitate distinction of these different units.

The largest Eocene igneous complex within the Canadian Cordillera is located within the Nechako plateau in central British Columbia. This igneous complex is located between the subduction-related Eocene Mount Skukum and Bennett Lake Igneous Complex in the Yukon (Morris and Creaser 1998) and the subduction- and extension-related Eocene Kamloops and Penticton Groups in south central British Columbia (Ewing 1981; Pearce et al. 1981; Smith 1986). Although Eocene volcanic and plutonic rocks are widespread in central British Columbia and related to copper porphyry and Au-Ag±Cu epithermal deposits (Andrew 1988; Leitch et al. 1991; MacIntyre et al. 1997), these rocks are poorly understood (Souther 1991).

Chapter 3 presents $^{40}Ar/^{39}Ar$ and U-Pb age determinations from the Eocene Ootsa Lake Group which constrain the timing of Ootsa Lake Group volcanism and associated plutonism in the Nechako plateau. These results augment the existing database of published K/Ar and $^{40}Ar/^{39}Ar$ dates for the Ootsa Lake Group within the region. The timing of Eocene magmatic activity is discussed relative to the Eocene structural and tectonic evolution of this region. In addition, geochemical results from the Eocene Newman volcanics and Ootsa Lake Group and tracer isotope results from the Newman volcanics, Endako and Ootsa Lake Groups are reported in Chapter 3. Geochemical and tracer isotope results from these Eocene igneous rocks in central British Columbia are compared to one another and to published data from the area, in order to gain a better understanding of the magmatic origin of these rocks and their relationship to the tectonic setting.

References

Anderson, R.G., Synder, L.D., Resnick, J. and Barnes, E. 1998. Geology of the Big Bend Creek map area, central British Columbia. *in;* Current Research 1998-A. Geological Survey of Canada. p. 145-154.

Andrew, K.P.E. 1988. Geology and genesis of the Wolf Precious Metal Epithermal Prospect and the Capoose Base amd Precious Metal Porphyry-style prospect, Capoose Lake area, Central British Columbia. University of British Columbia. Unpublished MSc thesis. 334 pages.

Ewing, T.E. 1981. Petrology and geochemistry of the Kamloops Group volcanics, British Columbia. Canadian Journal of Earth Sciences. 18;1478-1491.

Leitch, C.H.B., Hood, C.T., Cheng, X. and Sinclair, A.J. 1992. Tip Top Hill volcanics: Late Cretaceous Kasalka Group rocks hosting Eocene epithermal base- and precious-metal veins at Owen Lake, west-central British Columbia. Canadian Journal of Earth and Atmospheric Sciences. 29: 854-864.

L'Heureux, R. and Anderson, R.G. 1997. Early Cretaceous plutonic rocks and molybdenite showings in the Nithi mountain area, central British Columbia. *in;* Current Research 1997-A. Geological Survey of Canada. p. 117-124.

Lipman, P.W. and Glazner, A.F. 1991. Introduction to Middle Tertiary Cordilleran Volcanism: Magma Sources and Relations to Regional Tectonics. Journal of Geophysical Research. 96; 13193-13199.

Lowe, C. Enkin, R.J. and Dubois, J. 1998. Magnetic and plaeomagnetic constraints on Tertiary deformation in the Endako region, central British Columbia. *in;* Current Research 1998-A. Geological Survey of Canada. p. 125-134.

MacIntyre, D.G., Webster, I.C.L. and Villeneuve, M.E. 1997. Babine porphyry belt project: Bedrock geology of the Old Fort Mountain Map area (93M/1), British Columbia. *in;* Geological Fieldwork 1996. British Columbia Ministry of Employment and Investment. Paper 1997-1, p. 47-67.

Morris, G.A and Creaser, R.A. 1998. The petrogenesis of the Mount Skukum/Bennett Lak Igneous Complex, Yukon territory, and reflections on the Eocene tectonics of the Canadian Cordillera. *In;* Slave-NORthern Cordillera Lithoprobe Evolution (SNORCLE) and Cordilleran Tectonics Workshop. P.Erdmer and F.Cook (eds). Lithoprobe Report No 64. p. 165-169.

Price, R.A., Monger, J.W.H. and Muller, J.E. 1981. Cordilleran cross-section, Calgary to Victoria. Field guides to geology and mineral deposits; Calgary '81 annual meeting. R.I. Thompson and D.G. Cook (eds.). Geological Association of Canada. p. 261-334.

Resnick, J., Anderson, R.G., Russel, J.K., Edwards, B.R. and Grainger, N.C. 1999. Neogene basaltic flow rocks, xenoliths, and related diabase, northern Nechako River map area, central British Columbia. *in;* Current Research 1999-A. Geological Survey of Canada. P.157-167.

Smith, A.D. 1986. Isotopic and geochemical studies of Terrane I, South-Central British Columbia. Unpublished PhD thesis. University of Alberta. Edmonton, Alberta. 195 p.

Souther, J.G. 1991. Chapter 14, Volcanic Regimes. *In;* Geology of Cordilleran Orogen in Canada. (eds.) H. Gabrielse and C.J. Yorath; Geological Survey of Canada, Geology of Canada, no.4, p. 457-490.

Struik, L.C. and McMillan, W.J. 1996. Nechako project overview, central British Columbia. *in;* Current Research1996-A. Geological Survey of Canada. p.57-62.

Struik, L.C. and MacIntyre, D.G. 1999. Nechako NATMAP project overview, central British Columbia, year four: part 1. *in;* Current Research1999-A. Geological Survey of Canada. p.71-78.

Wetherup, S. 1997. Geology of the Nulki Hills and surrounding area, central British Columbia. *In;* Current Research 1997-A. Geological Survey of Canada. p.125-132.

CHAPTER 2

Geochronology and geochemistry of Middle Jurassic, Late Cretaceous and Late Tertiary igneous rocks in the Nechako plateau, central British Columbia

Introduction

Recent mapping within the Nechako plateau in central British Columbia has revealed remnant Neogene basaltic centers and lava flows in the Nechako River map sheet (NTS 93F) (Anderson et al., 1998a; Resnick et al., 1999). These rocks have been correlated with the Mio-Pliocene Chilcotin Group, based on the expansion of the original group designation by Bevier (1983a, b) north into the Nechako plateau by Mathews (1989). There are no age determinations reported for these rocks within the Nechako River map sheet and there are only a few reported K-Ar dates from adjacent areas. New $^{40}Ar/^{39}Ar$ age determinations for these rocks are reported here, in addition to Sr and Nd analyses of the basalt lavas and lherzolite xenoliths.

Difficulties correlating volcanic stratigraphy within the Nechako plateau are highlighted by new U-Pb age determinations of rocks initially correlated with the Eocene Ootsa Lake Group, now identified as Cretaceous and Middle Jurassic in age. Geochemistry and tracer isotope data for these rocks are also presented here.

These data, combined with available geochemical and tracer isotope data, provide an overview of the isotopic character of igneous rocks extruded or emplaced since the Jurassic within the Nechako plateau. These data can be used to provide insight into the geochemical nature of the subsurface of the Stikine terrane in central British Columbia.

Regional Geology

The Nechako plateau is located within the Stikine terrane in the Intermontane belt (Figure 2-1). The study area is at the eastern margin of Stikinia, and overlaps onto Cache Creek and the western margin of Quesnellia. Stikinia is composed of late Devonian to middle Jurassic volcanic and sedimentary strata and plutonic rocks. The volcanic and sedimentary units within the study area are predominantly rocks of the Lower to Middle Jurassic Hazelton Group which is composed of mafic flows, breccias, volcaniclastics and minor sediments of calc-alkaline volcanic arc affinity (Monger et al. 1991). The Cache Creek terrane is composed of sedimentary and volcanic rocks of oceanic affinity. Within the study area, the Cache Creek Group is composed of an imbricate thrust stack of Upper Paleozoic and Mesozoic limestones and chert, Mesozoic greywacke, siltstone, argillite and basalt with a layered cumulate ultramafic klippe of unknown age (Struik and Orchard 1998). Triassic to early Jurassic volcanic and sedimentary rocks of the Takla Group are exposed within the northeastern corner of the study area in the Quesnel terrane (Figure 2-2) (Struik and Orchard 1998). Quesnellia is widely considered a volcanic arc that was accreted onto the North American margin during the Jurassic (Yorath 1991), however, recent research suggests that pericratonic rocks underlie Quesnellia in southern British Columbia which would necessitate modification of the current tectonic model (e.g. Thompson et al. 1999; Heaman et al. 1999). Early Triassic sediment deposits in northern British Columbia suggest amalgamation of Stikinia, Cache Creek and Quesnellia with the Slide Mountain terrane between the Early Triassic and Early Jurassic, forming the Intermontane Superterrane (Gabrielse and Yorath 1991). Accretion of the Intermontane Superterrane onto the western North American margin likely occurred during the Early to Middle Jurassic (Yorath 1991). Middle Jurassic plutonism is partly coeval, but mostly postdates terrane amalgamation ca. 185-175 Ma (Anderson 1998b).

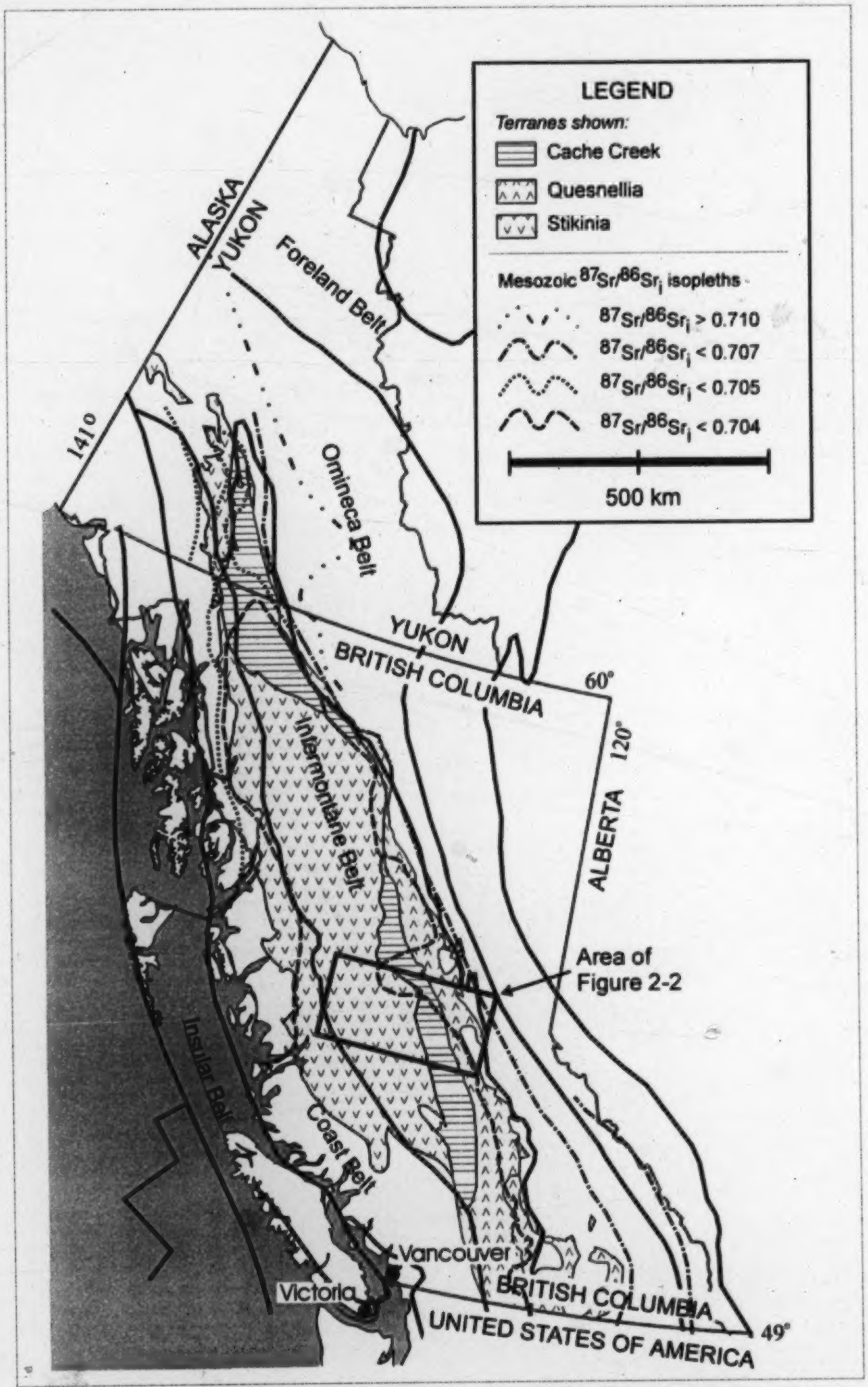
LEGEND
Terranes shown:
Cache Creek
Quesnellia
Stikinia
Mesozoic $^{87}Sr/^{86}Sr_i$ isopleths
$^{87}Sr/^{86}Sr_i > 0.710$
$^{87}Sr/^{86}Sr_i < 0.707$
$^{87}Sr/^{86}Sr_i < 0.705$
$^{87}Sr/^{86}Sr_i < 0.704$
500 km
ALASKA
YUKON
Foreland Belt
Omineca Belt
141°
YUKON
BRITISH COLUMBIA
60°
120°
ALBERTA
Intermontane Belt
Area of Figure 2-2
Insular Belt
Coast Belt
Vancouver
Victoria
BRITISH COLUMBIA
UNITED STATES OF AMERICA
49°

Figure 2-1. Terrane setting of study area showing $^{87}Sr/^{86}Sr_i$ isopleths (Armstrong 1988). (Yorath 1991).

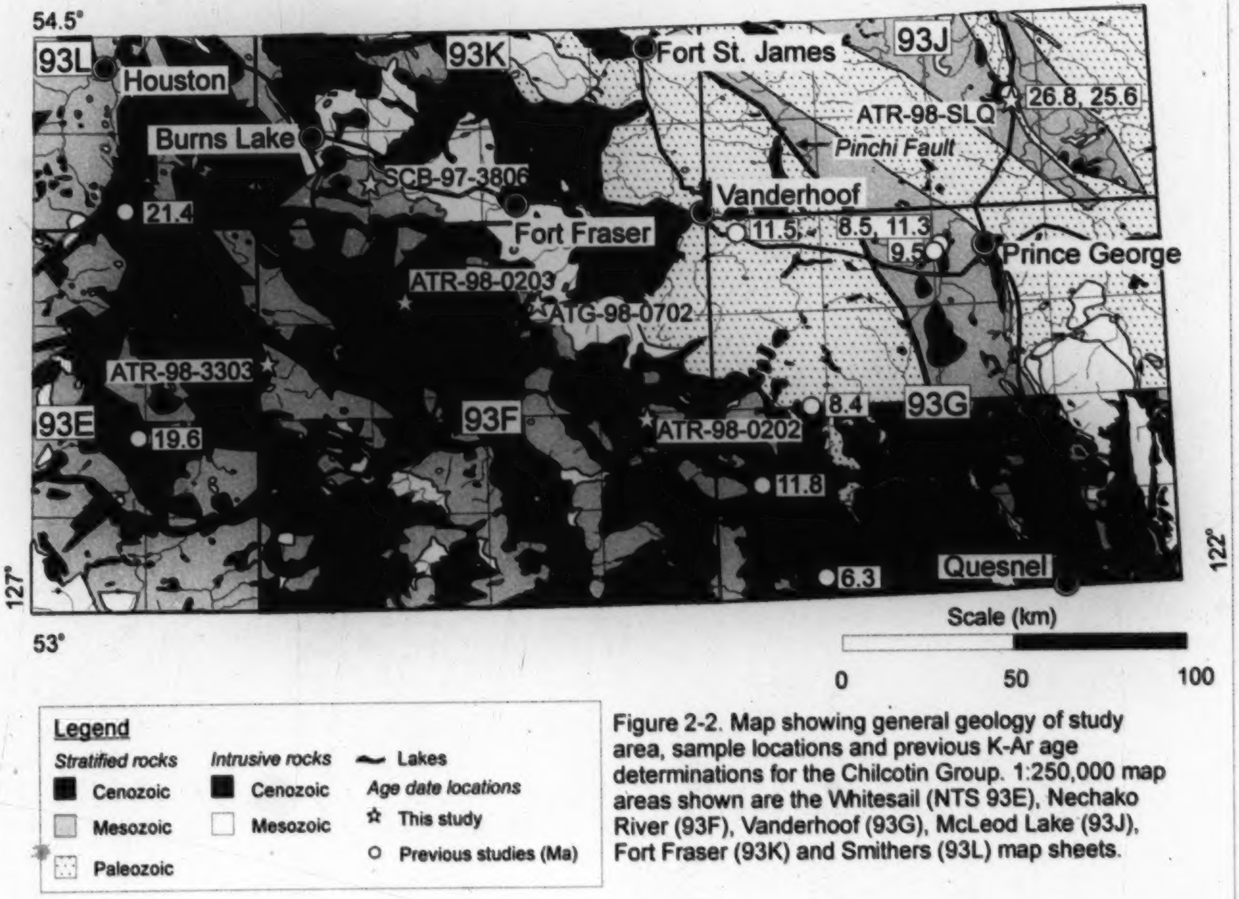
54.5°
53°
127°
122°
93L
93K
93J
93E
93F
93G
Houston
Burns Lake
Fort St. James
Fort Fraser
Vanderhoof
Prince George
Quesnel
ATR-98-SLQ
26.8, 25.6
Pinchi Fault
SCB-97-3806
21.4
11.5
8.5, 11.3
9.5
ATR-98-0203
ATG-98-0702
ATR-98-3303
19.6
8.4
ATR-98-0202
11.8
6.3
Scale (km)
0
50
100
Legend
Stratified rocks
Cenozoic
Mesozoic
Paleozoic
Intrusive rocks
Cenozoic
Mesozoic
Lakes
Age date locations
This study
Previous studies (Ma)

Figure 2-2. Map showing general geology of study area, sample locations and previous K-Ar age determinations for the Chilcotin Group. 1:250,000 map areas shown are the Whitesail (NTS 93E), Nechako River (93F), Vanderhoof (93G), McLeod Lake (93J), Fort Fraser (93K) and Smithers (93L) map sheets.

Middle Cretaceous uplift and thickening of the Coastal belt may be related to accretion of the Insular superterrane onto the North American margin or from intraplate contraction and plutonism related to a subduction zone further west (Monger et al. 1983; Gabrielse and Yorath 1991). Uplift of the Coast belt is approximately coeval with the eruption of the Kasalka Group volcanics (ca 87-100 Ma) located to the west of the study area within the central Intermontane belt (Yorath 1991). Magmatic activity occurred during the Late Cretaceous with the Tip Top Hill volcanics in the Nechako plateau and emplacement of the Bulkley plutons west of the study area (ca 70-84 Ma) (Carter 1981; Yorath 1991). Large scale motion along strike-slip faults, such as the Pinchi fault, during the Late Cretaceous to Eocene has been proposed and the magnitude of this motion is the subject of ongoing debate (e.g Irving et al. 1996; Ward et al. 1997; Paterson et al. 1998; Mahoney et al. 1999). Paleomagnetic data from Eocene rocks immediately to the west of the study area indicate that any northward motion that may have occurred in the Stikine terrane was completed by 50 Ma (Vandell and Palmer 1989).

Crustal extension and dextral translation occurred along northwest trending faults during the Early Eocene and along north trending en echelon transform faults during the Late Eocene to Early Oligocene in central British Columbia (Struik 1993). Eocene extension is evident within the Nechako plateau in the system of northwest, northeast and east-west faults and the Vanderhoof Metamorphic complex, which is interpreted as an extension-related core complex (NTS 93F/09 and 93F/16) (Wetherup and Struik 1996; Wethurup 1997; Lowe et al. 1998). Extension-related to the Vanderhoof Metamorphic Complex was northwesterly in orientation and cooling was completed circa 45 Ma (Wethurup 1997; M.E. Villeneuve unpublished data *in* Anderson et al. 1998b). During this period of transtensional stress widespread calc-alkaline volcanism and plutonism occurred throughout the Nechako plateau. Similar extension-related bimodal volcanic complexes are found in south central British Columbia.

Transitional to alkaline basalts of the Chilcotin Group were extruded over the Chilcotin plateau to the south and into the Nechako plateau during the Oligocene-Miocene in a back arc tectonic setting behind the Pemberton-Garibaldi arc to the west (Bevier 1983a; Mathews 1989; Souther 1991).

Previous Work

Oligocene - Micoene

Young basaltic rocks have been recognized in the Nechako River and adjacent map areas by the earliest mapping in the area (e.g. Armstrong 1949; Tipper 1963a). These rocks were initially designated the Endako Group (Armstrong 1949) and assigned an age of Miocene or younger (Tipper 1963a). Later mapping and K-Ar dating revealed that some of these rocks were Eocene in age (Mathews 1964; Stevens et al. 1982; Rouse & Mathews 1988; Diakow & Koyanagi 1988), while others were Oligocene-Miocene (Church 1972; Stevens et al. 1982; Mathews 1989). This problem was addressed by Mathews (1989) who expanded the original designation of the Chilcotin Group (Bevier 1983a and 1983b) to include basaltic rocks, indistinguishable in the field from those at the type section, which are between 26 and 1.1 Ma in age. The Endako Group has subsequently been used to designate only basaltic to andesitic rocks of Eocene age (e.g. Haskin et al. 1998).

Regionally the Chilcotin Group has three periods of abundant eruptions at 16-14, 9-6 and 3-1 Ma (Mathews 1989). Eleven K-Ar dates have been reported for Chilcotin Group basalts in the Nechako Plateau (Figure 2-2). Two dates west of the Nechako River map sheet, in the Whitesail (NTS 93E) and Smithers (NTS 93L) map sheets overlap and range from 19.6 to 21.4 (Church 1972; Stevens et al. 1982). Seven age determinations are reported from the Prince George (NTS 93G) map sheet, immediately east of Nechako River. These dates define at least four pulses of magmatism at 11.8 to 11.3 Ma, 9.5 Ma, 8.5 to 8.4 Ma and 6.3

Ma (Mathews 1989; Bevier 1983a).Two older dates, of 25.6 ± 1.0 and 26.8 ± 0.7 Ma, are reported from the Summit Lake center, north of Prince George (Mathews 1989).

The extent of Chilcotin Group rocks within the Nechako River map area is described by recent mapping (Anderson et al. 1998a; Anderson et al. 1999; Struik et al. 1999). Within the Nechako River map area these rocks typically display columnar jointing, lack amygdules or vesicles, and may contain phenocrysts of plagioclase, pyroxene and/or biotite. These rocks may contain xenocrysts of olivine or pyroxene and both mantle and crustal xenoliths are found at or near volcanic centers (Resnick et al. 1999). The localities sampled in this paper are described in detail in Resnick et al. (1999), with the exception of the Summit Lake locality which is described in Brearley et al. (1984) and Smith (1986). The locations for all samples analyzed in this study are given in Appendix I. A recent petrogenetic study of these rocks identifies them to be mostly basanites and hawaiites, alkaline, high-K, nepheline-normative, calc-alkaline, with within-plate affinities (Resnick 1999). These rocks are chemically distinct from type locality Chilcotin rocks described to the south which are transitional alkaline-subalkaline, nepheline-, hypersthene- and quartz normative (Bevier 1983b; Smith 1986; Dostal et al. 1996). Two-pyroxene equilibrium temperatures of spinel lherzolite xenoliths are consistently lower than the liquidus temperatures of the basalt lavas (Suh 1999). Thus, Resnick (1999) concludes that the source region for these lavas is the asthenosphere and formed from an upwelling of the asthenosphere. This agrees with the back-arc tectonic setting that is inferred for the type locality Chilcotin basalts (Bevier 1983b).

Cretaceous

Cretaceous volcanic and plutonic rocks have been recently mapped in the Fort Fraser (NTS 93K) and Nechako River map areas (e.g. Anderson & Synder 1998; Anderson et al. 1998a; Anderson et al. 1999; Struik et. al, 1999; Hrudey et al. 1999) modifying the distribution of these rocks on earlier maps (Armstrong 1949; Tipper 1963a). Cretaceous plutons range from diorite to monzonite to granodiorite. Volcanic rocks are composed predominantly of andesitic to dacitic flows and tuffaceous rocks with minor rhyolite flows and sedimentary rocks. A few dates have been reported regionally and these rocks are well dated where they host epithermal Au-Ag±Cu mineralization, e.g. the Silver Queen deposit (Leitch et al. 1992) and the Capoose prospect (Andrew 1988).

Five K-Ar dates are reported for intrusions within the Nechako River map sheet that overlap and range from 64.3 to 70.3 Ma (Andrew 1988; Friedman *in* Lane and Schroeter 1997). These rocks were correlated with the Quanchus intrusions by Andrew (1988). Nine K-Ar dates are reported from volcanic and intrusive rocks in the adjacent Whitesail and Smithers map sheets which give age ranges of 70 to 71.5 and 75 to 79 and a date of 85 Ma (Church 1972; Drobe 1991; Leitch et al. 1992). These ages correlate well with the Bulkley intrusions, west of the map area, which range from 70 to 84 Ma, with major pulses occurring at 70, 76 and 83 Ma (Carter 1981). The volcanics dated between 75-78 Ma, named the Tip Top Hill Formation by Church (1970 & 1972), are younger than the mid-Cretaceous Kasalka Group volcanics, to the west, which range in age from 87 to 100 Ma (Yorath 1991). Some authors have suggested including the Tip Top Hill volcanics as a formation within the Kasalka Group based on lithological similarities and the understanding that these K-Ar dates underestimate the true age (Leitch et al. 1992). Others have separated them into the Carmacks and South Fork Assemblages, respectively based strictly on the determined age ranges (Souther 1991). Other groups within the Late Cretaceous Carmacks Assemblage include the Carmacks Group in southwestern Yukon and the Brian Boru Formation, near Hazelton, in central British Columbia (Souther 1991). The Carmacks Group volcanics are potassic and calc-alkaline in nature. The Brian Boru Formation are porphyritic andesite breccias and massive flows which have been K-Ar dated to 70-72 Ma (Sutherland 1960).

Jurassic

The distribution and age of Jurassic plutonism is well known within the Nechako River and Fort Fraser map areas. The presence of a series of Jurassic intrusions was recognized in early mapping (Armstrong 1949) and numerous subsequent studies (e.g. Tipper 1963a; Carr 1966), particularly as they relate to the Endako molybdenum mine (e.g. Dawson 1972; Kimura et al. 1976; Bysouth and Wong 1995). Recent mapping of the region (Whalen et al. 1998; Anderson and Synder 1998) and an excellent review of the Endako batholith (Anderson et al. 1998b) divide local Jurassic plutonism into three phases; Middle Jurassic Stag Lake Suite (171-163 Ma), Late Jurassic 'older' Francois Lake plutonic suite (159-154 Ma) and the Jura-Cretaceous 'younger' Francois Lake suite (148-145 Ma). These were preceeded by the Late Triassic Boer Suite (220-215 Ma?). These age ranges are based primarily on 12 ^{40}Ar/^{39}Ar and 3 U-Pb ages (Villeneuve unpublished data *in* Anderson et al., 1998b) which provides more restricted age ranges than the approximately 20 K-Ar and 2 Rb-Sr dates (including Baadsgaard et al, 1961; Tipper 1963b; Lowdon 1963; White et al. 1968 and 1970; Kimura et al. 1976; Bysouth and Wong 1995).

Over 100 chemical analyses have been conducted on these rocks as part of the Nechako NATMAP project and are reported in Anderson et al. (1998b). All of the units are classified as calc-alkaline and subalkaline with a moderate to high K content and volcanic arc granite affinity. The results show an overall trend from a more primitive geochemistry in the Triassic to a more evolved arc signature by the end of the Jurassic. Preliminary isotopic data in Anderson et al. (1998b) supports published data indicating a primitive source material with initial $^{87}Sr/^{86}Sr_i \leq 0.704$ and $\delta O^{18} = +5$ to $+7^0/_{00}$ (Margaritz and Taylor 1976; Armstrong 1988; Woodsworth et al. 1991; R.L. Armstrong unpublished data *in;* Anderson et al. 1998b).

Major and Trace Element Geochemistry

Analytical Methods

Two Cretaceous samples were selected for analysis. These analyses are intended only to provide a initial sampling of the geochemistry of these Cretaceous volcanics and enable a preliminary comparison with the lithologically similar Eocene volcanics. Splits of each sample were powdered using both a Tungsten carbide and steel ring mill. Samples were analyzed in the laboratories at the Geological Survey of Ottawa. Samples were analyzed using X-ray flourescence for major and several trace elements (Ba, Nb, Rb, Sr and Zr). Trace elements were determined using inductively coupled plasma emission spectrometry (Ag, Ba, Be, Co, Cr, Cu, La, Ni, Mo, Pb, Sc, Sr, V, Y, Yb, Zn, Zr) or inductively coupled plasma mass spectrometry (Bi, Cd, Cs, Ga, Hf, In, Nb, Rb, Sn, Ta, Th, Tl, U, Ce, Dy, Er, Eu, Gd, Ho, La, Lu, Nd, Pr, Sm, Tb, Tm, Y and Yb). Precision is ± 1-5 % for the major elements and ± 5-10 % for the trace elements. Analytical errors are given with the data in Appendix II. A sample previously analyzed at the University of Alberta by wet chemistry (H. Baadsgaard 1964 unpublished data) was analyzed with those submitted to the GSC to compare reproducibility of results. Results of these comparative analyses are in good agreement for all elements determined.

Results

Only general comments can be made about the geochemical character of the Cretaceous volcanics based on these limited data and lack of available published data. These two Cretaceous flows, one andesite and one rhyolite, have SiO_2 contents of 59 and 74 wt.%, respectively. Both samples are calc-alkaline in character (Figure 2-3), fall within the subalkaline field on the ($Na_2O + K_2O$) vs SiO_2 plot (Figure 2-4) and are very high K (Figure 2-5). The chondrite normalized rare earth element (REE) plot (Figure 2-6) shows light rare earth element (LREE) enrichment, heavy rare earth element (HREE) depletion and a weak negative Eu anomaly. This gradual enrichment in REE from Yb to Ce is typical of continental margin arc magmatism (Condie 1989). The andesite sample shows less enrichment of LREE and greater HREE depletion than the rhyolite sample. The mixed trace element plot normalized to primitive mantle composition (Figure 2-7) shows both samples are enriched in the large ion lithophile elements (LILE), K, Rb, Cs, Sr and Ba, as well as LREE relative to the HREE and high field strength elements (HFSE), Ti, Zr, Hf, Nb and Ta. Both samples also show a negative Nb anomaly and positive K and Pb anomalies on this plot. The rhyolite

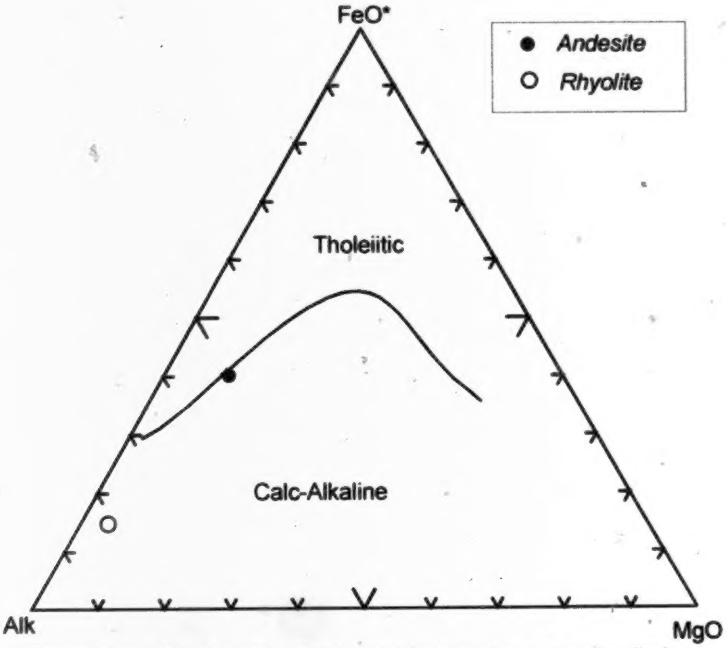

Figure 2-3. AFM classification for the Cretaceous volcanics (Irvine and Barager 1971).

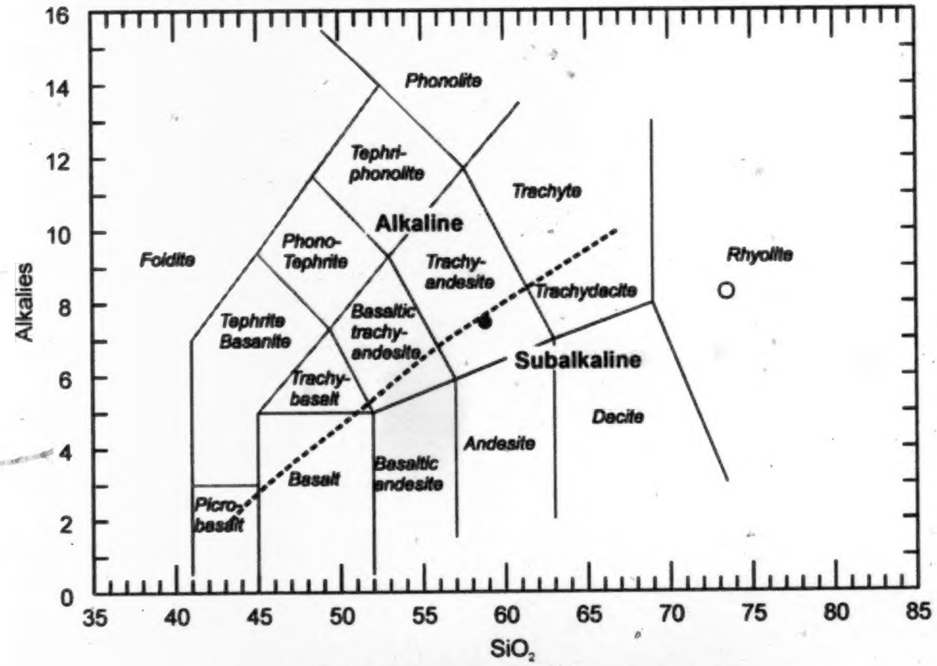

Figure 2-4. Alkalies versus silica volcanic classification scheme with alkaline-subalkaline division for the Cretaceous volcanics (Irvine and Barager 1971; LeBas et al. 1986). Symbols as defined in Figure 2-2.

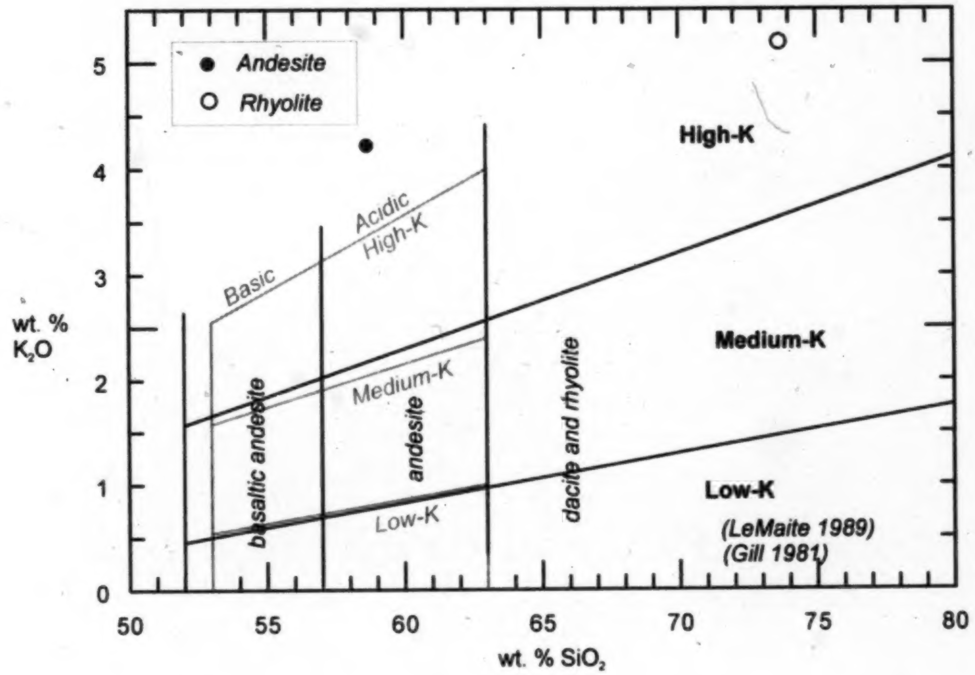

Figure 2-5. K_2O vs SiO_2 (wt. %) with potassic classification schemes for the Cretaceous volcanics.

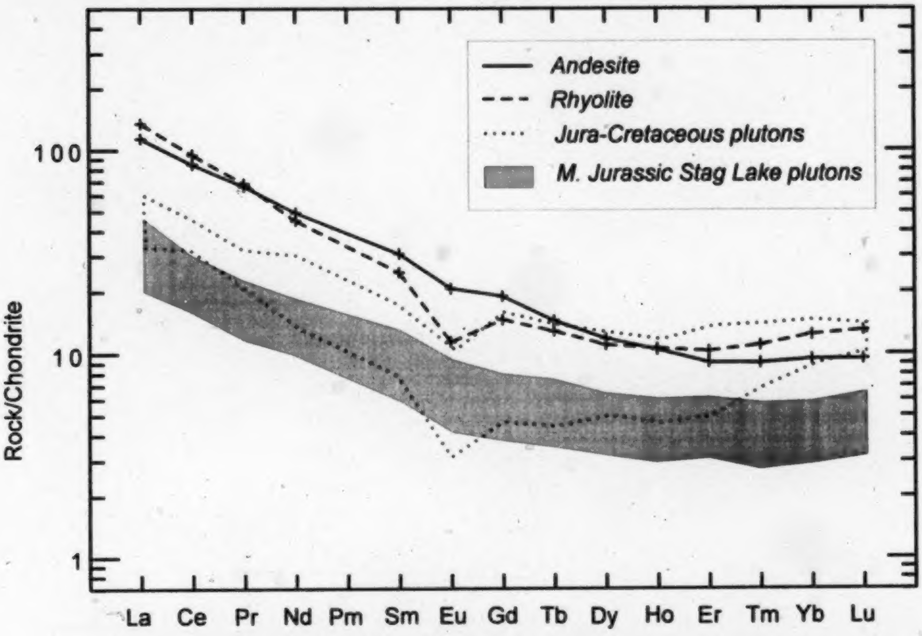

Figure 2-6. Chrondrite normalized REE plot for the Cretaceous volcanic samples. Comparison data from the Nechako River and Fort Fraser map areas (Anderson et al. 1998b). (Normalization values from Sun and McDonough 1989)

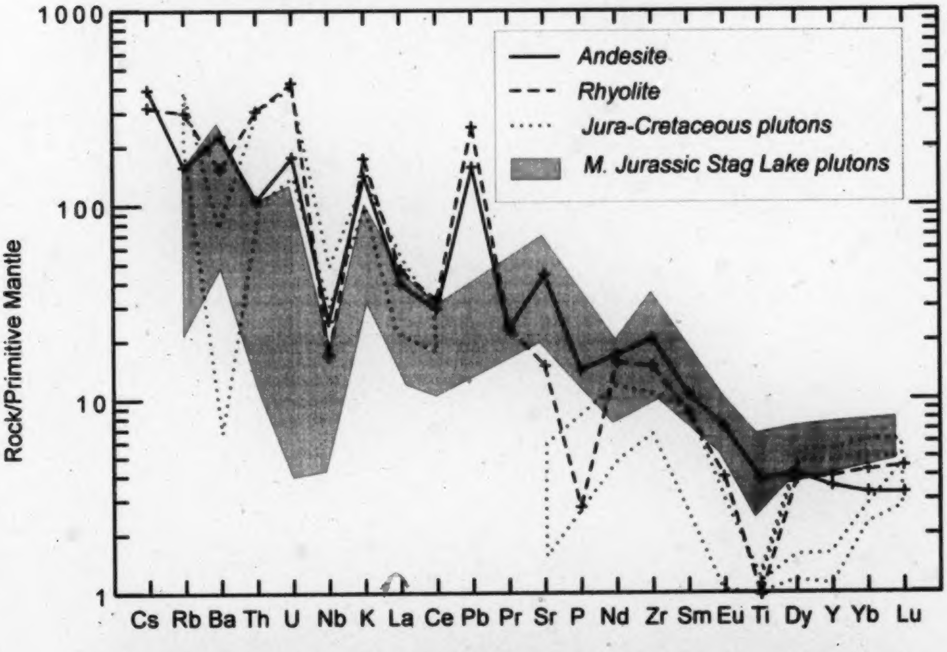

Figure 2-7. Primitive mantle normalized mixed plot for Cretaceous volcanic samples. Comparison data from the Nechako River and Fort Fraser map areas (Anderson et al. 1998b). (Normalization values from Sun and McDonough 1989)

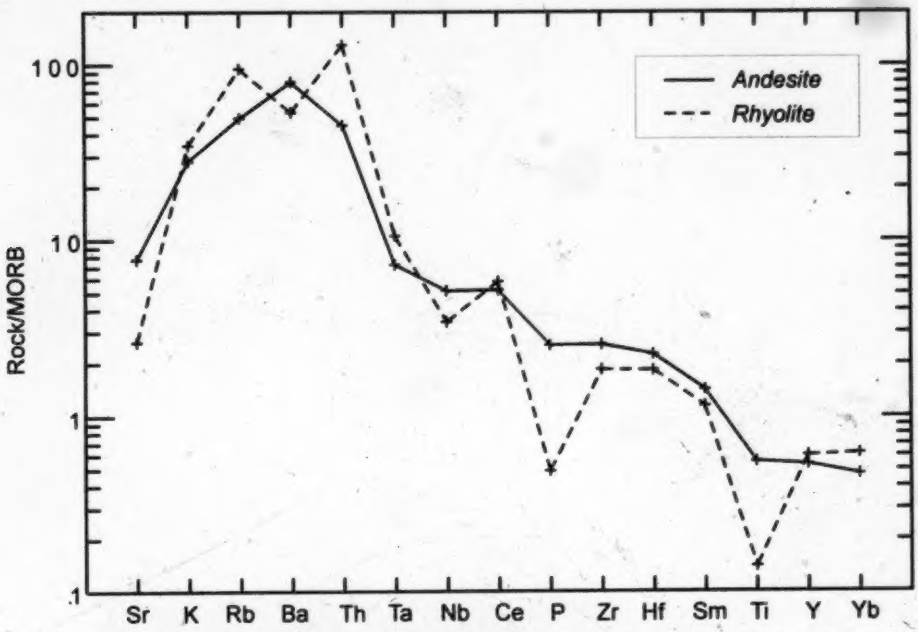

Figure 2-8. Mid-ocean ridge basalt normalized mixed element variation diagram for the Cretaceous volcanic samples (Pearce 1983)

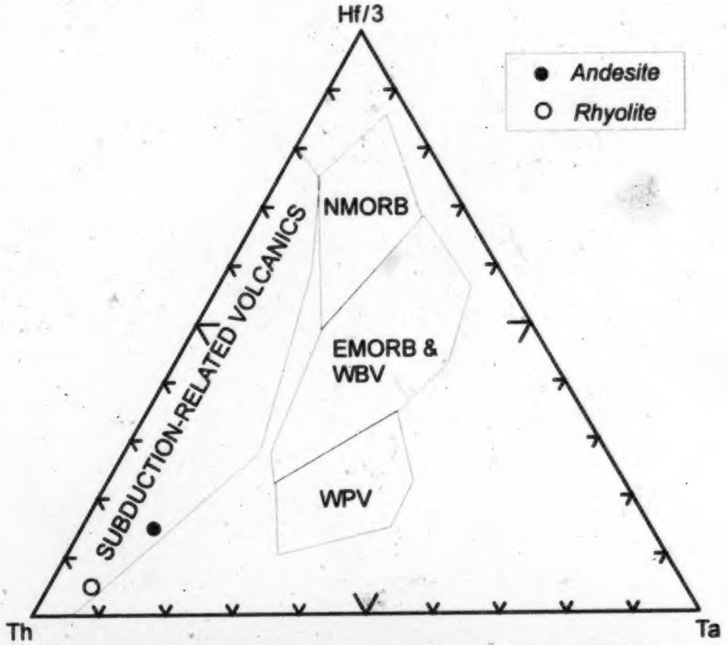

Figure 2-9. Hf/3-Ta-Th tectonic discrimination diagram for the Cretaceous volcanic samples (Wood 1980).

sample also shows negative P and Ti anomalies. The mixed element mid ocean ridge basalt (MORB) plot (Figure 2-8) shows these same trends in addition to a Ta-Nb depletion relative to the neighbouring LILEs. The rhyolite sample also shows a slight depletion in Ba, relative to the adjacent LILEs. This MORB normalized element pattern is typical of subduction-related high K calc-alkaline rocks like those in central Chile (Pearce 1983). The tectonic discrimination diagram from Wood (1980), shown in Figure 2-9, shows that both samples clearly plot in the subduction-related volcanic field.

Trace element data from the Middle Jurassic Stag Lake suite and Jura-Cretaceous plutons within the study area are shown in Figures 2-6 and 2-7 for comparison. The Cretaceous samples show a greater overall enrichment of REE than both plutonic suites, however, the Jura-Cretaceous rocks show a similar enrichment level of the HREE. All three suites show a similar overall pattern of greater LREE enrichment relative to HREE, generally decreasing from Ce to Lu, with either a weak negative or no Eu anomaly. This chondrite normalized REE pattern is typical of calc-alkaline or continental rift related rocks (Condie 1989). The three suites show a similar pattern of LILE enrichment with a strong negative Nb and variable negative Ti anomalies on the mixed element PM normalized plot. The Jura-Cretaceous rocks also show a strong negative Ba and Sr anomaly, not seen in the other two suites.

U-Pb Geochronology

Analytical Methods

The samples were prepared at the University of Alberta by standard crushing (jaw crusher and disk mill) and mineral separation (Wilfley table, heavy liquids, Frantz Isodynamic magnetic separator) techniques. Multi-grain zircon fractions were handpicked from different magnetic and morphological groups. Certain fractions, indicated in Table 1, were air abraded using the technique of Krogh (1982).

Samples were cleaned (Heaman and Machado 1992), weighed and spiked with a mixed ^{205}Pb-^{235}U spike before dissolution in teflon vessels. U and Pb were purified from dissolved samples by anion exchange chromatography on micro-columns using a method modified from Krogh (1973). U and Pb were loaded together onto single outgassed Re filaments using H_3PO_4 and silica gel. Isotopic compositions of U and Pb were determined using two thermal ionization mass spectrometers, a Sector 54 and VG 354. Both mass spectrometers were operated in single-collector mode using either a Faraday cup or Daly photomultiplier detector. Pb and U data collected using the Daly collector (most data) were corrected by a factor of 0.13%/amu and 0.15%/amu (VG 354) and 0.056%/amu and 0.024%/amu (Sector 54), respectively. All isotopic ratios were corrected for mass discrimination based on repeated analyses of the NIST SRM981 Pb and U500 standards. Mass discrimination corrections of 0.12%/amu and 0.15%/amu (VG354) and 0.11%/amu and 0.12%/amu (Sector 54) were applied to Pb and U, respectively. Repeated procedural blanks for U and Pb were measured as 6 pg ± 50% and 5 pg ± 20%, respectively. Decay constants used were $\lambda(^{238}U) = 1.55125 \times 10^{-10}$/yr and $\lambda(^{235}U) = 9.8485 \times 10^{-10}$/yr and an atomic ratio of $^{238}U/^{235}U=137.88$ (Steiger and Jäger 1977; Jaffey et al. 1971; Cowan and Adler 1976). The composition of initial Pb was calculated using the Stacey and Kramers (1975) growth curve. All calculations and errors were calculated using in-house software. All results are reported with errors at the 2 σ level (95% confidence interval). Weighted mean and linear regression age calculations were determined using Isoplot (Ludwig 1998).

Sample Descriptions and Results

Analytical results from U-Pb zircon analyses for two samples are shown in Table 1 and Concordia diagrams in Figure 2-10.

Table 2-1. Analytical results from U-Pb zircon analyses

			(ppm)					Atomic Ratios[4]			Apparent Age ± 2 σ Error (Ma)			
Fr.	Description[1]	Weight (µg)	U	Pb	Th[2]	Th/U	Common Pb (pg)[3]	^{206}Pb/^{238}U	^{207}Pb/^{235}U	^{207}Pb/^{206}Pb	^{206}Pb/^{238}U	^{207}Pb/^{235}U	^{207}Pb/^{206}Pb	% Dis.
	Savory Hill dacite												*SCB-97-3806*	
1	18 su;lp;MI↓	29	233	4	183	0.78	21	0.01156	0.07050	0.04424	74.08 ± 0.8	69.17 ± 2.8		
2	220 su;lp;NM@0.6A	247	276	4	245	0.89	52	0.01162	0.07590	0.04737	74.49 ± 0.8	74.29 ± 0.8	67.84 ± 11.0	-9.85
3	180 su;lp;NM@0.6A	262	328	5	266	0.81	87	0.01152	0.07577	0.04771	73.83 ± 0.8	74.16 ± 0.8	84.89 ± 12.4	13.11
4	161 su;lp;NM@0.6A	141	270	4	233	0.86	23	0.01158	0.07569	0.04742	74.20 ± 0.4	74.08 ± 0.6	70.38 ± 11.4	-5.45
	Hallett Lake Monzonite												*ATG-98-0702*	
1	170 eu;e;M@3°	52	726	19	321	0.44	30	0.02441	0.16723	0.04969	155.46 ± 1.0	157.01 ± 1.0	180.52 ± 6.2	14.05
2	180 su;lp;M@3°	86	632	17	354	0.56	39	0.02476	0.16982	0.04973	157.70 ± 1.2	159.26 ± 1.2	182.58 ± 5.2	13.80
3	137 eu;e;NM@3°	161	492	13	228	0.46	16	0.02493	0.17078	0.04968	158.76 ± 1.0	160.09 ± 1.0	179.90 ± 3.4	11.90
4	98 eu;e;ABR;NM@3°	61	383	11	219	0.57	7	0.02684	0.18257	0.04934	170.74 ± 1.6	170.27 ± 1.6	163.83 ± 7.2	-4.27
5	90 eu;e;ABR;NM@3°	7	344	10	188	0.55	10	0.02630	0.17954	0.04951	167.36 ± 0.8	167.67 ± 1.0	171.99 ± 7.4	2.73

[1] eu=euhedral, su=subhedral, e=equant, lp=prisms (L:W≥3:1), M=magnetic separate (all side tilt angles at 1.85A, unless otherwise specified), NM=non magnetic, all samples are -70 mesh and colourless, ABR = air abrasion treatment

[2] model concentration calculated based on ^{208}Pb and ^{207}Pb/^{206}Pb age

[3] initial + blank Pb

[4] atomic ratios corrected for blank (Pb= 6 pg ± 50% and U= 5 pg ± 20%) and initial common Pb

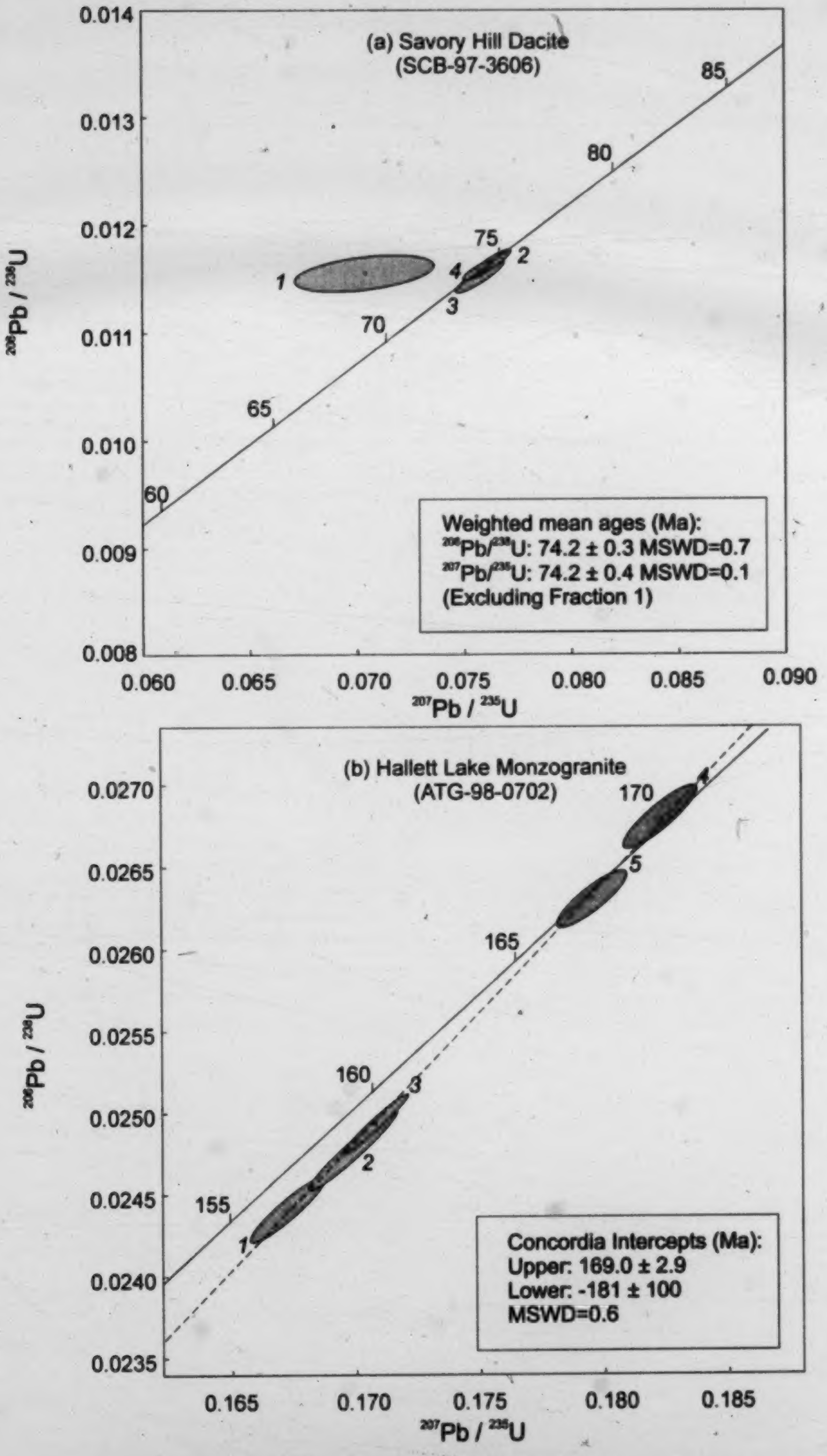

Figure 2-10. Concordia diagrams for the (a) Savoury Hill dacite (SCB-97-3806) and (b) Hallett Lake monzogranite (ATG-98-0702).

Savory dacite 93K/3 (SCB-97-3806)

This medium grey plagioclase dacite is a widespread unit in 93K3, particularly along Savory ridge, north and west of Tchesinkut River. Lower portions of this flow contain minor hornblende and it directly overlies a sequence of rhyolite, rhyolite breccia and conglomerate. Zircons from this sample are a mix of needles, many with inclusions along the length of the needle, and moderately to substantially resorbed, approximately equant, prisms. Analyses of four multi-grain fractions of needles produced slightly discordant results (Figure 2-10a). A linear regression gives a lower intercept of 74.2 ± 0.4 Ma. The upper intercept is unconstrained due to the clustering of analyses. In such cases the Pb/U ages may provide a better estimate of the zircon crystallization age. The individual $^{206}Pb/^{238}U$ and $^{207}Pb/^{235}U$ ages are in agreement for all fractions with the exception of the $^{207}Pb/^{235}U$ age from the first fraction. This fraction is excluded in the quoted weighted mean $^{206}Pb/^{238}U$ and $^{207}Pb/^{235}U$ ages. The weighted mean $^{206}Pb/^{238}U$ age for the three most concordant fractions, 74.2 ± 0.3 Ma, is taken as the best estimate of the crystallization age for this dacite.

Hallett Lake Monzogranite 93F/15 (ATG-98-0702)

Sporadic outcrops of this composite pluton occur in the south central area of the Hallett Lake map sheet (93 F/15) and the north central part of the Big Bend Creek map sheet. The pluton is composed primarily of mottled pink and white, medium grained, biotite monzogranite with minor felsic porphyritic and intrusive breccia phases, porphyritic dykes and stocks (Anderson and Synder 1998; Grainger and Anderson 1999). The majority of the zircons separated from this sample are clear, euhedral and equant in proportion with a minor population of clear needles. Some of the larger equant zircons are slightly to moderately resorbed. Four fractions from the equant zircon population and one representing the needle-like zircon morphology were analyzed from this sample (Figure 2-10b). The most concordant analyses are from air abraded fractions (4 & 5), indicating lead loss as the most probable cause of the discordant results. A discordia line using all five fractions gives an upper intercept of 169.0 ± 2.9 Ma, which is interpreted as the crystallization age of this sample. The lower intercept has a significant error and can be interpreted as intersecting at zero.

$^{40}Ar/^{39}Ar$ Geochronology

Analytical Methods

Four whole rock samples from the presumed Oligo-Miocene basalts were selected for analysis. Samples were crushed and sieved to 150-350 μm at the University of Alberta, then prepared and analyzed at the Geological Survey of Canada laboratories in Ottawa. Fine grained and homogeneous whole rock fragments were selected for analysis, placed into separate aluminum foil packets and loaded into an aluminum can. The age calculation for the $^{40}Ar/^{39}Ar$ dating method includes a parameter called the J value, which is, in part, a function of the neutron flux density and capture cross sections. These two variables are difficult to determine empirically, however, it is possible to determine the J value for a particular position by using a sample of known age, called a flux monitor (Faure 1986). Studies have found the Fish Canyon Tuff sanidine (FCT-SAN) to be suitably homogeneous for laser $^{40}Ar/^{39}Ar$ dating (Lanphere and Baadsgaard 1997; Renne et al. 1994). One FCT-SAN grain was loaded with each sample in the aluminum packets to act as a flux monitor. The aluminum can was irradiated for eight hours in the research reactor at McMaster University in an approximate fast neutron flux of $3x10^{16}$ neutrons/cm^2.

Several aliquots of, usually, five whole rock fragments from each sample were each loaded into a separate hole in a copper planchet. The monitor grain from each packet was also loaded into the planchet. Each monitor was fused in one step and used to calculate the J value for that sample, based on the reported age of 28.03 ± 0.1 Ma for FCT-SAN (Renne et al. 1994; McDougall and Harrison 1988). J values were interpolated for samples that did not contain monitors. Each aliquot was step heated in 3 to 11 increments, from 0.1 to 2 % of the nominal laser power, using a Merchantek® MIR-10 10 W CO_2 laser. This laser is equipped with a 2mm x 2mm flat-field lens, which evenly heats the sample. Each heating step was two minutes in length and typically corresponds to an increment of 50°C to 150°C. Analysis was conducted using a VG 3600 gas source mass spectrometer using either a Faraday cup or standard electron multiplier collector. The relative gain of the electron multiplier is approximately 50 and the sensitivity is typically $1.900\text{X}10^{-9}$ cm^3/V. Data collection protocols are described in Villeneuve and MacIntyre (1997). Decay constants and isotopic abundances used are $\lambda(^{40}K)=5.543 \times 10^{-10}/yr$, $^{39}K=93.2581$, $^{40}K=0.01167$ and $^{41}K=6.7302$ as recommended by Steiger and Jäger (1977) and determined by Beckinsale and Gale (1969) and Garner et al. (1976). Data reduction procedures are given in Roddick (1988) and is based primarily on the individual error associated with each step. The error in the J-factor (± 0.5%, 1σ) is applied to the final age, however, the monitor age uncertainty is not. All results are reported with errors at the $2\ \sigma$ level of uncertainty, unless otherwise stated.

Results

Both heating gas release and inverse isochron plots (Roddick et al. 1980) are used to display the results from four whole rock samples analyzed as shown in Figures 2-11 (a-g). A complete data summary is provided in Appendix III. Each gas release plot shows all of the aliquots analyzed from one sample placed side-by-side. Different aliquots are distinguished by the shaded backgrounds. The horizontal scale has been normalized to the total volume of ^{39}Ar gas produced for one sample (i.e. the combined amount of ^{39}Ar gas produced from all aliquots analyzed for one sample). This makes the relative quantity of gas released in different aliquots readily visible, but does not affect the gas release profile. For example, in Figure 2-11 (a) the second aliquot produced slightly more ^{39}Ar gas than the first aliquot (67% vs 43%), however, both produced comparable quantities of gas. Each step is indicated by a filled black rectangle (e.g. in Figure 2-11 (a) there are five steps in aliquot one, six in aliquot two). The rectangle is vertically centered about the calculated step age and the height of the polygon corresponds to the magnitude of the error associated with that calculated age. The rectangle width is proportional to the quantity of ^{39}Ar gas released in that step. Referring again to Fig 2-11 (a), the first step in aliquot one illustrates a calculated step age of 28.1 ± 1.1 Ma from 37% of the total ^{39}Ar released (or 85% of the ^{39}Ar gas released in aliquot one). Step two of aliquot one illustrates a calculated age of 28.4 ± 10.9 Ma from less than 2% of the total ^{39}Ar released (or just 4% of the gas released in aliquot one). These gas release plots show that in all of the aliquots analyzed most or all of the steps have a consistent calculated step age, referred to as a plateau age. In all of these samples, the plateau ages from the two aliquots analyzed are in good agreement and this combined plateau age is interpreted as the crystallization age of the sample. Some of the samples released only a small quantity of radiogenic argon, which increases the analytical error on the plateau age. In these cases, an inverse isochron plot can be used for analysis to obtain a more precise age.

Summit Lake Quarry basalt, 93J7 (ATR-98-SLQ)

Two aliquots of six and five whole rock fragments, respectively, were analyzed from this sample (Figure 2-11a). Most of the gas in the first aliquot was released in the first heating step and the remaining steps produced little gas and consequently have large errors associated with the calculated step ages. However, the steps in the first aliquot are in good agreement and agree well with the plateau in the second aliquot where the gas was more equally distributed among the heating steps. The two plateau ages combine to produce a total gas age of 28.0 ± 0.6 Ma.

Ootsa Main basalt, 93F/12 (ATR-98-3303)

Two aliquots of five whole rock fragments each were analyzed producing good plateaus with ages of 12.7 and 13.0 Ma (Figure 2-11b). The large errors are mostly due to the small quantity of radiogenic argon released as compared to significant quantities of atmospheric argon. The inverse isochron plot provides a more precise estimate of the crystallization age of the sample at 13.1 ± 0.3 Ma with an MSWD=0.6 (Figure 2-11c). Although less precise, the combined plateau age of 13.5 ± 1.2 Ma is in agreement with the inverse isochron age.

Figure 2-11. Gas release spectra and selected inverse isochron plots for samples analyzed. Separate aliquots are distinguished on the gas release plots by different backgrounds. Line with arrows indicates steps included in plateau and used to calculate sample age on gas release plots. Age calculated from linear regression of data and atmospheric air is shown on inverse isochron plots. (^{40}Ar/^{36}Ar = 295.5 for atmospheric air) Hyphenated numbers indicate aliquot and step number, respectively.

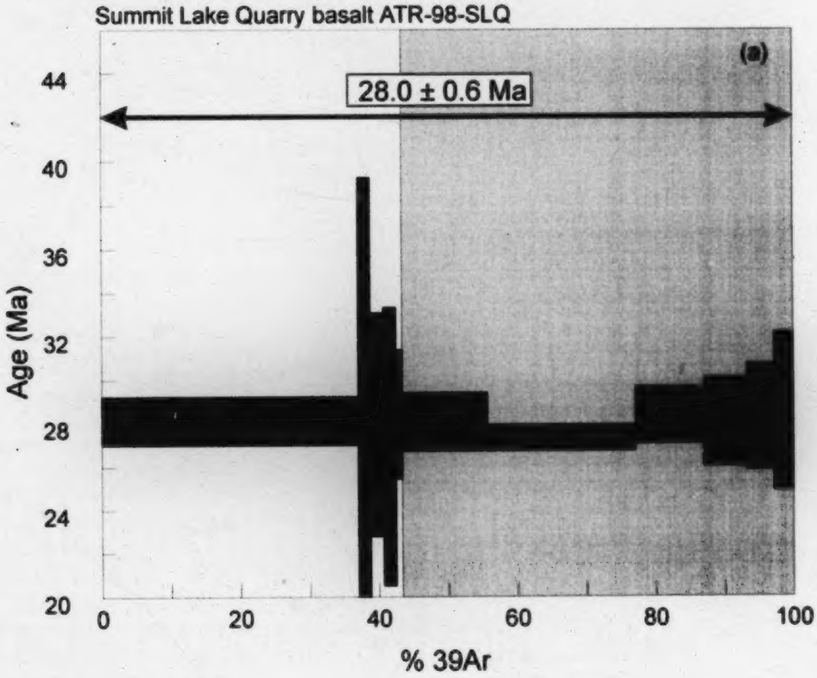

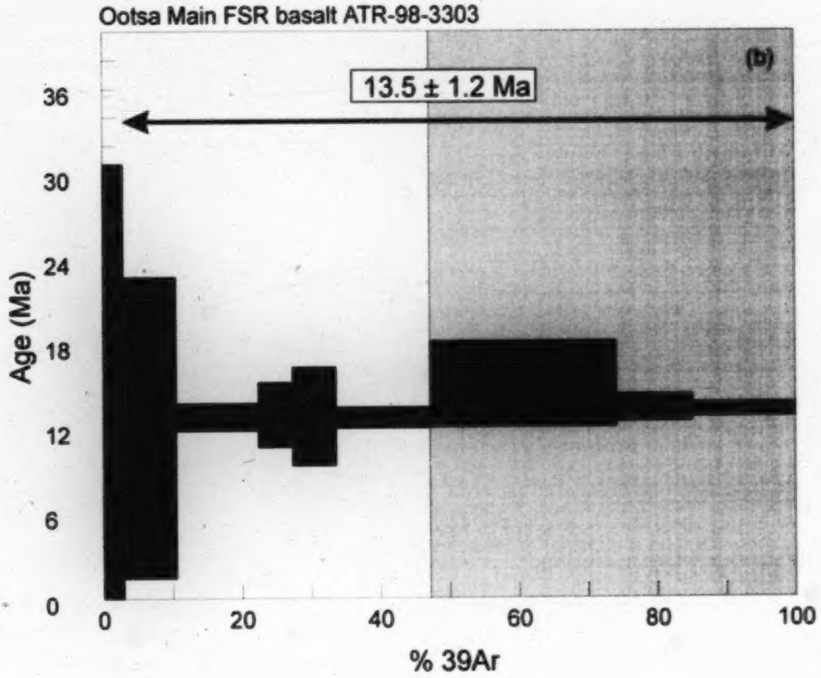

Ootsa Main FSR basalt ATR-98-3303

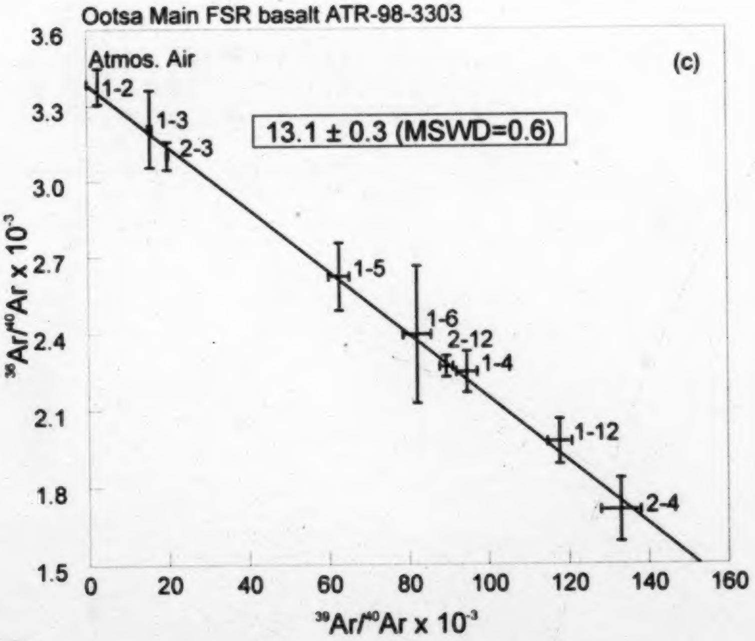

Ootsa Main FSR basalt ATR-98-3303

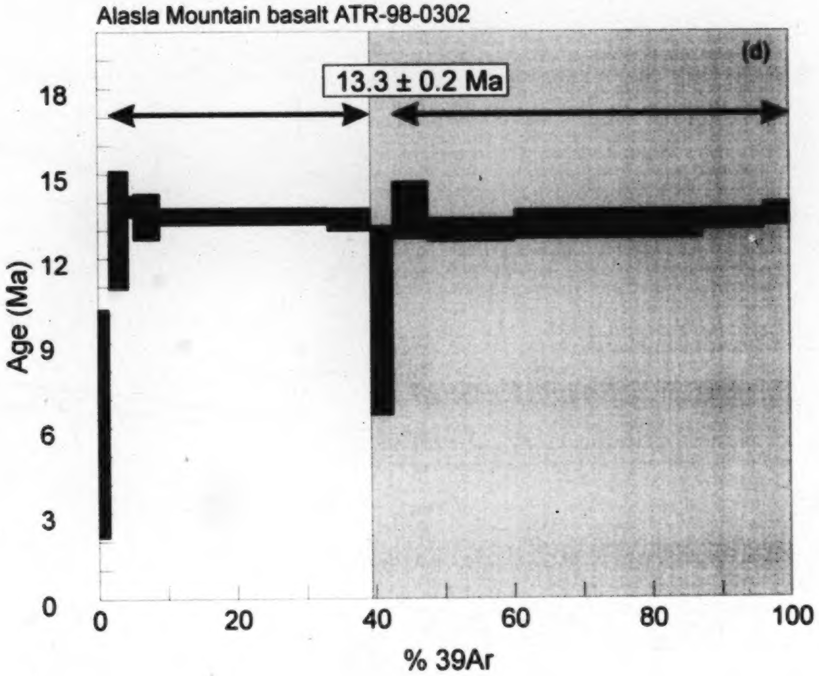

Alasla Mountain basalt ATR-98-0302

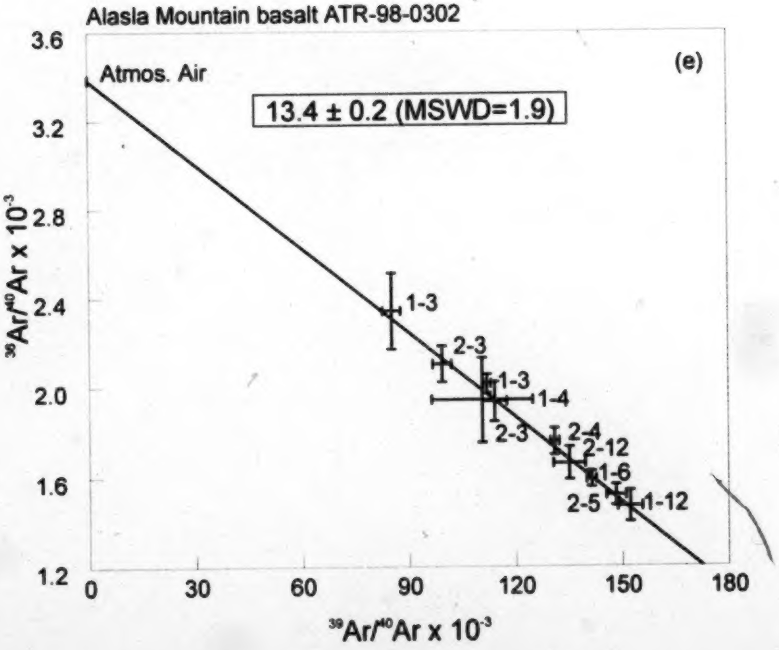

Alasla Mountain basalt ATR-98-0302

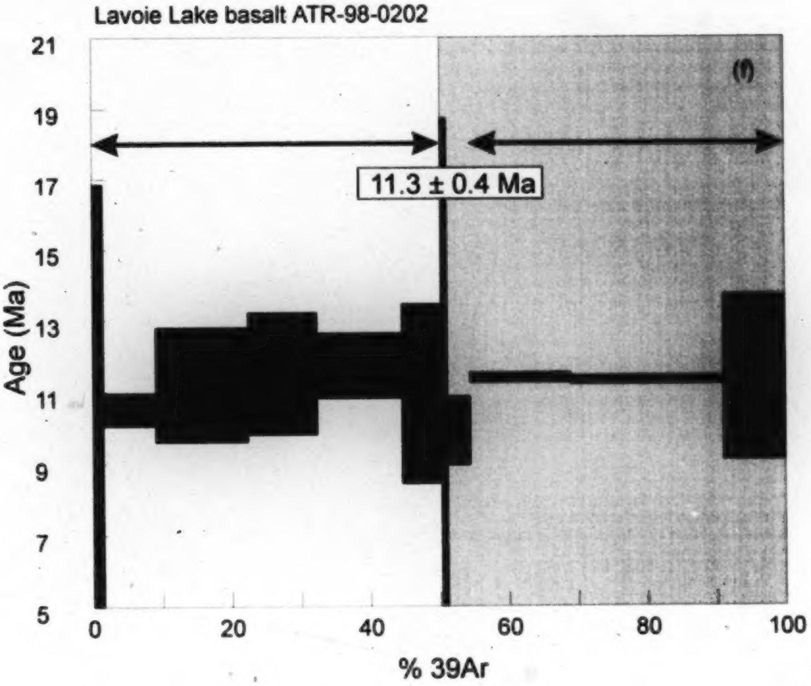
Lavoie Lake basalt ATR-98-0202
(f)
11.3 ± 0.4 Ma
Age (Ma)
21
19
17
15
13
11
9
7
5
0
20
40
60
80
100
% 39Ar

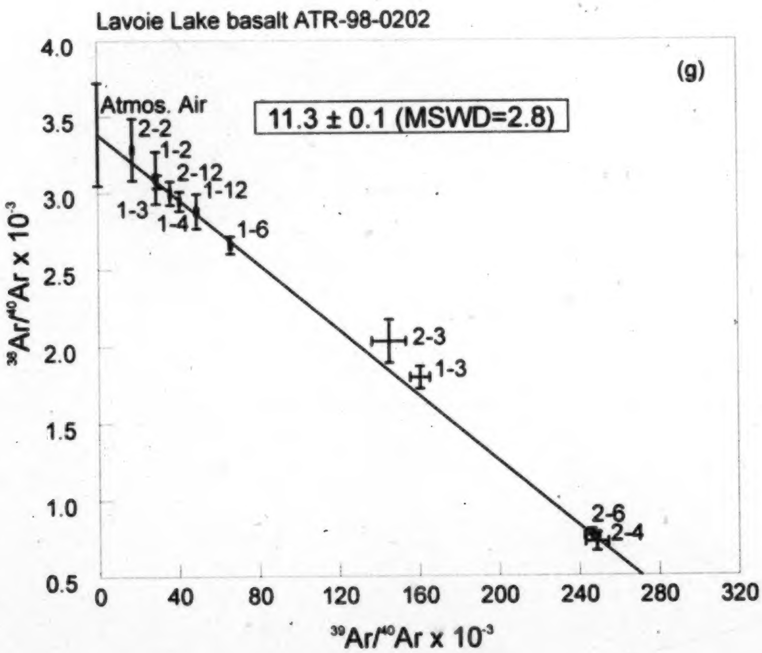
Lavoie Lake basalt ATR-98-0202
(g)
11.3 ± 0.1 (MSWD=2.8)
Atmos. Air
2-2
1-2
2-12
1-12
1-3
1-4
1-6
2-3
1-3
2-6
2-4
$^{36}Ar/^{40}Ar \times 10^{-3}$
4.0
3.5
3.0
2.5
2.0
1.5
1.0
0.5
0
40
80
120
160
200
240
280
320
$^{39}Ar/^{40}Ar \times 10^{-3}$

Alasla Mountain basalt, 93F/14 (ATR-98-0302)
Two aliquots of five whole rock fragments each were analyzed from this sample. Both aliquots produced a good plateau give a combined plateau age of 13.3 ± 0.2 Ma (Figure 2-11d). The argon loss in the early steps of both aliquots may be the result of a younger event in the vicinity. The inverse isochron plot provides a more precise age estimate for this sample of 13.4 ± 0.2 Ma with an MSWD=1.9 (Figure 2-11e). The two ages are in excellent agreement and the plateau age is taken as the best estimate of the crystallization age of this sample.

Lavoie Lake basalt, 93F/8 (ATR-98-0202)
Two aliquots, each of five whole rock fragments, produced excellent plateaux (Figure 2-11f) giving a combined plateau age of 11.3 ± 0.4 Ma. The inverse isochron age is in excellent agreement and gives an age of 11.3 ± 0.1 with an MSWD=2.8 for this sample (Figure 2-11g). The slightly elevated MSWD for the inverse isochron age suggests that the analytical error may be underestimated in this calculated age and thus the combined plateau age is taken as the crystallization age of this sample.

Sr and Nd isotope geochemistry

One Chilcotin basalt and one lherzolite xenolith from three different localities and one Middle Jurassic granitic sample were selected for analysis. Jurassic, Oligocene and Miocene samples were analyzed in order to compare with reported results for these units, to investigate the isotopic composition of the subsurface and the tectonic implications for this period. Constraining the mantle and crustal compositions from these units will also help provide a framework within which to interpret Eocene volcanism, which is relatively less well understood in this area.

Analytical Methods

Samples were prepared by standard crushing procedures (Jaw crusher and powdered in a tugsten carbide ring mill). Isotopic abundances and ratios for Rb-Sr and Sm-Nd were determined at the University of Alberta using isotope dilution mass spectrometry. Rb and Sm were measured on a Micromass 30. Sr and Nd were measured on a VG 354. Measured ratios were normalized to ^{86}Sr/^{88}Sr = 0.1194 and ^{146}Nd/^{144}Nd = 0.7219. Replicate analyses of standards run during this study produced results of ^{143}Nd/^{144}Nd = 0.512095 ± 4 for the Shin Etsu Nd standard (n=19) and ^{87}Sr/^{86}Sr = 0.710275 ± 7 for the NBS 987 Sr standard (n=18). Initial isotopic values were calculated using ^{40}Ar/^{39}Ar or U-Pb age determinations for samples where available and an average Miocene ^{40}Ar/^{39}Ar age of 12.7 Ma was used for the one Chilcotin sample lacking a direct age determination. Analytical results are shown in Table 2. Decay constants used were $\lambda(^{147}\text{Sm}) = 6.54 \times 10^{-12}$/yr and $\lambda(^{87}\text{Rb}) = 1.42 \times 10^{-11}$/yr (Lugmair and Marti 1978; Neumann and Huster 1976; Davis et al. 1977). Values of $^{143}\text{Nd}/^{144}\text{Nd}_{\text{CHUR}}=0.512638$, $^{147}\text{Sm}/^{144}\text{Nd}_{\text{CHUR}}=0.1967$, $^{143}\text{Nd}/^{144}\text{Nd}_{\text{DM}}=0.513163$, $^{147}\text{Sm}/^{144}\text{Nd}_{\text{DM}}=0.2137$ were used to calculate initial εNd and depleted mantle model ages using the following equations;

$$\varepsilon\text{Nd} = (^{143}\text{Nd}/^{144}\text{Nd}_{(T)} / ^{143}\text{Nd}/^{144}\text{Nd}_{\text{CHUR}(T)} - 1)\text{x}10^{4}$$

$$T_{\text{DM}} = \ln[(^{143}\text{Nd}/^{144}\text{Nd} - ^{143}\text{Nd}/^{144}\text{Nd}_{\text{DM}})/(^{147}\text{Sm}/^{144}\text{Nd} - ^{147}\text{Sm}/^{144}\text{Nd}_{\text{DM}}) + 1]/\lambda$$

where $^{143}\text{Nd}/^{144}\text{Nd}_{(T)} = {}^{143}\text{Nd}/^{144}\text{Nd} - ^{147}\text{Sm}/^{144}\text{Nd}(e^{-\lambda t} - 1)$.

Results

Oligocene and Miocene
There is a distinct difference in the Sr and Nd isotopic signature between the two basalt samples from the Nechako River map area, the Bird road locality (ATR-0203 93F/11) and Ootsa Main locality (ATR-3303 93F/12), and the third basalt sample from the Summit Lake locality (ATR-SLQ 93J/7) in the McLeod map sheet as shown in Figure 2-12. The Nechako River samples fall within the mantle array indicating a primitive source, whereas the Summit

Table 2-2. Analytical Results of tracer isotope analyses

Sample	T_{cryst} (Ma)	Rb ppm	Sr ppm	$^{87}Sr/^{86}Sr$	2 σ error	$^{87}Rb/^{86}Sr$	Sr_i	Sm ppm	Nd ppm	$^{143}Nd/^{144}Nd$	2 σ error	$^{147}Sm/^{144}Nd$	$^{143}Nd/^{144}Nd_i$	$εNd_0$	$εNd_i$	Goldstein (Ma)
Oligocene-Miocene Chilcotin Group Lherzolite xenoliths																
ATR-SLQ-LZ	28.0	1.59	5.88	0.70543	0.000012	0.7843	0.70512	0.05	0.23	0.512921	0.000006	0.1372	0.512896	5.5	5.7	483
ATR-0203-LZ	12.7	0.33	61.97	0.70444	0.000013	0.0152	0.70444	0.02	- no data -							
ATR-3303-LZ	13.5	5.43	129.37	0.70363	0.000012	0.1213	0.70360	0.38	6.00	0.512784	0.000017	0.0384	0.512781	2.8	3.1	330
Oligocene-Miocene Chilcotin Group Basalts																
ATR-SLQ	28.0	81.89	763.96	0.70594	0.000010	0.3101	0.70582	4.43	32.28	0.512544	0.000007	0.0830	0.512529	-1.8	-1.4	722
ATR-0203	12.7	61.24	1791.83	0.70350	0.000015	0.0989	0.70348	17.22	84.68	0.512821	0.000007	0.1229	0.512811	3.6	3.7	575
ATR-3303	13.5	194.93	1063.75	0.70358	0.000018	0.5301	0.70348	7.68	44.38	0.512853	0.000006	0.1046	0.512844	4.2	4.4	434
Middle Jurassic Hallett Lake Granite																
ATG-0702	169.0	111.34	283.84	0.70635	0.000012	1.1350	0.70363	3.79	23.00	0.512819	0.000006	0.0996	0.512709	3.5	5.6	460

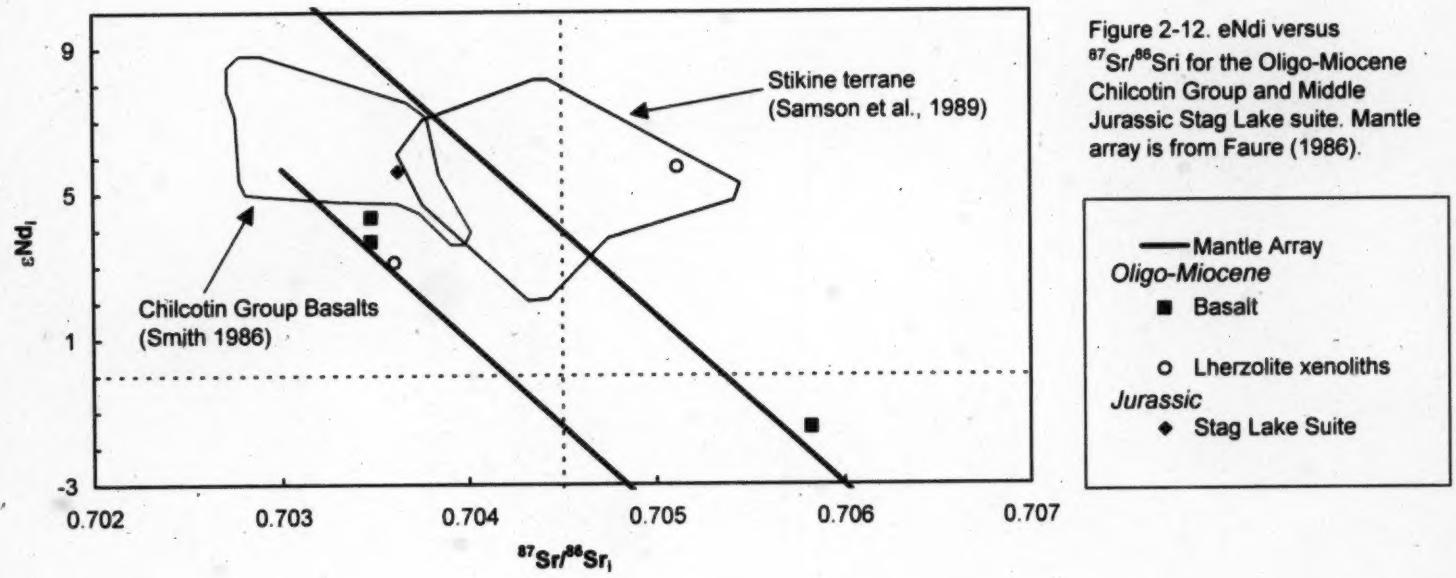

Figure 2-12. eNdi versus $^{87}Sr/^{86}Sri$ for the Oligo-Miocene Chilcotin Group and Middle Jurassic Stag Lake suite. Mantle array is from Faure (1986).

Lake sample plots outside the array and indicates contamination with more evolved crustal material.

The two primitive $^{87}Sr/^{86}Sr$ results of 0.7035 and 0.7036 agree well with published values from the type locality Chilcotin Group basalts (Farquharson 1973; Bevier 1983b). Twelve of these fourteen samples have measured values between 0.7031 and 0.7035 with two higher results of 0.7037 and 0.7038. Twenty-four analyses of Chilcotin Group basalts analyzed by Smith (1986) show a greater range with $^{87}Sr/^{86}Sr$=0.7028 to 0.7039 and εNd=+8.5 to +4.1. The two basalts analyzed here have slightly lower εNd values, but are close to the range defined by these analyses (Figure 2-12).

The spinel lherzolite xenolith samples from the same three sites have $^{87}Sr/^{86}Sr_i$ ranging from 0.7036 to 0.7051 and εNd_i of +5.7 and +3.1. The lherzolite $^{87}Sr/^{86}Sr_i$ result from the Ootsa Main locality agrees within error of the basalt, is slightly lower at the Summit Lake locality and higher at the Bird road locality. The εNd_i values are distinctly different at both the Summit Lake and Ootsa Main localities. Shi et al. (1998) concluded from a study of xenoliths in the northern Canadian Cordillera that spinel lherzolites represent the regional lithospheric upper mantle. If these results do accurately reflect the upper mantle composition, they indicate that there is significant heterogeneity in isotopic composition. Results from an isotopic study of mantle xenoliths, predominantly spinel lherzolites, in Chilcotin basalts within the Quesnel terrane indicated an even greater variation with $^{87}Sr/^{86}Sr$ ranging from 0.7040 to 0.7102 and εNd= -20.4 to +6.9 (Smith 1986).

Jurassic

The isotopic results from the one Stag Lake suite sample falls just slightly below the $^{87}Sr/^{86}Sr_i$ range for published results from igneous rocks in the Stikine terrane (Samson et al., 1989; Patchett et al., 1998) as shown in Figure 2-12. However, in general the results are similar and this analysis agrees well with unpublished data from the other Jurassic plutons in the Endako batholith of $^{87}Sr/^{86}Sr_i \cong 0.7039$ and εNdi ranging from +3 to +7 for other samples from the Stag Lake suite (Anderson et al. 1998b; Anderson, B.A. and Whalen, J.B., unpublished data). These data support previous findings that this pluton, like other Jurassic igneous rocks of the Stikine terrane, are composed of juvenile mantle derived material (Samson et al. 1989; Mihalynuk, et al. 1992).

Discussion

Timing of Magmatism

Jurassic

The Hallett Lake monzogranite sample was collected from a mapped outlier of the Copley Lake pluton near Hallett Lake. This locality has previously been correlated with the Eocene(?) Copley Lake pluton based on the lithological similarity with rocks cross-cutting Eocene Ootsa Lake Group volcanics elsewhere. Given the fact that there is no physical or analytical evidence among the zircon population of this sample to suggest that this sample is significantly younger than the U-Pb age determined here, this outlier is obviously not correlative with the Copley Lake pluton. Rather, this sample is age correlative with the Middle Jurassic Stag Lake suite which has been dated at 171-163 Ma (Villeneuve, M.E. unpublished data *in;* Anderson et al. 1998b). The composition of the pluton is consistent with the felsic Tintagel and Caledonia phases of this suite which are biotite quartz monzonite to monzogranite and known outcrops of these phases can be found within the vicinity of the Hallett Lake locality. Difficulties in distinguishing Jurassic from Eocene plutons are not surprising given the low metamorphic grade in the area and compositional similarity between the suites. Another example of this potential confusion is illustrated by the U-Pb dating of a felsic pluton near the Endako mine which yielded an Eocene age instead of the expected Jurassic age based on regional mapping (Villeneuve and Whalen, unpublished data).

The major element chemistry of the Middle Jurassic and Eocene plutons is similar, both are calc-alkaline, subalkaline, peraluminous, high K, LIL and LREE enriched. However, the Middle Jurassic plutons have volcanic arc affinities whereas the Eocene plutons have within-plate granite affinities on a Rb vs Y+Nb tectonic discrimination diagram (Peace et al. 1984; Anderson et al. 1998b). The Eocene plutons are more potassic, have greater LIL and LREE enrichment and have a more marked Eu anomaly. Isotopic differences might also be useful to distinguish these plutons. Unpublished εNd_i values for Middle Jurassic plutons range from +3 to +7 in the Endako batholith, whereas the Eocene Sam Ross pluton in the Fort Fraser map area has εNd_i values between 1 and 3, identical to the Eocene Ootsa Lake Group (Anderson et al. 1998a; R.G. Anderson and J.B. Whalen unpublished data).

Cretaceous

The Savoury dacite unit was initially mapped as a lower unit within the Ootsa Lake Group (Whalen et al. 1998). Given the precise U-Pb age of 74.2 ± 0.3 Ma, this unit may be correlative with the 75-79 Ma Tip Top Hill volcanics. This would extend the distribution of the Tip Top Hill volcanics east of the Buck Creek basin and indicates that Late Cretaceous volcanism may be significantly more widespread within the Nechako plateau than previously understood. The Savory dacite unit has been mapped throughout the Endako and Taltalpin map areas (93 K/3 and 93 K/6) (Whalen et al. 1998; Hrudey et al. 1999) and suggests that Eocene units mapped within these and adjacent areas need to be carefully reconsidered.

This new age highlights the need for a means to distinguish Eocene and Cretaceous volcanics. The lithologies of the rocks are similar and the only difference appears to be the greater frequency of hornblende phenocrysts within the Cretaceous volcanics. This can be used as an indicator, but can not be used to distinguish the two suites. Unfortunately the geochemical results for the Cretaceous samples analyzed fall within the elemental variation patterns of the Ecoene Ootsa Lake Group and are similar in all aspects. There are no differences between the two groups, based on these limited data, that can be used to distinguish them. Further geochemical and tracer isotope analyses from the Tip Top Hill volcanics are necessary to identify differences between these suites or confirm the apparent chemical similarity.

This age determination suggests there is a good correlation between the K-Ar and U-Pb isotopic systems and is in disagreeement with the suggestion by Leitch et al. (1992) that the younger 75-79 K-Ar ages are underestimating the crystallization ages in this area.

Oligocene and Miocene

The Summit Lake volcanic center is significantly older than the three sites from the Nechako River map sheet. The $^{40}Ar/^{39}Ar$ age is slightly older than the previously published K-Ar dates from Summit Lake, but they do overlap within error. This site was specifically included in the Chilcotin Group by Mathews (1989), therefore this new age slightly expands the defined age range from 28 to 1.1 Ma.

The three $^{40}Ar/^{39}Ar$ ages from the Nechako River map sheet combined with the regional compilation of Chilcotin age determinations by Mathews (1989) suggests that eruptive activity was regionally continuous from 6 to 16 Ma (Figure 2-13). The compilation by Mathews (1989) shows fewer reported ages between 9 and 14 Ma. Mathews (1989) suggested that this either represents a period of reduced volcanic activity or that the results in this interval are spurious. Three of the four ages determined here fall into the 9 to 14 Ma period indicating that the fewer results between 9 and 14 Ma are not due to spurious analyses, but may reflect a reduced rate of volcanic activity. Chilcotin Group volcanism in the Nechako plateau lacks any dated eruptions prior to 6 Ma.

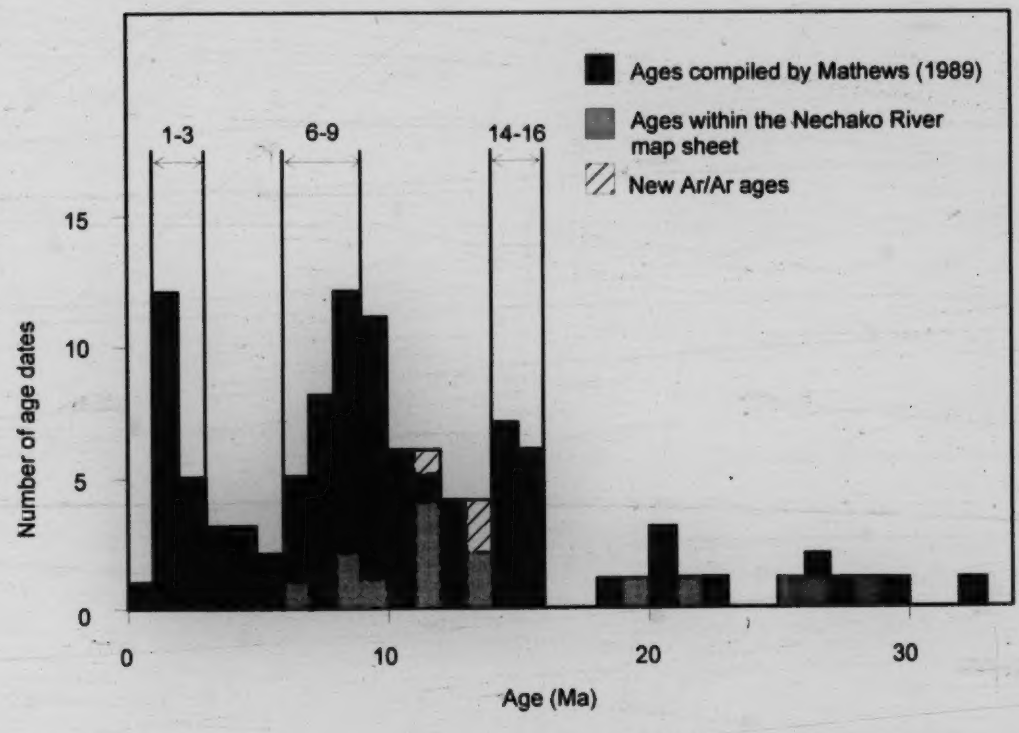

Figure 2-13. Histogram of regional K/Ar ages of Chilcotin Group basalts compiled by Mathews (1989). Results of Ar/Ar analyses included. Ranges of abundant Chilcotin magmatism as concluded by Mathews (1989) are shown for reference.

Magmatic and Tectonic Evolution

Jurassic to Cretaceous

Trace element data for the Jurassic plutons in the Nechako plateau (Anderson et al. 1998b) and Cretaceous Tip Tip Hill volcanics presented here, are both indicative of a subduction-related geochemical signature. The enrichment in LREE relative to HREE, LILE enrichment, negative Nb and Ti anomalies, and general increasing enrichment in incompatible trace elements from Yb to Ce are all characteristic of a subduction-related magmatic source (Condie, 1989). According to Condie (1989), the Ta-Nb depletion relative to LILE or subduction zone component (SZC) can only be derived in three ways; (1) directly from an arc related magma, (2) from a magma derived from melting arc-related rocks in the crust or (3) superimposed on a mantle lithosphere source possibly as a result of an earlier period of subduction.

The isotopic results from the Stag Lake suite (εNd=5.6, Sr_i=0.7036) suggest a primitive source which is consistent with formation in a volcanic arc setting. It has been argued that Stikine terrane formed in an intra-oceanic environment based on the lack of apparent crustal contamination (Samson et al. 1989). However, the emplacement of the Stag Lake suite post-dates accretion of the Intermontane Superterrane (Ricketts et al. 1992; Murphy et al. 1995). This fact, combined with the evolving chemical character of magmatism in the Nechako plateau from the Late Triassic to Late Jurassic (Anderson 1998b) suggests that the arc system operated relatively continuously throughout this time and that the subcontinental lithospheric mantle was not significantly altered by the migration or addition of other isotopic sources into the subsurface in this region. This implies that there was no North American continental crust beneath the Nechako plateau during the Middle Jurassic as the lower Sr isotopic boundary for rocks intruded through autochthonous rocks of continental affinity with North America is generally regarded as 0.706 (Kistler and Peterman 1978).

With only limited geochemical analyses from the Cretaceous volcanics, it is difficult to speculate on the origin of these rocks. MacIntyre et al. (1997) notes that the Cretaceous Kasalka Group and Bulkley intrusions located west of the study area are similar to the Eocene Newman volcanics and Babine intrusions northeast of Burns Lake and suggests that Cretaceous to Eocene magmatism may be explained by an eastward migrating continental arc. Recent geochronology, including results presented here, show active volcanism west of the study area between 100 and 87 Ma, followed by plutonism between 84 to 70 Ma and coeval volcanism at 70 to 72 Ma. Within the study area volcanism at 79 to 74 Ma is succeeded by plutonism from 70 to 64 Ma, then widespread volcanism occurred between 53 and 47 Ma with related plutonism at 55-57, 51-50 and 47 Ma.

Plate reconstructions by Engebretson et al. (1985) at the same latitude as the study area on the coast, show the motion of the Farallon and, subsequently, Kula plates between 100 and 74 Ma were obliquely convergent relative to the North American plate with increasing velocity and strike slip component through this period. Plate motions subsequently became increasingly convergent and decreased in velocity from 74 to 56 Ma. Engebretson et al. (1985) show a significant increase in the velocity of the Kula plate between 56 and 43 Ma, however, this is not supported by the results of Stock and Molnar (1988) who suggest Kula-Pacific relative motion slowed or even ceased after 55 Ma. Both plate reconstructions are in agreement, however, that the Kula plate was obliquely convergent along the western North American margin between 69 and 49 Ma.

These plate reconstructions suggest that volcanism during the Early Cretaceous was related to continental arc activity coincident with convergent plate motions, followed by continued, more sporadic and less voluminous magmatic arc activity through the Late Cretaceous as strike slip plate motions became more dominant. The spatial distributions of volcanism and plutonism are not easily resolved by a simple arc model. For example during the emplacement of the Bulkley plutons, coeval volcanic activity occurred to the east in the Nechako plateau and then migrated west. Godwin (1975) proposed the existence of imbricate subduction zones to explain these patterns. This is possible, however, the location and shape of the subducting slab would also have been subject to the varied plate motions throughout this period, such as roll back of the slab as the rate of convergence decreased, and these effects are more difficult to estimate. During the Tertiary plate motions again became obliquely convergent and widespread extension is coincident with volcanism and plutonism during the Eocene (see Chapter 3).

Oligocene and Miocene

The Chilcotin Group basalts within the Nechako River map area clearly indicate derivation from a primitive source (εNd_i=3.7 to 4.4, $^{87}Sr/^{86}Sr_i$=0.7035). A study of the Oligo-Miocene Chilcotin Group within the Nechako River map area and the Summit Lake locality, found that calculated liquidus temperatures for the basalts are consistently greater than two-pyroxene equilibration temperatures of spinel lherzolite xenoliths entrained in these lavas (Suh 1999). Resnick (1999) interpreted this result to infer an asthenosphere source for the Oligo-Miocene Chilcotin Group and an upper mantle origin for the spinel lherzolite xenoliths. The isotopic results from the Nechako River map area are in excellent agreement with analyses reported for the type locality Miocene Chilcotin Group basalts to the south (Farquharson 1973; Bevier 1983b; Smith 1986) and together suggest an isotopic composition for the Miocene asthenosphere of $^{87}Sr/^{86}Sr_i$=0.7028 to 0.7039 and εNd_i=3.7 to 8.5.

Geochemical differences identified between the Chilcotin Group within the Nechako River map area and Summit Lake locality have been attributed to regional differences in the chemical composition of the asthenosphere (Resnick 1999). It may also be significant that the Summit Lake site is at least 15 Ma older than any other Chilcotin Group basalt that has been analyzed, suggesting the possibility of a temporal variation in asthenosphere composition. Thus, the isotopic results from the Summit Lake locality basalt can be interpreted either as the result of a different asthenosphere composition or contamination of a more isotopically enriched component. The Summit Lake basalt center contains metamorphic crustal xenoliths which have been correlated with Upper Proterozoic paragneiss and orthogneisses of the Wolverine Metamorphic complex which outcrop approximately 10 to 30 km away (Resnick 1999). Xenoliths of this type are found only at this locality. This physical evidence indicates the presence of North American basement below Quesnellia and could explain the isotopic difference between this site and the Chilcotin samples from the Stikine terrane.

It is not possible to eliminate the possibility of contamination of Chilcotin magma from primitive Jurassic rocks at depth given their similar isotopic compositions (Figure 2-12). Bevier (1983b) concludes that contamination or assimilation of this material is unlikely given Pb isotopic results, the absence of crustal xenoliths and silicic differentiates or isotopic evidence for mixing trends. The presence of spinel lherzolite xenoliths within these basalts implies a rapid ascent which provides a limited opportunity for contamination. Within the Nechako River area crustal xenoliths of gabbroic to intermediate plutonic rocks are found, in addition to felsite xenoliths (Resnick et al. 1999). The inclusion of such material within the basalt lavas indicates that, at least at some level, assimilation of crustal material into the magma is likely. However, the primitive isotope results and excellent agreement between the isotopic composition of the Nechako River basalts and type locality Chilcotin Group basalts, which do not contain crustal xenoliths, suggests that crustal contamination appears to have had no significant effect on the overall chemistry.

Bevier (1983b) concluded that the variations in the isotopic composition of the Chilcotin Group basalts were due to heterogeneities in the mantle. Brearly et al. (1984) concluded that the upper mantle is heterogeneous on a scale of centimeters to meters in a study of mantle xenoliths from the Summit Lake locality. The isotopic results from the spinel lherzolite xenoliths in the Nechako River map area and Summit Lake locality also support this interpretation of a heterogeneous upper mantle.

An isotopic study of mantle xenoliths, predominantly spinel lherzolites, at the Summit Lake locality and two other locales in the Quesnel terrane further south reported $^{87}Sr/^{86}Sr$ values from 0.7036 to 0.7112 and εNd values of +7.6 to –20.4 (n=15; Smith 1986). The three analyses of spinel lherzolites in the Oligo-Miocene basalts from the Nechako River and Summit Lake locality reported here have $^{87}Sr/^{86}Sr$ values between 0.7036 and 0.7051. Of these eighteen analyses, three have $^{87}Sr/^{86}Sr = 0.7036$ and $\varepsilon Nd = +6$. This component is comparable to the asthenospheric composition defined by the Miocene basalts (see above). Half of these eighteen analyses have $^{87}Sr/^{86}Sr$ values of 0.7037 to 0.7046 and εNd values of +2 to +5.5. This isotopic component is widespread and thus inferred to represent the dominant upper mantle composition during the Oligo-Miocene. Three analyses from the Summit Lake locality have $^{87}Sr/^{86}Sr>0.7060$ and $\varepsilon Nd<-4$. This latter component is interpreted by Smith (1986) to represent old silicic continental crust, which may reside in the mantle, however, it may represent a strongly enriched mantle component. The few remaining analyses, all from the Summit Lake locality, have $^{87}Sr/^{86}Sr$ values between 0.7051 and 0.7058 with εNd from +3 to +7. The $^{87}Sr/^{86}Sr$ values of this component are similar to those returned from the Summit Lake basalt and may reflect variations in the composition of the asthenosphere at this time or locality.

Plate motions from 49.6 to 35.6 Ma could not be resolved by Stock and Molnar (1988). They determined oblique convergent motion of the Pacific plate towards North America from 10.6 to 19.9 Ma which is both preceeded and followed by primarily strike slip motion. Engebretson et al. (1995) show primarily strike slip motion throughout this period. The resolutions of Stock and Molnar (1988) do appear to agree well with the interpretation of a back arc model for the Chilcotin magmatism.

Conclusions

Middle Jurassic Stag Lake suite rocks are chemically and isotopically distinct from lithologically similar Eocene Ootsa Lake Group plutons. Geochemical and isotopic data are consistent with the emplacement of these rocks in a volcanic arc setting and indicates the absence of any isotopically evolved material, such as North American crust, beneath this area during the Middle Jurassic.

Late Cretaceous volcanism has been found to be significantly more widespread than previously recognized within the Nechako plateau. These rocks are lithologically and chemically similar to the Eocene Ootsa Lake Group, making distinction of these separate groups difficult. Geochemical data supports the interpretation of a continental volcanic arc setting related to the oblique convergence of the Kula plate during this time.

Chilcotin Group magmatism was regionally continuous between 6 and 16 Ma with scattered earlier events around 20 and 28 Ma. Within the Nechako River map area no Chilcotin Group magmatism has been dated earlier than 6 Ma. Sr and Nd results from Chilcotin basalts are isotopically primitive, which supports the interpretation of an asthenosphere source for these lavas and is consistent with a back arc tectonic setting. Results of tracer isotope analyses of spinel lherzolite xenoliths entrained in the Chilcotin Group basalts support the existence of isotopically enriched mantle components beneath the subsurface of the Nechako plateau.

References

Anderson, R.G. and Synder, L.D. 1998. Jurassic to Tertiary volcanic, sedimentary, and intrusive rocks in the Hallett Lake area, central British Columbia. *in;* Current Research 1998-A. Geological Survey of Canada. p. 135-144.

Anderson, R.G., Synder, L.D., Resnick, J. and Barnes, E. 1998a. Geology of the Big Bend Creek map area, central British Columbia. *in;* Current Research 1998-A. Geological Survey of Canada. p. 145-154.

Anderson, R.G., Whalen, J.B., Struik, L.C. and Villeneuve, M.E. 1998b. Mesozoic to Tertiary volcanism and plutonism in southern Nechako NATMAP area: Part 2. Triassic to Eocene composite intrusions and molybdenum metallogeny: the Endako Batholith redefined. *In;* New Geological Constraints on Mesozioc to Tertiary Metallogenesis and on Mineral Exploration in central British Columbia: Nechako NATMAP project; Geological Association of Canada, Cordilleran Section, March 27, 1998, Short Course notes.

Anderson, R.G., Synder, L.D., Resnick, J., Grainger, N.C. and Barnes, E. 1999. Bedrock geology of the Knapp Lake map area, central British Columbia. *in;* Current Research 1999-A. Geological Survey of Canada. p. 109-118.

Andrew, K.P.E. 1988. Geology and genesis of the Wolf Precious Metal Epithermal Prospect and the Capoose Base amd Precious Metal Porphyry-style prospect, Capoose Lake area, Central British Columbia. University of British Columbia. Unpublished MSc thesis. 334 pages.

Armstrong, J.E. 1949. Fort St. James Map-area, Cassiar and Coast Districts, British Columbia. Geological Survey of Canada, Memoir 252, 210 pages.

Armstrong, R.L. 1988. Mesozoic and early Cenozoic magmatic evolution of the Canadian Cordillera. Geological Society of America. Special Paper 218. p. 55-91.

Baadsgaard, H., Folinsbee, R.E. and Lipson, J. 1961. Potassium-argon age of biotites from Cordilleran granites. Geological Society of America. Bulletin. 72; 689-702.

Beckinsale, R.D. and Gale, N.H. 1969. A reappraisal of the decay constants and branching ratio of ^{40}K. Earth and Planetary Science Letters. 6; 289-294.

Brearley, M. Scarfe, C.M. and Fujii, T. 1984. The petrology of ultramafic xenoliths from Summit Lake, near Prince George, British Columbia. Contributions to Mineralogy and Petrology, v.88, p.53-63.

Bevier, M.L. 1983a. Regional stratigraphy and age of the Chilcotin Group basalts, south-central British Columbia. Canadian Journal of Earth Sciences. 20: 515-524.

Bevier, M.L. 1983b. Implications of chemical and isotopic composition for petrogenesis of Chilcotin Group basalts, British Columbia. Journal of Petrology. 24; 207-226.

Bysouth, G.D. and Wong, G.Y. 1995. The Endako molybdenum mine, central British Columbia: An update. *In;* Porphyry deposits of the Northwestern Cordillera of North America, T.G. Schroeter (ed). Canadian Institue for Mining, Metallurgy and Petroleum. Special volume 46; 697-703.

Carr, J.M. 1966. Geology of the Endako area, British Columbia. *in;* Lode metals in British Columbia, British Columbia Ministry of Mines and Petroleum Resources, Annual Report 1965, p. 114-135.

Carter, N.C. 1981. Porphyry Copper and Molybdenum deposits West-central British Columbia. British Columbia Ministry of Energy, Mines and Petroleum Resources. Bulletin 64. 150 pp.

Church, B.N. 1970. The Geology of The Owen Lake Area. British Columbia Department of Mines and Petroleum Resources. Geology, Exploration and Mining in British Columbia 1969; pp. 122-148.

Church, B.N. 1972. Geology of the Buck Creek area, British Columbia Ministry of Energy, Mines and Petroleum Resources. Geology, Exploration and Mining in British Columbia; pp. 353-363.

Condie, K.C. 1989. Plate Tectonics and Crustal Evolution. Pergamnon Press, Oxford. 467 p.

Cowan, G.A. and Adler, H.H. 1976. The variability of the natural abundance of ^{235}U. Geochimica et Cosmochimica Acta. 40; 1487-1490.

Davis, D.W., Gray, J., Cumming, G.L., Baadsgaard, H. 1977. Determination of the ^{87}Rb constant. Geochimica et Cosmochimica Acta. 41; 1745-1749.

Dawson, K.M. 1972. Geology of the Endako Mine, British Columbia. University of British Columbia. Unpublished PhD thesis. 337 pages.

Diakow, L.J. and Koyanagi, V. 1988. Stratigraphy and Mineral Occurences of Chikamin Mountain and Whitesail Reach map areas. British Columbia Ministry of Energy, Mines and Petroleum Resources. Geological Fieldwork 1987. pp. 155-168.

Dostal, J., Hamilton, T.S. and Church, B.N. 1996. The Chilcotin basalts, British Columbia (Canada): geochemistry, petrogenesis and tectonic significance. Neues Jahrbuch fur Mineralogie, Abhandlungen. 170; 207-229.

Drobe, J.R. 1991. Petrology and Petrogenesis of the Ootsa Lake Group in the Whitesail Range, West-central British Columbia. Queen's University. Unpublished MSc thesis. 199 pages.

Engebretson, D.C., Cox, A. and Gordon, R.G. 1985. Relative motions between oceanic and continental plates in the Pacific basin. Geological Society of America. Special Paper 206. 59 p.

Farquharson, R.B. 1973. The petrology of Late Tertiary dolerite plugs in the South Cariboo region, British Columbia. Canadian Journal of Earth Science. 10; 205-225.

Faure, G. 1986. Principles of Isotope Geology (2nd edition). John Wiley and Sons, Inc. New York. 589 p.

Gabrielse, H. and Yorath, C.J. 1991. Chapter 18. Tectonic synthesis. *In;* Geology of Cordilleran Orogen in Canada. (eds.) H. Gabrielse and C.J. Yorath; Geological Survey of Canada, Geology of Canada, no.4, p. 677-705.

Garner, E.L., Murphy, T.J., Gramlich, J.W., Paulsen, P.J. and Barnes, I.L. 1976. Absolute isotopic abundance ratios and the atomic weight of a reference sample of potassium. Journal of Research. U.S. National Bureau of Standards. Section A. 79A; 713-725.

Gill, J.B. 1981. Orogenic Andesites and Plate Tectonics. Springer, Berlin. 389 p.

Godwin, C.I. 1975. Imbricate subduction zones and their relationship with Upper Cretaceous to Tertiary porphyry deposits in the Canadian Cordillera. Canadian Journal of Earth Sciences. 12; 1362-1378.

Grainger, N.C. and Anderson, B.A. 1999. Geology of the Eocene Ootsa Lake Group in northern Nechako River and southern Fort Fraser map areas, central British Columbia. *in*; Current Research 1999-A, Geological Survey of Canada, p. 139-148.

Haskin, M.L., Synder, L.D. and Anderson, R.G. 1998. Tertiary Endako Group volcanic and sedimentary rocks at four sites in the Nechako River and Fort Fraser Map area, central British Columbia. In: Current Research 1998-A, Geological Survey of Canada. p.155-164.

Heaman, L.M., Erdmer, P., Thompson, R.I. and Daughtry, K.L. 1999. Preliminary U-Pb Geochronology Results from the Vernon area, British Columbia. *In;* Slave-NORthern Cordillera Lithoprobe Evolution (SNORCLE) and Cordilleran Tectonics Workshop. P.Erdmer and F.Cook (eds). Lithoprobe Report No 69. p. 196-200.

Heaman, L.M. and Machado, N. 1992.Timing and origin of midcontinent rift alkaline magmatism, North America: evidence from the Coldwell Complex. Contributions to Mineralogy and Petrology. 110; 289-303.

Hrudey, M.G., Struik, L.C. and Whalen, J.B. 1999. Geology of the Taltapin map area, central British Columbia. *in;* Current Research 1999-A. Geological Survey of Canada. p. 85-96.

Irvine, T.N. and Barager, W.R.A. 1971. A guide to the chemical classification of common volcanic rocks. Canadian Journal of Earth Science. 8;523-548.

Irving, E., Thorkelson, D.J. and Schiarizza, P. 1996. Large (1000 to 4000 km) northward movements of tectonic domains in the northern Cordillera, 83 to 45 Ma. Journal of Geophysical Research. 101; 17,901-17,916.

Jaffey, A.H., Flynn, K.F., Glendenin, L.F., Bentley, W.C., and Essling, A.M. 1971. Precision measurements of half-lives and specific activities or ^{235}U and ^{238}U. Physics Review. 4;1889-1906.

Kimura, E.T., Bysouth, G.D. and Drummond, A.D. 1976. Endako. *In;* Porphyry deposits of the Canadian Cordillera, Sutherland Brown, A. (ed.); Canadian Institute of Mining and Metallurgy, Special volume 15; 444-454.

Kistler, R.W. and Peterman, Z.E. 1978. Reconstruction of crustal blocks of California on the basis of initial strontium compositions of Mesozoic granitic rocks. U.S. Geological Survey Professional Paper. 17 p.

Krogh, T.E. 1973. A low-contamination method for hydrothermal decomposition of zircon and extraction of U and Pb for isotopic age determinations. Geochimica et Cosmochimica Acta. 37:485-494.

Krogh, T.E. 1982. Improved accuracy of U-Pb zircon ages by the creation of more concordant systems using an air abrasion technique. Geochimica et Cosmochimica Acta. 37; 485-494.

Lane, R.A. and Schroeter, T.G. 1997. A review of metallic mineralization in the Interior Plateau, central British Columbia (Parts of 93B, C and F); *in;* Interior Plateau Geoscience Project: Summary of Geological, Geochemical and Geophysical Studies, (ed.) L.J.Diakow and J.M. Newell; British Columbia Geological Survey Branch Open File 1996-2 and Geological Survey of Canada, Open File 3448, p.237-256.

Lanphere, M.A. and Baadsgaard, H. 1997. The Fish Canyon tuff; a standard for geochronology. Eos. 78; 326.

LeBas, M.J., LeMaitre, R.W., Streckeisen, A. and Zanettin, B. 1986. A chemical classification of volcanic rocks based on the total alkali silica diagram. Journal of Petrology. 27; 745-750.

Leitch, C.H.B., Hood, C.T., Cheng, X. and Sinclair, A.J. 1992. Tip Top Hill volcanics: Late Cretaceous Kasalka Group rocks hosting Eocene epithermal base- and precious-metal veins at Owen Lake, west-central British Columbia. Canadian Journal of Earth and Atmospheric Sciences. 29: 854-864.

LeMaitre, R.W. 1989. A Classification of Igneous Rocks and Glossary of Terms. Blackwell, Oxford. 193 p.

Lowdon, J.A. 1963. K-Ar measurement on mineral pairs. *In;* Part I – Age determinations by the Geological Survey of Canada, Isotopic Ages, Report 4; Age determinations and Geological Studies. Geological Survey of Canada. Paper 62-17, p.20-22.

Lowe, C. Enkin, R.J. and Dubois, J. 1998. Magnetic and paleomagnetic constraints on Tertiary deformation in the Endako region, central British Columbia. *in;* Current Research 1998-A. Geological Survey of Canada. p. 125-134.

Ludwig, K.R. 1998. Isoplot (Excel version). Berkeley Geochronology Center.

Lugmair, G.W. and Marti, K. 1978. Lunar initial ^{143}Nd/^{144}Nd: Differential evolution of the lunar crust and mantle. Earth and Planetary Science Letters. 35; 273-284.

MacIntyre, D.G., Webster, I.C.L. and Villeneuve, M.E. 1997. Babine porphyry belt project: Bedrock geology of the Old Fort Mountain Map area (93M/1), British Columbia. *in;* Geological Fieldwork 1996. British Columbia Ministry of Employment and Investment. Paper 1997-1, p. 47-67.

Mahoney, B.J., Mustard, P.S., Haggart, J.W., Friedman, R.M., Fanning, M.C. and McNicoll, V.J. 1999. Archean zircons in Cretaceous strata of the western Cordillera; the "Baja BC" hypothesis fails a "crucial test". Geology. 27; 195-198.

Margaritz, H. and Taylor, H.P. 1976. ^{18}O/^{16}O and D/H studies along a 500 km traverse across the Coast Range batholith and its country rocks, central British Columbia. Canadian Journal of Earth Sciences. 13;1514-1536.h

Mathews, W.H. 1964. Potassium-Argon age determinations of Cenozoic volcanic rocks from British Columbia. Geological Society of America Bulletin, v. 75, pp. 465-468.

Matthews, W.H. 1989. Neogene Chilcotin basalts in south-central British Columbia: geology, ages and geomorphic history. Canadian Journal of Earth Sciences. 26; 969-982.

McDougall, I. And Harrison, T.M. 1988. Geochronology and thermochronology by the ^{40}Ar/^{39}Ar method. Oxford University Press, New York. 212 p.

Mihalynuk, M.G., Smith, M.S., Gabites, J.E., Runkle, D., Lefebure, D. 1992. Age of emplacement and basement character of the Cache Creek terrane as constrained by new isotopic and geochemical data. Canadian Journal of Earth Science. 29; 2463-2477.

Monger, J.W.H., Price, R.A., Templeman-Kluit, D.J. 1983. Tectonic accretion and the origin of the two major metamorphic and plutonic welts in the Canadian Cordillera. Geology. 10; 70-75.

Monger, J.W.H., Wheeler, J.O., Tipper, H.W., Gabrielse, H., Harms, T., Struik, L.C., Campbell, R.B., Dodds, C.J., Gehrels, G.E. and O'Brien, J. 1991. Part B. Cordilleran terranes. Chapter 8. Upper Devonian to Middle Jurassic assemblages. *In;* Geology of Cordilleran Orogen in Canada. (eds.) H. Gabrielse and C.J. Yorath; Geological Survey of Canada, Geology of Canada, no.4, p. 281-327.

Murphy, D.C. and van der Heyden, P., Parrish, R.P., Klepacki, D.W., McMillan, W., Struik, L.C. and Gabites, J. 1995. New geochronological constraints on Jurassic deformation of the western edge of North America, southeastern Canadian Cordillera. *In;* Jurassic magmatism and tectonics of the North American Cordillera. D.M. Miller and C. Busby eds. Geological Society of America Special Paper 299. P. 159-171.

Neumann, W. and Huster, E. 1976. Discussion of the ^{87}Rb half-life determined by absolute counting. Earth and Planetary Science Letters. 33; 277-288.

Patchett, P.J., Gehrels, G.E. and Isachsen, C.E. 1998. Nd isotopic characteristics of metamorphic and plutonic rocks of the Coast Mountains near Prince Rupert, British Columbia. Canadian Journal of Earth Science. 35; 556-561.

Paterson, S.R., Miller, R.B., Brandon, M.T. and Ague, J.J. 1998. Regional tilt of the Mount Stuart Batholith, Washington, determined using aluminum in hornblende barometry; implications for northward translation of Baja British Columbia; discussion and reply. Geological Society of America Bulletin. 110; 685-690.

Pearce, J.A. 1983. Role of the sub-continental lithosphere in magma genesis at active continental margins. *In;* Continental basalts and mantle xenoliths. C.J. Hawkesworth and M.J. Norry eds. Shiva Publishing Ltd. Cheshire, UK. p.230-272.

Pearce, J.A., Harris, B.W. and Tindle, A.G. 1984. Trace element discrimination diagrams for the tectonic interpretation of granitic rocks. Journal of Petrology. 25; 956-983.

Renne, P.R., Deino, A.L., Walter, R.C., Turrin, B.D., Swisher, C.C., Becker, T.A., Curtis, G.H., Sharp, W.D. and Jaouni, A.-R. 1994. Intercalibration of astronomical and radioisotopic time. Geology. 22:783-786.

Resnick, J. 1999. Neogene magmatism from the northern Nechako and Summit Lake map areas, British Columbia: implications for the petrology of the lithosphere. Unpublished BSc thesis. University of British Columbia. Vancouver, British Columbia. 105p.

Resnick, J., Anderson, R.G., Russel, J.K., Edwards, B.R. and Grainger, N.C. 1999. Neogene basaltic flow rocks, xenoliths, and related diabase, northern Nechako River map area, central British Columbia. *in;* Current Research 1999-A. Geological Survey of Canada. P.157-167.

Ricketts, B.D., Evenchick, C.A., Anderson, R.G. and Murphy, D.C. 1992. Bowser Basin, northern British Columbia: Constraints on the timing of initial subsidence and Stikinia-North America terrane interactions. Geology. 20; 1119-1122.

Roddick, J.C. 1988. The assessment of errors in ^{40}Ar/^{39}Ar dating. *In;* Radiogenic age and isotopic studies. Report 2. Geological Survey of Canada. Paper 88-2. p. 7-16.

Roddick, J.C., Cliff, R.A. and Rex, D.C. 1980. The evolution of excess argon in alpine biotites – a $^{40}Ar/^{39}Ar$ analysis. Earth and Planetary Science Letters. 48; 185-208.

Rouse, G.E. and Matthews, W.H. 1988. Palynology and geochronology of Eocene beds from Cheslatta Falls and Nazko areas, central British Columbia: geology, ages and geomorphic history. Canadian Journal of Earth Sciences. 25; 1268-1276.

Samson, S.D., McClelland, W.C., Patchett, P.J., Gehrels, G.E. and Anderson, B.A. 1989. Evidence from neodymium isotopes for mantle contributions to Phanerozoic crustal genesis in the Canadian Cordillera. Nature. 337; 705-709.

Shi, L., Francis, D., Ludden, J., Fredricksen, A. and Bostock, M. 1998. Xenolith evidence for lithospheric melting above anomalously hot mantle under the northern Canadian Cordillera. Contributions to Mineralogy and Petrology. 131; 39-53.

Smith, A.D. 1986. Isotopic and geochemical studies of Terrane I, South-Central British Columbia. Unpublished PhD thesis. University of Alberta. Edmonton, Alberta. 195 p.

Souther, J.G. 1991. Chapter 14, Volcanic Regimes. *In;* Geology of Cordilleran Orogen in Canada. (eds.) H. Gabrielse and C.J. Yorath; Geological Survey of Canada, Geology of Canada, no.4, p. 457-490.

Stacey, J.S. and Kramers, J.D. 1975. Approximation of the terrestrial lead isotope evolution by a two-stage model. Earth and Planetary Science Letters. 26:207-221.

Steiger, R.H. and Jäger, E. 1977. Subcommission on Geochronology: Convention on the use of decay constants in geo- and cosmochronology. Earth and Planetary Science Letters. 36: 359-362.

Stevens, R.D., Delabio, R.N. and Lachance, G.R. 1982. Age determinations and geological studies, K-Ar isotope ages; in Report 15; Geological Survey of Canada, Paper 81-2, p.8-9.

Stock, J. and Molnar,P. 1988. Uncertainties and implications of the late Cretaceous and Tertiary position of North America relative to the Farallon, Kula and Pacific plates. Tectonics. 7; 1339-1384.

Struik, L.C. 1993. Intersecting intracontinent Tertiary transform fault systems in the North American Cordillera. Canadian Journal of Earth Sciences. 30; 1262-1274.

Struik, L.C., Anderson, R.G. and Plouffe, A. 1999. Geology of the Euchiniko map area, central British Columbia. *in;* Current Research 1999-A. Geological Survey of Canada. P.119-128.

Struik, L.C. and Orchard, M.J. 1998. Cache Creek Group: Its stratigraphy, structural stacking and paleoenvironment, central British Columbia. *In;* New Geological Constraints on Mesozioc to Tertiary Metallogenesis and on Mineral Exploration in central British Columbia: Nechako NATMAP project; Geological Association of Canada, Cordilleran Section, March 27, 1998, Short Course notes.

Suh, C. 1999. Petrology, chemistry and geothermometry of ultramafic xenoliths from the North Nechako River area, British Columbia, and the nature of the underlying mantle. Unpublished BSc thesis. University of British Columbia. Vancouver, British Columbia. 81 p.

Sun, S.-s. and McDonough, W.F. 1989. Chemical and isotopic systematics of oceanic basalts: implications for mantle composition and processes. *In;* Magmatism in the Ocean Basins. (eds.) Saunders,A.D. and Norry, M.J. Geological Society Special Publication 42. Pp. 313-345.

Sutherland, B.A. 1960. Geology of the Rocher Deboule Range. British Columbia Department of Energy, Mines and Petroleum Resources. British Columbia Department of Mines and Petroleum Resources Bulletin. 78p.

Thompson, R.I., Erdmer, P., Daughtry, K.L., Heaman, L. and Creaser, R.A. 1999. Tracking North American Basement west of the Okanagan Valley: insights from the Vernon, Ashcroft and Hope map areas. *In;* Slave-NORthern Cordillera Lithoprobe Evolution (SNORCLE) and Cordilleran Tectonics Workshop. P.Erdmer and F.Cook (eds). Lithoprobe Report No 69. p. 195.

Tipper, H.W. 1963a. Nechako River Map-area, British Columbia. Geological Survey of Canada, Memoir 324, 59 pages.

Tipper, H.W. 1963b. Topley intrusions; *in;* Age determinations and Geological studies; Geological Survey of Canada, Paper 62-17, p.134-136.

Vandall, T.A. and Palmer, H.C. 1989. Upper limit of docking time for Stikinia and Terrane I: paleomagnetic evidence from the Eocene Ootsa Lake Group, British Columbia. Canadian Journal of Earth Sciences. 27; 212-218.

Villeneuve, M.E. and MacIntyre, D.G. 1997. Laser ^{40}Ar/^{39}Ar ages of the Babine porphyries and Newman Volcanics, Fulton Lake map area, west-central British Columbia. *in;* Radiogenic Age and Isotopic Studies: report 10; Geological Survey of Canada, Current Research 1997-F, p.131-139.

Ward, P.D., Hurtado, J.M., Kirschivink, J.L. and Verosub, K.L. 1997. Measurements of the Cretaceous paleolatitude of Vancouver Island; consistent with the Baja-British Columbia hypothesis. Science. 277; 1642-1645.

Wetherup, S. 1997. Geology of the Nulki Hills and surrounding area, central British Columbia. *In;* Current Research 1997-A. Geological Survey of Canada. p.125-132.

Wetherup, S. and Struik, L.C. 1996. Vanderhoof Metamorphic Complex and surrounding rocks, central British Columbia. *In;* Current Research 1996-A. Geological Survey of Canada. p.63-70.

Whalen, J.B., Struik, L.C. and Hrudey, M.G. 1998. Bedrock geology of the Endako map area, central British Columbia. *In;* Current Research 1998-A. Geological Survey of Canada. p.113-123.

White, W.H., Harakal, J.E. and Carter, N.C. 1968. Potassium-argon ages of some ore deposits in British Columbia. Canadian Institute of Mining and Metallurgy. Bulletin. 61;1326-1334.

White, W.H., Sinclair, A.J., Harakal, J.E. and Dawson, K.M. 1970. Potassium-argon ages of Topley intrusions near Endako, British Columbia. Canadian Journal of Earth Sciences. 7; 1172-1178.

Wood, D.A. 1980. The application of a Th-Hf-Ta diagram to problems of tectonomagmatic classification and to establishing the nature of crustal contamination of basaltic lavas of the British Tertiary volcanic province. Earth and Planetary Science Letters. 50; 11-30.

Woodsworth, G.J., Anderson, R.G. and Armstrong, R.L. 1991. Chapter 15, Plutonic Regimes, *In;* Geology of Cordilleran Orogen in Canada. (eds.) H. Gabrielse and C.J. Yorath; Geological Survey of Canada, Geology of Canada, no.4, p. 491-531.

Yorath, C.J. 1991. Chapter 9; Upper Jurassic to Paleogene Assemblages. *In;* Geology of Cordilleran Orogen in Canada. (eds.) H. Gabrielse and C.J. Yorath; Geological Survey of Canada, Geology of Canada, no.4, p. 331-371.

Appendix I – Sample Locations

Sample Number	Unit	NTS Sheet	Latitude	Longitude
ATG-98-0702	mJ_{SL}	93F15	53.795	124.784
ATR-98-3303C	Mc	93F12	53.644	125.968
ATR-98-3303C-LZ	Mcx	93F12	53.644	125.968
ATR-98-0301	Mc	93F14	53.809	125.355
ATR-98-0203	Mc	93F11	53.620	125.098
ATR-98-0203-LZ	Mcx	93F11	53.620	125.098
ATR-98-0202	Mc	93F8	53.480	124.320
ATR-98-SLQ	Mc	93J7	54.305	122.637
ATR-98-SLQ-LZ	Mcx	93J7	54.305	122.637
SCB-98-3806	uKv	93K3	54.125	125.488
SCB-98-3808	uKv	93K3	54.125	125.481

Appendix II - Analytical results of geochemical analyses

Sample #	SiO_2	TiO_2	Al_2O_3	Fe_2O_3T	Fe_2O_3	FeO	MnO	MgO	CaO	Na_2O	K_2O	H_2OT	CO_2T	P_2O_5	TOTAL
							(wt. %)[1]								
SCB-98-3806	58.70	0.83	15.30	6.70	2.60	3.7	0.09	1.41	4.57	3.30	4.21	2.2	2.8	0.31	100.4
SCB-98-3808	73.60	0.21	13.40	1.70	1.00	0.6	0.03	0.42	1.10	3.10	5.18	1.1	0.2	0.06	100.1
Comparative analysis - Nass R. Basalt															
R-65	47.00	3.60	14.40	16.60	3.00	12.2	0.22	4.37	7.73	4.10	1.88	0.2	0.2	1.21	100.4
R-65[2]	47.55	3.54	14.58		9.32	6.18	0.20	4.31	7.67	4.00	1.92	0.2		1.28	100.8
Absolute error	0.5	0.02	0.2		0.06	0.2	0.01	0.04	0.01	0.03	0.05	0.1	0.1	0.01	

Sample #	Ag	Ba	Be	Co	Cr	Cs	Cu	Ga	Hf	In	Mo	Nb	Ni	Pb	Rb
								(ppm)[1]							
SCB-98-3806	0.2	1597	1.8	22	111	3.10	26	18.00	5.40	0.07	1.7	18.00	53	11	99.00
SCB-98-3808	-	1069	1.9	44	-	2.50	-	15.00	4.40	-	2.0	12.00	-	18	190.00
Absolute error	0.1	20	0.5	5	10	0.02	10	0.1	0.05	0.05	5	0.05	10	10	0.05

Sample #	Sb	Sc	Sn	Sr	Ta	Th	Tl	U	V	Zn	Zr	Ce	Dy	Er	Eu
															(ppm)[1]
SCB-98-3806	0.5	11.0	1.5	928	1.30	9.00	0.64	3.70	111	72	230.0	52.0	3.00	1.50	1.20
SCB-98-3808	0.2	3.4	1.6	317	1.90	26.00	1.20	8.90	13	27	166.0	58.0	2.80	1.70	0.66
Absolute error	0.2	0.5	0.5	10	0.2	0.02	0.02	0.02	5	5	10	0.1	0.02	0.02	0.02

Sample #	Gd	Ho	La	Lu	Nd	Pr	Sm	Tb	Tm	Y	Yb
						(ppm)[1]					
SCB-98-3806	3.90	0.59	27.0	0.24	23.0	6.30	4.70	0.54	0.23	16.00	1.60
SCB-98-3808	3.00	0.60	32.0	0.33	21.0	6.50	3.80	0.48	0.28	18.00	2.10
Absolute error	0.02	0.02	10	0.02	0.1	0.02	0.02	0.02	0.02	5	0.5

[1] Samples below detection are indicated by "-". Bi, Cd and Te were analyzed, but found to be below detection levels for all samples.

[2] Analyzed at the University of Alberta by H. Baadsgaard, 1964 (unpublished data)

Appendix III - Analytical results of laser $^{40}Ar/^{39}Ar$ analyses

(W)			x10-11cm3 STP							
[illegible]										
				Aliquot: A						
3.8	1.2306	3.1660	0.3765	11.4338	453.8742	80.1	28.12	±	1.12	37.0
4.3	0.1580	0.7882	0.0785	0.5274	50.9052	91.7	28.42	±	10.85	1.7
5.4	0.0967	1.9162	0.0375	0.5911	33.2028	86.0	27.93	±	5.17	1.9
7.0	0.1162	5.1013	0.0375	0.5606	38.5742	89.0	26.93	±	6.42	1.8
12.0	0.0538	6.7541	0.0252	0.2767	18.0921	87.8	28.42	±	2.98	0.9
				Aliquot: B						
2.3	0.3362	0.3863	0.0506	3.7939	129.2280	76.9	28.07	±	1.33	12.3
3.1	0.3001	1.3828	0.1846	6.6147	139.4437	63.6	27.35	±	0.60	21.4
3.8	0.1313	0.9561	0.0963	3.0744	63.2806	61.3	28.36	±	1.30	10.0
4.6	0.1657	1.1757	0.0641	1.9067	63.9686	76.5	28.06	±	2.04	6.2
6.2	0.1522	5.1414	0.0739	1.2166	54.6240	82.3	28.29	±	2.45	3.9
12.1	0.1809	13.6443	0.0507	0.8846	60.5431	88.3	28.54	±	3.66	2.9
Total°	**2.9217**	**40.412**	**1.075**	**30.881**	**1105.737**	**78.1**	**27.97**	**±**	**0.64**	
[illegible]										
				Aliquot: A						
2.3	0.2597	0.1721	0.0071	0.2109	76.9216	99.8	3.20	±	27.52	3.0
3.1	0.1109	0.4889	0.0091	0.5411	34.5863	94.8	12.06	±	10.65	7.6
3.8	0.0202	1.0790	0.0064	0.8492	8.9769	66.4	12.78	±	0.99	11.9
4.8	0.0146	0.8490	0.0105	0.3500	5.5774	77.5	12.93	±	2.30	4.9
6.2	0.0131	1.5384	0.0447	0.4498	5.4710	70.8	12.81	±	3.50	6.3
12.0	0.0162	10.5657	0.1381	0.9675	8.2156	58.4	12.73	±	0.76	13.6
				Aliquot: B						
2.7	0.2984	1.8285	0.0190	1.9217	96.2213	91.6	15.09	±	3.04	26.9
4.0	0.0101	1.3308	0.0220	0.7863	5.9113	50.5	13.40	±	0.96	11.0
12.0	0.0270	16.4645	0.2588	1.0653	11.9081	67.1	13.26	±	0.49	14.9
Total°	**0.7702**	**34.317**	**0.516**	**7.142**	**253.790**	**89.7**	**13.21**	**±**	**1.45**	
[illegible]										
				Aliquot: A						
2.3	0.0263	0.2985	0.0062	0.2460	8.4862	91.5	10.52	±	6.34	1.5
2.7	0.0134	1.2703	0.0048	1.1981	7.4610	53.1	10.51	±	0.47	7.5
3.4	0.2215	2.0585	0.0126	2.1359	72.0949	90.8	11.20	±	1.60	13.4
4.1	0.1153	1.6397	0.0215	1.5969	39.1747	87.0	11.51	±	1.71	10.0
5.5	0.0784	5.4387	0.2452	1.9525	29.5269	78.5	11.73	±	0.92	12.2
12.0	0.0528	7.3125	0.1526	0.9038	18.3375	85.0	10.94	±	2.51	5.7
				Aliquot: B						
2.3	0.0270	0.1860	0.0055	0.1423	8.2117	97.0	6.19	±	12.54	0.9
2.7	0.0074	0.6071	0.0033	0.5320	3.6639	60.0	9.91	±	0.96	3.3
3.7	0.0068	2.2162	0.0104	2.3233	9.3426	21.4	11.38	±	0.14	14.5
5.5	0.0110	6.0807	0.2088	3.5272	14.3280	22.6	11.32	±	0.12	22.1
12.0	0.1194	8.5742	0.2247	1.4381	39.8485	88.6	11.39	±	2.31	9.0
Total°	**0.6793**	**35.682**	**0.896**	**15.996**	**250.476**	**80.1**	**11.20**	**±**	**0.43**	

[illegible] Whole Rock; J=.001 [illegible]										
Aliquot: A										
2.3	0.0494	0.2179	0.1027	0.3607	15.2153	95.9	6.17	±	4.03	1.6
2.7	0.0170	0.2600	0.2174	0.6179	7.2534	69.2	13.02	±	2.11	2.8
3.4	0.0030	0.0924	0.0353	0.1716	1.5516	57.3	13.86	±	0.38	0.8
4.1	0.0144	0.3529	0.1898	0.8504	7.4545	57.2	13.49	±	0.82	3.8
5.5	0.0609	4.3142	0.7891	5.4174	38.3346	47.0	13.49	±	0.30	24.2
12.0	0.0134	12.6421	0.4067	1.3856	9.1034	43.4	13.37	±	0.40	6.2
Aliquot: B										
2.3	0.0705	0.3741	0.2166	0.7202	22.7812	91.4	9.79	±	3.35	3.2
2.7	0.0240	0.4286	0.3556	1.1348	11.4220	62.1	13.71	±	1.01	5.1
3.4	0.0504	1.2859	0.5702	2.8004	25.0169	59.5	13.00	±	0.41	12.5
4.3	0.0813	2.0448	0.8312	6.0629	46.2916	51.9	13.21	±	0.51	27.1
5.3	0.0204	5.1616	0.3361	1.9917	13.4355	44.8	13.37	±	0.36	8.9
12.0	0.0104	10.2692	0.3273	0.8453	6.2546	49.0	13.55	±	0.42	3.8
Total[d]	**0.4151**	**37.444**	**4.378**	**22.359**	**204.115**	**60.1**	**13.10**	**±**	**0.26**	

a:Nominal power as measured by laser

b: Gas quantities corrected for decay, isotopes derived from interfering neutron reactions

c: Errors are analytical only and do not reflect error in irradiation parameter J

d: Integrated age, uncertainty includes error in J (0.5%)

e: Nominal J, referenced to FCT-SAN=28.03 Ma (Renne et al., 1994)

CHAPTER 3

Timing and origin of the Ootsa Lake Group, Fort Fraser and Nechako Map areas, central British Columbia

Introduction

The Ootsa Lake Group along with coeval or correlative rocks of the Newman volcanics, Babine and Nanika intrusions, Francois Lake Group and overlying Endako Group form the largest Eocene calc-alkaline volcano-plutonic complexes within the Canadian Cordillera (Figure 3-1). Although the Ootsa Lake Group is one of a discontinuous series of Eocene igneous provinces that stretch along the Cordillera, from the Yukon south through British Columbia, Washington, Montana, Idaho and into Wyoming (Armstrong and Ward 1991), these rocks in central British Columbia are poorly understood (Souther 1991). They are located between the Sloko volcanic province in the Coastal Belt to the northwest and the Kamloops and Penticton Groups to the south within the Intermontane belt. A geochemical and isotopic study of the Mount Skukum and Bennett Lake Igneous Complex, within the Sloko province, concluded that these volcanics were directly mantle derived from contemporaneous subduction (Morris and Creaser 1998). To the south, rocks of the Kamloops Group have also been linked to subduction (Ewing 1981a; Smith 1986). However, coeval extensional tectonics are well documented throughout central and south-central British Columbia (Struik 1993) and volcanism of the Penticton Group was linked to crustal thinning and dextral strike slip motion (Price et al. 1981). Further to the south, calc-alkaline rocks of the Colville Igneous Complex in northeast Washington have recently been interpreted as the product of melting of mid and lower crust as a result of post-Larimide orogenic collapse (Morris and Hooper 1997). These studies indicate that all Eocene magmatic activity within the Cordillera can not be adequately explained by a simplistic continental margin volcanic arc model.

One of the outstanding problems within the Cordillera is whether these widespread Eocene igneous rocks are primarily the result of active subduction, in an Andean arc like setting, or the product of local extension-related to a tensional or transcurrent stress regime which resulted in crustal thinning and increased heat flow (Gabrielse and Yorath 1991; Souther 1991). Of course both of these processes may be involved in Eocene magmatism regionally. This problem also relates to the more fundamental question of how to chemically distinguish volcanic rocks formed from magmas with inherited subduction signatures, either from an overprinted mantle source or crustal contamination, from those which are the product of active subduction. These and other issues indicate the importance of studies, such as this, in order to improve our understanding of the tectonic evolution of convergent plate margins.

This study was undertaken to improve our understanding of the timing and origin of Eocene volcanism and related plutonism within the Nechako River and Fort Fraser map areas (NTS 93F and 93K) in central British Columbia (Figure 3-2). The timing of Ootsa Lake Group volcanism and associated plutonism is here constrained by U-Pb and $^{40}Ar/^{39}Ar$ geochronology. These data augment the existing published database of K-Ar dates for these rocks. Geochemistry of the Ootsa Lake Group and radiogenic tracer isotope data for the Babine Igneous Suite, Ootsa Lake and Endako Groups are also presented. These data, combined with available data from geochemical studies of Ootsa Lake Group volcanics in adjacent areas by Drobe (1991) and Dostal et al. (1998), enables a discussion of the petrogenesis of these rocks and their relationship to Eocene tectonics.

Geological Setting

The study area is located mostly within Stikinia, the largest terrane within the allochthonous Intermontane Superterrane (Figure 3-1). Stikinia is composed of late Devonian to middle

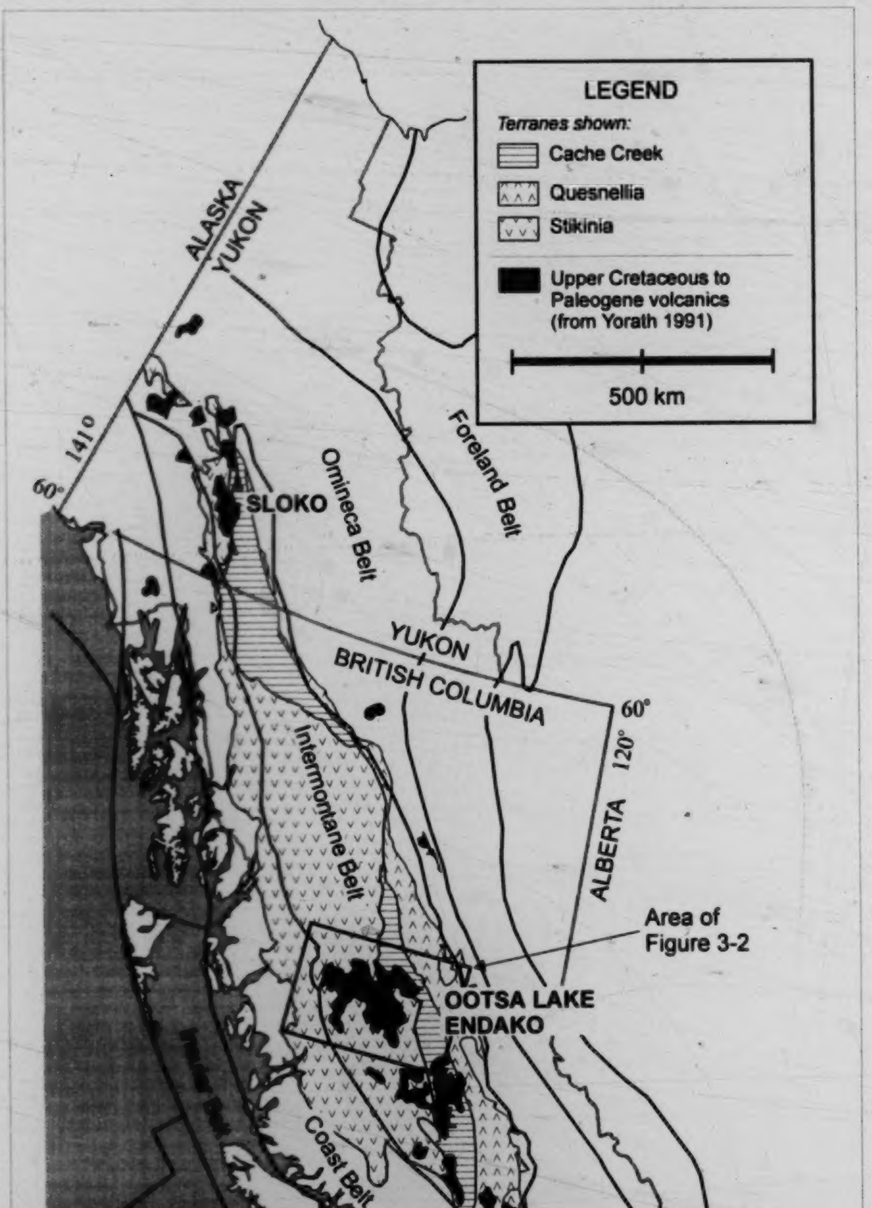
LEGEND
Terranes shown:
Cache Creek
Quesnellia
Stikinia
Upper Cretaceous to Paleogene volcanics (from Yorath 1991)
500 km
ALASKA
YUKON
141°
60°
SLOKO
Omineca Belt
Foreland Belt
YUKON
BRITISH COLUMBIA
60°
120°
ALBERTA
Intermontane Belt
Area of Figure 3-2
OOTSA LAKE
ENDAKO
Coast Belt
KAMLOOPS
Vancouver
Victoria
PENTICTON
BRITISH COLUMBIA
UNITED STATES OF AMERICA
49°

Figure 3-1. Terrane setting of study area showing the distribution of Upper Cretaceous to Paleogene volcanics in the Canadian Cordillera (from Yorath 1991). Names of Groups of Eocene volcanics indicated. (Yorath 1991)

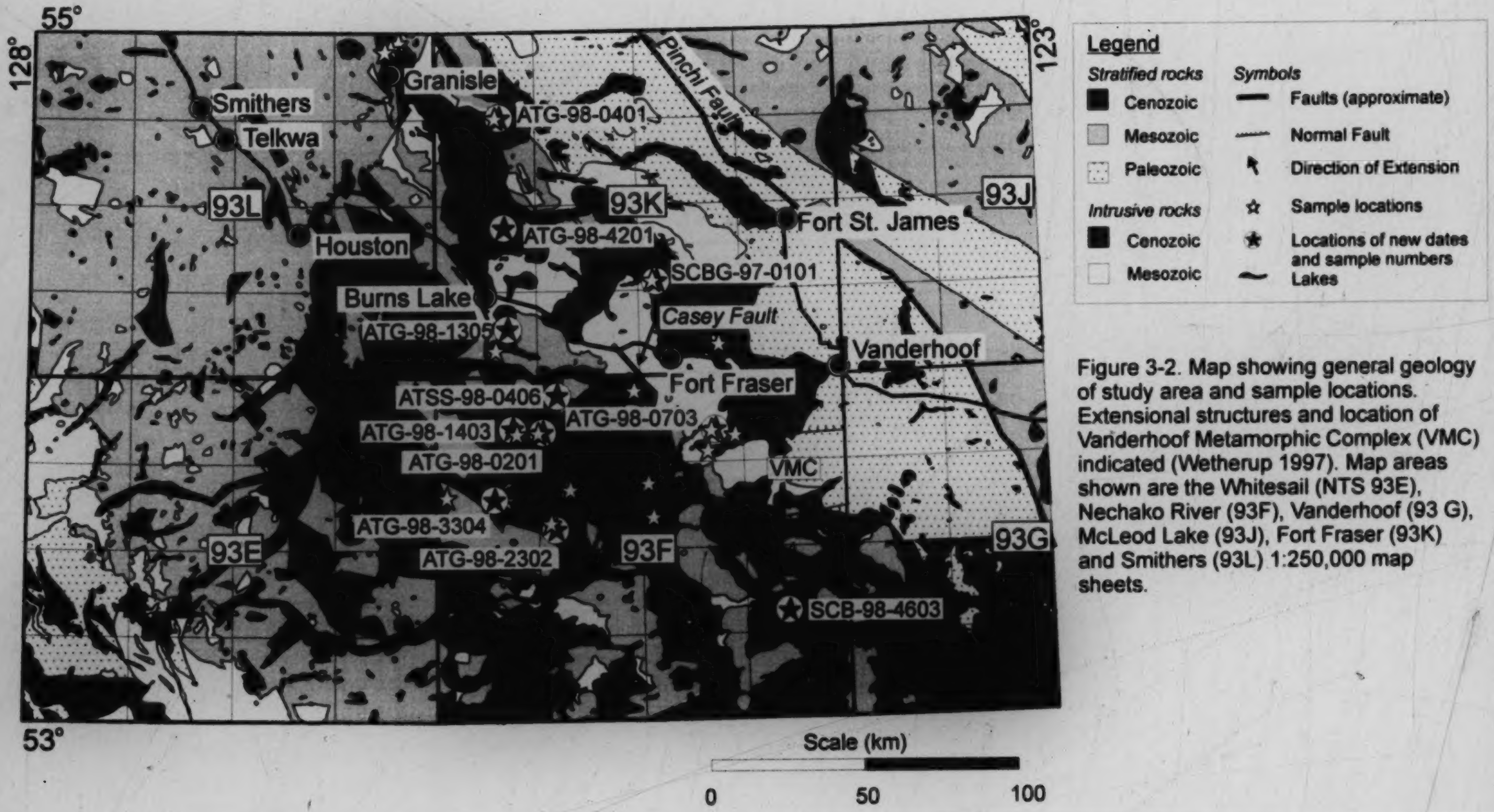
55°
128°
123°
53°
Smithers
Telkwa
Granisle
Houston
Burns Lake
Fort St. James
Fort Fraser
Vanderhoof
Pinchi Fault
Casey Fault
VMC
93L
93K
93J
93E
93F
93G
ATG-98-0401
ATG-98-4201
SCBG-97-0101
ATG-98-1305
ATSS-98-0406
ATG-98-0703
ATG-98-1403
ATG-98-0201
ATG-98-3304
ATG-98-2302
SCB-98-4603
Scale (km)
0
50
100
Legend
Stratified rocks
Cenozoic
Mesozoic
Paleozoic
Intrusive rocks
Cenozoic
Mesozoic
Symbols
Faults (approximate)
Normal Fault
Direction of Extension
Sample locations
Locations of new dates and sample numbers
Lakes

Figure 3-2. Map showing general geology of study area and sample locations. Extensional structures and location of Vanderhoof Metamorphic Complex (VMC) indicated (Wetherup 1997). Map areas shown are the Whitesail (NTS 93E), Nechako River (93F), Vanderhoof (93 G), McLeod Lake (93J), Fort Fraser (93K) and Smithers (93L) 1:250,000 map sheets.

Jurassic volcanic and sedimentary strata and comagmatic plutonic rocks. The most widespread of these within the study area is the Jurassic Hazelton Group composed of mafic flows, breccias, volcaniclastics and minor sediments of calc-alkaline volcanic arc affinity (Monger et al. 1991). The study area also overlaps the Cache Creek and western margin of the Quesnel terrane. The Cache Creek terrane is composed of sedimentary and volcanic rocks of oceanic affinity. Within the study area the Cache Creek Group is composed of an imbricate thrust stack of Upper Paleozoic and Mesozoic limestones and chert, Mesozoic greywacke, siltstone, argillite and basalt with a layered cumulate ultramafic klippe of unknown age (Struik and Orchard 1998). Quesnellia is of volcanic arc affinity and Triassic to early Jurassic volcanic and sedimentary rocks of the Takla Group are exposed within the northeastern corner of the study area (Struik and Orchard 1998). Early Triassic sediment deposits in northern British Columbia suggest amalgamation of these terranes with the Slide Mountain terrane between the Early Triassic and Early Jurassic, forming the Intermontane Superterrane (Gabrielse and Yorath 1991). Accretion of the Intermontane Superterrane onto the western North American margin likely occurred during the Early to Middle Jurassic (Yorath 1991). Recent research indicates that pericratonic rocks underlie Quesnellia in southern British Columbia which would necessitate modification of the current tectonic model (Thompson et al. 1999; Heaman et al. 1999). Middle Jurassic plutonism within the Nechako plateau is partly coeval, but mostly post-dates terrane amalgamation ca. 185-175 Ma (Anderson et al. 1998a).

Uplift and cooling of the Coast belt west of the study area during the Cretaceous is marked by the appearance of Coast belt derived sediments in the Intermontane belt around 98 Ma and cooling K-Ar ages reported from the Coast belt (Woodsworth et al. 1991). This uplift is approximately coeval with the eruption of the Kasalka Group volcanics (ca. 87-100 Ma) within the central Intermontane belt, to the west of the study area (Yorath 1991). Volcanic activity in the study area occurred during the Late Cretaceous with the Tip Top Hill volcanics (ca. 75-79 Ma) and emplacement of the Bulkley plutons west of the study area (ca 70-84 Ma) (Carter 1981; Yorath 1991; Chapter 2). The magnitude of northward movement along strike-slip faults, such as the Pinchi fault, in the Cordillera during the Late Cretaceous to Eocene is the subject of ongoing debate (e.g. Irving et al. 1996; Ward et al. 1997; Paterson et al. 1998; Mahoney et al. 1999). Paleomagnetic data from Eocene rocks immediately west of the study area indicate that any northward motion of the Stikine terrane was completed by 50 Ma (Vandell and Palmer 1989).

Struik (1993) identified three transform fault systems active during the Tertiary in central British Columbia. Early Eocene extension and dextral translation occurred along northwest trending faults followed by Late Eocene to Early Oligocene dextral translation along north trending en echelon transform faults, such as the Pinchi fault. Extension is evident in abundant northeasterly oriented synvolcanic and northwesterly faults distributed across the study area (e.g. Anderson and Synder 1998; Whalen et al. 1998; Barnes and Anderson 1999; Struik et al. 1999). Younger east-west brittle faults have been described in the northeast portion of the Nechako River map area (Wetherup 1997). Up to 4km of horizontal displacement is estimated on the northwesterly Casey fault in the south central portion of the Fort Fraser map area, however, timing of motion on this fault is unconstrained (Lowe et al. 1998). The northeasterly faults are likely coeval with northwesterly extension which formed the Vanderhoof Metamorphic complex, interpreted as an extension-related core complex (NTS 93F/09 and 93F/16) (Wetherup and Struik 1996; Wethurup 1997; Anderson and Synder 1998). ^{40}Ar/^{39}Ar biotite analyses record cooling and the completion of extension on the Vanderhoof Metamorphic complex circa 45 Ma (Anderson 1998). During this period of transtensional stress, widespread calc-alkaline volcanism and less voluminous plutonism occurred across the Nechako plateau. Other Eocene calc-alkaline volcanic complexes included in the Kamloops Assemblage are the Kamloops and Penticton Groups located in south central British Columbia (Ewing1981b; Yorath 1991). This period of magmatism in the Intermontane belt also corresponds to an intense period of uplift and widespread emplacement of granitic plutons in the Coast and Omineca belts (Gabrielse and Yorath 1991).

Alkaline basalts of the Oligocene-Miocene Chilcotin Group were extruded over the Chilcotin plateau to the south and into the study area in a back arc tectonic setting (Souther 1991; Matthews 1989). Miocene and younger Basin and Range style faulting related to this volcanism may have disrupted the Eocene fault systems (Struik 1993).

Eocene Stratigraphy

Early work in the Fort St James (NTS 93N), Fort Fraser, Nechako River and Whitesail (NTS 93E) map sheets recognized a widespread Upper Cretaceous to Oligocene package of mainly felsic flows with minor intermediate to mafic flows, tuffs, breccia and conglomerate (Armstrong 1949; Tipper 1955; Duffel 1959; Tipper 1963). Named the Ootsa Lake Group, this package is unconformably overlain by andesite and basalt flows of the Oligocene or younger Endako Group. Reconnaissance geochronology later indicated that both the Endako Group and Ootsa Lake Group are Eocene in age and the presence of a younger package of Oligocene-Miocene basalts, which have been correlated with the Chilcotin Group volcanics (Matthews 1964; Church 1970; 1972; Carter 1981; Stevens et al. 1982; Matthews 1989).

The correlation of rocks with the Ootsa Lake Group has proceeded primarily on the basis of lithology. Typically, most felsic rocks have been associated with the Ootsa Lake Group and mafic rocks with the Endako Group (Souther 1991). There are two problems with this approach. First, geochronology studies have demonstrated that some rocks correlated with these groups are actually correlative with the Upper Cretaceous Kasalka Group or the Miocene Chilcotin Group (e.g. Church 1972; Drobe 1991; see also Chapter 2). Second, it may be difficult to distinguish mafic rocks of the Ootsa Lake Group from those of the Endako Group (e.g. Diakow & Koyanagi 1988). These problems are further exacerbated by the limited exposure and discontinuous nature of the units (i.e. thin and/or localized flows) which renders correlation of volcanic units within the Ootsa Lake Group across large areas difficult, if not impossible. Consequently, mapping reports within this region provide a local stratigraphic framework for the Ootsa Lake Group, which may not be applicable to adjacent areas. These are summarized in Figure 3-3. Correlations shown in Figure 3-3 are made primarily on the basis of existing age constraints.

Previous Work

The distribution and description of volcanic rocks of the Ootsa Lake and Endako Groups is well known from recent mapping in the Fort Fraser and Nechako River map areas (Anderson et al. 1998b; Anderson and Synder 1998; Whalen et al. 1998; MacIntyre et al. 1998; Struik et al. 1999; Anderson et al. 1999; Hrudey et al. 1999). The Ootsa Lake and Endako Groups were first loosely constrained by Duffell (1959) and Tipper (1963) using paleontological data (Figure 3-3). At least seventeen K-Ar dates have subsequently been reported for the Ootsa Lake Group (Figure 3-4). Three K-Ar dates reported for the Ootsa Lake and correlated volcanics within the Fort Fraser and Nechako River map areas range from 48 to 54 Ma (Matthews 1964; Andrew 1988). An additional fourteen K-Ar and ^{40}Ar/^{39}Ar dates are reported from the adjacent Whitesail and Smithers (NTS 93L) map areas (Figure 3-4; Church 1972; Stevens et al. 1982; Diakow and Koyanagi 1988; Drobe 1991; Dostal et al., 1998). These determinations overlap and range from 47 to 56 Ma. More recent ^{40}Ar/^{39}Ar dating has locally defined a more restricted range of 49 to 53 Ma (NTS 93F/15 & 10, 93K/1 & 7) (M.E. Villeneuve unpublished data *in;* Anderson 1998).

Two geochemical analyses from the Ootsa Lake Group were reported by Souther (1977) who classified the volcanics as calc-alkaline and sub- to mildly alkaline. A petrologic study of the Ootsa Lake volcanics, including thirty-seven geochemical analyses from samples collected in

Figure 3-3. Stratigraphy of the Endako Group, Ootsa Lake Group and correlated units within the Whitesail, Nechako River, Fort Fraser and Smithers map sheets (NTS 93E, 93F, 93K and 93L).

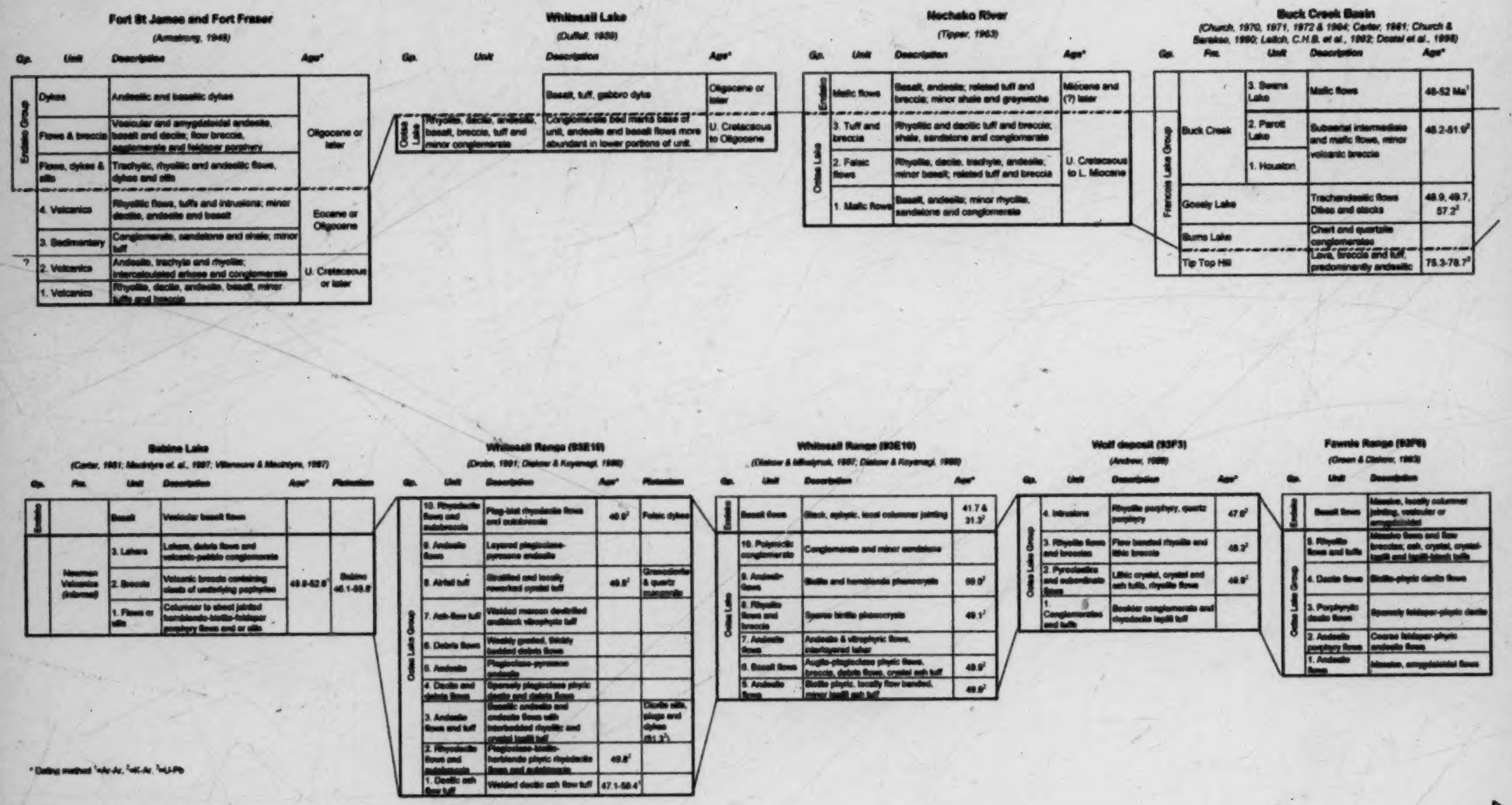

Fort St James and Fort Fraser

(Armstrong, 1949)

Gp.	Unit	Description	Age*
Endako Group	Dykes	Andesitic and basaltic dykes	Oligocene or later
	Flows & breccia	Vesicular and amygdaloidal andesite, basalt and dacite; flow breccia, agglomerate and feldspar porphyry	
	Flows, dykes & sills	Trachytic, rhyolitic and andesitic flows, dykes and sills	
	4. Volcanics	Rhyolitic flows, tuffs and intrusions; minor dacite, andesite and basalt	Eocene or Oligocene
	3. Sedimentary	Conglomerate, sandstone and shale; minor tuff	
?	2. Volcanics	Andesite, trachyte and rhyolite; intercalculated arkose and conglomerate	U. Cretaceous or later
	1. Volcanics	Rhyolite, dacite, andesite, basalt, minor tuffs and breccia	

Whitesail Lake

(Duffell, 1959)

Gp.	Unit	Description	Age*
		Basalt, tuff, gabbro dyke	Oligocene or later
Ootsa Lake	Rhyolite, dacite, andesite, basalt, breccia, tuff and minor conglomerate	Conglomerate bed marks base of unit, andesite and basalt flows more abundant in lower portions of unit.	U. Cretaceous to Oligocene

Nechako River

(Tipper, 1963)

Gp.	Unit	Description	Age*
Endako	Mafic flows	Basalt, andesite; related tuff and breccia; minor shale and greywacke	Miocene and (?) later
Ootsa Lake	3. Tuff and breccia	Rhyolitic and dacitic tuff and breccia; shale, sandstone and conglomerate	U. Cretaceous to L. Miocene
	2. Felsic flows	Rhyolite, dacite, trachyte, andesite; minor basalt; related tuff and breccia	
	1. Mafic flows	Basalt, andesite; minor rhyolite, sandstone and conglomerate	

Buck Creek Basin

(Church, 1970, 1971, 1972 & 1984; Carter, 1981; Church & Barakso, 1990; Leitch, C.H.B. et al., 1992; Dostal et al., 1998)

Gp.	Fm.	Unit	Description	Age*
	Buck Creek	3. Swans Lake	Mafic flows	48-52 Ma[1]
Francois Lake Group		2. Parrott Lake	Subaerial intermediate and mafic flows, minor volcanic breccia	48.2-51.9[2]
		1. Houston		
	Goosly Lake		Trachandesitic flows Dikes and stocks	48.9, 49.7, 57.2[2]
	Burns Lake		Chert and quartzite conglomerates	
	Tip Top Hill		Lava, breccia and tuff, predominantly andesitic	75.3-78.7[2]

Babine Lake

(Carter, 1981; MacIntyre et al., 1997; Villeneuve & MacIntyre, 1997)

Gp.	Fm.	Unit	Description	Age*	Plutonism
Endako		Basalt	Vesicular basalt flows		
	Newman Volcanics (informal)	3. Lahars	Lahars, debris flows and volcanic-pebble conglomerate	49.9-52.6[1]	Babine 45.1-55.6
		2. Breccia	Volcanic breccia containing clasts of underlying porphyries		
		1. Flows or sills	Columnar to sheet jointed hornblende-biotite-feldspar porphyry flows and or sills		

Whitesail Range (93E10)

(Drobe, 1991; Diakow & Koyanagi, 1988)

Gp.	Unit	Description	Age*	Plutonism
Ootsa Lake Group	10. Rhyodacite flows and autobreccia	Plag-biot rhyodacite flows and autobreccia	49.9[2]	Felsic dykes
	9. Andesite flows	Layered plagioclase-pyroxene andesite		
	8. Airfall tuff	Stratified and locally reworked crystal tuff	49.8[2]	Granodiorite & quartz monzonite
	7. Ash-flow tuff	Welded massive devitrified and black vitrophyric tuff		
	6. Debris flows	Weakly graded, thickly bedded debris flows		
	5. Andesite	Plagioclase-pyroxene andesite		
	4. Dacite and debris flows	Sparsely plagioclase phyric dacite and debris flows		
	3. Andesite flows and tuff	Basaltic andesite and andesite flows with interbedded rhyolitic and crystal lapilli tuff		Diorite sills, plugs and dykes (51.3[2])
	2. Rhyodacite flows and autobreccia	Plagioclase-biotite-hornblende phyric rhyodacite flows and autobreccia	49.8[2]	
	1. Dacitic ash flow tuff	Welded dacitic ash flow tuff	47.1-50.4[1]	

Whitesail Range (93E10)

(Diakow & Mihalynuk, 1987; Diakow & Koyanagi, 1988)

Gp.	Unit	Description	Age*
Endako	Basalt flows	Black, aphyric, local columnar jointing	41.7 & 31.3[2]
Ootsa Lake	10. Polymictic conglomerate	Conglomerate and minor sandstone	
	9. Andesite flows	Biotite and hornblende phenocrysts	50.0[2]
	8. Rhyolite flows and breccia	Sparse biotite phenocrysts	49.1[2]
	7. Andesite flows	Andesite & vitrophyric flows, interlayered lahar	
	6. Basalt flows	Augite-plagioclase phyric flows, breccia, debris flows, crystal ash tuff	49.9[2]
	5. Andesite flows	Biotite phyric, locally flow banded, minor lapilli ash tuff	49.9[2]

Wolf deposit (93F3)

(Andrew, 1988)

Gp.	Unit	Description	Age*
Ootsa Lake Group	4. Intrusions	Rhyolite porphyry, quartz porphyry	47.6[2]
	3. Rhyolite flows and breccias	Flow banded rhyolite and lithic breccia	48.2[2]
	2. Pyroclastics and subordinate flows	Lithic crystal, crystal and ash tuffs, rhyolite flows	49.9[2]
	1. Conglomerates and tuffs	Boulder conglomerate and rhyodacite lapilli tuff	

Fawnie Range (93F8)

(Green & Diakow, 1993)

Gp.	Unit	Description
Endako	Basalt flows	Massive, locally columnar jointing, vesicular or amygdaloidal
Ootsa Lake Group	5. Rhyolite flows and tuffs	Massive flows and flow breccias; ash, crystal, crystal-lapilli and lapilli-block tuffs
	4. Dacite flows	Biotite-phyric dacite flows
	3. Porphyritic dacite flows	Sparsely feldspar-phyric dacite
	2. Andesite porphyry flows	Coarse feldspar-phyric andesite flows
	1. Andesite flows	Massive, amygdaloidal flows

* Dating method: [1]Ar-Ar, [2]K-Ar, [3]U-Pb

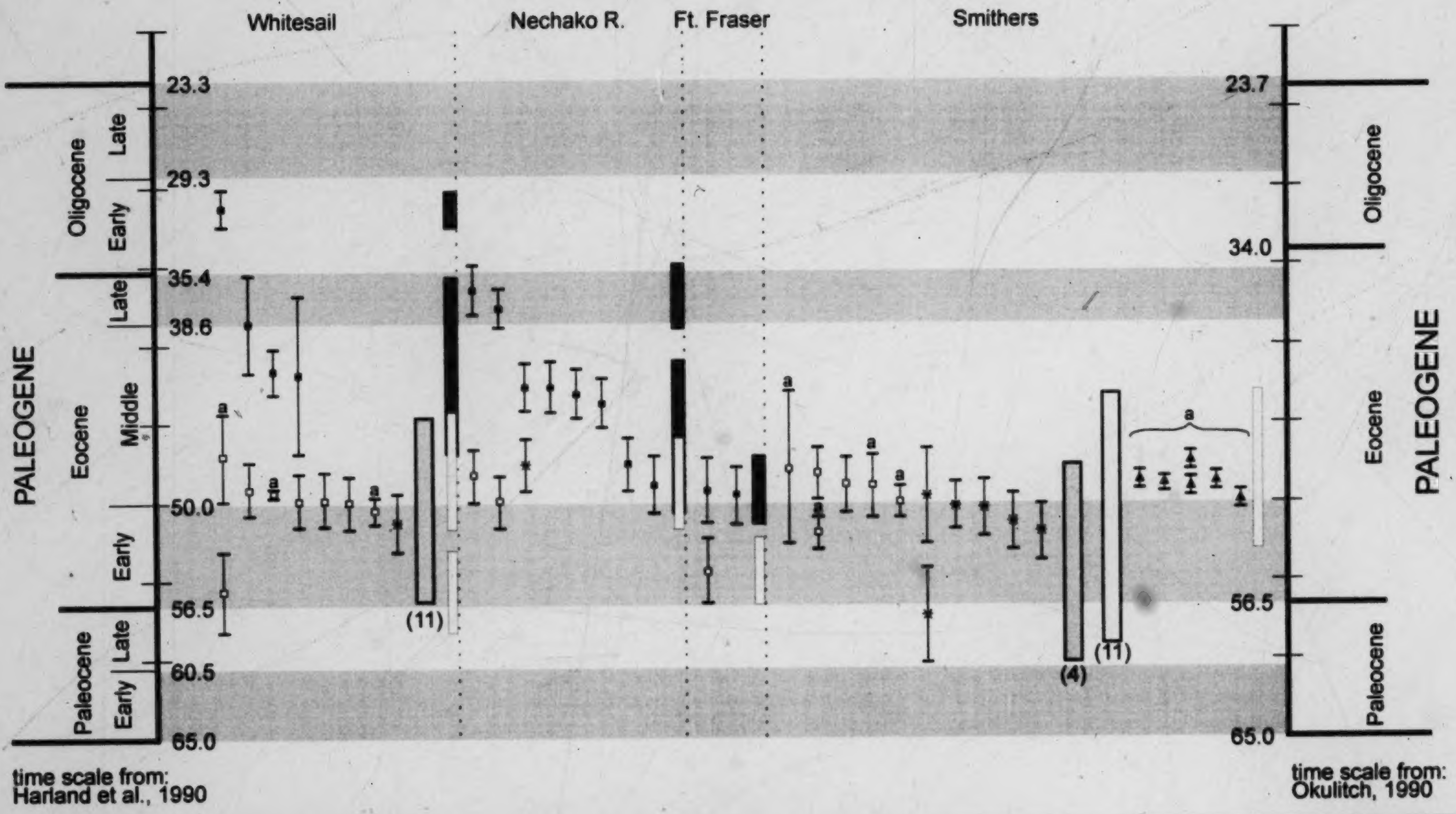

Figure 3-4. Compilation of published K-Ar and Ar-Ar ages for the Eocene within the Whitesail, Nechako River, Fort Fraser and Smithers map areas. All K-Ar ages have been corrected where necessary to conform with the decay constants recommended by Steiger and Jäger (1977). Ranges of Endako Group and Ootsa Lake Group volcanism are indicated based on existing age constraints for areas where age dates have been published. All age data are tabulated in Appendix I (Mathews 1964; Church 1970; 1972; Wanless 1974; Carter 1981; Stevens et al. 1982; Andrew 1988; Diakow and Koyanagi 1988; Rouse and Mathews 1988; Drobe 1991; Leitch et al. 1992; Villeneuve and MacIntyre 1997; Dostal et al. 1998).

the adjacent Whitesail map sheet (NTS 93E/10), was completed by Drobe (1991). This study also indicated that the volcanics are calc-alkaline in character, but subalkaline, high K and quartz normative. Similar results were published for forty-eight samples from the Buck Creek basin (NTS 93L/1 & 2) for the Buck Creek Formation and Swan Lake volcanic suite correlated with the Ootsa Lake and Endako Groups, respectively (Leitch et al. 1992; Dostal et al. 1998). The Swan Lake suite is more tholeiitic in character, but the two groups are otherwise similar and are geochemically similar to subduction-related calc-alkaline or continental intraplate basalts.

The Babine Igneous Suite is located in the Smithers map sheet near Granisle (Figure 3-2). This Suite consists of intermediate volcanics, informally named the Newman volcanics by Tipper and Richards (1976), and the related Babine intrusions. These rocks have been included as part of the Ootsa Lake Group by recent mapping (MacIntyre et al. 1996; 1997). The volcanics are quite localized and consist of a sequence of hornblende-plagioclase porphyry flows, breccias and lahars unconformably overlying Triassic and Jurassic volcanic and sedimentary rocks (MacIntyre et al. 1997). K-Ar dates for the Babine Igneous suite range from 45 to 56 Ma (Wanless 1974; Carter 1981). Recent $^{40}Ar/^{39}Ar$ dating has established a more restricted age range of 50 to 53 Ma through dating samples from many of the same sites previously analyzed (Villeneuve and MacIntyre 1997). This contrast is shown clearly in Figure 3-4.

Only a few K-Ar dates are reported for Eocene intrusive rocks associated with the Ootsa Lake Group within the Nechako plateau. The Nanika intrusions are found in the Whitesail and Smithers map areas and are spatially associated with the Ootsa Lake Group (Souther 1991). These intrusions are commonly small stocks or plugs of quartz monzonite which overlap and range in age from 48 to 54 Ma (Carter 1981). The Goosly Lake syenomonzonite and granite intrusions located in the Buck Creek basin in the Smithers map sheet have been dated at 50 and 57 Ma, respectively (Church 1970 and 1972). The Goosly Lake granite was included with the Nanika intrusions by Carter (1981) thus increasing the age range for these intrusions to 48 to 57 Ma. Three dykes have been dated at the Silver Queen mine, also in the Smithers map area, at 50-52 Ma (Leitch et al. 1992). A rhyolite dyke at the Wolf Lake prospect within the Nechako River map sheet was dated at 47 Ma and an andesite sill in the Whitesail map area was dated at 51 Ma (Andrew 1988; Diakow unpublished data *in* Drobe 1991). More recent U-Pb dating has identified two Eocene plutons in the Nechako River map area; the Frank Lake pluton (93 F/16 & 9) and the Sam Ross pluton (93F/14) have U-Pb dates, interpreted as crystallization ages, of circa 55 and 50.5 Ma, respectively (M.E.Villeneuve pers. comm.).

Recent mapping has identified granite to syenite intrusions associated with the Ootsa Lake Group in the Nechako River map sheet (Sellwood et al. 1999). Geochemical analyses of the intrusions studied by Sellwood et al. (1999) show these plutons to be silicic, subalkaline, calc-alkaline, peraluminous, high K, large ion lithophile element-enriched and within-plate granite affinities (S. Sellwood unpublished data). These plutons are compositionally and geochemically similar to the Sam Ross pluton and Ootsa Lake Group volcanics (Anderson unpublished data).

A geochemical and petrographic study of the Endako Group determined that this group is composed of basaltic andesite to andesite flows (Haskin et al. 1998). Chemically these rocks are mildly alkaline to subalkaline, high-K, transitional tholeiitic to calc-alkaline exhibiting within-plate basalt characteristics (Anderson et al. 1998a). Ten K-Ar dates reported for the Endako Group within the Fort Fraser and Nechako River map areas overlap and range from 37 to 50 Ma (Figure 3-4; Matthews 1964; Rouse and Matthews 1988). Five more K-Ar dates have been reported from the adjacent Whitesail (NTS 93E) and Vanderhoof (NTS 93G) map areas (Stevens et al. 1982; Diakow and Koyanagi 1988; Rouse and Matthews 1988). These dates fall within the above range, with the exception of one anomalous determination of 31.3 ± 1.2 Ma from the Whitesail map sheet. Recent $^{40}Ar/^{39}Ar$ dating has determined a more restricted age range of 45 to 51 Ma for the Endako Group based on analyses of twelve samples across the Fort Fraser and northeastern Nechako River map sheets (M.E.Villeneuve pers. comm. 1999).

Local Geology of the Ootsa Lake Group

The Ootsa Lake Group in the northern Nechako River and southern Fort Fraser map areas consists predominantly of rhyolitic flows and domes, crystal and lithic-crystal tuff, less abundant pyroclastic and autoclastic breccias and minor dacitic and andesitic flows (Grainger and Anderson 1999 – Appendix IV). Examples of these are shown in Figure 3-5. Phenocrysts observed within the Ootsa Lake Group, in order of decreasing frequency of occurrence, are plagioclase, biotite, alkali feldspar, quartz and hornblende. A general stratigraphy consists of a basal reworked lithic rhyolite tuff and overlying hornblende-plagioclase andesite with amethyst-calcite bearing amygdules (Figure 3-5D), medial flow laminated rhyolite flow rocks (Figure 3-5F and G) and breccia (Figure 3-5C) and upper felsic tuff and breccia (Figure 3-5B). Rhyolite ash-lignite interbeds mark the top of the sequence (Figure 3-5A). The lignite interbeds, in addition to quenched glassy rhyolite flow bases and basal reworked rhyolite tuffs indicate the presence of shallow water environments throughout eruption of the Ootsa Lake Group volcanics.

Samples were collected from across the northern and eastern portions of the Nechako River map sheet and southern and western regions of the Fort Fraser map sheet which represent the lithological and temporal variation of the Ootsa Lake Group volcanics in these areas. Samples were contributed from other studies on related Eocene plutonic rocks (Sellwood et al. 1999) and the Endako Group (Haskin et al. 1998). Samples from the Babine Igneous Suite were also collected as part of this study (Figure 3-5E). Locations for all samples analyzed are provided in Appendix II. These samples were included in this study in order to investigate whether these coeval rocks share a similar petrogenetic origin.

Major and Trace Element Geochemistry

Analytical Methods

Twenty two samples from the Ootsa Lake volcanics and three samples from the Babine Igneous Suite were selected for analysis. Samples were powdered using both a Tungsten carbide and steel ring mill at the University of Alberta and were analyzed at the Geological Survey of Canada (GSC) analytical chemistry laboratory in Ottawa. Samples were analyzed using X-ray flourescence (XRF) for major and several trace elements (Ba, Nb, Rb, Sr and Zr). Trace elements were determined using either inductively coupled plasma emission spectrometry (ICP-ES) (Ag, Ba, Be, Co, Cr, Cu, La, Ni, Mo, Pb, Sc, Sr, V, Y, Yb, Zn, Zr) or inductively coupled plasma mass spectrometry (ICP-MS). Analytical errors are given with the data in Appendix III. Precision is ± 1-5% for the major elements and ± 5-10% for the trace elements. A sample previously analyzed at the University of Alberta by wet chemistry (H. Baadsgaard unpublished data 1964) and two replicate samples were also analyzed at the GSC to test the reproducibility of results. These comparative analyses are very close for all elements determined.

Results

The Ootsa Lake Group volcanics have SiO_2 contents ranging from 54.8 to 79.8 wt %. On the volcanic classification diagram of LeBas et al. (1986), the Ootsa Lake Group volcanics show a continuous range from basaltic trachyandesite to rhyolite, with the majority of the samples falling into the trachydacite to rhyolite range (Figure 3-6). This range is similar to results from the Kamloops Group (Ewing 1981a; Smith 1986) and differs somewhat from the distinctly bimodal distribution from the Mount Skukum and Bennett Lake Igneous Complex (Morris and

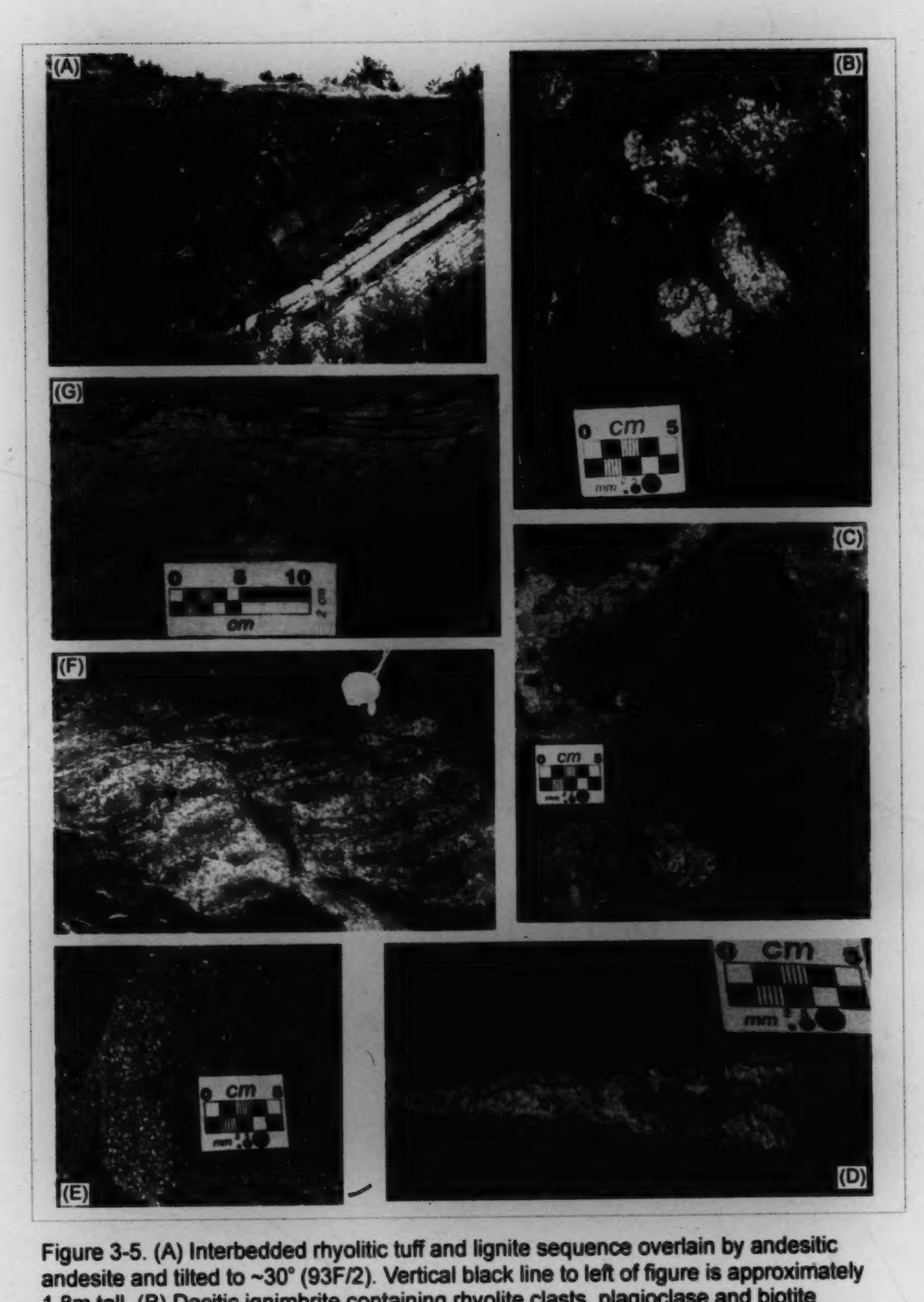

Figure 3-5. (A) Interbedded rhyolitic tuff and lignite sequence overlain by andesitic andesite and tilted to ~30° (93F/2). Vertical black line to left of figure is approximately 1.8m tall. (B) Dacitic ignimbrite containing rhyolite clasts, plagioclase and biotite phenocrysts from Dayeezcha Mtn (ATG-1403: 93F/13). (C) Rhyolitic pyroclastic breccia showing a subrounded dark grey perlitic rhyolite clast above the basal unit contact (93F/12). (D) Basal andesite unit containing amygdules of amethyst (A) and inner calcite (c) (93F/14). (E) Plagioclase porphyry andesite from the Newman volcanics (93L/16). (F and G) Typical flow laminated rhyolites at the sample site ATG-0201 (G: 93F/14) and containing rotated rhyolite clasts (F: 93F/12).

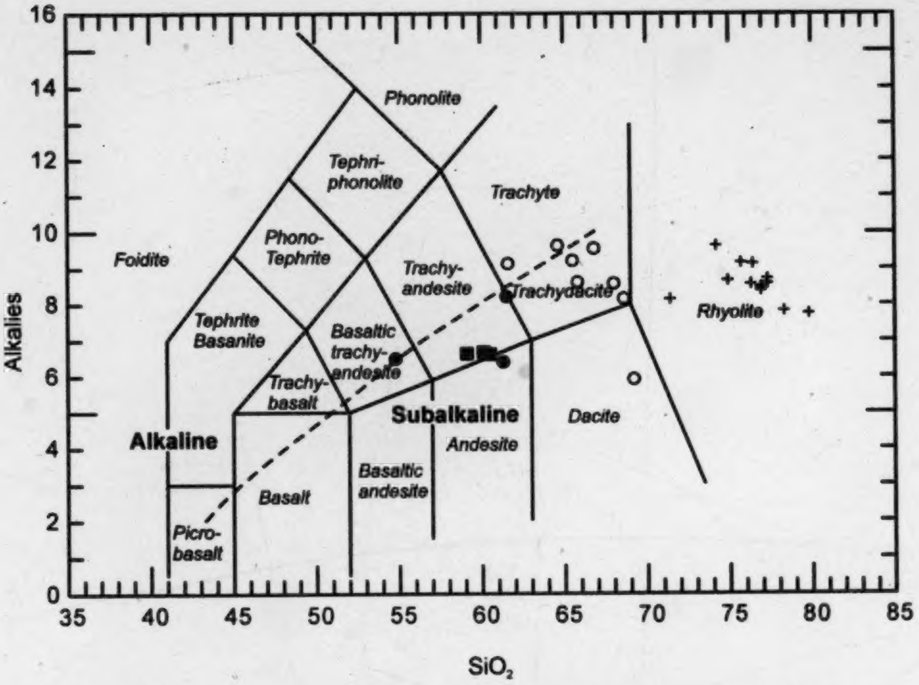

Figure 3-6. Alkalies versus silica plot for the Ootsa Lake Group volcanics and Babine Igneous suite with alkaline-subalkaline division (Irvine and Barager 1971) and volcanics classification scheme (LeBas et al. 1986)

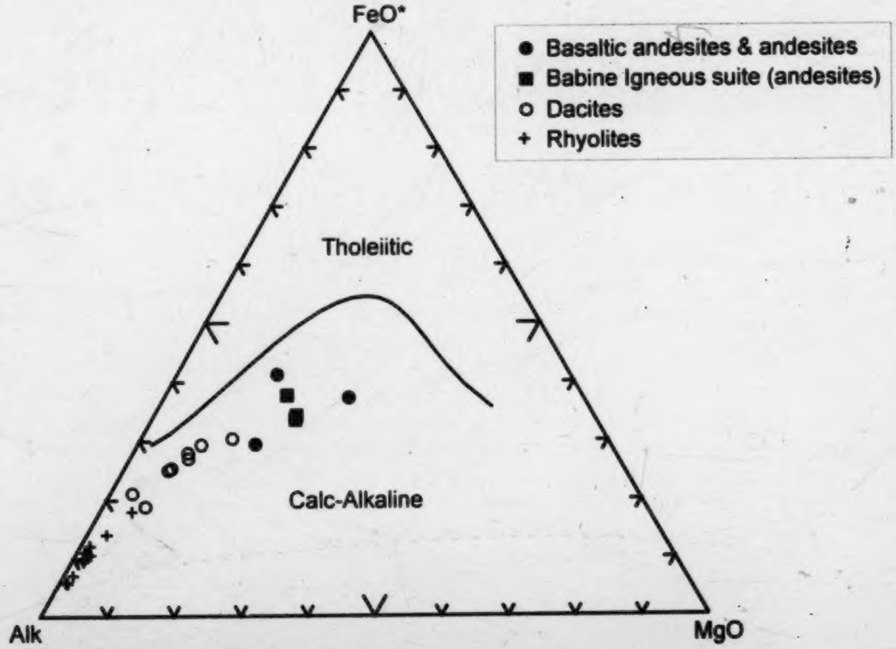

Figure 3-7. AFM classification for the Ootsa Lake Group volcanics and the Babine Igneous Suite (Irvine and Barager 1971)

Creaser 1998). The Babine Igneous Suite has a much more restricted SiO_2 content between 59.1 to 60.5 wt % and all analyses fall into the trachyandesite range (LeBas et al. 1986). The three samples from the Babine Igneous Suite are from a biotite-hornblende-plagioclase porphyry intrusion, an andesite flow and the third is either another andesite flow or, possibly, a late stage sill (Villeneuve and MacIntyre 1997). Thus, although only three samples were analyzed, the suite is fairly well represented and further analyses are not expected to substantially expand the compositional range determined here. All samples are classified as calc-alkaline on the AFM classification diagram (Figure 3-7) and a FeO*/MgO versus SiO_2 plot (not shown, Miyarshiro 1974). The samples are mildly alkaline to subalkaline as shown in the total alkalies versus SiO_2 classification (Irvine and Barager 1971; Figure 3-6). The Babine Igneous Suite and the few mafic samples from the Ootsa Lake Group fall within the ranges of arc andesite compositions given by Condie (1989), with high Al_2O_3 (>16%), low Fe_2O_3 (5-9%) and low TiO_2 (<1%). The K_2O versus SiO_2 (wt %) plot shows most samples plot as high K (Figure 3-8). One sample, the most southeasterly, plots in the medium K dacite-rhyolite field. Most other elements plotted relative to silica decrease with increasing silica content (Figure 3-9), with the exceptions of K_2O and Rb which increase (Figures 3-9g and k). Na_2O remains relatively consistent with changing SiO_2 content, while Al_2O_3 increases slightly from 55 % to 67% SiO_2 before decreasing (Figure 3-9a and e). Ba, Sr and Zr show considerable scatter in concentration relative to silica (Figure 3-9i, j and l). Ba and Sr are generally high, 1050 to 2550 ppm and 150 to 1450 ppm, respectively while the high silica rhyolite samples, with SiO_2 >75 wt %, have significantly lower concentrations of <270 and <40 ppm, respectively. Both Cr and Ni are generally below detection limits, however are as high as 180 and 86 ppm, respectively, in the most mafic sample. These low Cr and Ni values are typical of high-K andesites (Condie 1989).

The chondrite normalized rare earth element (REE) plot shows enrichment of the light rare earth elements (LREE) relative to the heavy rare earth elements (HREE) (Figure 3-10). This gradual increasing enrichment in the REE from Yb to Ce is typical of calc-alkaline rocks from continental margin arcs (Condie 1989). A weak slightly negative Eu anomaly becomes pronounced in the high silica rocks (Figure 3-10c). The mixed trace element plot normalized to primitive mantle (PM) shows the enrichment of large-ion lithophile elements (LILE) (K, Rb, Cs, Sr and Ba) in addition to the LREE relative to the HREE and high field strength elements (HFSE) (Ti, Zr, Hf, Nb and Ta) (Figure 3-11). Negative Nb, Ti and positive Pb anomalies are noticeable in all samples. A weak positive Ba anomaly in the intermediate samples becomes a pronounced negative anomaly in the high silica rhyolites (Figure 3-11c). The high silica rhyolites also show strong negative Sr and P anomalies. The element variation patterns observed on the mid-ocean ridge basalt (MORB) normalized diagrams in Figure 3-12 are typical of active continental margin related potassic calc-alkaline volcanics, like those in central northern Chile (Pearce 1983). These plots show a depletion in Ta and Nb relative to the adjacent LILE, which is characteristic of arc related rocks (Condie 1989). The tectonic discrimination diagram of Wood (1980) shows that most of the Ootsa Lake Group and Babine Igneous Suite samples plot in or adjacent to the subduction-related volcanic field (Figure 3-13).

There are no clear spatial trends in the geochemistry of these samples as have been identified in some arc related systems (e.g. Ewing 1981a). Plots of K_2O (%) versus distance, along an east-west transect of approximately 140 km, show no consistent trend as has been demonstrated within the Kamloops Group (Ewing 1981a). Overall the silica variation diagrams show clear coherent trends, suggesting these rocks may share a common magmatic origin. The Babine Igneous Suite, while showing a lower overall level of rare earth element enrichment as compared to the mafic Ootsa Lake Group volcanics (Figure 3-10a), fall within the range defined by the Ootsa Lake Group volcanics. Subtle chemical differences between samples do appear in the trace element patterns. For example, dacitic samples show variable enrichment of Hf and Zr relative to MORB (Figure 3-12a) as well as Y and Yb (Figure 3-12b). Endako Group samples also have distinct trace element characteristics which are site dependent (Anderson 1998).

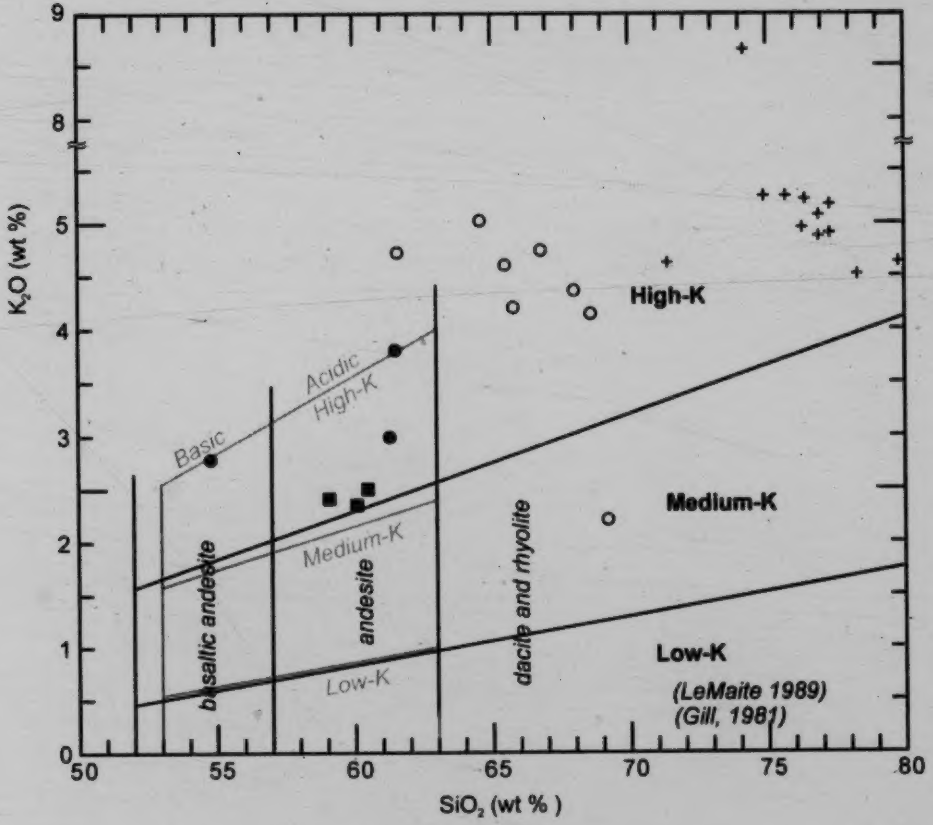

Figure 3-8. K_2O versus SiO_2 (wt %) with potassic classification schemes for the Ootsa Lake Group volcanics and Babine Igneous suite.

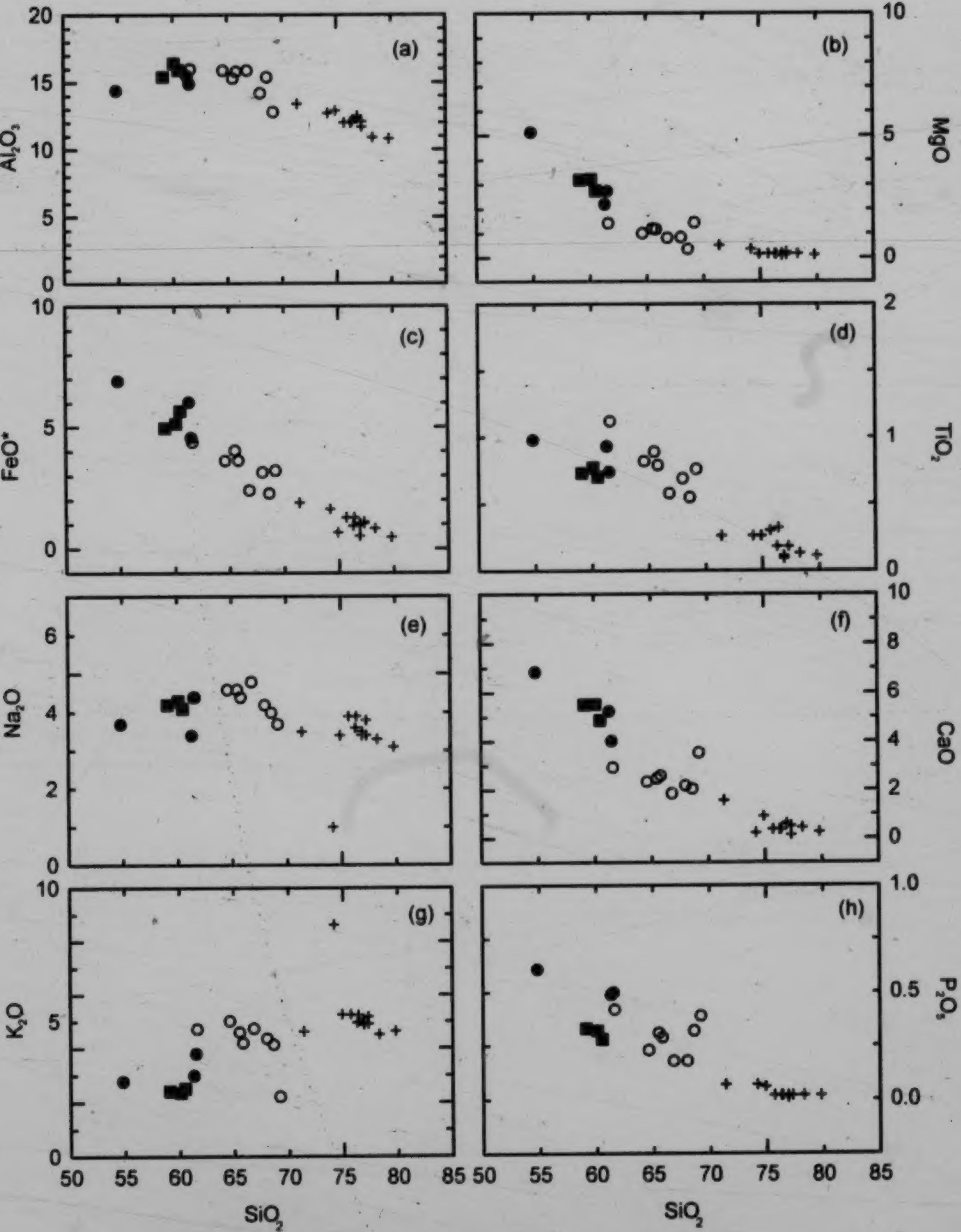

Figure 3-9. Harker diagrams for Ootsa Lake Group volcanics and Babine Igneous Suite. (symbols as defined in Figure 6).

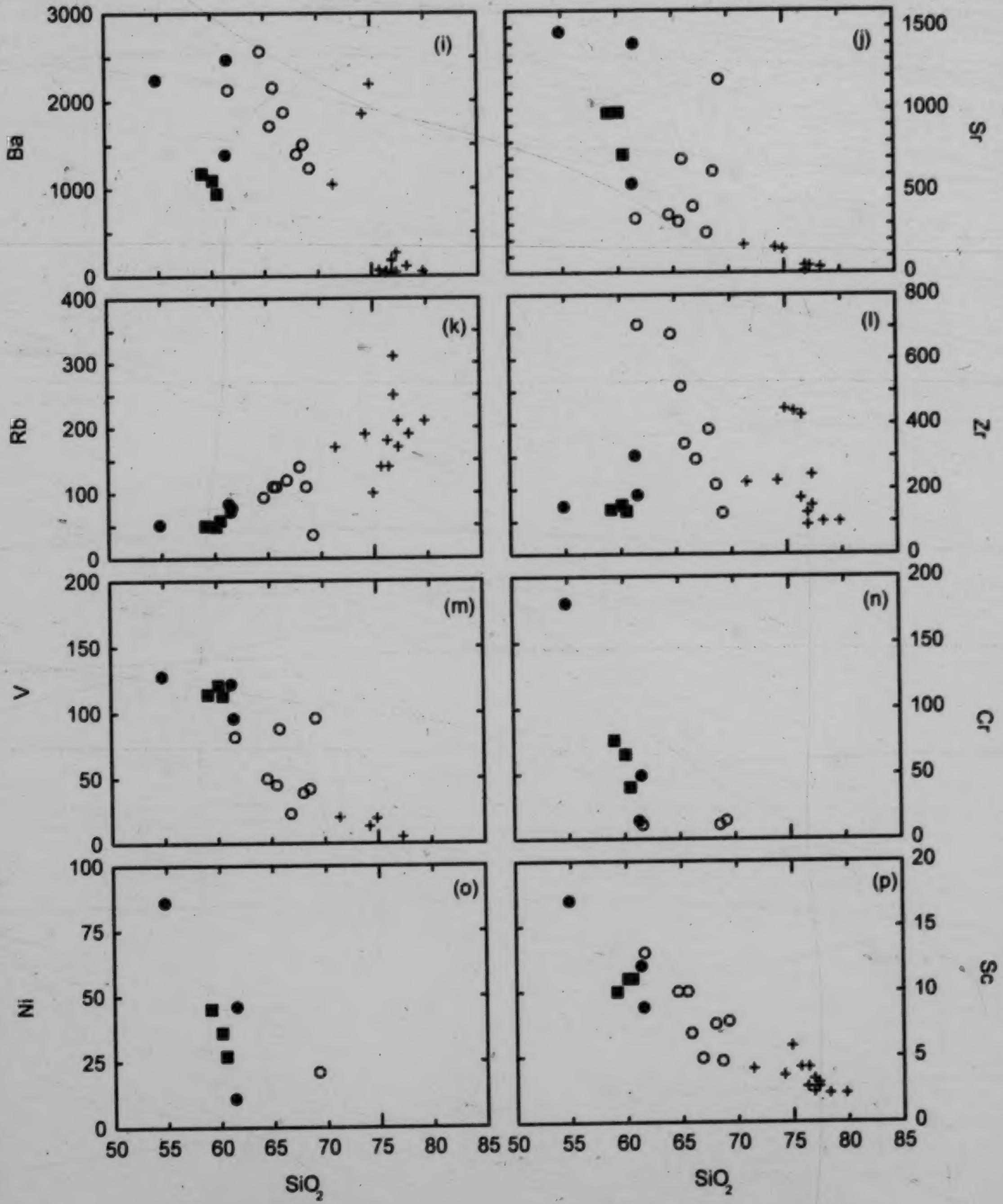

Figure 3-9. Harker diagrams for Ootsa Lake Group volcanics and Babine Igneous Suite.

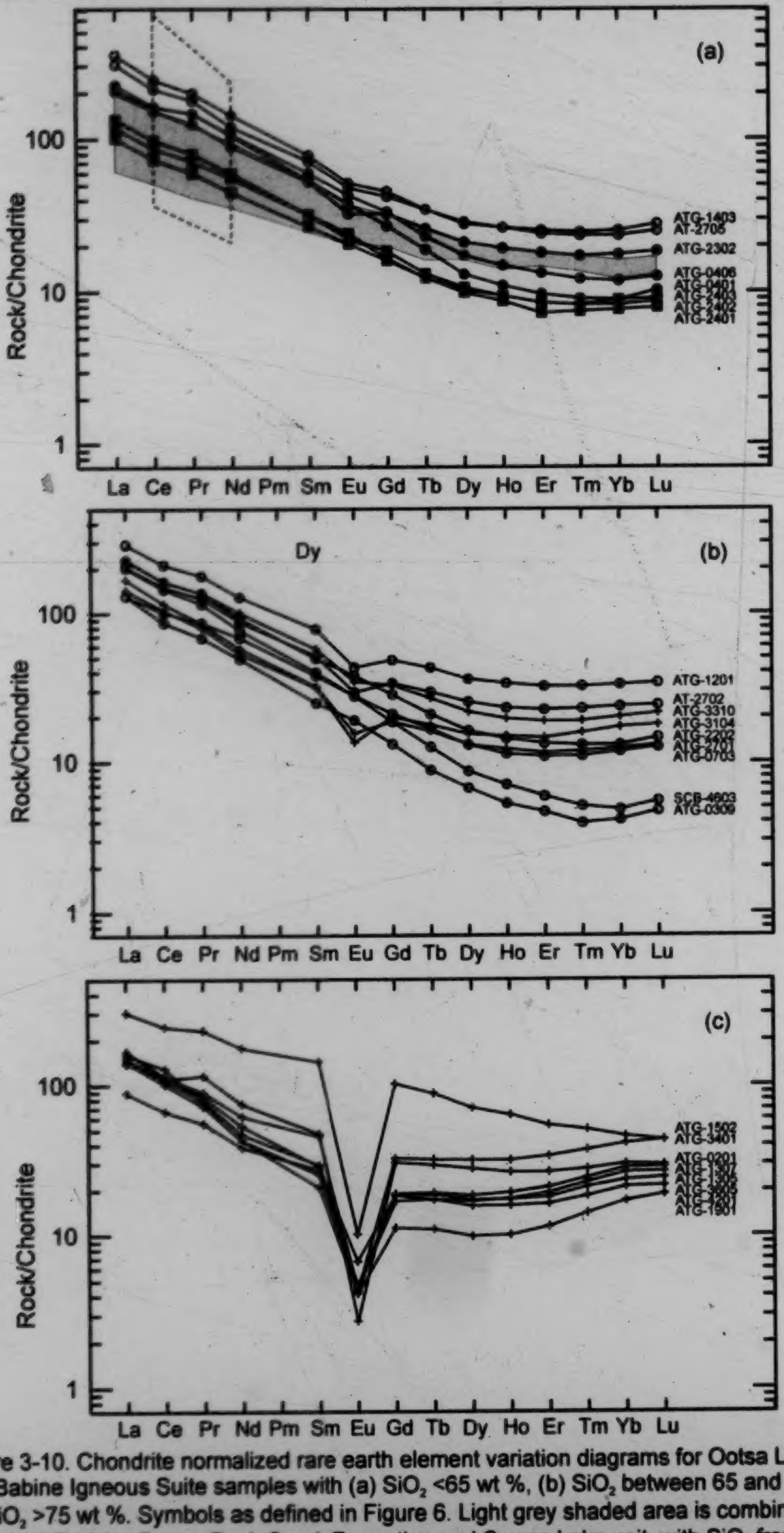

Figure 3-10. Chondrite normalized rare earth element variation diagrams for Ootsa Lake Group and Babine Igneous Suite samples with (a) SiO_2 <65 wt %, (b) SiO_2 between 65 and 75 wt % and (c) SiO_2 >75 wt %. Symbols as defined in Figure 6. Light grey shaded area is combined range of published Endako Group, Buck Creek Formation and Swans Lake unit with SiO_2 from 48 to 61 wt % (Dostal et al. 1998; Anderson 1998). Outlined area is Kamloops Group volcanics with SiO_2 from 47 to 64 wt % (Ewing 1981a). (Normalization values from Sun and McDonough, 1989)

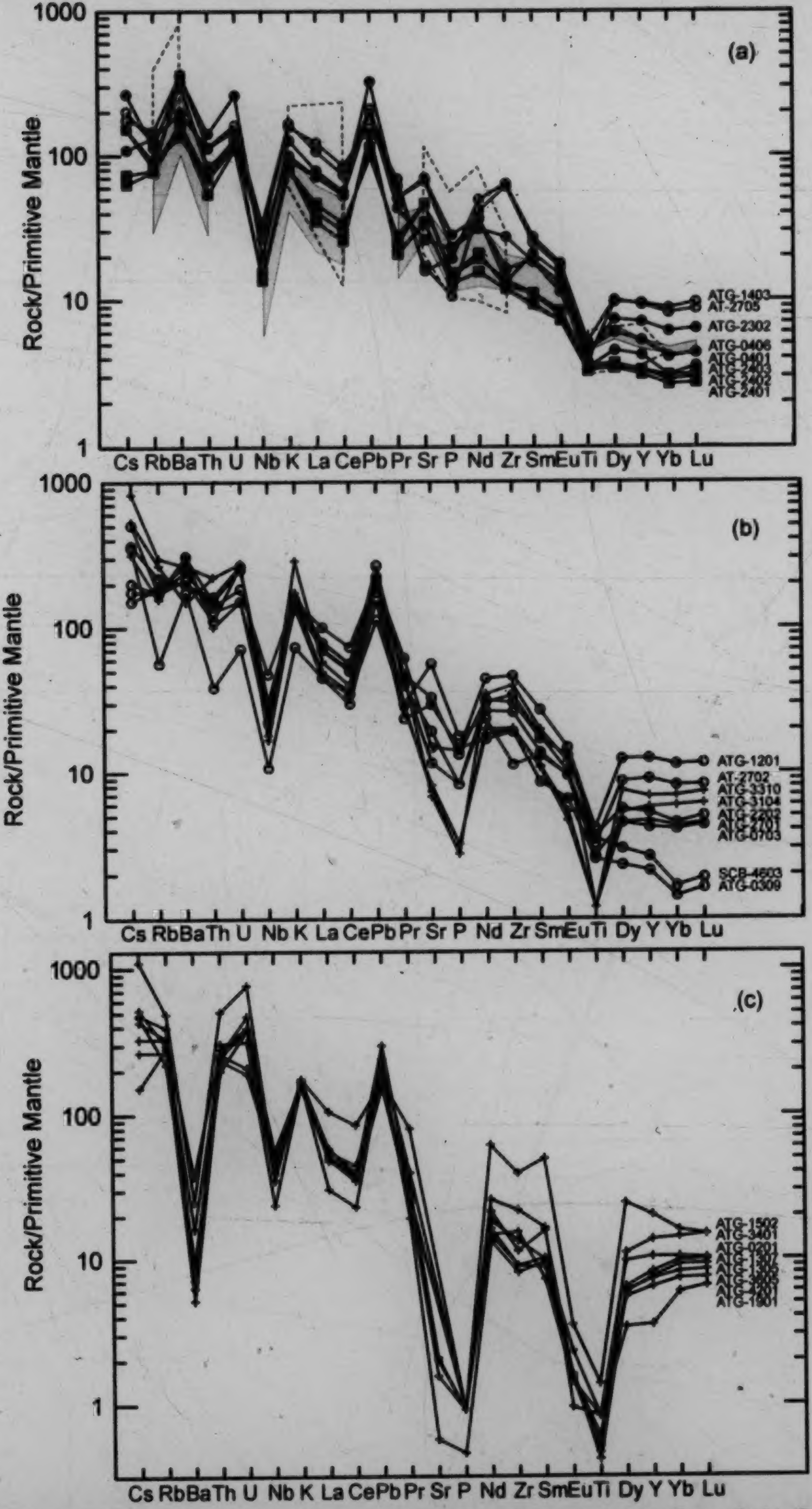

Figure 3-11. Primitive mantle normalized element variation diagrams for the Ootsa Lake Group and Babine Igneous Suite with (a) SiO_2 <65 wt %, (b) SiO_2 between 65 and 75 wt % and (c) SiO_2 >75 wt %. Symbols as defined in Figure 6. Light grey shaded area is range of published Endako Group samples with SiO_2 from 50 to 61 wt % (Anderson 1998). Outlined area from the Kamloops Group volcanics with SiO_2 from 47 to 64 wt % (Ewing 1981a). (Normalization values from Sun and McDonough 1989)

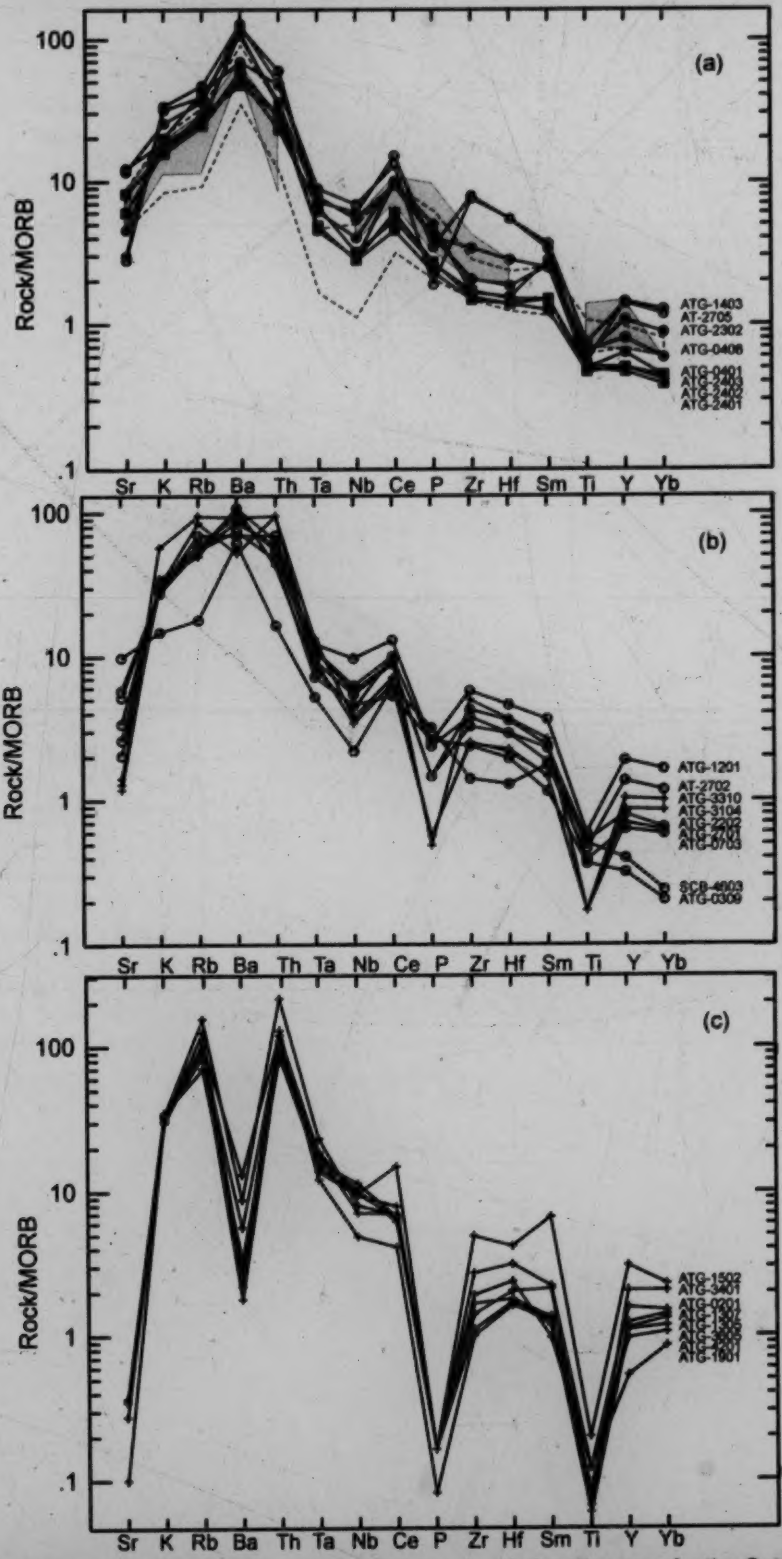

Figure 3-12. Mid-ocean ridge basalt normalized element variation diagrams for the Ootsa Lake Group and Babine Igneous Suite with (a) SiO_2 <65 wt %, (b) SiO_2 between 65 and 75 wt % and (c) SiO_2 >75 wt %. Symbols as defined in Figure 6. Light grey shaded area is range of Buck Creek Formation and Swans Lake unit with SiO_2 from 48 to 58 wt % (Dostal et al. 1998). Outlined area is range of Endako Group with SiO_2 from 50 to 61 wt % (Anderson 1998). (Normalization values from Pearce 1983)

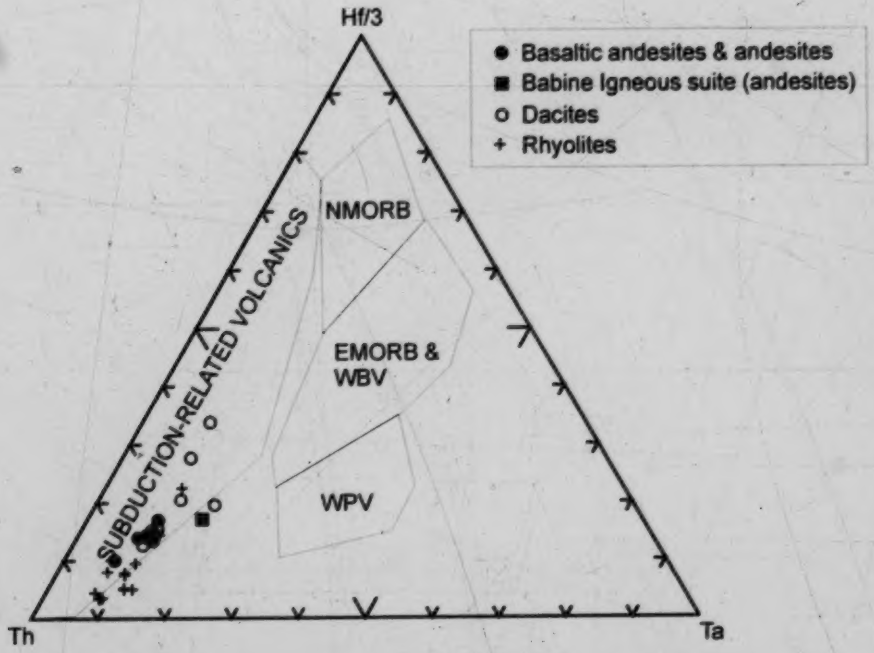

Figure 3-13. Hf/3-Ta-Th tectonic discrimination diagram for the Ootsa Lake Group and Babine Igneous Suite (Wood 1980).

Compared to published geochemical results from correlative rocks, the Ootsa Lake Group volcanics are substantially more felsic. Samples from the Buck Creek formation and Swans Lake unit range from 50 to 67 wt % SiO_2 (n=48; Dostal et al. 1998) and the Ootsa Lake Group from the Whitesail map area ranges from 51 to 69 wt % SiO_2 (n=37; Drobe 1991) as compared to 55 to 80 wt % determined here. This may be in part the result of sampling bias, i.e. that felsic samples were preferentially sampled due to their similarity with known Ootsa Lake Group volcanics. However, in general, felsic rocks are dominant within the Fort Fraser and Nechako map areas and may not be in areas to the west. Comparing only the more mafic samples, the results of these two studies follow similar elemental trends in the major and trace elements to those determined here. The PM and MORB normalized plots show a slightly greater enrichment in the LREE and particularly the LILE in the samples reported here. The results from analyses of Endako Group samples (n=19; Anderson 1998) closely agree with the results of Dostal et al. (1998) for the Buck Creek Formation and Swans Lake volcanics.

Published analyses from the Kamloops Group in south central British Columbia are chemically similar to the Ootsa Lake Group (n=73; Ewing 1981a; n=52; Smith 1986). The Kamloops Group, as defined by Ewing (1981a), is a calc-alkaline suite containing high K basalt to rhyolite, with high Sr and Ba, low Zr, Ti and Ni concentrations and no Fe enrichment. Analyses by Smith (1986) identified more samples of andesitic composition, as compared to the more dominant basaltic or basaltic andesitic composition determined by Ewing (1981a). Samples analyzed by Smith (1986) were in general less potassic than the results of Ewing (1981a). Given that both of these studies sampled from the same general area, Smith (1986) attributed these differences to sampling bias.

U-Pb Geochronology

Analytical Methods

Four samples were prepared at the University of Alberta Radiogenic Isotope Facility by standard crushing (jaw crusher and disk mill) and mineral separation techniques (Wilfley table, heavy liquids, Frantz Isodynamic magnetic seperator). Zircons generally free of fractures, inclusions and turbidity were handpicked from different magnetic and morphological groups for multi-grain fraction analysis. Certain fractions, indicated in Table 3-1, were air abraded prior to cleaning using the technique of Krogh (1982). The samples were cleaned (Heaman and Machado 1992) prior to being weighed and spiked with a mixed ^{205}Pb-^{235}U spike. U and Pb were purified from dissolved samples by anion exchange chromatography on micro-columns using a method modified from Krogh (1973).

U and Pb were loaded together onto single outgassed Re filaments using H_3PO_4 and silica gel. Isotopic compositions of U and Pb were determined using two thermal ionization mass spectrometers, a Micromass Sector 54 and VG 354. Both mass spectrometers were operated in single-collector mode using either a Faraday cup or Daly photomultiplier detector. All data obtained using the Daly collector (most ratios) were corrected by a factor of 0.13%/amu and 0.15%/amu (VG 354) and 0.056%/amu and 0.024%/amu (Sector 54) for Pb and U, respectively. All isotopic ratios were corrected for mass discrimination based on repeated analyses of the NIST SRM981 Pb and U500 standards. Mass discrimination corrections of 0.09%/amu and 0.16%/amu (VG354) and 0.15%/amu and 0.14%/amu (Sector 54) were applied to Pb and U, respectively. Procedural blanks for U and Pb during this study were measured as 5 ± 20% pg and 6 ± 50% pg. Decay constants used were $\lambda(^{238}U) = 1.55125 \times 10^{-10}$/yr and $\lambda(^{235}U) = 9.8485 \times 10^{-10}$/yr and an atomic ratio of $^{238}U/^{235}U=137.88$ as recommended by Steiger and Jäger (1977) (Jaffey et al. 1971; Cowan and Adler 1976). The composition of initial Pb was calculated using the Stacey and Kramers (1975) growth curve. All data listed in Table 3-1 were calculated using in-house software. Errors were calculated by propagating all known sources of uncertainty. All results are reported with errors at the 2 σ

Table 3-1. Analytical results from U-Pb zircon analyses

Fr.	Description [1]	Weight (µg)	(ppm) U	Pb	Th [2]	Th/U	Common Pb (pg) [3]	Atomic Ratios [4] ^{206}Pb/^{238}U	^{207}Pb/^{235}U	^{207}Pb/^{206}Pb	Apparent Age ± 2 σ Error (Ma) ^{206}Pb/^{238}U	^{207}Pb/^{235}U	^{207}Pb/^{206}Pb	% Dis.
Twenty-six Mile Lake granite pluton													*ATSS-98-0406*	
1	205 eu;e;M@1.85A	47	1623	15	1448	0.89	40	0.00741	0.04807	0.04707	47.57 ± 0.4	47.67 ± 0.6	52.66 ± 11.8	9.69
2	143 eu;e;M@1.85A	152	1069	10	1153	1.08	136	0.00741	0.04782	0.04681	47.59 ± 0.8	47.43 ± 0.8	39.44 ± 15.6	-20.75
3	154 eu;e;NM@1.85A	79	809	7	604	0.75	26	0.00732	0.04781	0.04737	47.02 ± 0.4	47.42 ± 0.4	67.69 ± 11.2	30.65
Binta Lake flow laminated rhyolite													*ATG-98-0201*	
1	200 eu;e;M@1.4A	39	460	4	354	0.77	20	0.00763	0.04959	0.04713	49.02 ± 0.2	49.15 ± 0.8	55.62 ± 34.0	11.91
2	173 su;lp;M@1.4A	123	10411	67	6671	0.64	108	0.00573	0.03722	0.04714	36.81 ± 5.0	37.11 ± 4.8	56.08 ± 3.6	34.46
3	186 eu;e;NM@1.4A	58	338	3	263	0.78	13	0.00754	0.04893	0.04708	48.42 ± 0.2	48.51 ± 0.6	53.14 ± 29.0	8.92
4	222 eu;e;NM@1.4A	70	389	3	288	0.74	14	0.00754	0.04908	0.04722	48.42 ± 0.2	48.65 ± 0.6	60.12 ± 21.2	19.53
5	90 su;lp;NM@1.4A	51	6892	55	3780	0.55	78	0.00735	0.04766	0.04706	47.18 ± 1.6	47.28 ± 1.6	52.47 ± 5.2	10.12
Flow laminated rhyolite													*SCBG-97-0101*	
1	181 eu;e;M@5°	104	742	7	348	0.47	23	0.00760	0.05026	0.04797	48.80 ± 0.4	49.79 ± 0.6	97.95 ± 9.2	50.37
2	138 eu;e;M@1°	85	554	5	470	0.85	13	0.00771	0.05032	0.04734	49.50 ± 0.4	49.85 ± 0.4	66.61 ± 12.4	25.78
3	178 eu;e;M@3°	154	572	6	506	0.88	35	0.00797	0.05200	0.04732	51.17 ± 0.6	51.47 ± 0.6	65.48 ± 9.0	21.94
4	163 su;lp;M@5°	145	616	6	594	0.96	56	0.00787	0.05110	0.04709	50.54 ± 0.6	50.60 ± 0.6	53.60 ± 12.0	5.74
5	198 eu;e;M@1°	126	477	5	417	0.87	36	0.00788	0.05133	0.04723	50.61 ± 0.4	50.82 ± 0.6	61.05 ± 13.0	17.18
Dayeezcha Mtn Bi-plag dacitic ignimbrite													*ATG-98-1403*	
1	239 su;af+lp;M@2°	229	83	1	64	0.78	26	0.00777	0.05063	0.04724	49.91 ± 0.4	50.15 ± 0.8	61.45 ± 34.8	18.85
2	58 su;sp;r;M@2°	410	64	1	57	0.88	35	0.00765	0.04963	0.04705	49.14 ± 0.4	49.19 ± 0.6	51.43 ± 27.2	4.46
3	49 su;sp;r;NM@2°	299	129	1	102	0.79	18	0.00741	0.04801	0.04702	47.56 ± 0.4	47.56 ± 0.4	50.10 ± 16.2	5.08
4	1 su;e;r;NM@2°; ABR	10	90	1	74	0.52	9	0.00951	0.06275	0.04783	61.05 ± 0.6	61.79 ± 12.8	90.90 ± 200	33.00
5	48 su;sp;r;NM@2°	18	60	1	49	0.82	11	0.00750	0.04867	0.04708	48.15 ± 0.2	48.25 ± 1.2	53.42 ± 52.8	9.90

[1] eu=euhedral, su=subhedral, e=equant, sp=prisms (L:W≧2:1), lp=prisms (L:W≥3:1), af=angular fragments, r=resorbed, M=magnetic separate (all side tilt angles at 1.85A, unless otherwise specified), NM=non magnetic, all samples are -70 mesh and colourless or pink (p), ABR= air abrasion treatment

[2] model concentration calculated based on ^{208}Pb and ^{207}Pb/^{206}Pb age

[3] initial + blank Pb

[4] atomic ratios corrected for blank (Pb= 6 pg ± 50% and U= 5 pg ± 20%) and initial common Pb

level (95% confidence interval). Ages determined by either a weighted means or linear regression approach were calculated using Isoplot (Ludwig 1998).

Sample Descriptions and Results

U-Pb zircon analytical results for four samples are shown in Table 3-1 and the data are displayed on concordia diagrams in Figures 3-14(a-d). Linear regression lines (discordia) were calculated for all of these samples using Isoplot (Ludwig 1998). The intercepts are generally poorly constrained for most samples due to the tight clustering of analyses. As a result, the weighted mean Pb/U ages provide a more precise estimate of the sample age. The weighted mean $^{206}Pb/^{238}U$ age is taken as the best age estimate, as this ratio is less sensitive to corrections for common lead and lead loss than the $^{207}Pb/^{235}U$ ratio.

'Island' Lake pluton 93F/14 (ATSS-98-0406)

This pluton is one of several small, high-level, felsic plutons distributed sporadically throughout the northern Nechako River map sheet. This sample was collected from the informally named 'Island' Lake locality and is a miarolitic, fine grained, equigranular biotite granite. This locality and the Twenty-six Mile Lake pluton (93 F/15) are described in Sellwood et al. (1999). Similar and other presumed Eocene intrusions from the Uncha Mountain area (93 F/13) are described in Barnes and Anderson (1999). North-northeasterly faults within the Uncha Mountain area are interpreted as facilitating the emplacement of intrusions similar to this one (Barnes and Anderson 1998). Thus the crystallization age of this pluton should provide an estimate of the timing of Eocene extensional motion along these north-northeasterly faults. Zircons separated from this sample were beautiful clear, euhedral, approximately equant prisms. Most of the zircons were small, approximately 40 microns in length, with a subordinate population of larger zircons. There was also a minor population of pale pink, opaque, tetragonal dipyramidal zircons. Three multi-grain fractions of small equant zircons were analyzed and the weighted mean $^{206}Pb/^{238}U$ and $^{207}Pb/^{235}U$ ages agree well within error (Figure 3-14a). A concordia regression gives an upper intercept of 47.6 +0.9/-0.4 Ma which is in excellent agreement with the Pb/U ages, however, it is poorly constrained (no lower intercept could be calculated) due to the tight cluster of results. The weighted mean $^{206}Pb/^{238}U$ age of 47.3 ± 0.8 Ma is interpreted as the crystallization age of this pluton.

Flow laminated rhyolite, Mount Lorenz area 93K/7 (SCBG-97-0101)

This variegated pale yellow and purple biotite-quartz-plagioclase flow laminated rhyolite locally underlies pale purple, biotite-plagioclase rhyolite flows, tuff and crystal tuff. It is overlain by basaltic andesite breccia of the Endako Group. The local geology is described in Struik et al. (1997). The predominant zircon morphology from this sample is small, clear, equant and euhedral grains with a subordinate population of subhedral, clear needles. Five fractions, mostly from the equant population, were analyzed from this sample. The weighted mean $^{206}Pb/^{238}U$ and $^{207}Pb/^{235}U$ ages agree within error for all five fractions, however, the two most discordant fractions were excluded from the final calculated ages (Figure 3-14b). The discordant results are interpreted to be a result of lead loss. A regression calculation gives an upper intercept of 52 Ma, but is poorly constrained due to the cluster of analyses. The weighted mean $^{206}Pb/^{238}U$ age of 50.7 ± 0.8 Ma is taken as the crystallization age of this sample.

Dayeezcha Mountain biotite-plagioclase dacitic ignimbrite 93F/13 (ATG-98-1403)

Dayeezcha Mountain is a distinctive landmark, rising to an elevation of 1170m. The mountain itself is composed entirely of a glassy, hornblende-biotite-plagioclase dacitic crystal ignimbrite containing partly welded flow laminated and tuffaceous rhyolite clasts (Figure 3-5B). The mountain is surrounded by rhyolite and dacite flows, welded ignimbrites ash, lapillistone, rhyolitic tuff and crystal tuff. The geology of the Dayeezcha Mountain area is described in further detail by Grainger and Anderson (1999). Clasts from this sample were carefully removed during crushing to prevent contribution of zircons from these, possible older, fragments. Zircons from this sample are clear to faint tan in colour, generally slightly to

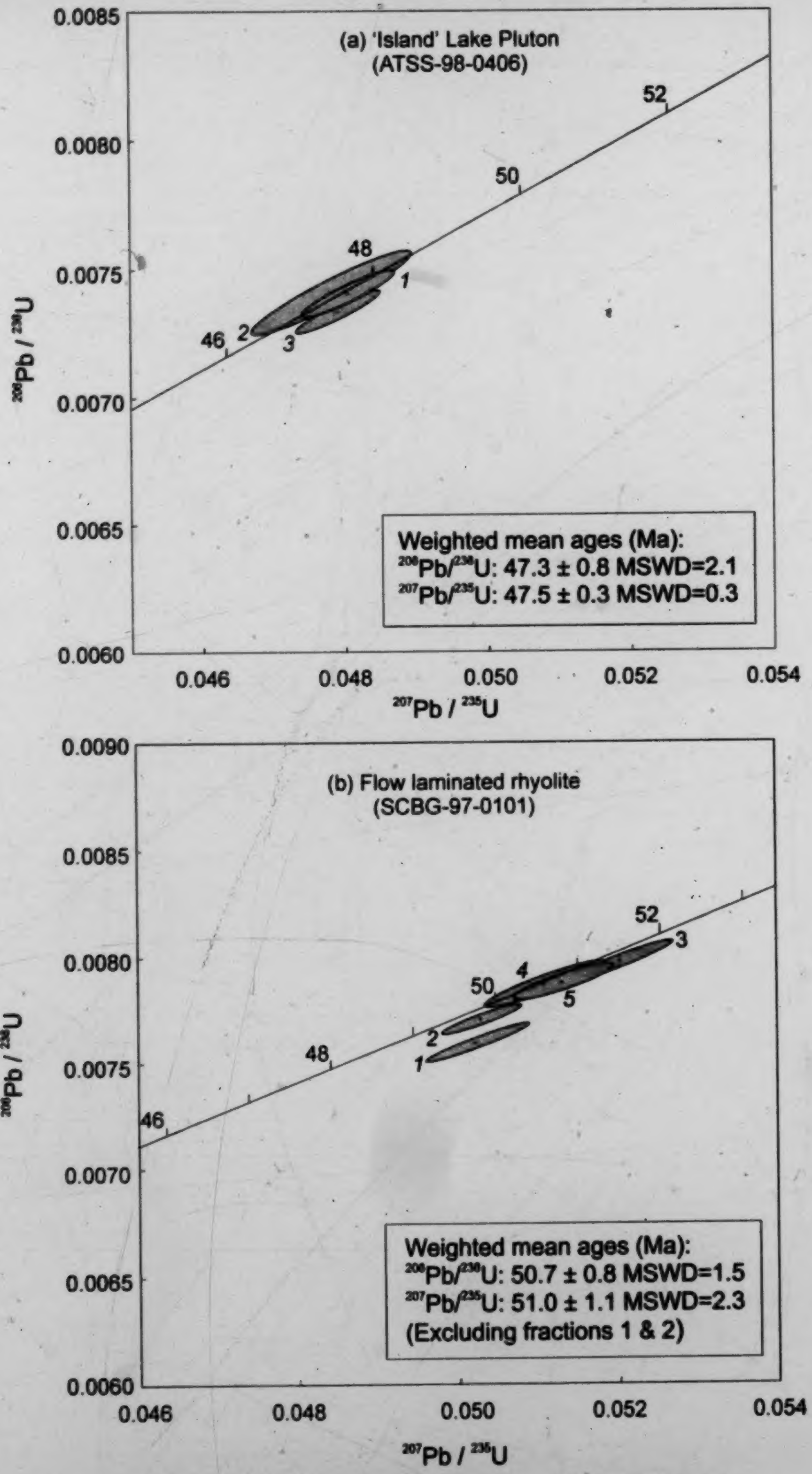

Figure 3-14. Concordia diagrams for the (a) 'Island' Lake granite pluton (ATSS-98-0406) and (b) Flow laminated rhyolite (SCGB-97-0101).

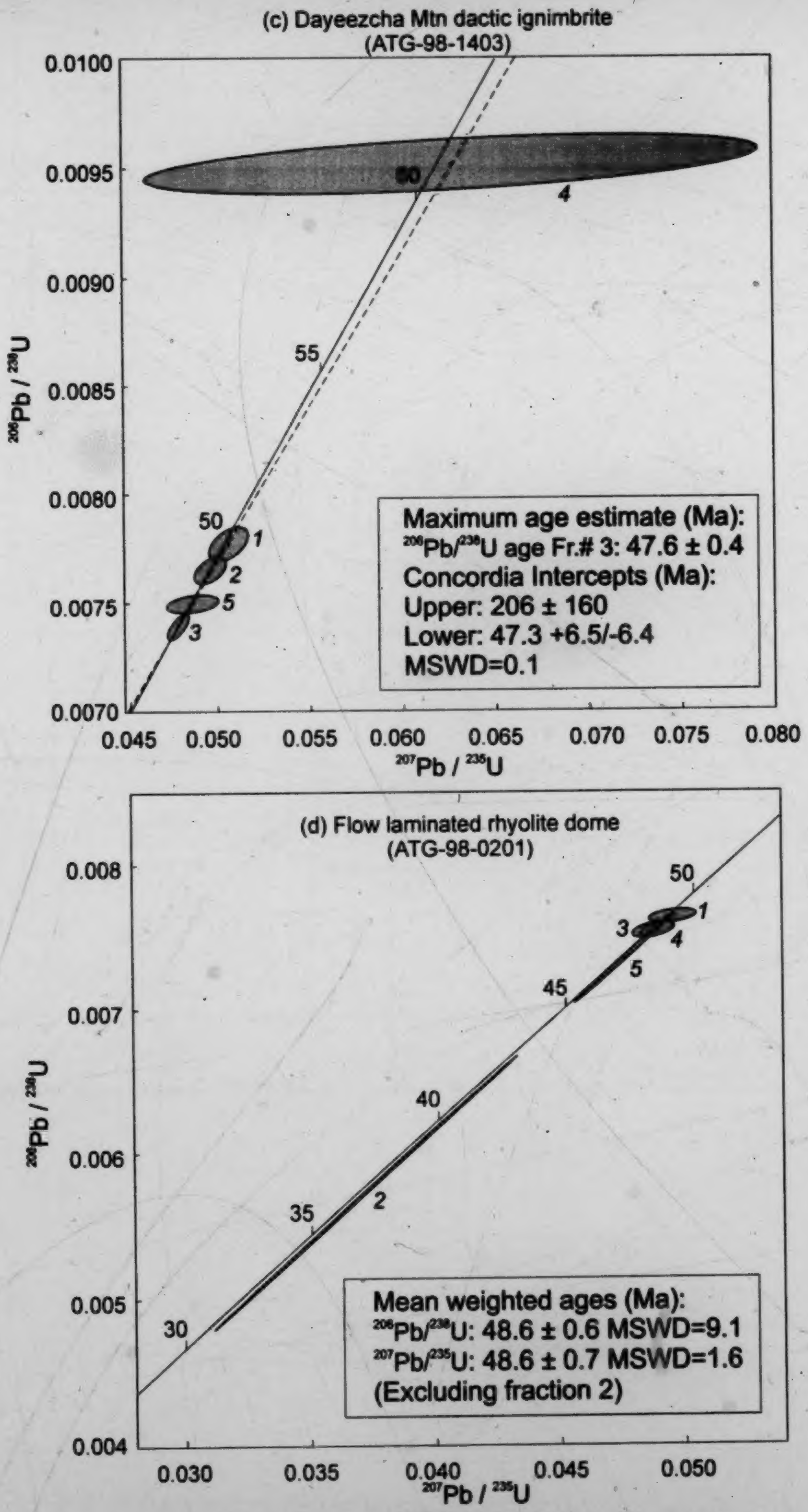

Figure 3-14. Concordia diagrams for the (c) Dayeezcha mountain dacitic ignimbrite (ATG-98-1403) and Flow laminated rhyolite dome (ATG-98-

moderately resorbed and vary in proportion from needles to approximately equant prisms. Five fractions were analyzed from this sample (Figure 3-14c). Scatter in the data was interpreted as indicating the presence of inheritance and confirmed by the analysis of a single air abraded resorbed zircon (fraction 4), which is significantly older than the other analyses. The upper intercept on a linear regression is loosely constrained, but suggests the inheritance is of Early Jurassic age. The lower intercept is also poorly constrained giving a crystallization age of 47.3 +6.5/-6.4 Ma. The $^{206}Pb/^{238}U$ age from the third fraction provides a maximum age estimate for this sample of 47.6 ± 0.4 Ma. Assuming that no inherited zircons are included in this fraction, this analysis would represent the true crystallization age of this sample and thus is taken as the best age estimate for this sample.

Binta Lake flow laminated rhyolite dome 93F/14 (ATG-98-0201)
This pink and white flow laminated rhyolite dome with associated rhyolite breccia is one of a series of domes that surround felsic to intermediate flows, pyroclastic breccias and tuffs around Dayeezcha Mountain from the northwest to east. The rhyolite domes are interpreted as comagmatic with the volcanics in the Dayeezcha mountain area and may have been emplaced late in the development of the volcanic complex. Zircons separated from this sample were predominantly clear, small, euhedral and approximately equant grains. A minor population of subhedral, clear needles was also present. Five fractions were analyzed from this sample (Figure 3-14d). The second fraction is quite discordant and has a significant error, thus is excluded from the age calculations. Both Pb/U ages agree within error and the weighted mean $^{206}Pb/^{238}U$ age is taken as the crystallization age of the sample at 48.6 ± 0.6 Ma.

$^{40}Ar/^{39}Ar$ Geochronology

Analytical Methods

Seven samples were selected for laser $^{40}Ar/^{39}Ar$ dating. Samples were prepared by crushing and sieving to 150-350 μm. Biotite was selected for analysis in samples containing fresh grains, otherwise whole rock fragments were used. Biotite is preferred for analysis, because whole rock material is more likely to contain minerals susceptible to alteration and may have a lower potassium content. Fine grained and homogeneous fragments were selected for whole rock analysis. Euhedral biotite grains containing few inclusions and no evidence of alteration were selected for mineral analysis. Most samples were prepared at the University of Alberta. Samples were loaded and analyzed at the Geological Survey of Canada laboratories in Ottawa. Each fraction was loaded into a separate aluminum foil packet and arranged inside an aluminum can. The age calculation for the $^{40}Ar/^{39}Ar$ dating method includes a parameter called the J value. The J value is, in part, a function of the neutron flux density and capture cross sections. These two variables are difficult to determine empirically, however, it is possible to determine the J value for a particular position by using a sample of known age, called a flux monitor (Faure 1986). Studies have found the Fish Canyon Tuff sanidine (FCT-SAN) to be suitably homogeneous for laser $^{40}Ar/^{39}Ar$ dating (Lanphere and Baadsgaard 1997; Renne et al. 1994). One FCT-SAN grain was loaded with each sample in the aluminum packets to act as a flux monitor. The samples were sent to the research reactor at McMaster University and irradiated for eight hours in an approximate fast neutron flux of 3×10^{16} neutrons/cm^2.

Upon return from the reactor, the foil packets were opened, the best grains selected and divided into aliquots of five whole rock fragments or 1 to 4 flakes of biotite. Each aliquot and the flux monitor from each sample were loaded into separate holes in a copper planchet for analysis. Each monitor was fused in one step and used to calculate the J value for that sample, based on the reported age of 28.03 ± 0.1 Ma for FCT-SAN (McDougall and Harrison 1988; Renne et al. 1994). J values were interpolated for samples that did not contain monitors. Each aliquot was step heated in 3 to 11 increments, from 0.1 to 2 % of the nominal laser power, using a Merchantek® MIR-10 10 W CO_2 laser. This laser is equipped with a

2mm x 2mm flat-field lens, which evenly heats the sample. Each heating step was two minutes in duration and typically corresponds to an increment of 50°C to 150°C. Analysis was conducted using a VG 3600 gas source mass spectrometer using either a Faraday cup or standard electron multiplier collector. The relative gain of the electron multiplier is approximately 50 and the sensitivity is typically 1.900X10^{-9} cm^3/V. Data collection protocols are described in Villeneuve and MacIntyre (1997). Decay constants and isotopic abundances used are $\lambda(^{40}K)=5.543$ x 10^{-10}/yr, ^{39}K=93.2581, ^{40}K=0.01167 and ^{41}K=6.7302 as recommended by Steiger and Jäger (1977) and determined by Beckinsale and Gale (1969) and Garner et al. (1976). Data reduction procedures are given in Roddick (1988). The error in the J-factor (± 0.5%, 1σ) is applied to the final age, however, the monitor age uncertainty is not. All results are reported with errors at the 2 σ level of uncertainty, unless otherwise stated.

Sample Descriptions and Results

The results for the seven samples analyzed are displayed in heating gas release plots, shown in Figures 3-15(a-g). A complete data summary is provided in Appendix IV. Each gas release plot shows all of the aliquots analyzed from one sample placed side-by-side. Different aliquots are distinguished by the shaded backgrounds. The horizontal scale has been normalized to the total volume of ^{39}Ar gas produced from analyses of a given sample (i.e. the combined amount of ^{39}Ar gas produced from all aliquots analyzed for one sample). This makes the relative quantity of gas released in different aliquots readily visible, but does not affect the gas release profile. For example, in Figure 3-15 (a) the second aliquot produced only slightly more ^{39}Ar gas than the first aliquot (52% vs 48%). Each heating step is indicated by one filled black rectangle (e.g. in Figure 3-15 (a) there are seven steps in aliquot one, six in aliquot two). The rectangle is vertically centered about the calculated step age and the height of the polygon corresponds to the magnitude of the error associated with that calculated age. The rectangle width is proportional to the quantity of ^{39}Ar gas released in that step. Thus in Fig 3-15 (a), the first step in aliquot one corresponds to a calculated step age of 48.7 ± 16.2 Ma from 2.3% of the total ^{39}Ar released (or 5% of the ^{39}Ar gas released in aliquot one). Step two of aliquot one illustrates a calculated age of 52.7 ± 0.3 Ma from 10.3% of the total ^{39}Ar released (or 21% of the gas released in aliquot one). These two examples clearly illustrate that steps which release greater volumes of gas will result in more precise calculated step ages. For most samples, each aliquot produced a good multistep plateau and the two aliquots are in excellent agreement. For these samples the combined plateau age is interpreted as the crystallization age of the sample.

Andesite, east of Babine Lake 93K/12 (ATG-98-0401)

This medium gray andesite contains sparse large plagioclase and partially resorbed quartz phenocrysts. This thin flow overlies a sequence of hornblende-biotite-feldspar phyric to aphyric rhyodacite ash flows and plagioclase phyric andesite. This sequence is overlain by vesicular basalts which are correlated with the Endako Group (MacIntyre et al. 1997). The andesite will provide an age for the upper portion of the volcanic sequence at the most northern exposure of Ootsa Lake Group rocks mapped. Two aliquots of five whole rock fragments each were analyzed and produced excellent multistep plateaux (Figure 3-15a). The combined plateau age of 52.0 ± 0.5 Ma is interpreted as the crystallization age of the andesite flow.

Rhyolite dyke, northwest of Augier Lake 93K/5 (ATG-98-4201)

This biotite-plagioclase-quartz rhyolite dyke cross cuts a black massive basalt with plagioclase microlites and minor pyroxene correlated with the Endako Group. This is one of very few localities which show a felsic rock associated with the Ootsa Lake Group cross cutting or overlying basaltic rocks associated with the generally younger Endako Group. This sample was selected for dating to determine the age of these late stage rhyolitic intrusions and their relation to the age of the Endako Group. Two biotite aliquots of four grains each were analyzed and both produced a good multistep plateau (Figure 3-15b). These ages are

Figure 3-15. Gas release spectra for samples analyzed. Separate aliquots for each sample are distinguished by different backgrounds. Line with arrows indicates steps included in plateau and used to calculate sample age. Material analyzed indicated as WR = whole rock or BIOT = biotite.

Andesite, Babine Lake (93 K/12) ATG-98-0401 WR

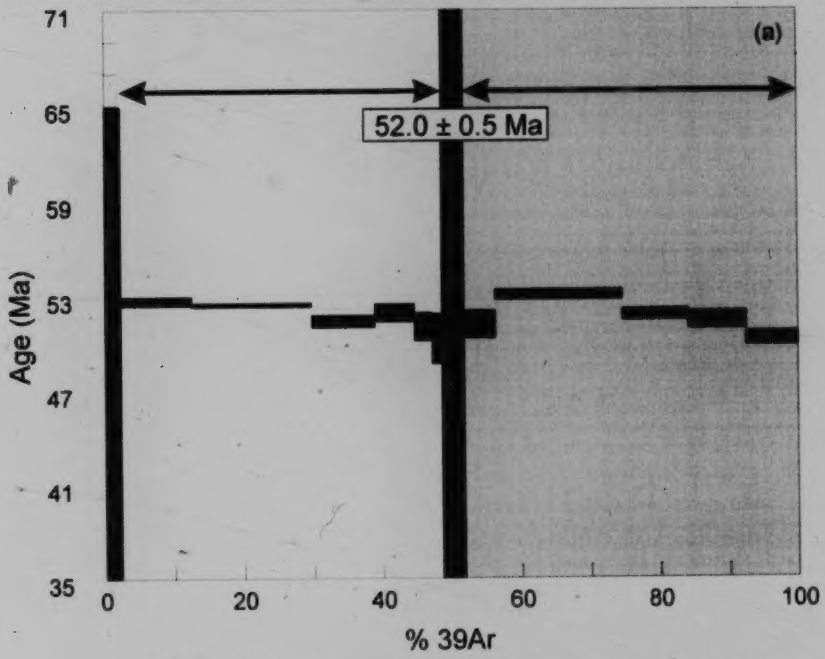

Rhyolite dyke, Augier Lake (93 K/5) ATG-98-4201 BIOT

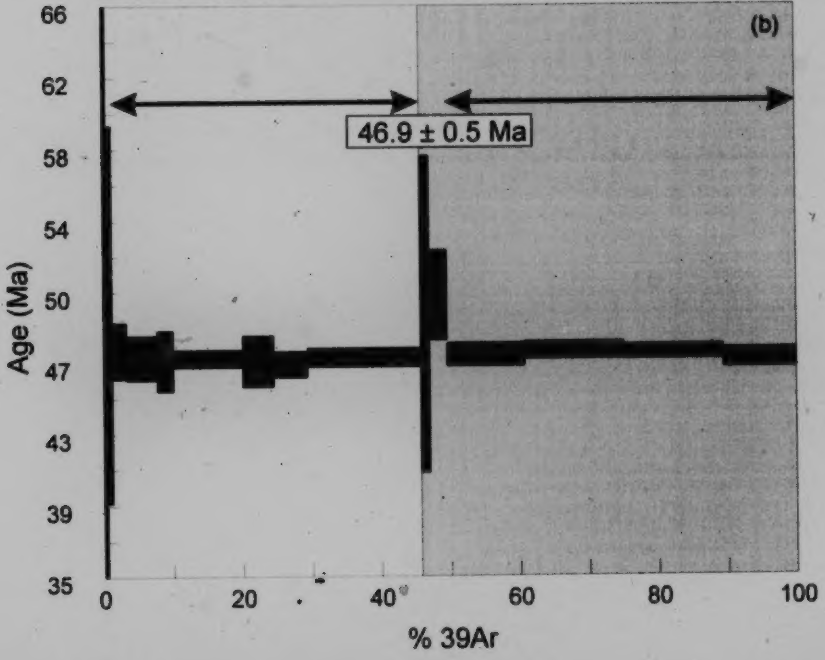

Banded biotite rhyolite, Burns Lake (93 K/4)
ATG-98-1305 BIOT

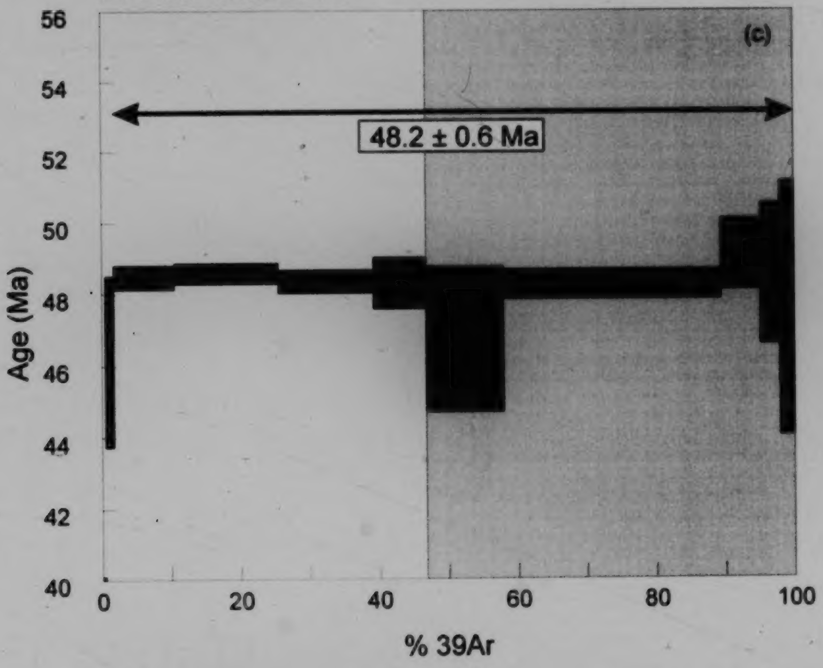

Biotite-plagioclase rhyolite,Tahultzu Lake (93 F/15)
ATG-98-0703 BIOT

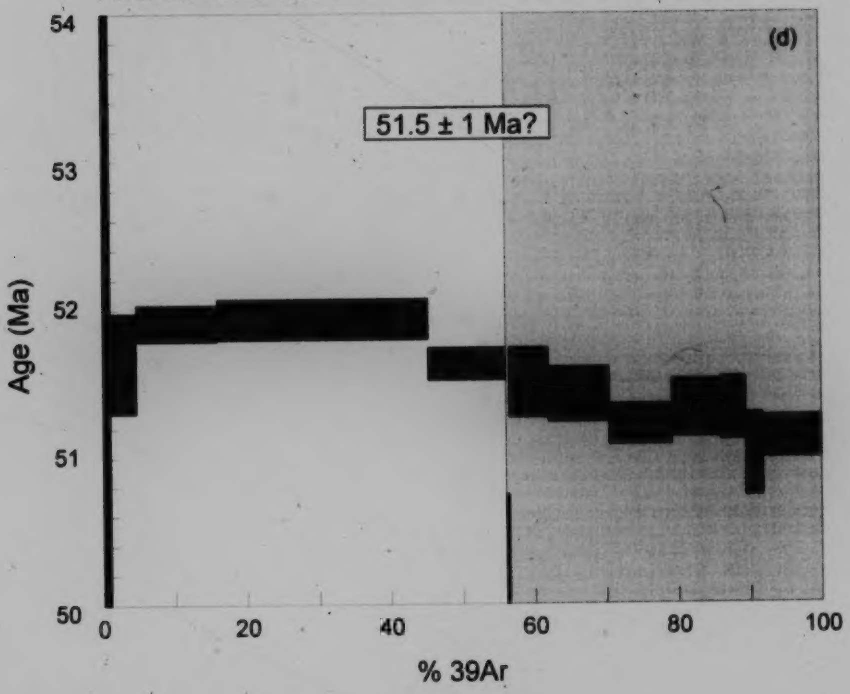

Andesite, Deerhorn FSR (93 F/11) ATG-98-2302 WR

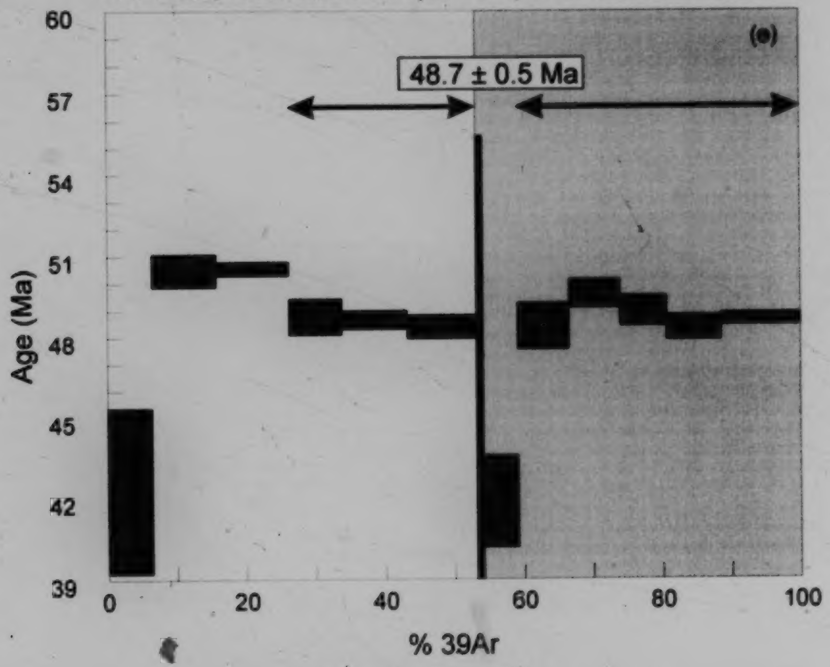

Biotite-quartz-plagioclase rhyolite ignimbrite, Henson Hills (93 F/12) ATG-98-3304 BIOT

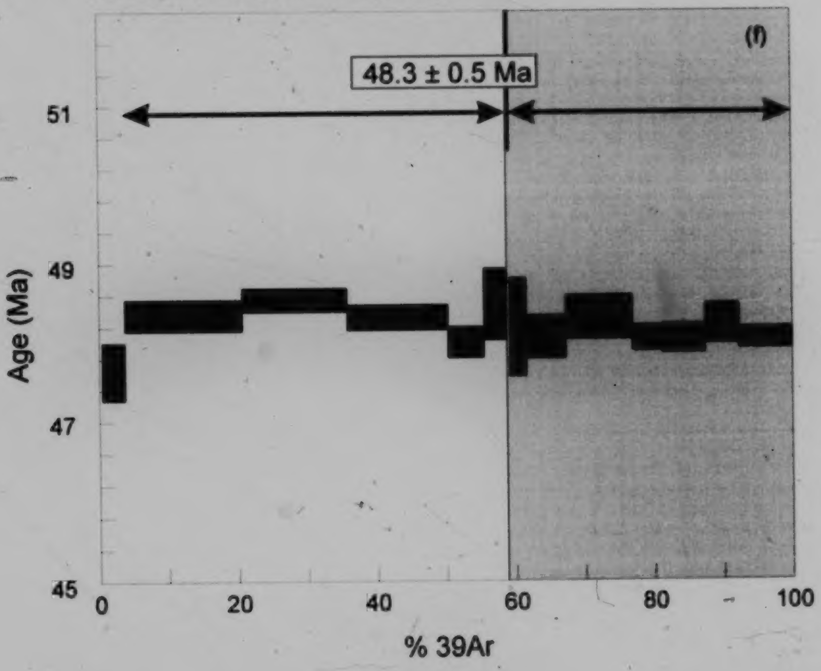

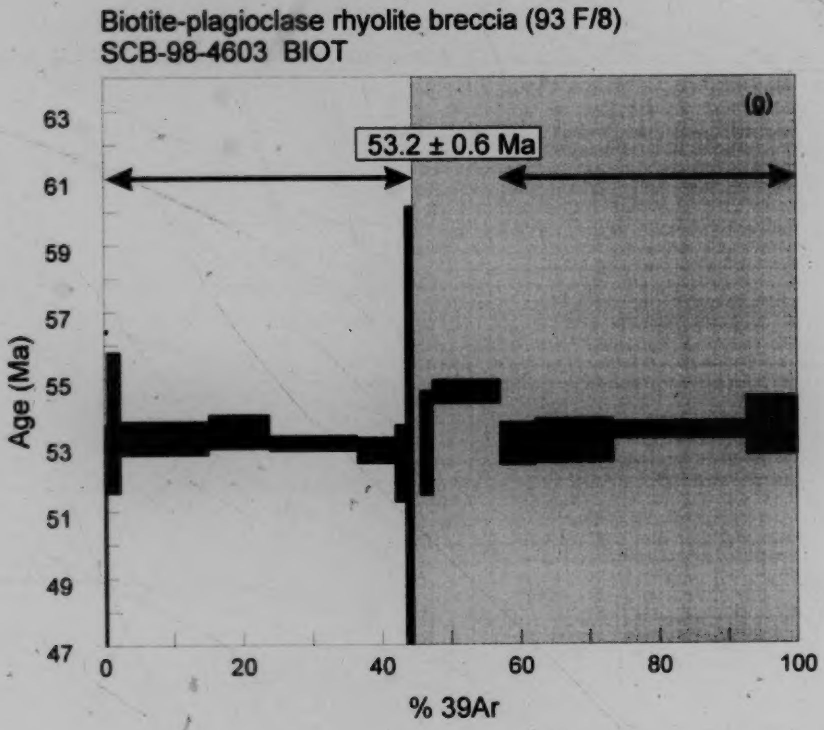
Biotite-plagioclase rhyolite breccia (93 F/8)
SCB-98-4603 BIOT
(g)
53.2 ± 0.6 Ma
Age (Ma)
63
61
59
57
55
53
51
49
47
0
20
40
60
80
100
% 39Ar

in excellent agreement and the combined plateau age of 46.9 ± 0.5 Ma is interpreted as the crystallization age of this dyke.

Banded biotite rhyolite, south of Burns Lake 93K/4 (ATG-98-1305)
This glassy, red and medium gray banded biotite rhyolite contains lithophysae, spherulitic and perlitic textures and is overlain by Endako Group basaltic andesite flows. This unit should provide an age for the final stage of Ootsa Lake Group volcanism in this area. Both aliquots analyzed, each with four biotite flakes, produced good plateaux (Figure 3-15c). These combine to produce a composite age of 48.2 ± 0.6 Ma which is interpreted as the cystallization age of this unit.

Biotite-plagioclase dacite, east of Tahultzu Lake 93F/15 (ATG-98-0703)
This pale grey biotite-plagioclase dacite immediately and unconformably overlies the Limit Lake phase of the Middle Jurassic Stag Lake plutonic suite (Anderson and Synder 1998). This unit was selected for dating in order to determine the timing of the onset of volcanic activity in the area. Two aliquots of three biotite flakes each were analyzed and produced plateau ages of 51.8 and 51.3 Ma (Figure 3-15d). The steps analyzed in the second aliquot produced scattered results and fail to provide a well defined plateau. This poorly defined plateau combined with poor agreement between the two aliquots results in an inconclusive result for this sample. This sample is likely 52 ± 1 Ma, however this age should be taken as a best estimate on the basis of these results.

Andesite, Deerhorn FSR 93F/11 (ATG-98-2302)
This slightly greenish, light grey andesite characteristically contains amygdules of calcite and amethyst and, rarely, hornblende phenocrysts. This distinct unit is found both in the Knapp Lake (93F/14) and Cheslatta Lake (93F/11) map sheets and is a lower unit within the Ootsa Lake Group (Anderson et al. 1999; Grainger and Anderson 1999). Two aliquots of five whole rock fragments each were analyzed and both gas release spectra appear to have been disturbed. Recent argon loss is indicated in the first step of aliquot one and first and second steps in aliquot two (Figure 3-15e). The second and third steps in aliquot one also suggest possible excess argon. Despite this disturbance to the isotopic system, the two aliquots did produce a multistep plateau in the latter portions of the analyses which agree well and combine to give an age of 48.7 ± 0.5 Ma.

Biotite-quartz-plagioclase rhyolite ignimbrite, Henson Hills 93F/12 (ATG-98-3304)
This unit is located in the Henson Hills area. It is light grey in colour with large biotite, quartz and plagioclase crystals, with resorption rims on some of the quartz crystals. The unit also contains slightly flattened vesicles, tuffaceous rhyolite and andesitic fragments and becomes quite glassy in areas. This unit is interpreted as an eruptive center for the abundant felsic flows, tuffs and breccias found locally. A more detailed description of the local geology is given in Grainger and Anderson (1999). Two aliquots of one biotite flake were analyzed (Figure 3-15f). Both aliquots produced a good plateau and give a combined plateau age of 48.3 ± 0.5 Ma.

Biotite-plagioclase dacite breccia, Swede Creek FSR 93F/8 (SCB-98-4603)
This medium grey biotite-plagioclase dacite breccia to agglomerate is fairly extensive within the Euchiniko River map sheet (93F/8). It is unconformably overlain by olivine-bearing basalts which have been correlated with the Chilcotin Group (Struik et al. 1999). Two aliquots of one biotite flake each were analyzed (Figure 3-15g). Both aliquots produced a good plateau which give a combined plateau age of 53.2 ± 0.6 Ma. This age is interpreted as the crystallization age of this unit.

Sr and Nd isotope geochemistry

Analytical Methods

Twelve andesitic to rhyolitic volcanic samples were selected for analysis from the Ootsa Lake Group to represent both the stratigraphic and regional variation of the Ootsa Lake Group. One sample from the 'Island' Lake granite pluton related to the Ootsa Lake Group was included to compare with the volcanics. Two samples from the Babine Igneous Suite and twelve samples from the Endako Group were selected for tracer isotope analysis. Samples were prepared by standard crushing procedures (Jaw crusher and powdered in a tungsten carbide ring mill). Isotopic abundances and ratios for Rb-Sr and Sm-Nd were determined at the University of Alberta using isotope dilution mass spectrometry. Rb and Sm were measured on a Micromass 30 thermal ionization mass spectrometer. Sr and Nd were measured on a VG 354. Measured ratios were normalized to $^{86}Sr/^{88}Sr = 0.1194$ and $^{146}Nd/^{144}Nd = 0.7219$. Replicate analyses of standards run during this study produced results of $^{87}Sr/^{86}Sr = 0.710275 \pm 7$ for the NBS 987 Sr standard (n=27). The La Jolla standard used during analyses of the Endako Group samples was measured as $^{143}Nd/^{144}Nd = 0.511833 \pm 11$ (n=4) and the Shin Etsu Nd standard used during analysis of the remaining samples was measured as $^{143}Nd/^{144}Nd = 0.512095 \pm 4$ (n=18). For all samples, initial isotopic values were calculated using precise $^{40}Ar/^{39}Ar$ or U-Pb age results from the same or proximal sample as determined here for the Ootsa Lake Group volcanics and 'Island' Lake granite, in Villeneuve and MacIntyre (1988) for the Babine Igneous Suite and by Villeneuve (unpublished data *in* Anderson 1998 and pers. comm.) for the Endako Group. A median value of 51.5 Ma from the age range of 51 to 53 Ma determined for the Babine Igneous Suite (Villeneuve and MacIntyre 1997) was used for the one Babine porphyry sample (ATG-2403) that lacked either a direct or proximal age determination. An age of 49.5 Ma was assumed for a rhyolite dome in the Henson Hills area (ATG-3605) based on the assumption of similar age relationships between a rhyolite dome and eruptive center in the Dayeezcha mountain area (ATG-0201 and ATG-1403, respectively) and a $^{40}Ar/^{39}Ar$ date of 48.3 ± 0.5 Ma, determined here, for an eruptive center within the Henson Hills area (ATG-3304). Decay constants used were $\lambda(^{147}Sm) = 6.54 \times 10^{-12}$/yr and $\lambda(^{87}Rb) = 1.42 \times 10^{-11}$/yr (Neumann and Huster 1974; Davis et al. 1977; Lugmair and Marti 1978). Values of $^{143}Nd/^{144}Nd_{CHUR} = 0.512638$, $^{147}Sm/^{144}Nd_{CHUR} = 0.1967$, $^{143}Nd/^{144}Nd_{DM} = 0.513163$, $^{147}Sm/^{144}Nd_{DM} = 0.2137$ were used to calculate initial εNd and depleted mantle model ages using the following equations:

$$\varepsilon Nd = (^{143}Nd/^{144}Nd_{(T)} / ^{143}Nd/^{144}Nd_{CHUR(T)} - 1) \times 10^4$$

$$T_{DM} = \ln[(^{143}Nd/^{144}Nd - ^{143}Nd/^{144}Nd_{DM})/(^{147}Sm/^{144}Nd - ^{147}Sm/^{144}Nd_{DM}) + 1]/\lambda$$

where $^{143}Nd/^{144}Nd_{(T)} = ^{143}Nd/^{144}Nd - ^{147}Sm/^{144}Nd(e^{-\lambda t} - 1)$.

Results

The twelve results for the Endako Group basalt to andesite flows (Table 3-2) are highly consistent and define a narrow range of $^{87}Sr/^{86}Sr_i$ from 0.7040 to 0.7044 with $\varepsilon Nd_i = +1.4$ to $+3.2$. These results all form a tight cluster that plot within the mantle array (Faure 1986), as shown in Figure 3-16. The isotopic results are close to bulk earth values, with slightly lower $^{87}Sr/^{86}Sr_i$ and higher εNd_i relative to bulk earth.

The two samples from the Babine Igneous Suite/Newman volcanics fall within or close to the range of values defined by the Endako Group with $^{87}Sr/^{86}Sr_i$ of 0.7044 to 0.7045 and εNd_i of +2.2 to +2.3.

Table 3-2. Analytical Results of trace isotope analyses

Sample*	Lithology	t_{cryst} (Ma)	Rb ppm	Sr ppm	^{87}Sr/^{86}Sr	2 σ error	^{87}Rb/^{86}Sr	Sr$_i$	Sm ppm	Nd ppm	^{143}Nd/^{144}Nc	2 σ error	^{147}Sm/^{144}Nd	^{143}Nd/^{144}Ndi	εNd$_0$	εNd$_i$	TDM Goldstein (Ma)
Endako Group - basalt to andesite																	
ATH97-0202	basalt	49.60	32.22	715.88	0.70426	0.000017	0.1302	0.70414	10.49	53.05	0.512739	0.000007	0.1195	0.512700	2.0	2.5	687
ATH97-0216	basalt	42.00	36.42	700.05	0.70432	0.000014	0.1505	0.70420	10.50	53.30	0.512755	0.000011	0.1191	0.512755	2.3	2.7	658
ATH97-0304A	basalt	45.30	47.11	652.65	0.70420	0.000018	0.2088	0.70403	11.06	55.85	0.512737	0.000007	0.1197	0.512702	1.9	2.4	691
AT97-1601B	basalt	49.00	38.37	725.16	0.70429	0.000016	0.1530	0.70416	10.82	37.59	0.512712	0.000008	0.1740	0.512656	1.4	1.6	1727
ATH97-0103	basaltic andesite	51.20	66.98	1029.30	0.70452	0.000013	0.1882	0.70435	8.24	45.25	0.512701	0.000008	0.1101	0.512664	1.2	1.8	681
ATH97-0113	basaltic andesite	51.20	96.85	1023.76	0.70454	0.000019	0.2736	0.70431	8.23	45.17	0.512746	0.000008	0.1102	0.512709	2.1	2.7	615
ATH97-0215	basaltic andesite	49.60	23.06	631.27	0.70411	0.000014	0.1056	0.70401	11.55	56.74	0.512779	0.000007	0.1231	0.512739	2.8	3.2	647
ATS97-1702C	basaltic andesite	48.80	47.73	666.08	0.70442	0.000014	0.2073	0.70425	6.22	47.48	0.512752	0.000007	0.0792	0.512727	2.2	3.0	467
ATH97-0402	andesite	45.20	25.89	559.64	0.70426	0.000019	0.1338	0.70414	9.36	46.58	0.512760	0.000008	0.1215	0.512724	2.4	2.8	667
ATH97-0313	andesite	45.20	48.86	557.32	0.70431	0.000018	0.2536	0.70412	9.72	47.69	0.512710	0.000013	0.1233	0.512674	1.4	1.8	764
ATH97-0406	andesite	45.20	27.66	560.19	0.70427	0.000014	0.1428	0.70415	9.54	47.58	0.512776	0.000015	0.1212	0.512740	2.7	3.1	639
ATS97-1702B	andesite	48.80	41.22	695.96	0.70437	0.000015	0.1713	0.70422	6.65	35.43	0.512682	0.000008	0.1134	0.512646	0.9	1.4	732
Ootsa Lake Group - andesite to rhyolite																	
ATG-2302	andesite	48.70	86.78	527.11	0.70564	0.000021	0.4763	0.70531	7.26	40.67	0.512745	0.000008	0.1079	0.512710	2.1	2.6	604
SCB-4603	dacite	53.20	34.56	1176.63	0.70455	0.000016	0.0850	0.70448	5.54	31.60	0.512720	0.000020	0.1060	0.512683	1.6	2.2	628
ATG-1403	dacite	47.60	90.51	344.65	0.70505	0.000016	0.7598	0.70454	10.25	58.88	0.512722	0.000007	0.1053	0.512690	1.6	2.2	620
AT-2705	dacite	48.50	83.93	316.45	0.70498	0.000015	0.7673	0.70445	11.20	67.67	0.512725	0.000095	0.1001	0.512693	1.7	2.3	588
ATG-2202	dacite	50.70	151.04	674.50	0.70490	0.000016	0.6478	0.70444	7.29	42.97	0.512683	0.000007	0.1026	0.512649	0.9	1.5	659
ATG-0703	dacite	51.50	119.29	397.39	0.70503	0.000017	0.8685	0.70439	5.86	35.16	0.512776	0.000007	0.1009	0.512742	2.7	3.3	524
ATG-1305	rhyolite	48.20	189.71	32.14	0.71720	0.000015	17.0966	0.70549	3.91	20.40	0.512736	0.000007	0.1160	0.512700	1.9	2.4	666
ATG-0201	rhyolite	48.60	173.44	1.47	0.94931	0.000023	348.6184	0.70864	8.27	37.10	0.512726	0.000008	0.1348	0.512684	1.7	2.1	843
ATG-3605	rhyolite	49.50	255.11	12.14	0.74747	0.000017	61.0619	0.70453	3.46	15.37	0.512853	0.000011	0.1362	0.512809	4.2	4.6	610
AT-2702	rhyolite	48.50	133.78	237.37	0.70540	0.000014	1.6305	0.70428	7.69	40.05	0.512782	0.000008	0.1161	0.512745	2.8	3.3	596
ATH97-0301	rhyolite	52.70	171.30	41.82	0.71255	0.000015	11.8580	0.70365	7.04	42.62	0.512733	0.000007	0.0999	0.512699	1.9	2.5	577
ATS97-1701B	rhyolite	51.60	143.27	108.58	0.70717	0.000014	3.8177	0.70434	10.71	62.10	0.512756	0.000007	0.1043	0.512721	2.3	2.9	568
Ootsa Lake Group related Intrusions - granite																	
ATSS-0406	granite	47.30	165.23	3.19	0.81525	0.000014	151.3168	0.71358	4.38	- no data -							
ATSS-0406-2	granite	47.30	213.74	4.11	0.81103	0.000011	152.0292	0.70888	4.44	- no data -							
ATSS-0406-3	granite	47.30	212.71	4.06	0.81098	0.000016	153.1006	0.70811									
Babine Igneous Suite																	
ATG-2401-2	andesite	51.30	48.56	987.20	0.70450	0.000016	0.1423	0.70440	4.82	27.40	0.512725	0.000024	0.1063	0.512689	1.7	2.3	0
ATG-2403-2	biot-hb-plag porphyr	51.50	54.75	720.32	0.70463	0.000015	0.2199	0.70447	3.33	20.83	0.512719	0.000007	0.0966	0.512686	1.6	2.2	0

* Replicate analyses are indicated as "-2", "-3" etc.

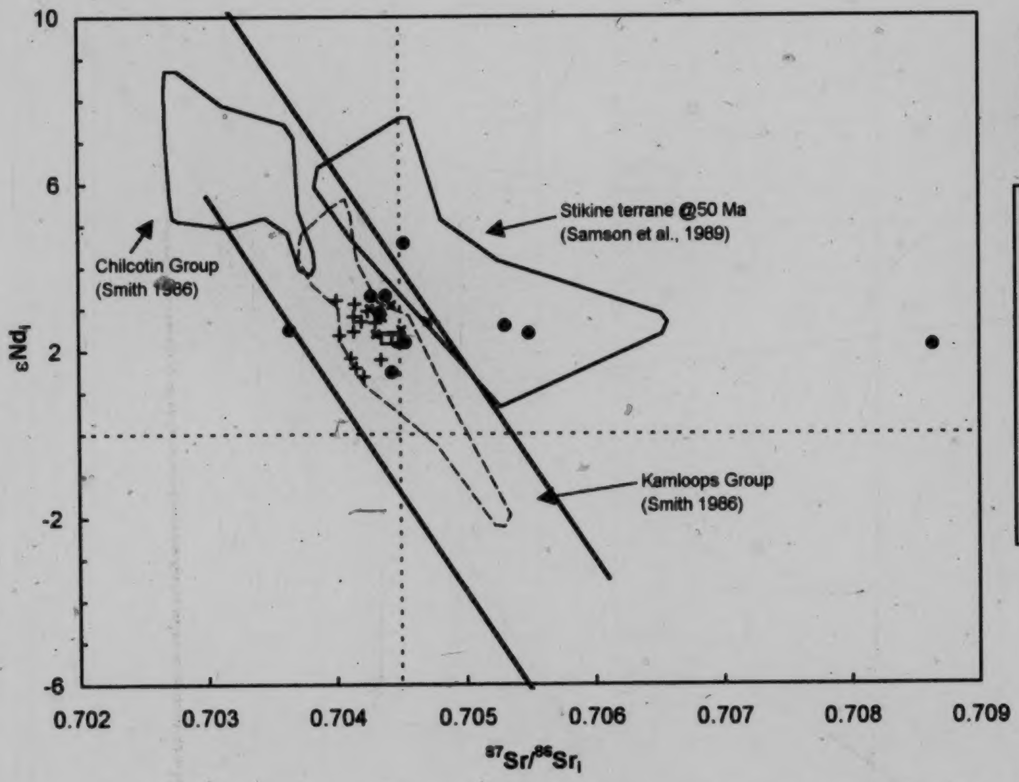

Figure 3-16. εNdi versus ^{87}Sr/^{86}Sri for the Ootsa Lake and Endako Groups. Data from the Buck Creek Formation shown for comparison (Dostal et al. 1998).

Values of εNd_i for the Ootsa Lake Group volcanics range from +1.5 to +4.6, with eleven of the twelve analyses falling into a narrower range from +1.5 to +3.3. Thus, the range of εNd_i values compares very well with the results from the Endako Group and Babine Igneous Suite/Newman volcanics. Eight of the twelve samples have $^{87}Sr/^{86}Sr_i$ values between 0.7043 and 0.7045, which overlaps with both the Babine Igneous Suite/Newman volcanics and Endako Group. Of the four remaining samples, one falls below this range with $^{87}Sr/^{86}Sr_i$ = 0.7037. Two others have $^{87}Sr/^{86}Sr_i$ values of 0.7053-0.7055 and together with the one sample with a high εNd_i fall into the range of crustal values. A fourth sample is substantially higher with $^{87}Sr/^{86}Sr_i$ = 0.7086. Thus while most of the Ootsa Lake Group volcanics have $^{87}Sr/^{86}Sr_i$ values of 0.7043 to 0.7045 and εNd_i of +1.5 to +3.3, there are deviations from this range.

Two analyses from one sample of the 'Island' Lake granite pluton give different $^{87}Sr/^{86}Sr_i$ values of 0.7136 and 0.7089. This sample also has a high $^{87}Rb/^{86}Sr$ value (~152) and these results are interpreted as the result of an increased sensitivity to variations in the measured isotopic concentrations. Despite the obvious inaccuracy of these results, they do suggest that this pluton has a $^{87}Sr/^{86}Sr_i$ value of ~0.709, higher than the values for the Ootsa Lake Group volcanics. No Nd isotopic data was obtained for this sample, likely due to a very low Nd concentration.

Six samples from the Buck Creek Formation and Swan Lake volcanics in the Smithers map area (NTS 93L) have $^{87}Sr/^{86}Sr_i$ values ranging from 0.7043 to 0.7047 and εNd_i from +2.4 to +3.1 (Dostal et al. 1998). These results are shown in Figure 3-16 and overlap well with the bulk of the Ootsa Lake Group volcanics. $^{87}Sr/^{86}Sr_i$ results from Ewing (1981a) for the Kamloops Group range from 0.7034 to 0.7078 (n = 11), with the bulk of the analyses falling within the 0.7034 to 0.7046 range (n=8). Further analyses of the Kamloops Group by Smith (1986) have $^{87}Sr/^{86}Sr_i$ results that range from 0.7038 to 0.7052 and εNd_i between -1.9 and +5.4 (n=17). These results are plotted in Figure 3-16 and show significantly more variation in Nd isotopic composition than any of these other studies. Ewing (1981a) identified a trend of increasing $^{87}Sr/^{86}Sr_i$ values from west to east which was interpreted as corresponding to an origin above an east dipping subduction zone. Additional analyses by Smith (1986) do not support the existence of such a trend.

Discussion

Geochronology

Comparison of $^{40}Ar/^{39}Ar$ and U-Pb results

In order to evaluate the robustness of the $^{40}Ar/^{39}Ar$ dating method for these young felsic volcanics, samples for both $^{40}Ar/^{39}Ar$ and U-Pb were collected from a flow laminated rhyolite (SCBG-97-0101). The $^{40}Ar/^{39}Ar$ date determined at the Geological Survey of Canada laboratories in Ottawa using the same laser $^{40}Ar/^{39}Ar$ methodology as described here of 50.5 ± 0.5 Ma (M.E. Villeneuve pers. comm.) is in excellent agreement with the U-Pb date of 50.7 ± 0.8 Ma determined in this study. The $^{40}Ar/^{39}Ar$ system does not appear to have been affected by later events at this locality and suggests that, in general, the $^{40}Ar/^{39}Ar$ isotope system should provide accurate age determinations within the area. Thus both $^{40}Ar/^{39}Ar$ and U-Pb determinations reported here can be directly compared.

Timing of Eocene Plutonism

The 47.3 ± 0.8 Ma U-Pb zircon crystallization age of the 'Island' Lake granite pluton is the only age of an intrusive body related to the Ootsa Lake Group determined here. The 'Island' Lake pluton intrudes volcanic and volcaniclastic rocks of the Middle Jurassic Hazelton Group to the east and volcanic and volcaniclastic rocks of the Ootsa Lake Group to the west (Sellwood et al. 1999). Thus, this age determination constrains the local Ootsa Lake Group volcanics as older than 47.3 Ma. This age determination is younger than any previously reported age for the Eocene Goosly Lake or Babine intrusions (50-53 Ma; see Figure 3-4). However, it does overlap within error of the age range of the Nanika intrusions (48 to 57 Ma).

The earliest plutonic activity related to the Ootsa Lake Group is the emplacement of the Goosly Lake granite at 57 ± 3 Ma in the Smithers map sheet (Carter 1981). This is followed shortly by the emplacement of the Frank Lake granite pluton in the northeastern Nechako River map sheet circa 55 Ma (M.E. Villeneuve pers. comm.). The Frank Lake pluton was intruded into Middle Jurassic volcanic and plutonic rocks that are now largely obscured by Miocene basalt flows (Wetherup 1997). These two ages indicate that the onset of Eocene plutonic activity occurred within 2 Ma at two localities, located more than 100 km apart, at the eastern and western margins of the study area. Although only two ages are reported, these data suggest that processes controlling Eocene magmatism influenced a large area at the onset. These age determinations also indicate that Eocene plutonism preceded volcanic activity by at least 2 Ma (see below).

The determined age range of emplacement for the Nanika intrusions indicates continuous plutonism regionally within the Smithers and Whitesail map areas from the onset at 57 Ma until 48 Ma (Carter 1981). The age range for intrusion of the Nanika plutons is quite large and based on K-Ar ages with fairly substantial errors of 1.5 to 3.0 Ma. More precise age dating may determine a more restricted age range, just as recent ^{40}Ar/^{39}Ar age dating of the Babine Igneous suite reduced this period of magmatism from 10 Ma to 3 Ma (Villeneuve and MacIntyre 1997). Of the published K-Ar ages for the Babine igneous suite, 8 of the previous 11 age dates fall within the 50 to 53 Ma age range determined by the more precise ^{40}Ar/^{39}Ar age results.

There are only three more precise age determinations for intrusions associated with the Ootsa Lake Group available; the age of the 'Island' Lake pluton, reported here, and the unpublished ages of the Sam Ross pluton, circa 50.5 Ma, and the Frank Lake pluton, circa 55 Ma (M.E. Villeneuve pers. comm.). Of the seventeen ages reported for the Nanika and Goosly Lake instrusions, ten fall into the period between 49.5 and 51.5 Ma (Carter 1981; Church 1970 and 1972). Two others are just slightly older than the age of the 'Island' Lake pluton at 47.7 and 47.9 Ma (Carter 1981). Two ages bracket the emplacement age of the Frank Lake pluton at 54 and 57 Ma. These data correspond well to the more precise age determinations and suggest that Eocene plutonism may be more restricted to three periods at roughly 47-48, 49.5-51.5 and 54-57 Ma. Fourteen of the seventeen reported K-Ar ages for the Nanika and Goosly Lake instrusions are included in these intervals. In conclusion, precise age dating indicates three periods of Eocene plutonism, which is supported by the bulk of reported K-Ar ages. It is clear, however, that further geochronology is necessary to confirm these more restricted intervals of Eocene plutonism.

Relationships between local structure and Eocene plutonism

The Frank Lake pluton is located within the core of the Vanderhoof Metamorphic Complex and is terminated by a shallow dipping north-northeast shear zone with a normal northwest sense of motion (Wethurup 1997). These relationships indicate that the emplacement of the Frank Lake pluton, circa 55 Ma, predates northwest extension on the Vanderhoof Metamorphic Complex. A ^{40}Ar/^{39}Ar biotite cooling age circa 45 Ma indicates extension on this shear zone was completed between 55 and 45 Ma (M.E. Villeneuve unpublished data *in* Anderson 1998).

Both the 'Island' Lake and the Sam Ross plutons are spatially associated with north-northeast and northeast faults, respectively (Whalen et al. 1998; Anderson et al. 1999). A similar relationship was observed in detailed mapping of Uncha Mountain between the north-northeast trending Uncha fault and various Eocene intrusions, including syenite to granite intrusions which strongly resemble the 'Island' Lake and Twenty-Six mile Lake pluton (Barnes and Anderson 1999). Barnes and Anderson (1999) observe that the intrusions have an elongate nature parallel to the fault and suggest that emplacement of the plutons was facilitated by extensional motion on these faults. Although more detailed work is necessary, this suggests that extension along northeast faults, such as that associated with the Sam

Ross pluton, occurred circa 50.5 Ma, prior to north-northeast extension along faults such as the Uncha Fault and that associated with the 'Island' Lake pluton at 47 Ma.

The Nulki Shear zone has a trend of 220° (Wetherup 1997) which is approximately parallel to the northeast orientated extensional faults, such as that associated with the Sam Ross pluton. If there is only one regional northwest extensional event responsible for motion along these northeast faults and northwest extension on the Vanderhoof Metamorphic Complex, this extensional event likely occurred circa 50.5 Ma.

Regional timing of Ootsa Lake Group volcanism
Figure 3-17 shows that the ranges of U-Pb and $^{40}Ar/^{39}Ar$ age dates determined here for the Ootsa Lake Group volcanics within the Nechako River and Fort Fraser map areas are similar. Four ages from the Nechako River map area overlap and range from 47.6 to 48.7 Ma, with two older ages of 51.5 (?) and 53.2 Ma. Within the Fort Fraser map area there are two younger ages of 46.9 and 48.2 Ma and two older ages that overlap giving a range of 50.7 to 52.0 Ma. Eleven other precise $^{40}Ar/^{39}Ar$ age dates from Ootsa Lake Group volcanics in the northeastern Nechako River and the eastern Fort Fraser map areas overlap and range from 49.4 to 52.7 Ma (Villeneuve unpublished data *in* Anderson 1998 and pers. comm.). Taken together these ages overlap and establish that Ootsa Lake Group volcanism was regionally continuous between 47.6 and 53.2 Ma.

This age range is slightly more restricted, but compares well with the age ranges of Ootsa Lake Group volcanism established from previously reported less precise K-Ar and $^{40}Ar/^{39}Ar$ ages (see Figure 3-4). K-Ar ages for the Nechako River and Fort Fraser map areas define an age range for Ootsa Lake Group volcanism between 48 and 54 Ma (Matthews 1964; Andrew 1988). The age range for the Whitesail and Smithers map sheets, based on both K-Ar and $^{40}Ar/^{39}Ar$ ages, is slightly greater from 47 to 56 Ma (Church 1972; Stevens et al. 1982; Diakow and Koyanagi 1988; Drobe 1991; Dostal et al. 1998). Only three of the seventeen previously reported K-Ar and $^{40}Ar/^{39}Ar$ ages fall outside the age range defined by the more precise U-Pb and $^{40}Ar/^{39}Ar$ age dates determined here and in Villeneuve (*in* Anderson 1998 and pers. comm.). Of these three, two agree within error of the precisely determined age range. Thus, it is clear that the regional volcanism of the Ootsa Lake Group is well defined and continuous between 47.5 and 53 Ma and that the three radiogenic systems appear to be in good overall agreement.

Local timing of Ootsa Lake Group volcanism
Locally there appear to be more restricted periods of Ootsa Lake Group volcanic activity. All six of the age determinations in this study from the northwestern quadrant of the Nechako River map sheet (93 F/11,12,13 and 14) and southwestern corner of the Fort Fraser map area (93 K/4 and 5) fall into the range from 47 to 49 Ma. Within these six ages both basal and upper units are well represented. An andesite flow (ATG-2302), which was mapped as the most basal flow unit within this region, produced the oldest age determination of this group at 48.7 ± 0.5 Ma. This unit is older, outside error, of the eruption at Dayeezcha Mountain, dated as 47.6 ± 0.4 Ma from a dacitic ignimbrite, and a rhyolite dyke (ATG-4201) which crosscuts Endako Group basaltic andesites and is dated at 46.9 ± 0.5 Ma. These results support the Ootsa Lake Group volcanic stratigraphy determined within this area (Grainger and Anderson 1999).

Three K-Ar ages from the nearby Wolf deposit (93 F/3) are in overall agreement with an age range of 47 to 49 Ma for this area. A rhyolite dyke and rhyolite flow both fall within this range

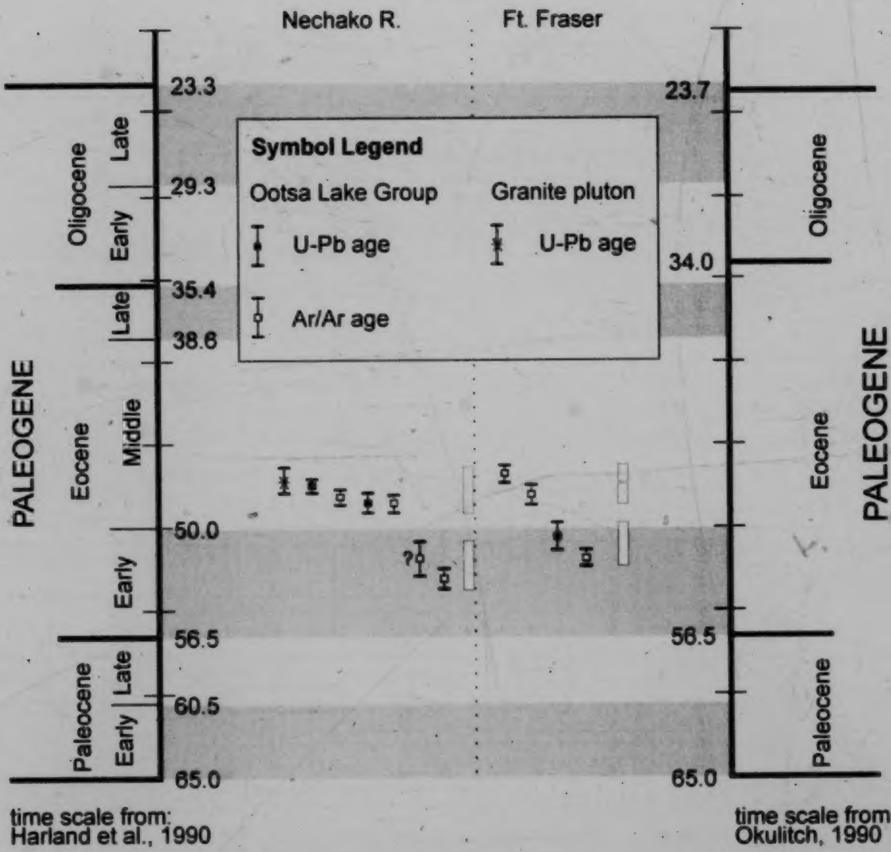

Figure 3-17. Summary of U-Pb and Ar/Ar age dates determined in this study for the Nechako River and Fort Fraser map areas. Ranges of Ootsa Lake Group volcanism are indicated by the open boxes for the two areas based only on these age constraints. The same vertical scale as Figure 3 was used to facilitate comparison with previously reported data.

and the age of a crystal tuff, 49.9 ± 1.7 Ma, agrees within error (Andrew 1988). The only other published age within this area is for a dacite in the southwestern Fort Fraser map area (93 K/4) which is significantly older at 54 ± 2 Ma (Matthews 1964). With the exception of this latter age, eight age determinations within the western half of the Nechako River (93 F/3, 11, 12, 13 and 14) and southwest corner of the Fort Fraser (93 K/4 and 5) map areas are all between 47 and 49 Ma in age with a ninth determination that agrees within error.

By contrast, two age determinations reported here for Ootsa Lake Group volcanics from the eastern portion of the Nechako River map sheet (93 F/8 and 15) are both older at 51.5 ± 1 (?) and 53.2 ± 0.6 Ma. Eight other precise $^{40}Ar/^{39}Ar$ age dates in the eastern Nechako River map area (Villeneuve unpublished data *in* Anderson 1998 and pers. comm.) are similar in age. These ten age determinations combined give an age range from 51 to 53 Ma for this area. Almost all of these age determinations are from units that almost immediately underlie Endako Group basaltic andesites or Chilcotin Group basalts and thus represent uppermost units within the Ootsa Lake Group. The one exception is the biotite-plagioclase rhyolite (ATG-0703: 93 F/15) which unconformably overlies the Limit Lake phase of the Middle Jurassic Stag Lake-Twenty-six Mile Lake plutonic suite (Anderson and Synder 1998) and thus should represent the lowermost Ootsa Lake Group within this area. Unfortunately, the $^{40}Ar/^{39}Ar$ age date for this sample was inconclusive and only a best estimate of 51 to 52 Ma could be obtained. These results do suggest that Ootsa Lake Group volcanism occurred over a short period of approximately 2 Ma within this area.

Within the southeast quadrant of the Fort Fraser map sheet there is one U-Pb zircon age reported here, and a $^{40}Ar/^{39}Ar$ age determination for a rhyolite flow (93 K/7) and two additional ages (93 K/1) by Villeneuve (unpublished data *in* Anderson 1998 and pers. comm.). These ages overlap and define an interval of volcanism from 49.5 to 51 Ma. All three of these units are from the upper Ootsa Lake Group, however, so further age dating may extend this age range.

The final age reported here, of 52.0 ± 0.5 Ma, is from the northwestern Fort Fraser map area, just south of the Babine Igneous suite. There are no other ages reported from this area.

Further age determinations may reduce these apparent local differences, however, several of these locations are well constrained. Other studies have dated magmatism of the Babine Igneous Suite (93 L/16) between 53 and 50 Ma (Villeneuve and MacIntyre 1997) and Ootsa Lake volcanism in the Whitesail range (93 E/10) between 49 and 50 Ma (Diakow and Koyanagi 1988; Drobe 1991).

In summary, a total of 27 $^{40}Ar/^{39}Ar$, 8 K-Ar and 4 U-Pb age determinations indicate a short duration of 6 Ma for Ootsa Lake Group volcanism between 53 and 47 Ma. Felsic volcanism was initiated in the eastern Fort Fraser map area, in the vicinity of the Vanderhoof Metamorphic Complex, between 53 and 51 Ma (see Figure 3-2). Coeval more mafic magmatism of the Babine Igneous Suite, near Granisle, also occurred during this time and ended by 50 Ma. Ootsa Lake Group predominantly felsic volcanism occurred in the southeastern portion of the Fort Fraser map sheet between 51 to 49.5 Ma and more intermediate volcanism in the Whitesail range between 50 and 49 Ma. The final stage of predominantly felsic Ootsa Lake Group volcanism occurred between 49 and 47 Ma in the southwestern portion of the Fort Fraser and western half of the Nechako River map areas. In general, it would appear that intermediate to mafic volcanism is more abundant in the Whitesail and Smithers map areas, with more predominant felsic volcanism in much of the Nechako River and Fort Fraser map areas. However, there do not appear to be any temporal trends towards one more dominant composition in any particular area. All areas contain units that describe the full compositional range of the Ootsa Lake Group volcanics.

Twelve precise $^{40}Ar/^{39}Ar$ age dates for the Endako Group (M.E. Villeneuve unpublished data *in* Anderson 1998 and pers. comm.) indicate that the period of Endako Group volcanism, from circa 51 to 45 Ma, overlaps regional Ootsa Lake Group volcanism for 4 Ma, between 51 to 47 Ma. This implies that any age relation of these two groups is possible. However, field mapping has shown that the Endako Group is almost always locally younger than the Ootsa Lake Group volcanics. There is only one location where reversion of the usual field relations was observed. This site (sample ATG-4201) is in the southwestern corner of the Fort Fraser map area where Ootsa Lake Group volcanism is the youngest.

Petrogenesis

Geochemical and tracer isotope analyses were completed on samples from the Ootsa Lake Group to investigate the magmatic origin of these rocks. One geochemical and petrographic study was completed on the Ootsa Lake Group within the Whitesail range (Drobe 1991) and a combined geochemical and isotopic study, west of Burns Lake, was recently published for the Buck Creek Formation and Swans Lake unit, which are correlated with the upper Ootsa Lake Group and Endako Groups, respectively (Figure 3-3; Dostal et al 1998). Samples analyzed for geochemistry and tracer isotopes in this study are predominantly from the northwest portion of the Nechako River map area, but regional samples were collected across the northern Nechako River and south and western portions of the Fort Fraser map areas to obtain better coverage. This is the first geochemical and tracer isotopic study of the Ootsa Lake Group within the Nechako River and Fort Fraser map areas. Combined use of trace element geochemistry and tracer isotopes has proven useful in many studies to obtain a better understanding of the magmatic origin of igneous rocks. Comparison with the geochemistry and tracer isotope values of known crustal and mantle components within the Nechako plateau will, hopefully, provide a better understanding of the origin of the Ootsa Lake Group volcanics.

Samples from the Babine Igneous Suite and Endako Group were also analyzed for comparison with the Ootsa Lake Group. All of these suites are at least partly coeval and overlap in geographic extent and lithology. Comparison of these suites is important in order to obtain a more complete understanding of the origin of Eocene magmatism and the relationship to coeval tectonism.

Isotopic components of the Nechako plateau subsurface

72 crustal xenoliths were collected as part of a study of Neogene basaltic magmatism within the Nechako River map area and Summit Lake locality by Resnick (1999). Crustal xenoliths within the Nechako River map area are of four types; granulite, anorthosite, granite and gabbro. Granulite xenoliths are confined to the eastern portion of the Nechako River map area and are correlated with the Vanderhoof Metamorphic Complex. Anorthosite xenoliths are found at only three localities and cannot be correlated to the surface geology. Granitic xenoliths are correlated with the Eocene plutons described by Sellwood et al. (1999). The gabbroic xenoliths might be correlative with plutonic rocks in Stikinia, such as those found within the Endako batholith (Anderson et al. 1998a). Using these crustal xenoliths to infer the compostion of the upper and lower crust, this study concludes that the lower crust is composed predominantly of gabbro, as these are the most widespread variety of crustal xenoliths. There may also exist either localized bodies or a regional body of anorthosite in the lower crust and granulite within the eastern portion of the Nechako River map area (Resnick 1999). Of these components, isotopic values from Middle Jurassic plutons and regional values for Stikinia can be used to approximate the gabbroic lower crustal component. Within the Nechako plateau $^{87}Sr/^{86}Sr_i$ values of Middle Jurassic plutons range from 0.7035 to 0.7043 and εNd from +3 to +7 (Anderson et al 1998a; R.G. Anderson and J.B. Whalen unpublished data; Chapter 2). Regional values for Stikina are similar with $^{87}Sr/^{86}Sr_i$ values of 0.7037 to 0.7053 and εNd from +2.3 to +7.7 (Samson et al. 1989; Patchett et al 1998).

Calculated liquidus temperatures for Oligo-Miocene basalts are consistently greater than two-pyroxene equilibration temperatures of spinel lherzolite xenoliths in the Nechako River map area and at the Summit Lake locality (Suh 1999). Resnick (1999) interpreted this result to infer an asthenospheric source for the Oligo-Miocene basalts and an upper mantle origin for the spinel lherzolite xenoliths. Two isotopic results available for the Oligo-Miocene basalts within the Nechako plateau suggest a uniform composition of this source with $^{87}Sr/^{86}Sr_i$ values of 0.7035 and εNd_i of +3.7 to +4.4 (see Chapter 2). These results are consistent with analyses reported for Miocene basalts in the Chilcotin plateau to the south (Farquharson 1973; Bevier 1983; Smith 1986). The isotopic results for the Oligocene Summit Lake basalt, $^{87}Sr/^{86}Sr_i = 0.7058$ and $\varepsilon Nd_i = -1$ (Smith 1986; Chapter 2), are significantly different from other Miocene basalts. Resnick (1999) noted that there are substantial chemical differences between the Summit Lake locality and all other sites in the Nechako River map area and interpreted this as a reflection of regional differences in the chemical composition of the asthenosphere. Alternatively, these isotopic differences may be due to temporal variations in asthenosphere composition as the Summit Lake locality is at least 15 Ma older than any other locality that has been analyzed to date. Thus, these isotopic values may be only applicable during the Miocene and may not reflect the Eocene composition of the asthenosphere.

Studies of mantle xenoliths entrained within Oligo-Miocene basalts within the Nechako River map area and Summit Lake locality have concluded that the mantle is heterogeneous on a large (Resnick 1999) and small scale (Brearly et al. 1984). An isotopic study of mantle xenoliths, predominantly spinel lherzolites, at the Summit Lake locality and two other locales in the Quesnel terrane further south reported $^{87}Sr/^{86}Sr$ values from 0.7036 to 0.7112 and εNd values of +7.6 to –20.4 (n=15; Smith 1986). Three analyses of spinel lherzolites in the Oligo-Miocene basalts from the Nechako River and Summit Lake locality have $^{87}Sr/^{86}Sr$ values between 0.7036 and 0.7051 (Chapter 2). Of these eighteen analyses, three have $^{87}Sr/^{86}Sr = 0.7036$ and $\varepsilon Nd = +6$. This component is comparable to the asthenospheric composition defined by the Miocene basalts (Farquharson 1973; Bevier 1983; Smith 1986; Chapter 2). Half of these eighteen analyses have $^{87}Sr/^{86}Sr$ values of 0.7037 to 0.7046 and εNd values of +2 to +5.5. This isotopic component (MC1) is widespread and thus inferred to represent the dominant upper mantle composition during the Oligo-Miocene. Three analyses from the Summit Lake locality have $^{87}Sr/^{86}Sr > 0.7060$ and $\varepsilon Nd < -4$. This latter component (MC2) is interpreted by Smith (1986) to represent old silicic continental crust, which may reside in the mantle, however it may represent a strongly enriched mantle component. The few remaining analyses, all from the Summit Lake locality, have $^{87}Sr/^{86}Sr$ values between 0.7051 and 0.7058 with εNd from +3 to +7. The $^{87}Sr/^{86}Sr$ values of this component (MC3) are similar to those returned from the Summit Lake basalt and may be related to variations in the composition of the asthenosphere at this time or locality.

Comagmatism of the Ootsa Lake Group

Peace element ratios can be used to test if a suite of igneous rocks are derived from a common source or comagmatic. Pearce element ratios have a denominator which is a conserved element, i.e. an element that is insensitive to a system undergoing change (Nicholls 1988). Tests are suggested by Nicholls (1988) to recognize these conserved elements. The data reported here for the Ootsa Lake Group do not contain sufficient conserved elements in order to test the hypothesis of comagmatism for the Ootsa Lake Group volcanics and thus, according to the Pearce element ratio test, these rocks are not comagmatic. However, the results from the geochemical analyses show that these rocks are similar and suggest that the Ootsa Lake Group volcanics share a similar origin. Furthermore, the geochemistry of the Ootsa Lake Group volcanics is similar to that of the Babine Igneous Suite and the Endako Group (Anderson 1998; Dostal et al. 1998) suggestive of a similar magmatic origin. The geochemical differences between these suites and within the Ootsa Lake Group may be the result of an inhomogeneous source or, alternatively, a homogeneous magma may have been modified by crustal contamination, magma mixing or fractionation (Russell and Nicholls 1988). These various processes are each considered below.

Crustal contamination

The isotopic results of the Endako Group and Babine Igneous Suite are quite homogeneous and argue against significant crustal contamination for these rocks. However, several samples from the Ootsa Lake Group volcanics and the granite pluton have isotopic values which may suggest that crustal contamination does occur in some of the Ootsa Lake Group rocks. In general, there is a lack of physical evidence, such as xenoliths, to support crustal contamination of the Ootsa Lake Group volcanics. One sample (ATG-1403), which was age dated by U-Pb zircon analyses, does contain significant zircon inheritance. Although poorly constrained, the upper intercept on a linear regression (Figure 3-14c) suggests Early Jurassic inheritance.

One of the main difficulties in defining the magmatic origin of these rocks is the isotopic heterogeneity of the upper mantle, as illustrated by the range of results from spinel lherzolite xenoliths analyzed by Smith (1986; $^{87}Sr/^{86}Sr_i = 0.7036$ to 0.7112 and $\varepsilon Nd = +7.6$ to –20.4). Bevier (1983) concluded that variations in isotopic results for the Miocene basalts were entirely due to mantle heterogeneity. It is possible that the same case might be made here. The Endako Group, Babine Igneous Suite and the bulk of the Ootsa Lake Group volcanics have $^{87}Sr/^{86}Sr_i$ values between 0.7040 and 0.7045 and εNd_i of +1.3 to +3.3. Of the subsurface components described above, the most similar to these rocks is the dominant upper mantle component (MC1:$^{87}Sr/^{86}Sr = 0.7037$ to 0.7046 and $\varepsilon Nd = +2$ to +5.5). The one sample with a low $^{87}Sr/^{86}Sr_i$ value of 0.7037 could also have been derived from this source. The incorporation of a minor quantity of older silicic material from within the mantle (MC2: $^{87}Sr/^{86}Sr>0.7060$ and $\varepsilon Nd<-4$) or crustal material of Middle Jurassic composition ($^{87}Sr/^{86}Sr_i = 0.7035$ to 0.7043 and $\varepsilon Nd_i = +3$ to +7) could produce the four more evolved samples from the Ootsa Lake Group volcanics and 'Island Lake' pluton.

Magma mixing

Physical evidence for magma mixing includes disequilibrium among phenocrysts, outrange glass inclusions in phenocrysts, quenched mafic melt inclusions in felsic rocks or convergence to a common composition (Gill 1981). Quartz phenocrysts with reaction rims found at several sites (e.g. ATG-3304 and ATG-0401) are not in disequilibrium with their host magma. These features are commonly found in quartz phenocrysts as SiO_2 solubility decreases with decreasing pressure during the rise and eruption of the magma, resulting in partial resorption of the quartz crystal (McPhie et al. 1993). There is no evidence for convergence towards a common composition over time. Felsic, intermediate and mafic volcanics are found throughout the stratigraphy and intermediate compositions do not become more dominant towards the upper portions of the stratigraphy. Thus physical evidence for magma mixing appears weak, although no detailed analyses were made of phenocrysts or glass inclusions.

Drobe (1991) found weak evidence to support magma mixing, based on one outrange glass analysis and resorption textures and reverse zoning in one andesite flow. However, he concluded that magma mixing was at best a minor process in the evolution of the Ootsa Lake Group volcanics.

Fractionation

Previous studies have found it possible to derive felsic lavas from a basaltic or andesitic parent (Gill 1981; Ewing 1981a; Drobe 1991). The elemental data presented here seems consistent with the same conclusion. The CIPW norm composite variation diagram shown in Figure 3-18 suggests fractionation of orthopyroxene, clinopyroxene, Fe-Ti oxides, apatite and plagioclase. Fractionation of these phases is supported by the major and trace element data. For instance, a decrease in CaO, Sc, MgO and Fe^*O relative to silica under relatively stable Al_2O_3 supports fractionation of the pyroxenes. Similarly decreasing Fe^*O and TiO_2 support fractionation of Fe-Ti oxides. The decrease in P_2O_5 relative to silica may reflect fractionation of apatite. The rapid decrease in Sr when $SiO_2>70\%$ may reflect fractionation of plagioclase. There is also a significant decrease in Ba above $SiO_2 = 75\%$, which may reflect fractionation

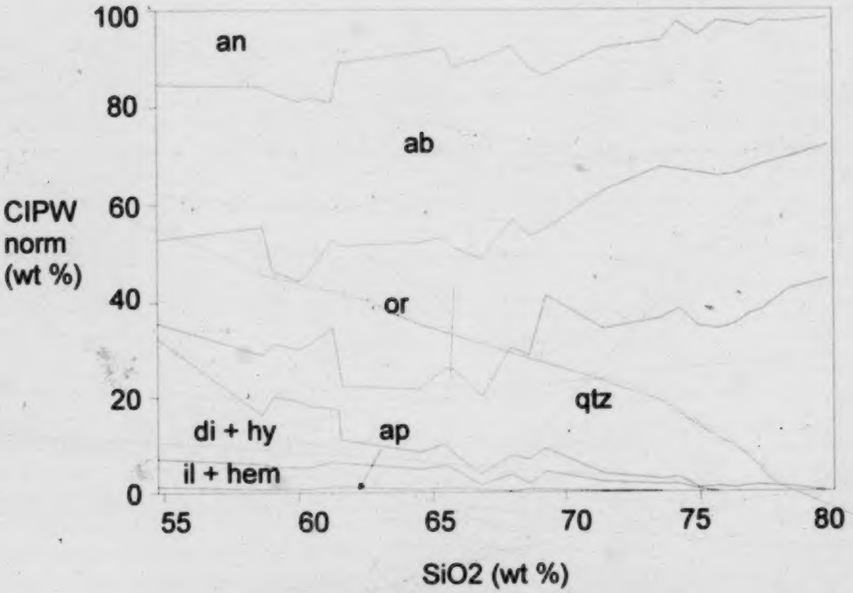

Figure 3-18. Composite variation diagram using CIPW norms calculated for the Ootsa Lake Group.

of alkali feldpsar. This fractionation assemblage of plagioclase, orthopyroxene, clinopyroxene, Fe-Ti oxides and apatite is identical to that suggested by Drobe (1991) and similar to that of Ewing (1981a). Drobe (1991) also suggests that above SiO_2 = 66% orthopyroxene fractionation is replaced by biotite and hornblende. This would seem reasonable for these samples as both of these minerals are found as phenocrysts. There is a minimal decrease in the HFSE among the more felsic samples to support this process, however, the decrease in Ba may reflect fractionation of biotite. This fractionation assemblage affects most elements and thus, as outlined by Russell and Nicholls (1988), it is possible that the lack of conserved elements is solely the result of fractionation.

In summary, geochemical data indicates the Ootsa Lake Group magmas were generated by fractionation of a mafic magma derived from an isotopically enriched upper mantle source. Isotopic data also suggests contamination in some of the Ootsa Lake Group volcanics and the 'Island Lake' pluton with either different enriched mantle components or lower crustal material. The Ootsa Lake Group, Babine Igneous Suite/Newman volcanics and Endako Groups are geochemically similar and are characterized as high K and calc-alkaline with LIL and LREE enrichment relative to HFSE and Ta-Nb depletion. Of these three suites, the Ootsa Lake Group is the most geochemically evolved and the Endako Group the least evolved. These suites are isotopically similar, mostly falling into a range with $^{87}Sr/^{86}Sr_i$ = 0.7040 to 0.7045 and εNd_i = 1.4 to 3.3. These similarities suggest a common magmatic origin for these rocks. The parental magma, prior to fractionation, was likely basalt or basaltic andesite with moderate Al and Na contents, high K, Sr and Ba and isotopically primitive. The subduction character of this magma must also be accounted for and is discussed below.

Tectonic Setting

Plate reconstructions for the Late Cretaceous and Paleogene place the Kula-Farallon ridge from northern California to northern Washington between 85 to 56 Ma providing rapid plate convergence in this area, likely contributing to the Laramide orogeny (Engebretson et al. 1985). Alternatively, the ridge may have intersected the continental margin farther south providing a mechanism for the northward translation during this time (Engebretson et al. 1985). Between 56 and approximately 43 Ma, when the Kula plate was subducted under the western North American margin, movement of the Kula plate adjacent to the central Canadian Cordillera became rapid and obliquely convergent to the north-northeast. Linear velocities calculated on the coast at the latitude of the study area are greater than 200 mm/yr during this period (Engebretson et al. 1985). Subsequent velocities estimated in this same area are considerably lower, between 40 and 25 mm/yr, for the Pacific plate between 43 and 37 Ma and plate motions evolve to become essentially strike-slip following this period (Stock and Molnar 1988; Engebretson et al. 1985). The plate reconstructions of Stock and Molnar (1988) do not support a rapid increase in Kula plate motion between 56 and 43 Ma, but suggest that the Kula-Pacific relative motion slowed or even ceased after 55 Ma. Both plate reconstructions agree that the Kula plate was obliquely convergent along the western North American margin between 69 and 49 Ma and subsequently evolved to essentially stike-slip motion. Struik (1993) concluded that the primary control on crustal extension and displacement is plate motions. The timing of extension and volcanism within the study area correlates well with the timing of these plate motions.

The first phase of plutonism within the Nechako plateau, 57-54 Ma, corresponds to a change in the rate of motion of the Kula plate. Regional volcanism, between 53 and 47 Ma, overlaps the timing of the two younger plutonic events between 51.5 to 49.5 Ma and 47 to 48 Ma and coincides with oblique convergence of the Kula plate. Based on the exisiting geochronology database for this area, sparse, if any, magmatism occurs between 44 and 29 Ma, which overlaps the period of dominantly strike-slip motion of the Pacific plate. Thus the timing of Eocene magmatic activity within the Nechako plateau corresponds with the motion and subduction of the Kula plate (56 to 43 Ma) and with extension in the Nechako plateau (post ~55 Ma to ca. 45 Ma).

According to Condie (1989) the subduction related geochemical character can only be derived directly from an arc related magma, from a magma derived from melting arc-related rocks in the crust or superimposed on a mantle lithosphere source (Johnson et al. 1978). While some of the Ootsa Lake Group samples do show evidence of crustal contamination, most of these rocks do not and this process can not be interpreted as responsible for producing the observed geochemical subduction character. Plate reconstructions indicate that the subduction of the Kula plate coincides with Eocene magmatism and suggests that the generation of magmas extruded in the Nechako plateau was initiated by active subduction of the Kula plate. Thus the subduction character of the Eocene volcanics is the result of mantle modification by active subduction processes. The magmas were variably modified by fractionation and contamination and extruded in a distal volcanic arc setting. The tectonic setting of the Kamloops Group and Buck Creek Formation has been interpreted as a continental arc (Ewing 1981a; Smith 1986; Dostal et al. 1998).

Tectonic discrimination diagrams show a transitional volcanic arc to within-plate association for the Ootsa Lake Group volcanics (Figure 3-19). Most of the Endako Group, almost all of the Eocene plutons and the three Babine Igneous Suite/Newman volcanics fall in the within plate field (Anderson 1998; Anderson 1999; J.B. Whalen unpublished data 1999). These data suggest that the tectonic setting of these rocks may have been transitional from subduction to extension dominated. Eocene extension within the Nechako plateau is well documented (Wetherup 1997; Lowe et al. 1998; Whalen etal. 1998; Stuik et al. 1999) and is responsible for localizing magmatism (Anderson and Synder 1998; Barnes and Anderson 1999). Basalts of the Oligo-Miocene Chilcotin Group plot consistently in the within plate field (Anderson 1999) and are interpreted as situated in a back arc tectonic setting (Bevier 1983; Resnick 1999), indicating that, by the Oligocene, tectonism in the Nechako plateau is extension dominated. The suggestion of a transitional tectonic setting for Eocene volcanics in the Nechako plateau was also made by Dostal et al. (1998) and has been described for a sequence of Cretaceous to Cenozoic volcanic rocks in southwestern Idaho by Norman and Leeman (1989).

Stratigraphy

Eocene volcanic and plutonic rocks of the Babine Igneous suite, Endako and Ootsa Lake Groups studied here and elsewhere, in addition to the Buck Creek Formation and Swans Lake unit volcanics (Diakow and Koyanagi 1988; Drobe 1991; Dostal et al. 1998), are all in part coeval and show an overall geochemical and tracer isotopic similarity that implies a similar magmatic origin. A revised regional stratigraphy for these units is proposed here for general use in order to emphasize these similarities (Table 3-3). The units are maintained as formations within the Ootsa Lake Group. There are lithological, spatial and age distinctions between these units that merits the retention of these names. The Ootsa Lake Group should be restricted to Eocene volcanic or plutonic rocks in order to maintain its relevance. Key references describing the members, recently determined age ranges and a general description are given in Table 3-3.

The one new unit proposed here is the Henson Hills Formation. This member is named for its type area in Henson Hills (93 F/12) which contains excellent exposures of the felsic flows, tuffs and breccias that are distinctive of what is commonly recognized as the Ootsa Lake Group volcanics. This formation is added in order to permit the distinction of these dominantly felsic volcanics within the Ootsa Lake Group from other more intermediate to mafic formations. No one locale contains the full stratigraphy identified within the northern Nechako River map area and southern Fort Fraser map areas, however, this is the most complete and best exposed location. Sites containing other units described in this stratigraphy are given in Grainger and Anderson (1999). Although the volcanics in the Henson Hills area are younger than most other areas of Ootsa Lake volcanism, the lithologies and style of volcanism is representative of the Ootsa Lake Group felsic volcanics. Rocks within this area are among those dated and analyzed in this study. Work by Andrew (1988) provides a detailed study of these rocks at the Wolf Prospect (93 F/3).

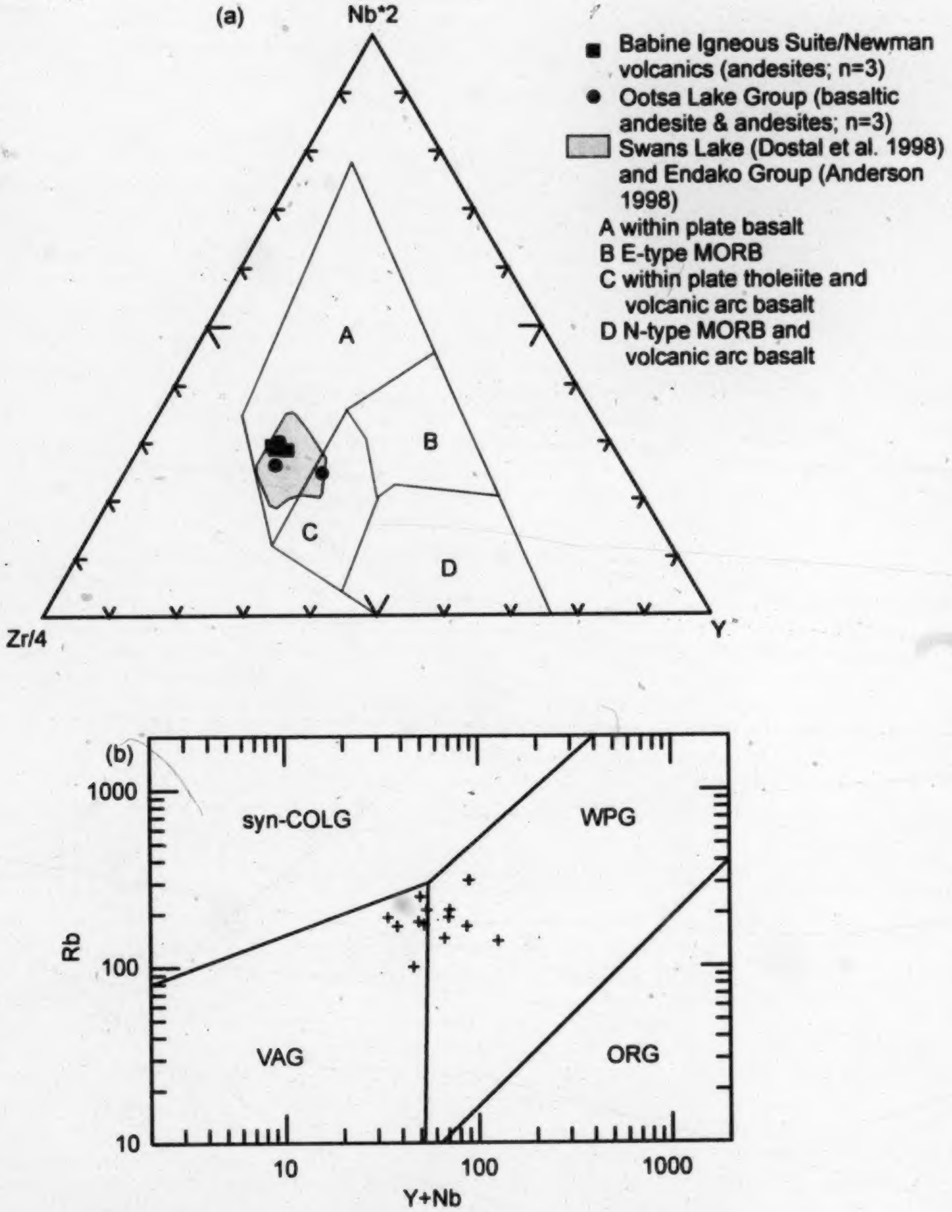

Figure 3-19. Tectonic discrimination diagrams showing (a) Mafic Ootsa Lake Group and Babine Igneous Suite/Newman volcanics (Meschede 1986) and (b) Ootsa Lake Group rhyolites (Pearce et al. 1984).

Ootsa Lake Group rocks within the Whitesail area (Drobe 1991; Diakow and Mihalynuk 1987) appear to be more intermediate to mafic in composition than those found in the Henson Hills Formation and may be most closely related to rocks of the Buck Creek Formation. However, they are not assigned to any particular formation here and are left within the Ootsa Lake Group.

The stratigraphy as outlined here contains the volcanic formations of the Ootsa Lake Group. However, the Nanika and Babine intrusions are related to the Ootsa Lake Group and Newman Formation, respectively (Carter 1981; Villeneuve and MacIntyre 1997).

Table 3-3. Stratigraphy of the Ootsa Lake Group volcanics

Formation	Age (Ma)	Description	Key references
Endako	45-51	Basaltic andesite flows	Haskin et al. 1998
Henson Hills	47-49	Felsic flows, tuffs and breccias	Grainger and Anderson 1999
Buck Creek	47-50	Intermediate to mafic flows and breccia	Dostal et al. 1998; Church 1971 & 1972
Newman	51-53	Andesite flows, breccias and lahars	Villeneuve and MacIntyre 1997; MacIntyre et al. 1995 & 1996
Goosly Lake	48-56	Trachyandesitic flows, dikes and stocks	Church 1971 & 1972
Burns Lake		Chert and quartzite conglomerates	Church 1971 & 1972

Conclusions

Ootsa Lake Group volcanism was regionally continuous between 47 and 53 Ma. Local age determinations show well constrained, more restricted periods of volcanic activity. Age determinations suggest local magmatic activity may be more episodic. Plutonism related to the Ootsa Lake Group volcanic activity has dated events between 47 and 48, 49.5 and 51.5, and 54 to 57 Ma. Further age dating may show plutonic activity to be more continuous within the Nechako plateau.

Analyses show the Babine Igneous Suite, Ootsa Lake and Endako Groups are geochemically and isotopically similar. The combined tracer isotope results predominantly fall into a range of $^{87}Sr/^{86}Sr_i = 0.7040$ to 0.7045 and $\varepsilon Nd_i = 1.4$ to 3.3. These values indicate derivation of these rocks from an enriched upper mantle source with $^{87}Sr/^{86}Sr_i = 0.7037$ to 0.7046 and $\varepsilon Nd_i = 2$ to 5.5. Isotopic variations from this range determined in the Ootsa Lake Group volcanics and 'Island Lake' pluton may be the result of contamination with other enriched mantle components or lower crustal material. The observed compositional range of the Ootsa Lake Group can be produced by fractionation of a basaltic andesite magma. There appears to be little evidence to support magma mixing.

A revised regional stratigraphy is suggested for use, to emphasize the similarities of these Eocene rocks in the Nechako plateau. A new unit is proposed, the Henson Hills Formation, which contains the predominantly felsic flows, tuffs and breccias studied in detail in the northern Nechako River map area and found throughout the Nechako plateau.

Eocene magmatism within the Nechako plateau is coeval with the rapid motion of the Kula plate and regional extension in central British Columbia. Parental magmas were generated as the result of eastward subduction of the Kula plate and erupted in a distal volcanic arc setting. Extension was important in localizing Eocene magmatism within the Nechako plateau. Eocene rocks display a transitional geochemical character interpreted to reflect a shift from a subduction to extension dominated tectonic setting which was completed by the Oligocene.

References

Anderson, R.G. 1998. Influence of Eocene tectonics and magmatism on the Mesozoic arc and orogenic collapse: New developments in Nechako River map area. *In;* New Geological Constraints on Mesozioc to Tertiary Metallogenesis and on Mineral Exploration in central British Columbia: Nechako NATMAP project; Geological Association of Canada, Cordilleran Section, March 27, 1998, Short Course notes.

Anderson, R.G. 1999. Eocene-Neogene continental magmatism in Nechako River area, central British Columbia, Canada. XXII IUGG General Assembly, Birmingham, U.K. July 19-30, 1999.

Anderson, R.G. and Synder, L.D. 1998. Jurassic to Tertiary volcanic, sedimentary, and intrusive rocks in the Hallett Lake area, central British Columbia. *in;* Current Research 1998-A. Geological Survey of Canada. P. 135-144.

Anderson, R.G., Whalen, J.B., Struik, L.C. and Villeneuve, M.E. 1998a. Mesozoic to Tertiary volcanism and plutonism in southern Nechako NATMAP area: Part 2. Triassic to Eocene composite intrusions and molybdenum metallogeny: the Endako Batholith redefined. *In;* New Geological Constraints on Mesozioc to Tertiary Metallogenesis and on Mineral Exploration in central British Columbia: Nechako NATMAP project; Geological Association of Canada, Cordilleran Section, March 27, 1998, Short Course notes.

Anderson, R.G., Synder, L.D., Resnick, J. and Barnes, E. 1998b. Geology of the Big Bend Creek map area, central British Columbia. *in;* Current Research 1998-A. Geological Survey of Canada. p. 145-154.

Anderson, R.G., Synder, L.D., Resnick, J., Grainger, N.C. and Barnes, E.M. 1999. Bedrock geology of the Knapp Lake map area, central British Columbia. *in;* Current Research 1999-A. Geological Survey of Canada. p.109-118.

Andrew, K.P.E. 1988. Geology and genesis of the Wolf Precious Metal Epithermal Prospect and the Capoose Base amd Precious Metal Porphyry-style prospect, Capoose Lake area, Central British Columbia. University of British Columbia. Unpublished MSc thesis. 334 pages.

Armstrong, J.E. 1949. Fort St. James Map-area, Cassiar and Coast Districts, British Columbia. Geological Survey of Canada, Memoir 252, 210 pages.

Armstrong, R.L. and Ward, P. 1991. Evolving geographic patterns of Cenozoic magmatism in the North American Cordillera: The temporal and spatial association of magmatism and metamorphic core complexes. Journal of Geophysical Research. 96; 13201-13224.

Barnes, E.M. and Anderson, R.G. 1999. Bedrock geology of the Uncha Mountain area, northwestern Nechako River map area, central British Columbia. *in;* Current Research 1999-A. Geological Survey of Canada. p. 129-138.

Beckinsale, R.D. and Gale, N.H. 1969. A reappraisal of the decay constants and branching ratio of ^{40}K. Earth and Planetary Science Letters. 6; 289-294.

Bevier, M.L. 1983. Implications of chemical and isotopic composition for petrogenesis of Chilcotin Group Basalts, British Columbia. Journal of Petrology. 24; 207-226.

Brearley, M. Scarfe, C.M. and Fujii, T. 1984. The petrology of ultramafic xenoliths from Summit Lake, near Prince George, British Columbia. Contributions to Mineralogy and Petrology, v.88, p.53-63.

Carter, N.C. 1981. Porphyry Copper and Molybdenum deposits West-central British Columbia. British Columbia Ministry of Energy, Mines and Petroleum Resources. Bulletin 64. 150 p.

Church, B.N. 1970. The Geology of The Owen Lake Area. British Columbia Department of Mines and Petroleum Resources. Geology, Exploration and Mining in British Columbia 1969; p. 122-148.

Church, B.N. 1971. Geology of the Owen Lake, Parrott Lakes and Goosly Lake area. British Columbia Department of Mines and Petroleum Resources. Geology, Exploration and Mining in British Columbia 1970; p. 119-125.

Church, B.N. 1972. Geology of the Buck Creek area, British Columbia Ministry of Energy, Mines and Petroleum Resources. Geology, Exploration and Mining in British Columbia; pp. 353-363.

Church, B.N. 1984. Geology of the Buck Creek Tertiary outlier. British Columbia Ministry of Energy, Mines and Petroleum Resources. Map H78 (1:100,000).

Church, B.N. and Barakso, J.J. 1990. Geology, lithogeochemistry and mineralization in the Buck Creek area, British Columbia. British Columbia Ministry of Energy, Mines and Petroleum Resources.Paper 1990-2.

Condie, K.C. 1989. Plate Tectonics and Crustal Evolution. Pergamnon Press, Oxford. 467 p.

Cowan, G.A. and Adler, H.H. 1976. The variability of the natural abundance of ^{235}U. Geochimica et Cosmochimica Acta. 40; 1487-1490.

Davis, D.W., Gray, J., Cumming, G.L., Baadsgaard, H. 1977. Determination of the ^{87}Rb constant. Geochimica et Cosmochimica Acta. 41; 1745-1749.

Diakow, L.J. and Mihalynuk, M. 1987. Geology of Whitesail Reach and Troitsa Lake Areas. British Columbia Ministry of Energy, Mines and Petroleum *Resources. Geological Fieldwork 1986.* Paper 1987-1. p. 171-179.

Diakow, L.J. and Koyanagi, V. 1988. Stratigraphy and Mineral Occurences of Chikamin Mountain and Whitesail Reach map areas. British Columbia Ministry of Energy, Mines and Petroleum Resources. Geological Fieldwork 1987. p. 155-168.

Dostal, J., Robichaud, D.A., Church, B.A. and Reynolds, P.H. 1998. Eocene Challis-Kamloops volcanism in central British-Columbia: an example from the Buck Creek basin. Canadian Journal of Earth Sciences. 35: 951-963.

Drobe, J.R. 1991. Petrology and Petrogenesis of the Ootsa Lake Group in the Whitesail Range, West-central British Columbia. Queen's University. Unpublished MSc thesis. 199 pages.

Duffel, S. 1959. Whitesail Lake Map-area, British Columbia. Geological Survey of Canada, Memoir 299, 119 pages.

Engebretson, D.C., Cox, A. and Gordon, R.G. 1985. Relative motions between oceanic and continental plates in the Pacific basin. Geological Society of America. Special Paper 206. 59 p.

Ewing, T.E. 1981a. Petrology and geochemistry of the Kamloops Group volcanics, British Columbia. Canadian Journal of Earth Sciences. 18;1478-1491.

Ewing, T.E. 1981b. Regional stratigraphy and structural setting of the Kamloops Group, south-central British Columbia. Canadian Journal of Earth Sciences. 18;1464-1477.

Farquharson, R.B. 1973. The petrology of Late Tertiary dolerite plugs in the South Cariboo region, British Columbia. Canadian Journal of Earth Science. 10; 205-225.

Faure, G. 1986. Principles of Isotope Geology (2nd edition). John Wiley and Sons, Inc. New York. 589 p.

Gabrielse, H. and Yorath, C.J. 1991. Chapter 22, Outstanding Problems. *In;* Geology of Cordilleran Orogen in Canada. (eds.) H. Gabrielse and C.J. Yorath; Geological Survey of Canada, Geology of Canada, no.4, p. 817-823.

Garner, E.L., Murphy, T.J., Gramlich, J.W., Paulsen, P.J. and Barnes, I.L. 1976. Absolute isotopic abundance ratios and the atomic weight of a reference sample of potassium. Journal of Research. U.S. National Bureau of Standards. Section A. 79A; 713-725.

Gill, J.B. 1981. Orogenic Andesites and Plate Tectonics. Springer, Berlin. 389 p.

Grainger, N.C. and Anderson, B.A. 1999. Geology of the Eocene Ootsa Lake Group in northern Nechako River and southern Fort Fraser map areas, central British Columbia. *in*; Current Research 1999-A, Geological Survey of Canada, p. 139-148.

Green, K.C. and Diakow, L.J. 1993. The Fawnie Range project – Geology of the Natalkuz Lake map area (93F/6) . British Columbia Ministry of Energy, Mines and Petroleum Resources. Geological Fieldwork 1992. Paper 1993-1. p. 57-67.

Harland, W.B., Armstrong, R.L., Cox, A.V., Craig, L.E., Smith, A.G. and Smith, D.G. 1990. A geological time scale 1989. Cambridge University Press. Cambridge, United Kingdom. 279 p.

Haskin, M.L., Synder, L.D. and Anderson, R.G. 1998. Tertiary Endako Group volcanic and sedimentary rocks at four sites in the Nechako River and Fort Fraser Map area, central British Columbia. In: Current Research 1998-A, Geological Survey of Canada. p.155-164.

Heaman, L.M., Erdmer, P., Thompson, R.I. and Daughtry, K.L. 1999. Preliminary U-Pb Geochronology Results from the Vernon area, British Columbia. *In;* Slave-NORthern Cordillera Lithoprobe Evolution (SNORCLE) and Cordilleran Tectonics Workshop. P.Erdmer and F.Cook (eds). Lithoprobe Report No 69. p. 196-200.

Heaman, L.M. and Machado, N. 1992.Timing and origin of midcontinent rift alkaline magmatism, North America: evidence from the Coldwell Complex. Contributions to Mineralogy and Petrology. 110; 289-303.

Hrudey, M.G., Struik, L.C. and Whalen, J.B. 1999. Geology of the Taltapin map area, central British Columbia. *in;* Current Research 1999-A. Geological Survey of Canada. p. 85-96.

Irvine, T.N. and Barager, W.R.A. 1971. A guide to the chemical classification of common volcanic rocks. Canadian Journal of Earth Science. 8;523-548.

Irving, E., Thorkelson, D.J. and Schiarizza, P. 1996. Large (1000 to 4000 km) northward movements of tectonic domains in the northern Cordillera, 83 to 45 Ma. Journal of Geophysical Research. 101; 17,901-17,916.

Jaffey, A.H., Flynn, K.F., Glendenin, L.F., Bentley, W.C., and Essling, A.M. 1971. Precision measurements of half-lives and specific activities or ^{235}U and ^{238}U. Physics Review. 4;1889-1906.

Johnson, R.W., MacKenzie, D.E. and Smith, I.E.M. 1978. Delayed partial melting of subduction-modified mantle in Papua New Guinea. Tectonophysics. 46; 197-216.

Krogh, T.E. 1973. A low-contamination method for hydrothermal decomposition of zircon and extraction of U and Pb for isotopic age determinations. Geochimica et Cosmochimica Acta. 37:485-494.

Krogh, T.E. 1982. Improved accuracy of U-Pb zircon ages by the creation of more concordant systems using an air abrasion technique. Geochimica et Cosmochimica Acta. 37; 485-494.

Lanphere, M.A. and Baadsgaard, H. 1997. The Fish Canyon tuff; a standard for geochronology. Eos. 78; 326.

LeBas, M.J., LeMaitre, R.W., Streckeisen, A. and Zanettin, B. 1986. A chemical classification of volcanic rocks based on the total alkali silica diagram. Journal of Petrology. 27; 745-750.

Leitch, C.H.B., Hood, C.T., Cheng, X. and Sinclair, A.J. 1992. Tip Top Hill volcanics: Late Cretaceous Kasalka Group rocks hosting Eocene epithermal base- and precious-metal veins at Owen Lake, west-central British Columbia. Canadian Journal of Earth and Atmospheric Sciences. 29: 854-864.

LeMaitre, R.W. 1989. A Classification of Igneous Rocks and Glossary of Terms. Blackwell, Oxford. 193 p.

Lowe, C. Enkin, R.J. and Dubois, J. 1998. Magnetic and paleomagnetic constraints on Tertiary deformation in the Endako region, central British Columbia. *in;* Current Research 1998-A. Geological Survey of Canada. p. 125-134.

Ludwig, K.R. 1998. Isoplot (Excel version). Berkeley Geochronology Center.

Lugmair, G.W. and Marti, K. 1978. Lunar initial ^{143}Nd/^{144}Nd: Differential evolution of the lunar crust and mantle. Earth and Planetary Science Letters. 35; 273-284.

MacIntyre, D.G., Webster, I.C.L. and Bellefontaine, K.A. 1996. Babine porphyry belt project: Bedrock geology of the Fulton Lake Map area (93L/16), British Columbia. *in;* Geological Fieldwork 1995. British Columbia Ministry of Employment and Investment. Paper 1996-1, p. 1-25.

MacIntyre, D.G., Webster, I.C.L., Villeneuve, M.E. 1997. Babine porphyry belt project: Bedrock geology of the Old Fort Mountain Area(93M/1), British Columbia. *in;* Geological Fieldwork 1996. British Columbia Ministry of Employment and Investment. Paper 1997-1, p. 47-67.

MacIntyre, D. G., Schiarizza, P. and Struik, L.C. 1998. Preliminary bedrock geology of the Tocha Lake map area (93K/13), British Columbia. *in;* Geological Fieldwork 1997. British Columbia Ministry of Employment and Investment. Paper 1998-1, p. 3-1 to 3-14.

Mahoney, B.J., Mustard, P.S., Haggart, J.W., Friedman, R.M., Fanning, M.C. and McNicoll, V.J. 1999. Archean zircons in Cretaceous strata of the western Cordillera; the "Baja BC" hypothesis fails a "crucial test". Geology. 27; 195-198.

Matthews, W.H. 1964. Potassium-Argon age determinations of Cenozoic volcanic rocks from British Columbia. Geological Society of America Bulletin, v. 75, pp. 465-468.

Matthews, W.H. 1989. Neogene Chilcotin basalts in south-central British Columbia: geology, ages and geomorphic history. Canadian Journal of Earth Sciences. 26; 969-982.

McDougall, I. And Harrison, T.M. 1988. Geochronology and thermochronology by the ^{40}Ar/^{39}Ar method. Oxford University Press, New York. 212 p.

McPhie, J., Doyle, M. and Allen, R. 1993. Volcanic textures: a guide to the interpretation of textures in volcanic rocks. University of Tasmania. 198 p.

Meschede, M. 1986. A method of discriminating between different types of mid-ocean ridge basalts and continental tholeiites with the Nb-Zr-Y diagram. Chemical Geology. 56; 207-218.

Miyashiro, A. 1974. Volcanic rocks series in island arcs and active continental margins. American Journal of Science. 274; 321-355.

Monger, J.W.H., Wheeler, J.O., Tipper, H.W., Gabrielse, H., Harms, T., Struik, L.C., Campbell, R.B., Dodds, C.J., Gehrels, G.E. and O'Brien, J. 1991. Part B. Cordilleran terranes. Chapter 8. Upper Devonian to Middle Jurassic assemblages. *In;* Geology of Cordilleran Orogen in Canada. (eds.) H. Gabrielse and C.J. Yorath; Geological Survey of Canada, Geology of Canada, no.4, p. 281-327.

Morris, G.A and Creaser, R.A. 1998. The petrogenesis of the Mount Skukum/Bennett Lak Igneous Complex, Yukon territory, and reflections on the Eocene tectonics of the Canadian Cordillera. *In;* Slave-NORthern Cordillera Lithoprobe Evolution (SNORCLE) and Cordilleran Tectonics Workshop. P.Erdmer and F.Cook (eds). Lithoprobe Report No 64. p. 165-169.

Morris, G.A. and Hooper, P.R. 1997. Petrogenesis of the Colville Igneous Complex, northeast Washington: Implications for Eocene tectonics in the northern U.S. Cordillera. Geology. 25; 831-834.

Neumann, W. and Huster, H. 1974. The half-life of ^{87}Rb measured as a difference between the isotopes ^{87}Rb and ^{85}Rb. Z. Physik. 270; 121-127.

Nicholls, J. 1988. The statistics of Pearce element diagrams and the Chayes closure problem. Contributions to Mineralogy and Petrology. 99;11-24.

Norman, M.D. and Leeman, W.P. 1989. Geochemical evolution of Cenozoic-Cretaceous magmatism and its relation to tectonic setting, southwestern Idaho, U.S.A. Earth and Planetary Science Letters. 94; 78-96.

Okulitch, A.V. 1995. Geological time scale, 1995. Geological Survey of Canada. Open File 3040 (National Earth Science series, Geological Atlas). 1 p.

Patchett, P.J., Gehrels, G.E. and Isachsen, C.E. 1998. Nd isotopic characteristics of metamorphic and plutonic rocks of the Coast mountains near Prince Rupert, British Columbia. Canadian Journal of Earth Sciences. 35; 556-561.

Paterson, S.R., Miller, R.B., Brandon, M.T. and Ague, J.J. 1998. Regional tilt of the Mount Stuart Batholith, Washington, determined using aluminum in hornblende barometry; implications for northward translation of Baja British Columbia; discussion and reply. Geological Society of America Bulletin. 110; 685-690.

Pearce, J.A. 1983. Role of the sub-continental lithosphere in magma genesis at active continental margins. *In;* Continental basalts and mantle xenoliths. C.J. Hawkesworth and M.J. Norry eds. Shiva Publishing Ltd. Cheshire, UK. p.230-272.

Pearce, J.A., Harris, N.B.W. and Tindle, A.G. 1984. Trace element discrimination diagrams for the tectonic interpretation of granitic rocks. Journal of Petrology. 25; 956-983.

Price, R.A., Monger, J.W.H. and Muller, J.E. 1981. Cordilleran cross-section, Calgary to Victoria. Field guides to geology and mineral deposits; Calgary '81 annual meeting. R.I. Thompson and D.G. Cook (eds.). Geological Association of Canada. p. 261-334.

Renne, P.R., Deino, A.L., Walter, R.C., Turrin, B.D., Swisher, C.C., Becker, T.A., Curtis, G.H., Sharp, W.D. and Jaouni, A.-R. 1994. Intercalibration of astronomical and radioisotopic time. Geology. 22:783-786.

Resnick, J. 1999. Neogene magmatism from the northern Nechako and Summit Lake map areas, British Columbia: implications for the petrology of the lithosphere. Unpublished BSc thesis. University of British Columbia. Vancouver, British Columbia. 105p.

Roddick, J.C. 1988. The assessment of errors in ^{40}Ar/^{39}Ar dating. *In;* Radiogenic age and isotopic studies. Report 2. Geological Survey of Canada. Paper 88-2. p. 7-16.

Rouse, G.E. and Matthews, W.H. 1988. Palynology and geochronology of Eocene beds from Cheslatta Falls and Nazko areas, central British Columbia: geology, ages and geomorphic history. Canadian Journal of Earth Sciences. 25; 1268-1276.

Russell, J.K. and Nicholls, J. 1988. Analysis of petrologic hypotheses with Pearce element ratios. Contributions to Mineralogy and Petrology. 99;25-35.

Samson, S.D., McClelland, W.C., Patchett, P.J., Gehrels, G.E. and Anderson, B.A. 1989. Evidence from neodymium isotopes for mantle contributions to Phanerozoic crustal genesis in the Canadian Cordillera. Nature. 337; 705-709.

Sellwood, S.M., Synder, L.D. and Anderson, B.A. 1998. Geology of two high-level Tertiary granite plutons, northern Nechako River map area, central British Columbia. *in;* Current Research 1999-A. Geological Survey of Canada, p. 149-156.

Smith, A.D. 1986. Isotopic and geochemical studies of Terrane I, South-Central British Columbia. Unpublished PhD thesis. University of Alberta. Edmonton, Alberta. 195 p.

Souther, J.G. 1977. Volcanism and tectonic environments in the Canadian Cordillera – a second look. *In;* Volcanic Regimes in Canada. (ed.) W.R.A. Barager, I.C. Coleman and J.M. Hall. Geological Association of Canada. Special Paper 16; p. 3-24.

Souther, J.G. 1991. Chapter 14, Volcanic Regimes. *In;* Geology of Cordilleran Orogen in Canada. (eds.) H. Gabrielse and C.J. Yorath; Geological Survey of Canada, Geology of Canada, no.4, p. 457-490.

Stacey, J.S. and Kramers, J.D. 1975. Approximation of the terrestrial lead isotope evolution by a two-stage model. Earth and Planetary Science Letters. 26:207-221.

Steiger, R.H. and Jäger, E. 1977. Subcomission on Geochronology: Concention on the use of decay constants in geo- and cosmochronology. Earth and Planetary Science Letters. 36: 359-362.

Stevens, R.D., Delabio, R.N. and Lachance, G.R. 1982. Age determinations and geological studies, K-Ar isotope ages; in Report 15; Geological Survey of Canada, Paper 81-2, p.8-9.

Stock, J. and Molnar,P. 1988. Uncertainties and implications of the late Cretaceous and Tertiary position of North America relative to the Farallon, Kula and Pacific plates. Tectonics. 7; 1339-1384.

Struik, L.C. 1993. Intersecting intracontinent Tertiary transform fault systems in the North American Cordillera. Canadian Journal of Earth Sciences. 30; 1262-1274.

Struik, L.C. and Orchard, M.J. 1998. Cache Creek Group: Its stratigraphy, structural stacking and paleoenvironment, central British Columbia. *In;* New Geological Constraints on Mesozioc to Tertiary Metallogenesis and on Mineral Exploration in central British Columbia: Nechako NATMAP project; Geological Association of Canada, Cordilleran Section, March 27, 1998, Short Course notes.

Struik, L.C., Whalen, J.B., Letwin, J.M. and L'Heureux, R.L. 1997. General Geology of southeast Fort Fraser map area, central British Columbia. *in;* Current Research 1997-A. Geological Survey of Canada. p.65-75.

Struik, L.C., Anderson, R.G. and Plouffe, A. 1999. Geology of the Euchiniko map area, central British Columbia. *in;* Current Research 1999-A. Geological Survey of Canada. P.119-128.

Suh, C. 1999. Petrology, chemistry and geothermometry of ultramafic xenoliths from the North Nechako River area, British Columbia, and the nature of the underlying mantle. Unpublished BSc thesis. University of British Columbia. Vancouver, British Columbia. 81 p.

Sun, S.-s. and McDonough, W.F. 1989. Chemical and isotopic systematics of oceanic basalts: implications for mantle composition and processes. *In;* Magmatism in the Ocean Basins. (eds.) Saunders,A.D. and Norry, M.J. Geological Society Special Publication 42. Pp. 313-345.

Thompson, R.I., Erdmer, P., Daughtry, K.L., Heaman, L. and Creaser, R.A. 1999. Tracking North American Basement west of the Okanagan Valley: insights from the Vernon, Ashcroft and Hope map areas. *In;* Slave-NORthern Cordillera Lithoprobe Evolution (SNORCLE) and Cordilleran Tectonics Workshop. P.Erdmer and F.Cook (eds). Lithoprobe Report No 69. p. 195.

Tipper, H.W. 1955. Nechako River, British Columbia. Geological Survey of Canada, Paper 54-11.

Tipper, H.W. 1963. Nechako River Map-area, British Columbia. Geological Survey of Canada, Memoir 324, 59 pages.

Tipper, H.W. and Richards, T.A. 1976. Jurassic stratigraphy and history of north-central British Columbia. Geological Survey of Canada. Bulletin 270. 73 p.

Vandall, T.A. and Palmer, H.C. 1989. Upper limit of docking time for Stikinia and Terrane I: paleomagnetic evidence from the Eocene Ootsa Lake Group, British Columbia. Canadian Journal of Earth Sciences. 27; 212-218.

Villeneuve, M.E. and MacIntyre, D.G. 1997. Laser ^{40}Ar/^{39}Ar ages of the Babine porphyries and Newman Volcanics, Fulton Lake map area, west-central British Columbia. *in;* Radiogenic Age and Isotopic Studies: report 10; Geological Survey of Canada, Current Research 1997-F, p.131-139.

Wanless, R.K. 1974. Age determinations and geological studies, K-Ar isotopic ages; in Report 11; Geological Survey of Canada, Paper 73-2, p.22-23.

Ward, P.D., Hurtado, J.M., Kirschivink, J.L. and Verosub, K.L. 1997. Measurements of the Cretaceous paleolatitude of Vancouver Island; consistent with the Baja-British Columbia hypothesis. Science. 277; 1642-1645.

Wetherup, S. 1997. Geology of the Nulki Hills and surrounding area, central British Columbia. *In;* Current Research 1997-A. Geological Survey of Canada. p.125-132.

Wetherup, S. and Struik, L.C. 1996. Vanderhoof Metamorphic Complex and surrounding rocks, central British Columbia. *In;* Current Research 1996-A. Geological Survey of Canada. p.63-70.

Whalen, J.B., Struik, L.C. and Hrudey, M.G. 1998. Bedrock geology of the Endako map area, central British Columbia. *in;* Current Research 1998-A. Geological Survey of Canada, p.113-123.

Wood, D.A. 1980. The application of a Th-Hf-Ta diagram to problems of tectonomagmatic classification and to establishing the nature of crustal contamination of basaltic lavas of the British Tertiary volcanic province. Earth and Planetary Science Letters. 50; 11-30.

Woodsworth, G.J., Anderson, R.G. and Armstrong, R.L. 1991. Chapter 15, Plutonic Regimes. *In;* Geology of Cordilleran Orogen in Canada. (eds.) H. Gabrielse and C.J. Yorath; Geological Survey of Canada, Geology of Canada, no.4, p. 491-531.

Yorath, C.J. 1991. Chapter 9; Upper Jurassic to Paleogene Assemblages. *In;* Geology of Cordilleran Orogen in Canada. (eds.) H. Gabrielse and C.J. Yorath; Geological Survey of Canada, Geology of Canada, no.4, p. 331-371.

Appendix I - Compilation of Published ages for the Ootsa Lake Group, Endako Group, Babine Igneous Suite, Nanika intrusions and correlative rocks

Age [1]	Mineral [2]	Unit [3]	Lithology	Rock Description	NTS Sheet	Lat	Long	Reference
Whitesail map area (NTS 93E)								
31.3 ± 1.2	WR	Ee	basalt	aphyric lava flow	93E10	53°43.89'	126°48.96'	Diakow and Koyanagi 1988
38.7 ± 3.1	WR	Ee	basalt	fine grained, fresh, black basalt with zoned plag crystals, small cpx & rare olivine	93E12	53°44.0'	127°47.1'	Stevens et al. 1982
41.7 ± 1.5	WR	Ee	basalt	remnant of columnar jointed aphyric laval	93E10	53°37.15'	127°01.27'	Diakow and Koyanagi 1988
41.9 ± 5	WR	Ee	basalt	fine grained, fresh, olivine basalt	93E1	53°01.2'	126°20.3'	Stevens et al. 1982
47.1 ± 2.7 [a]	PLAG	Eolv	tuff	ash-flow tuff	93E10			Drobe 1991
49.1 ± 1.7	BIOT	Eolv	rhyodacite	overlies platy basalt/tuff	93E10	53°37.06'	127°01.34'	Diakow and Koyanagi 1988
49.4 ± 0.2 [a]	WR	Eolv	tuff	ash-flow tuff	93E10			Drobe 1991
49.8 ± 1.7	BIOT	Eolv	tuff	crystal ash tuff interbed within a platy plagiocalse basaltic flow; overlies dacite	93E10	53°38.60'	126°53.18'	Diakow and Koyanagi 1988
49.8 ± 1.7	BIOT	Eolv	dacite	biotite phyric dacitic flow; bottom of section	93E10	53°37.46'	126°59.89'	Diakow and Koyanagi 1988
50 ± 1.7	BIOT	Eolv	andesite	vitrophyric andesite flow overlies rhyodacite	93E10	53°39.20'	126°46.54'	Diakow and Koyanagi 1988
50.4 ± 0.8 [a]	PLAG	Eolv	tuff	ash-flow tuff	93E10			Drobe 1991
55.6 ± 2.5	BIOT	Eolv	dacite	light grey dacite with biotite and calcite, chlorite & zeolite filled amygdules	93E15	53°52.5'	126°30.6'	Stevens et al. 1982
51.3 ± 1.8	PLAG	Eoli	andesite	porphryritic andesite sill; intrudes andesite	93E10	53°35.48'	127°04.16'	Drobe 1991
47.7 ± 1.5	BIOT	Enni	quartz diorite		93E14			Carter 1981
47.9 ± 3	BIOT	Enni	porphyry	quartz latite porphyry	93E14			Carter 1981
48.9 ± 3	BIOT	Enni	porphyry	quartz latite porphyry	93E14			Carter 1981
49.9 ± 2	BIOT	Enni	porphyry	quartz monzonite porphyry	93E6			Carter 1981
49.9 ± 3	BIOT	Enni	porphyry	quartz monzonite porphyry	93E6			Carter 1981
50.8 ± 2.1	BIOT	Enni	quartz diorite	metamorphosed	93E14			Carter 1981
50.9 ± 1.7	WR	Enni	biotite hornfels		93E6			Carter 1981
50.9 ± 3	BIOT	Enni	porphyry	quartz monzonite porphyry	93E6			Carter 1981
51.4 ± 2.2	BIOT	Enni	granite	porphyritic granite	93E8	53°23.5'	126°23'	Stevens et al. 1982

53 ± 3	BIOT	Enni	porphyry	quartz monzonite porphyry	93E14			Carter 1981
53 ± 3	WR	Enni	biotite hornfels		93E14			Carter 1981
Nechako River map area (NTS 93F)								
36.5 ± 1.6	WR	Ee	lava		93F10	53°38.5'	124°57.0'	Rouse and Mathews 1988
37.7 ± 1.3	WR	Ee			93F10	53°38.8'	124°56.5'	Rouse and Mathews 1988
42.7 ± 1.5	WR	Ee			93F10	53°34.4'	124°52'	Rouse and Mathews 1988
42.7 ± 1.6	WR	Ee			93F16	53°50.5'	124°28.3'	Rouse and Mathews 1988
43.1 ± 1.6	WR	Ee			93F16	53°50.5'	124°28.3'	Rouse and Mathews 1988
43.7 ± 1.5	WR	Ee			93F16	53°50.5'	124°29'	Rouse and Mathews 1988
47.6 ± 1.7	WR	Ee	basalt		93F10	53°38.5'	124°56.4'	Rouse and Mathews 1988
48.9 ± 1.8	WR	Ee			93F10	53°37.5'	124°51.8'	Rouse and Mathews 1988
48.3 ± 1.7	WR	Eolv	rhyolite	spherulitic and flow banded rhyolite flow	93F3	53°11'50"	125°27'15"	Andrew 1988
49.9 ± 1.7	WR	Eolv	tuff	crystal tuff	93F3	53°11'15"	125°29'30"	Andrew 1988
47.6 ± 1.7	WR	Eoli	rhyolite	coarse-grained rhyolite porphyry	93F3	53°11'15"	125°29'30"	Andrew 1988
Vanderhoof map area (NTS 93G)								
46.5 ± 1.6	WR	Ee			93G13	53°57.9'	123°43.2'	Rouse and Mathews 1988
Fort Fraser map area (NTS 93K)								
49.3 ± 2	BIOT	Ee	lava		93K3	54°07.3'	125°19.0'	Mathews 1964
54.4 ± 2	BIOT	Eolv	dacite		93K4	54°03.5'	125°57.1'	Mathews 1964
48 ± 5 [a]	WR	Eolv	basalt		93L8	54°21.60'	126°12.14'	Dostal 1998
Smithers map area (NTS 93L)								
48.9 ± 1.8	WR	Eolv		lavas and pyroclastic rocks	93L1	54°09.4'	126°18.1'	Church 1972
49 ± 2 [a]	WR	Eolv	basalt		93L8	54°27.40'	126°18.75'	Dostal 1998
50 ± 1 [a]	WR	Eolv	basalt		93L8	54°20.81'	126°07.36'	Dostal 1998
52 ± 1 [a]	WR	Eolv	basalt		93L8	54°26.66'	126°20.39'	Dostal 1998
49.7 ± 1.3	BIOT	Eoli	syenomonzonite		93L1	54°11.4'	126°15.4'	Church 1970
50.3 ± 1.5	BIOT	Eoli	syenomonzonite		93L2	54°07.3'	126°36.0'	Church 1972
50.4 ± 1.8	WR	Eoli	basalt	diabase dyke	93L2			Leitch. et al. 1992
51.3 ± 1.8	WR	Eoli		amygdular dyke	93L2			Leitch. et al. 1992
51.9 ± 1.8	WR	Eoli		bladed feldspar porphyry dyke	93L2			Leitch. et al. 1992
57.2 ± 3	BIOT	Eoli	granite		93L1	54°11.2'	126°16.8'	Church 1970
49.6 ± 1.9	BIOT	Enni	quartz monzonite		93L15			Carter 1981

50.8 ± 2.3	WR	Enni	biotite hornfels		93L4			Carter 1981
53.9 ± 2.2	BIOT	Enni	quartz monzonite		93L2			Carter 1981
57.2 ± 2.3	BIOT	Enni	porphyry	quartz monzonite porphyry	93L1			Carter 1981
45.1 ± 2	BIOT	Eni	porphyry	biotite feldspar porphyry	93L16	54°56.11'	126°13.93'	Wanless et. al. 1974
46.8 ± 2.7	HB	Eni	porphyry	hornblende feldspar porphyry	93L16	54°58.03'	126°24.52'	Wanless et. al. 1974
50.2 ± 3	HB	Eni	porphyry	hornblende feldspar porphyry	93L16	54°55.70'	126°27.50'	Wanless et. al. 1974
50.2 ± 3	BIOT	Eni	porphyry	hornblende biotite feldspar porphyry	93L16	54°55.70'	126°27.50'	Wanless et. al. 1974
50.7 ± 2.1	BIOT	Eni	porphyry	biotite feldspar porphyry	93L16			Carter 1981
51.1 ± 2.1	BIOT	Eni	vein	quart-biotite sulphide vein	93L16			Carter 1981
51.2 ± 0.6 [a]	BIOT	Eni	porphyry	hornblende biotite feldpsar porphyry	93L16			Villeneuve and MacIntyre 1997
51.5 ± 0.5 [a]	BIOT	Eni	porphyry	hornblende biotite feldpsar porphyry	93L16			Villeneuve and MacIntyre 1997
51.7 ± 0.6 [a]	HB	Eni	porphyry	hornblende biotite feldpsar porphyry	93L16			Villeneuve and MacIntyre 1997
51.9 ± 2	BIOT	Eni	porphyry	biotite feldspar porphyry	93L16			Carter 1981
51.9 ± 2	BIOT	Eni	porphyry	biotite feldspar porphyry	93L16			Carter 1981
51.9 ± 3	BIOT	Eni	porphyry	biotite feldspar porphyry	93L16			Carter 1981
52.4 ± 1.9	BIOT	Eni	porphyry	hornblende feldspar porphyry	93L16			Carter 1981
56 ± 3	BIOT	Eni	porphyry	biotite feldspar porphyry	93L16			Carter 1981
49.9 ± 0.6 [a]	HB	Env	porphyry	columnar jointed hornblende porphyry flow or sill	93L16			Villeneuve and MacIntyre 1997
51.3 ± 0.6 [a]	HB	Env	porphyry	hornblende feldpsar porphyry	93L16			Villeneuve and MacIntyre 1997
52.6 ± 0.6 [a]	HB	Env	porphyry	medium to fine grained hornblende feldpsar porphyry	93L16			Villeneuve and MacIntyre 1997
Hazelton map area (NTS 93M)								
49.8 ± 1.5	BIOT	Eni	porphyry	biotite feldspar porphyry	93M1			Carter 1981
49.9 ± 2	BIOT	Eni	porphyry	biotite feldspar porphyry	93M1			Carter 1981
53 ± 2	BIOT	Eni	porphyry	bioitite quartz monzonite	93M1			Carter 1981
53.1 ± 2.1	BIOT	Eni	porphyry	biotite feldspar porphyry	93M1			Carter 1981

[1] Errors are 2σ. Ages have been corrected to conform with the decay constant of Steiger and Jäger (1977). All ages are K/Ar determinations unless indicated as Ar/Ar ([a]).

[2] Material analyzed is; WR=whole rock, BIOT=biotite, HB=hornblende

[3] Units designation is: Ee=Endako Group, Eolv=Ootsa Lake Group volcanics, Eoli=Ootsa Lake Group intrusion, Env=Newman volcanics, Eni=Babine intrusion, Enni=Nanika intrusion

Appendix II – Sample Locations

Sample Number	Unit[1]	NTS Sheet	Latitude	Longitude
AT-97-1601B	Ee	93F10	53.682	124.925
ATH-97-0103	Ee	93K2	54.093	124.605
ATH-97-0113	Ee	93K2	54.093	124.605
ATH-97-0202	Ee	93F10	53.573	124.952
ATH-97-0215	Ee	93F10	53.573	124.952
ATH-97-0216	Ee	93F10	53.579	124.952
ATH-97-0304A	Ee	93F15/16	53.828	124.549
ATH-97-0313	Ee	93F15/16	53.833	124.533
ATH-97-0402	Ee	93F15/16	53.839	124.478
ATH-97-0406	Ee	93F15/16	53.837	124.478
ATS-97-1702B	Ee	93F15	53.775	124.677
ATS-97-1702C	Ee	93F15	53.775	124.677
ATG-98-2403	Eni	93L6	54.919	126.231
ATG-98-2401	Env	93L6	54.957	126.168
ATG-98-2402	Env	93L6	54.930	126.212
ATSS-98-0406	Eoli	93F14	53.943	125.401
AT-98-2702	Eolv	93F11	53.676	125.346
AT-98-2705	Eolv	93F11	53.671	125.349
ATG-98-0201	Eolv	93F14	53.836	125.471
ATG-98-0309	Eolv	93F14	53.956	125.036
ATG-98-0401	Eolv	93K12	54.759	125.685
ATG-98-0406	Eolv	93K12	54.748	125.705
ATG-98-0703	Eolv	93F15	53.835	124.671
ATG-98-1201	Eolv	93F13	53.828	125.600
ATG-98-1305	Eolv	93K4	54.161	125.640
ATG-98-1307	Eolv	93K4	54.082	125.724
ATG-98-1403	Eolv	93F13	53.853	125.636
ATG-98-1502	Eolv	93F13	53.837	125.504
ATG-98-1901	Eolv	93F15	53.829	124.681
ATG-98-2202	Eolv	93K7	54.279	124.896
ATG-98-2302	Eolv	93F11	53.561	125.418
ATG-98-2701	Eolv	93F11	53.562	125.420
ATG-98-3104	Eolv	93F12	53.645	125.679
ATG-98-3304	Eolv	93F12	53.654	125.727
ATG-98-3310	Eolv	93F12	53.665	125.739
ATG-98-3401	Eolv	93F12	53.648	125.969
ATG-98-3605	Eolv	93F12	53.641	125.707
ATG-98-4201	Eolv	93K5	54.432	125.673
ATH-97-0301	Eolv	93F15/16	53.813	124.573
ATS-97-1701B	Eolv	93F15	53.773	124.678

SCB-98-4603-2	Eolv	93F8	53.316	124.304
SCBG-98-0101	Eolv	93K7	54.279	124.882

[1] Unit abreviations: Ee – Endako Group; Eol – Ootsa Lake Group; En – Babine Igneous Suite where v = volcanic and i = intrusion.

Appendix III - Analytical results of geochemical analyses

Sample #	SiO_2	TiO_2	Al_2O_3	Fe_2O_3T	Fe_2O_3	FeO	MnO	MgO	CaO	Na_2O	K_2O	H_2OT	CO_2T	P_2O_5	TOTAL	Ag	Ba	Be
							(wt. %)[1]										(ppm)[1]	
Newman Volcanics																		
ATG-98-2401	59.10	0.73	15.40	5.50	3.50	1.8	0.09	3.18	5.50	4.20	2.42	2.5	1.9	0.33	100.9	-	1176	1.3
ATG-98-2402	60.10	0.77	16.40	5.70	3.60	1.9	0.08	3.21	5.52	4.30	2.36	1.6	0.3	0.32	100.8	-	1096	1.5
ATG-98-2403	60.50	0.70	15.90	6.30	4.40	1.7	0.06	2.74	4.87	4.10	2.51	2.0	0.4	0.28	100.2	-	944	1.5
Ootsa Lake Group																		
AT-98-2702	68.00	0.69	14.20	3.50	1.50	1.8	0.07	0.85	2.18	4.20	4.37	2.7	0.1	0.18	100.9	-	1396	2.5
AT-98-2705	61.60	1.12	16.00	4.90	4.10	0.7	0.08	1.43	2.93	4.40	4.73	2.0	0.3	0.42	100.2	0.2	2130	1.5
ATG-98-0201	77.30	0.18	11.70	1.20	1.00	0.2	0.02	0.12	0.14	3.80	4.91	0.6	0.1	0.02	100.1	0.1	44	4.7
ATG-98-0309	68.60	0.55	15.40	2.60	2.20	0.3	0.01	0.36	2.04	4.00	4.15	2.1	0.3	0.32	100.7	0.1	1503	2.3
ATG-98-0401	61.50	0.74	14.90	5.00	4.30	0.7	0.05	2.73	4.02	4.40	3.81	2.2	0.1	0.50	100.3	-	2476	2.0
ATG-98-0406	54.80	0.98	14.40	7.70	6.80	0.8	0.10	5.14	6.85	3.70	2.79	2.6	0.3	0.61	100.4	0.1	2247	1.7
ATG-98-0703	66.80	0.58	15.90	3.00	2.90	-	0.06	0.82	1.85	4.80	4.75	1.1	0.2	0.18	100.2	-	1876	2.8
ATG-98-1201	65.50	0.89	15.30	4.50	2.60	1.7	0.11	1.20	2.47	4.60	4.61	0.7	0.2	0.31	100.4	0.2	1718	2.5
ATG-98-1305	78.30	0.13	10.90	0.90	0.70	0.2	0.04	0.16	0.45	3.30	4.52	1.3	0.1	0.02	100.1	-	113	4.9
ATG-98-1307	79.80	0.11	10.80	0.50	0.30	0.2	0.02	0.11	0.26	3.10	4.64	0.8	0.4	0.02	100.7	-	50	5.3
ATG-98-1403	64.60	0.82	15.90	4.10	2.80	1.1	0.08	1.01	2.34	4.60	5.03	1.1	0.2	0.23	100.1	0.2	2568	2.0
ATG-98-1502	75.70	0.30	12.00	1.50	1.20	0.2	0.05	0.16	0.37	3.90	5.26	0.8	0.1	0.02	100.1	0.1	67	2.8
ATG-98-1502-B	76.40	0.32	12.10	1.40	1.20	0.2	0.05	0.15	0.37	3.90	5.23	0.8	0.1	0.02	100.9	0.1	53	2.7
ATG-98-1901A	76.30	0.18	12.00	1.10	0.70	0.3	0.04	0.16	0.37	3.60	4.96	1.1	0.2	0.02	100.0	-	36	4.6
ATG-98-2202A	65.80	0.79	15.80	4.00	3.70	0.3	0.05	1.18	2.58	4.40	4.21	1.4	0.1	0.29	100.9	0.3	2156	2.5
ATG-98-2302	61.30	0.93	15.50	6.70	3.60	2.8	0.08	2.20	5.25	3.40	3.00	2.0	0.1	0.49	100.9	0.2	1391	1.8
ATG-98-2701	74.20	0.26	12.70	1.80	0.70	1.0	0.03	0.35	0.23	1.00	8.63	1.2	0.2	0.07	100.9	0.1	1854	1.8
ATG-98-3104E	71.40	0.26	13.40	2.10	1.10	0.9	0.05	0.51	1.56	3.50	4.63	3.0	0.1	0.07	100.7	-	1049	2.0
ATG-98-3310	74.90	0.26	12.90	0.80	0.40	0.3	0.00	0.14	0.91	3.40	5.26	1.1	0.2	0.06	100.1	0.2	2193	2.0
ATG-98-3401	76.90	0.10	12.40	1.10	0.50	0.5	0.05	0.17	0.56	3.40	5.08	0.7	0.1	0.02	100.6	-	176	6.8
ATG-98-3401-B	76.90	0.11	12.50	1.10	0.60	0.5	0.05	0.18	0.59	3.40	5.08	0.7	0.2	0.02	100.9	0.1	184	7.1
ATG-98-3605	76.90	0.09	12.30	0.90	0.80	-	0.01	0.09	0.61	3.50	4.88	0.9	0.1	0.01	100.5	-	55	3.6
ATG-98-4201	77.30	0.18	12.10	1.20	0.60	0.5	0.03	0.23	0.51	3.40	5.18	0.5	0.2	0.02	100.8	-	264	4.1
SCB98-4603-2	69.20	0.76	12.80	3.60	2.80	0.7	0.04	1.45	3.53	3.70	2.22	2.2	0.1	0.39	100.2	-	1235	1.1
Comparative analysis - Nass R. Basalt																		
R-65	47.00	3.60	14.40	16.60	3.00	12.2	0.22	4.37	7.73	4.10	1.88	0.2	0.2	1.21	100.4			
R-65[2]	47.55	3.54	14.58		9.32	6.18	0.20	4.31	7.67	4.00	1.92	0.2		1.28	100.8			
Absolute error	0.5	0.02	0.2		0.06	0.2	0.01	0.04	0.01	0.03	0.05	0.1	0.1	0.01		5	20	0.5

[1] Samples below detection are indicated by "-". Bi and Cd were analyzed, but found to be below detection levels for all samples

[2] Analyzed at the University of Alberta by H. Baadsgaard, 1964 (unpublished data)

Co	Cr	Cs	Cu	Ga	Hf	In	Mo	Nb	Ni	Pb	Rb	Sb	Sc	Sn	Sr	Ta	Te	Th	Tl	U
									(ppm)[1]											
26	76	0.58	12	19.00	3.30	0.05	1.1	9.90	45	7	50.00	-	10.0	0.9	978	0.82	-	5.80	0.27	2.40
44	65	0.50	33	20.00	3.60	-	1.4	11.00	36	8	49.00	0.2	11.0	1.0	980	1.20	-	4.60	0.24	2.30
28	40	1.20	34	19.00	3.30	0.05	1.4	9.70	27	10	58.00	0.3	11.0	2.0	722	0.87	-	5.90	0.26	2.80
67	-	2.90	-	18.00	8.60	0.06	5.7	20.00	-	16	140.00	0.3	7.5	1.9	246	2.00	-	14.00	0.93	5.60
32	11	1.60	-	19.00	13.00	0.07	2.3	21.00	-	11	78.00	8.5	13.0	2.0	334	1.30	0.2	7.20	0.41	2.40
83	-	2.10	-	16.00	7.50	0.11	2.3	40.00	-	17	170.00	0.6	2.7	5.6	-	2.90	-	21.00	0.98	8.20
38	11	4.00	19	20.00	4.70	-	1.3	16.00	-	11	110.00	0.3	4.7	0.9	620	1.30	-	9.50	0.65	5.60
25	49	2.10	18	19.00	4.40	0.06	1.1	14.00	46	23	72.00	-	8.8	1.0	1400	1.10	-	12.00	0.26	5.50
42	180	1.20	71	17.00	3.70	0.09	1.3	10.00	86	14	52.00	-	17.0	7.1	1470	0.81	-	6.80	0.07	2.70
61	-	1.20	-	18.00	7.00	-	2.6	19.00	-	19	120.00	-	4.9	1.8	407	1.70	-	11.00	0.82	3.20
33	-	1.60	-	19.00	11.00	0.09	2.0	34.00	-	15	110.00	-	10.0	2.9	314	2.20	-	12.00	0.53	3.90
69	-	4.10	-	15.00	4.10	-	3.0	36.00	-	11	190.00	0.2	2.2	1.1	33	3.00	-	22.00	0.74	9.90
78	-	2.60	-	15.00	4.00	-	2.7	34.00	-	13	210.00	0.3	2.2	0.8	-	3.40	-	22.00	0.74	4.40
31	-	1.40	-	19.00	13.00	0.08	1.6	24.00	-	15	94.00	0.2	10.0	2.3	357	1.60	-	9.70	0.52	3.40
75	-	3.70	-	18.00	10.00	0.05	3.6	34.00	-	12	140.00	0.3	4.2	2.2	-	2.70	-	17.00	0.97	7.90
76	-	3.70	-	17.00	10.00	0.07	3.6	33.00	-	12	140.00	0.4	4.2	2.4	-	2.80	-	17.00	0.96	8.00
33	-	1.20	-	16.00	5.70	-	1.4	33.00	-	12	180.00	-	2.7	1.9	-	2.50	-	20.00	1.10	4.00
60	-	1.40	31	19.00	7.00	0.07	2.9	22.00	-	14	110.00	0.3	6.8	3.0	694	2.00	-	13.00	0.20	5.30
39	14	0.86	25	19.00	6.70	0.08	2.0	19.00	11	14	84.00	0.4	12.0	1.8	545	1.40	-	9.50	0.42	3.10
99	-	6.50	-	12.00	5.20	-	3.0	13.00	-	15	190.00	3.2	3.6	2.6	155	2.40	-	19.00	1.60	5.80
52	-	4.20	-	15.00	5.40	-	4.7	12.00	-	14	170.00	0.3	4.1	1.3	171	1.70	-	19.00	1.30	5.80
96	-	2.50	-	16.00	8.80	-	2.4	15.00	-	18	100.00	0.6	5.8	1.4	143	1.50	-	8.60	0.67	3.20
90	-	8.70	-	17.00	4.90	-	3.3	28.00	-	21	310.00	0.3	3.3	2.6	44	4.20	-	43.00	1.90	16.00
89	-	8.60	-	17.00	4.90	0.05	3.4	28.00	-	21	310.00	0.3	3.3	4.4	45	4.20	-	41.00	1.90	16.00
118	-	3.80	-	16.00	3.90	-	2.6	17.00	-	16	250.00	0.4	2.3	2.4	12	2.20	-	26.00	1.50	6.60
92	-	3.40	-	16.00	4.30	-	3.0	25.00	-	13	210.00	0.3	3.0	1.6	42	3.30	-	24.00	1.10	8.20
32	14	2.80	25	16.00	3.10	-	1.0	7.70	21	8	36.00	-	7.7	0.6	1180	0.94	-	3.30	0.16	1.50
5	10	0.02	10	0.10	0.05	0.05	5	0.05	10	10	0.05	0.2	0.5	0.5	10	0.2	0.02	0.02	0.02	0.02

V	Zn	Zr	Ce	Dy	Er	Eu	Gd	Ho	La	Lu	Nd	Pr	Sm	Tb	Tm	Y	Yb
							(ppm)^1										
114	57	138.0	60.0	2.50	1.20	1.40	3.40	0.49	32.0	0.20	28.0	7.60	4.90	0.46	0.19	14.00	1.30
121	54	152.0	53.0	2.70	1.40	1.30	3.80	0.53	28.0	0.22	26.0	6.80	4.90	0.49	0.21	15.00	1.40
113	52	132.0	45.0	2.60	1.40	1.20	3.30	0.53	24.0	0.23	21.0	5.70	4.10	0.46	0.21	15.00	1.50
39	52	383.0	92.0	6.40	3.70	1.70	6.90	1.30	49.0	0.61	41.0	12.00	7.90	1.10	0.58	41.00	4.00
82	92	708.0	150.0	7.30	4.00	3.00	9.40	1.50	84.0	0.64	67.0	19.00	12.00	1.30	0.60	42.00	4.00
-	66	244.0	67.0	7.10	4.40	0.16	6.30	1.50	40.0	0.75	35.0	11.00	7.30	1.10	0.71	47.00	5.10
42	61	214.0	53.0	1.70	0.77	1.10	2.70	0.30	31.0	0.12	23.0	6.50	3.80	0.33	0.10	9.60	0.70
96	55	183.0	100.0	3.30	1.60	2.20	5.60	0.62	54.0	0.26	49.0	14.00	8.30	0.71	0.23	19.00	1.50
128	64	148.0	99.0	4.40	2.20	2.50	6.90	0.84	49.0	0.32	50.0	14.00	9.20	0.87	0.31	24.00	2.00
23	57	292.0	89.0	3.30	1.80	1.60	4.30	0.64	48.0	0.32	36.0	11.00	6.10	0.62	0.28	19.00	2.00
45	79	517.0	130.0	9.10	5.30	2.50	9.90	1.90	69.0	0.86	60.0	17.00	12.00	1.60	0.82	57.00	5.60
-	16	100.0	62.0	4.30	3.20	0.26	3.50	1.00	34.0	0.68	20.0	6.90	3.90	0.65	0.58	34.00	4.50
-	16	100.0	66.0	4.70	3.50	0.25	3.90	1.10	36.0	0.73	22.0	7.50	4.50	0.72	0.62	37.00	4.80
50	72	680.0	130.0	7.10	4.20	2.80	8.70	1.50	73.0	0.71	56.0	17.00	11.00	1.30	0.63	43.00	4.30
-	46	440.0	150.0	18.00	9.00	0.59	21.00	3.60	72.0	1.10	83.0	22.00	22.00	3.30	1.30	92.00	7.80
-	46	427.0	160.0	19.00	8.80	0.58	20.00	3.60	73.0	1.10	85.0	22.00	22.00	3.20	1.20	93.00	7.70
-	24	172.0	79.0	2.50	1.90	0.24	2.30	0.57	38.0	0.48	20.0	7.10	3.20	0.41	0.36	16.00	2.90
88	61	340.0	100.0	4.10	2.20	2.20	5.80	0.81	54.0	0.37	43.0	13.00	7.60	0.78	0.33	24.00	2.20
122	77	303.0	94.0	5.40	3.00	1.90	6.70	1.10	49.0	0.47	42.0	12.00	8.10	0.98	0.44	32.00	3.00
13	29	226.0	71.0	3.30	1.90	0.90	3.80	0.69	40.0	0.33	27.0	8.10	4.90	0.60	0.30	21.00	2.10
20	34	221.0	64.0	3.90	2.40	0.78	4.10	0.84	34.0	0.45	25.0	7.60	4.80	0.66	0.40	26.00	2.90
19	20	447.0	100.0	5.50	3.10	2.00	6.70	1.10	55.0	0.54	47.0	13.00	8.80	1.00	0.48	31.00	3.40
-	26	127.0	69.0	8.10	5.60	0.25	6.70	1.80	33.0	1.10	29.0	8.50	7.00	1.20	0.95	62.00	7.00
-	27	128.0	67.0	8.30	5.50	0.23	6.60	1.90	32.0	1.00	28.0	8.30	7.10	1.20	0.95	61.00	7.10
-	22	90.0	41.0	4.40	3.00	0.27	3.80	0.99	21.0	0.62	18.0	5.30	4.20	0.70	0.54	33.00	4.00
5	23	150.0	70.0	4.00	2.70	0.39	3.80	0.90	40.0	0.55	25.0	8.00	4.40	0.65	0.47	29.00	3.60
96	53	127.0	62.0	2.20	0.98	1.60	3.80	0.40	31.0	0.14	32.0	8.20	5.80	0.47	0.13	12.00	0.82
5	5	10	0.1	0.02	0.02	0.02	0.02	0.02	10	0.02	0.1	0.02	0.02	0.02	0.02	5	0.5

Appendix IV - Analytical results of laser $^{40}Ar/^{39}Ar$ analyses

Power (W)	[illegible]	[illegible]	[illegible] x10-11cm3 STP[b]	[illegible]	[illegible]	[illegible] ^{40}Ar	[illegible] (Ma)			(%)
ATG-98-3193 Biotite; J=.00200100										
Aliquot: A										
3.8	0.8151	0.1235	0.3279	3.9954	298.0764	80.8	50.97	±	3.60	1.1
5.0	0.1879	0.2125	1.1089	13.6234	253.2308	21.9	51.64	±	0.34	3.6
6.2	0.2787	1.0706	3.5324	42.5446	703.0119	11.7	51.91	±	0.12	11.3
7.8	0.2758	11.8216	11.0802	110.5659	1695.1905	4.8	51.93	±	0.14	29.4
12.0	0.0367	7.8627	4.6210	40.2897	595.4021	1.8	51.63	±	0.11	10.7
Aliquot: B										
3.8	0.5556	0.0889	0.1603	1.8416	186.8454	87.9	43.88	±	6.86	0.5
5.0	0.2295	0.3703	1.6779	20.4784	364.2093	18.6	51.51	±	0.24	5.4
6.2	0.0561	1.8263	2.8429	31.9962	478.9240	3.5	51.42	±	0.18	8.5
6.9	0.0346	2.8574	3.1557	32.7431	481.4689	2.1	51.22	±	0.14	8.7
7.5	0.0271	2.2791	2.4741	25.5442	376.4279	2.1	51.33	±	0.19	6.8
8.1	0.0233	1.7443	1.3881	13.2785	198.3842	3.5	51.33	±	0.21	3.5
8.8	0.0230	1.3229	0.9281	8.7620	132.3915	5.1	51.01	±	0.28	2.3
12.0	0.0330	3.9951	3.2427	31.0660	456.0866	2.1	51.13	±	0.14	8.3
Total[c]	**2.5764**	**35.575**	**36.540**	**376.729**	**6219.650**	**12.2**	**51.56**	**±**	**0.51**	
ATG-98-3194 Biotite; J=.00199960										
Aliquot: A										
3.7	0.5831	0.0480	0.0995	0.7335	178.8893	96.3	32.07	±	9.90	0.4
5.0	0.0737	0.2327	0.8140	5.5069	95.4754	22.8	47.64	±	0.37	3.3
6.2	0.0943	3.3998	4.6484	28.2596	411.7680	6.8	48.35	±	0.20	16.9
6.9	0.0586	2.8706	4.0414	25.2460	361.6506	4.8	48.54	±	0.15	15.1
7.4	0.0497	2.6080	3.9695	24.2835	344.3321	4.3	48.32	±	0.16	14.6
7.8	0.0208	0.8615	1.4164	8.5918	122.0023	5.0	48.00	±	0.20	5.2
12.0	0.0165	0.5434	0.8951	5.4367	78.9256	6.2	48.48	±	0.45	3.3
Aliquot: B										
3.7	0.4200	0.0330	0.0214	0.0828	125.6050	98.8	64.51	±	311.92	0.1
5.2	0.0528	0.0814	0.1376	0.7020	26.3125	59.3	54.22	±	3.80	0.4
6.2	0.0385	0.5490	0.7934	3.9280	64.5616	17.6	48.19	±	0.62	2.4
6.9	0.0470	1.3609	1.7664	9.4918	142.0436	9.8	48.06	±	0.27	5.7
7.4	0.0607	1.2894	2.5783	16.0739	236.1054	7.6	48.31	±	0.28	9.6
7.9	0.0295	0.5905	1.1301	7.1440	105.1601	8.3	48.05	±	0.16	4.3
8.6	0.0336	0.3709	1.4975	10.3387	149.4696	6.6	48.04	±	0.19	6.2
9.3	0.0263	0.3318	1.1981	8.1926	118.7900	6.5	48.23	±	0.26	4.9
12.0	0.0427	2.3829	2.4004	12.8956	186.6796	6.8	48.05	±	0.14	7.7
Total[c]	**1.6478**	**17.554**	**27.408**	**166.907**	**2747.771**	**17.7**	**48.21**	**±**	**0.51**	
ATG-98-0491 Whole Rock; J=.00199750										
Aliquot: A										
2.3	2.5312	0.4457	0.0307	1.2027	764.4568	97.8	48.70	±	16.22	2.3
3.1	0.0422	1.5400	0.0299	5.4913	93.9423	13.3	52.69	±	0.28	10.3
3.8	0.0275	2.0256	0.0482	9.2550	144.8065	5.6	52.45	±	0.12	17.3
4.6	0.0208	1.2366	0.0653	4.8763	76.6824	8.0	51.39	±	0.39	9.1
5.6	0.0174	3.6926	0.2892	3.0532	49.7823	10.3	51.93	±	0.59	5.7
7.0	0.0208	6.5422	0.3008	1.3711	25.8286	23.7	51.04	±	0.91	2.6
12.0	0.0194	0.9730	0.0831	0.7593	16.4596	34.7	50.27	±	1.60	1.4
Aliquot: B										
2.0	3.0531	0.6416	0.0375	1.7209	921.2236	97.9	39.41	±	33.87	3.2
2.9	0.0449	0.7212	0.0116	2.3983	47.8298	27.8	51.18	±	0.89	4.5
3.4	0.0503	2.2500	0.0415	9.8165	161.5555	9.2	53.06	±	0.31	18.3
4.0	0.0196	1.0537	0.0312	5.1230	80.4799	7.2	51.79	±	0.37	9.6
4.6	0.0269	1.4162	0.1047	4.4595	72.5208	11.0	51.43	±	0.55	8.3
12.0	0.0630	5.4472	0.3244	4.0350	75.6809	24.6	50.27	±	0.44	7.5
Total[c]	**5.9371**	**27.986**	**1.398**	**53.562**	**2531.249**	**69.3**	**51.52**	**±**	**1.25**	

[illegible] Biotite; J=.00199550										
Aliquot: A										
3.4	0.2718	0.0347	0.0138	0.2489	81.7811	98.2	20.94	±	32.67	0.4
5.1	0.0541	0.0430	0.1658	1.2475	34.8679	45.9	53.67	±	2.14	1.9
6.2	0.0651	0.0626	1.1004	8.2242	142.5808	13.5	53.20	±	0.52	12.7
6.9	0.0270	0.0418	0.7381	5.6428	92.8979	8.6	53.38	±	0.52	8.7
7.4	0.0295	0.0573	1.0272	8.1737	130.9109	6.7	53.03	±	0.23	12.7
7.9	0.0239	0.0467	0.4573	3.5303	59.6055	11.8	52.81	±	0.40	5.5
8.9	0.0494	0.0197	0.1296	0.9602	28.7819	50.7	52.42	±	1.17	1.5
12.0	0.1829	0.0266	0.1098	0.7093	64.7741	83.5	53.59	±	6.56	1.1
Aliquot: B										
3.8	0.8225	0.0719	0.0372	0.6868	245.2423	99.1	11.49	±	21.17	1.1
5.2	0.0708	0.0533	0.1280	1.1115	37.5256	55.7	53.03	±	1.58	1.7
6.2	0.1015	0.1328	0.8465	6.3026	127.0303	23.6	54.59	±	0.36	9.8
6.9	0.0455	0.0608	0.4426	3.2919	62.6252	21.5	53.01	±	0.65	5.1
7.4	0.0605	0.0780	1.0004	7.2344	126.1456	14.2	53.09	±	0.67	11.2
8.4	0.0704	0.1250	1.7129	12.4704	208.5514	10.0	53.40	±	0.27	19.3
12.0	0.1973	0.5286	0.7184	4.7442	129.9257	44.9	53.54	±	0.89	7.4
Total*	**2.0722**	**1.383**	**8.628**	**64.579**	**1573.246**	**38.9**	**52.79**	**±**	**0.60**	
ATG-98-[illegible] Whole Rock; J=.00196[illegible]										
Aliquot: A										
2.3	0.5414	1.2211	0.0285	2.4118	189.0536	84.6	42.29	±	3.08	6.5
2.7	0.0538	1.1798	0.0095	3.4520	65.6685	24.2	50.47	±	0.62	9.3
3.4	0.0220	1.5437	0.0205	3.9112	62.9661	10.3	50.53	±	0.26	10.5
4.0	0.0256	1.2610	0.0311	2.8397	47.0962	16.1	48.76	±	0.67	7.6
4.6	0.0506	3.5549	0.1370	3.4964	63.5002	23.5	48.65	±	0.35	9.4
12.0	0.0669	6.0379	0.1923	3.7194	71.1294	27.8	48.38	±	0.45	10.0
Aliquot: B										
2.0	0.3450	0.2430	0.0135	0.3473	105.3592	96.8	34.46	±	20.98	0.9
2.3	0.1266	0.8584	0.0125	1.8711	59.7426	62.6	41.88	±	1.71	5.0
2.7	0.0586	0.8183	0.0067	2.7621	55.4683	31.2	48.40	±	0.87	7.4
3.4	0.0200	1.0138	0.0098	2.7509	44.8657	13.2	49.60	±	0.52	7.4
4.0	0.0255	1.2463	0.0384	2.5120	42.6522	17.7	48.97	±	0.56	6.7
4.6	0.0409	2.2079	0.0801	2.9153	52.3266	23.1	48.35	±	0.46	7.8
12.0	0.0674	6.5712	0.1881	4.2912	79.5252	25.0	48.67	±	0.23	11.5
Total*	**1.4443**	**27.757**	**0.768**	**37.280**	**939.354**	**45.4**	**48.17**	**±**	**0.57**	
ATG-98-[illegible] Biotite; J=.00199280										
Aliquot: A										
3.2	0.1178	0.0112	0.0142	0.1693	35.0393	99.4	4.80	±	35.30	0.5
3.9	0.0212	0.0082	0.0405	0.4370	11.9325	52.4	46.12	±	2.39	1.3
5.1	0.0282	0.0142	0.3041	3.0181	49.5737	16.8	48.46	±	0.34	8.8
6.3	0.0308	0.0277	0.4982	5.1594	79.7351	11.4	48.56	±	0.29	15.0
8.0	0.0270	0.0352	0.4746	4.7430	72.6079	11.0	48.33	±	0.33	13.8
12.1	0.0174	0.0107	0.2477	2.6036	40.5796	12.7	48.28	±	0.72	7.6
Aliquot: B										
3.8	0.7736	0.0691	0.3788	3.8456	279.2153	81.9	46.72	±	2.03	11.2
5.0	-2504370	-835.860	6.40E+10	-6.00E+12	########	-0.5	-0.09	±	0.00	100.0
6.2	0.1529	0.1747	1.0475	10.8342	192.5443	23.5	48.25	±	0.42	31.4
7.1	0.0913	0.0678	0.1936	1.9756	54.3076	49.7	49.08	±	1.01	5.7
7.8	0.0680	0.0112	0.0772	0.9533	33.1292	60.6	48.54	±	1.97	2.8
12.0	0.0720	0.0078	0.0737	0.7249	30.9823	68.6	47.57	±	3.55	2.1
Total*	**1.4002**	**0.438**	**3.350**	**34.464**	**879.647**	**47.0**	**47.96**	**±**	**0.59**	

ATG-[illegible] Biotite; J=.00198758										
Aliquot: A										
1.6	0.0340	0.0050	-0.0007	0.0072	10.3625	97.0	150.1	±	2599.4	0.0
2.2	0.0506	0.0071	0.0026	0.0101	15.4999	96.4	189.5	±	6051.3	0.0
3.4	0.0170	0.0072	0.0125	0.0993	6.4632	77.6	51.47	±	22.95	0.4
3.8	0.0113	0.0077	0.0222	0.1755	5.7698	57.7	49.15	±	10.20	0.8
4.3	0.0110	0.0095	0.0570	0.4667	9.4789	34.3	47.20	±	1.53	2.1
5.0	0.0230	0.0091	0.1179	0.9800	19.7506	34.4	46.80	±	1.21	4.4
5.5	0.0133	0.0070	0.0684	0.5385	11.0180	35.6	46.64	±	1.63	2.4
6.2	0.0136	0.0256	0.2799	2.2497	33.7524	11.9	46.76	±	0.49	10.0
7.0	0.0127	0.0165	0.1270	1.0108	17.0559	21.9	46.62	±	1.38	4.5
7.8	0.0136	0.0253	0.1306	1.0959	18.3952	21.8	46.45	±	0.71	4.9
12.0	0.0143	0.0208	0.4438	3.6589	52.6070	8.0	46.80	±	0.51	16.3
Aliquot: B										
3.1	0.0844	0.0060	0.0380	0.3049	29.1782	85.5	49.12	±	8.55	1.4
3.8	0.0165	0.0105	0.0665	0.5611	12.8355	38.0	50.17	±	2.46	2.5
5.0	0.0302	0.0444	0.3030	2.5279	42.4472	21.0	46.93	±	0.62	11.2
6.2	0.0257	0.0497	0.3679	3.2052	50.3134	15.1	47.15	±	0.46	14.2
7.7	0.0404	0.0160	0.3827	3.2434	55.0720	21.7	47.06	±	0.39	14.4
11.9	0.0217	0.0106	0.2721	2.3801	37.8186	16.9	46.73	±	0.51	10.6
Total[d]	**0.4333**	**0.278**	**2.691**	**22.515**	**427.818**	**29.9**	**47.12**	**±**	**3.11**	

a:Nominal power as measured by laser

b: Gas quantities corrected for decay, isotopes derived from interfering neutron reactions

c: Errors are analytical only and do not reflect error in irradiation parameter J

d: Integrated age, uncertainty includes error in J (0.5%)

e: Nominal J, referenced to FCT-SAN=28.03 Ma (Renne et al., 1994)

Appendix V

Geology of the Eocene Ootsa Lake Group in northern Nechako River and southern Fort Fraser map areas, central British Columbia[1]

N.C. Grainger[2] and R.G. Anderson
GSC Pacific, Vancouver

Grainger, N.C. and Anderson, R.G., 1999: Geology of the Eocene Ootsa Lake Group in northern Nechako River and southern Fort Fraser map areas, central British Columbia; in *Current Research 1999-A; Geological Survey of Canada, p. 139–148.*

Abstract: Eocene Ootsa Lake Group in northern Nechako River map area comprises variegated, flow-laminated rhyolitic flows and domes, crystal and lithic-crystal tuff, less common pyroclastic and autoclastic breccia, and minor dacite and andesite flows. Rotated rhyolite clasts, flow folding, vesicles, perlite and spherulites, and minor lithophysae and eutaxitic textures and phenocrysts of plagioclase, biotite, alkali feldspar, quartz, and rare hornblende are distinctive.

A local stratigraphy comprises basal hornblende-plagioclase porphyritic andesite with distinctive amethyst-bearing amygdules, medial flow-laminated rhyolite flow rocks and breccia, and upper felsic tuff and breccia. Distinct rhyolite ash-lignite beds mark the top of the unit and in addition to glassy quenched flow bases and reworking of lithic rhyolite tuff units, suggest local shallow-water environments.

The Dayeezcha Mountain, Henson Hills, and Mackenzie Lake study areas provide the most complete stratigraphy. Ongoing petrographic, geochronological, geochemical, and isotopic tracer studies will elucidate the age, correlation, composition, tectonic setting, and petrogenesis of the unit.

Résumé : Le Groupe d'Ootsa Lake de l'Éocène, dans le nord de la région cartographique de la rivière Nechako, comporte des coulées et dômes rhyolitiques bariolés à litage de flux, des tufs cristallins et cristallolithiques, des brèches pyroclastiques et autoclastiques moins abondantes ainsi que des coulées de dacite et d'andésite en quantités mineures. Des clastes de rhyolite hélicitiques, des plis ptygmatiques, des vacuoles, de la perlite et des sphérulites, des lithophyses et textures eutaxitiques en quantités mineures, ainsi que des phénocristaux de plagioclase, de biotite, de feldspath alcalin, de quartz et de rare hornblende sont caractéristiques.

La stratigraphie locale comprend à la base des andésites porphyriques à hornblende et plagioclase avec des amygdales à améthyste caractéristiques, puis des coulées de roches et de brèches rhyolitiques à litage de flux et enfin, des brèches et tufs felsiques. Des lits distincts de rhyolite à cendres et lignite marquent le sommet de l'unité et, avec les bases de coulées vitreuses figées rapidement et les unités de tufs à rhyolite lithique remaniées, suggèrent des milieux locaux d'eau peu profonde.

Les régions d'étude du mont Dayeezcha, des collines Henson et du lac Mackenzie offrent la stratigraphie la plus complète. Les études pétrographiques, géochronologiques et géochimiques et celles des marqueurs isotopiques en cours permettront de définir l'âge, la corrélation, la composition, le cadre tectonique et la pétrogenèse de cette unité.

---

[1] Contribution to the Nechako NATMAP Project

[2] Department of Earth and Atmospheric Sciences, University of Alberta, #1-26 Earth Sciences Building, Edmonton, Alberta T6G 2E3

INTRODUCTION

Eocene mafic and felsic volcanic rocks dominate the geology of northern Nechako River (NTS 93F) and southern Fort Fraser (NTS 93 K) map areas (e.g. Armstrong, 1949; Tipper, 1963; Bellefontaine et al., 1995; Williams, 1997). Paleogene Ootsa Lake and Endako group rocks were included in the Kamloops assemblage by Wheeler and McFeely (1991) and considered to represent a transtensional volcanic arc (e.g. Souther, 1991). Locally, the volcanic rocks are well known and dated (e.g. Struik et al., 1997; Villeneuve and MacIntyre, 1997; Anderson and Snyder, 1998; Anderson et al., 1998; Struik, 1998; Struik and Whalen, 1998; Whalen et al., 1998). Similarly, extensional tectonics coeval with some or all of the volcanism in the area is well documented (e.g. Wetherup and Struik, 1996; Wetherup, 1997, 1998). However, regionally, the felsic component of the Eocene magmatism, represented in the rocks of the Ootsa Lake Group, continues to be poorly known and understood. Moreover, the relationships amongst the sequence of magmatism and the timing and structural style of extensional tectonics remain unresolved.

Fieldwork undertaken in 1998 sought to better define the nature, timing, and petrogenesis of the Ootsa Lake Group and is the basis of a M.Sc. thesis by the senior author. This study will also contribute to two objectives of the Nechako NATMAP Project, 1) to test the hypothesis that the Eocene magmatic complex represents the tectonic and magmatic expression of an Eocene regional extensional event and 2) to improve our understanding of the potential for precious metal, epithermal and intrusion-related copper-gold and molybdenum deposits related to felsic magmatism (Andrew, 1988; Struik and McMillan, 1996).

PREVIOUS WORK AND STRATIGRAPHIC NOMENCLATURE

Previous and recent mapping first recognized the felsic volcanic Ootsa Lake Group in and around the study area (Armstrong, 1949; Tipper, 1955, 1963; Church, 1972; Kimura et al., 1980; Diakow et al., 1997; Struik et al., 1997; Wetherup, 1997; Anderson and Snyder, 1998; Anderson et al., 1998; T. Richards, pers. comm., 1998). The unit was first defined by Duffell (1959), who proposed the name Ootsa Lake Group for an Upper Cretaceous to late Oligocene series of mainly felsic flows with minor basalt, andesite, tuff, breccia, and rare conglomerate within the Whitesail Lake map area (NTS 93 E) to the west of the study area (Fig. 1). He correlated the unit with Eocene–Oligocene volcanic rocks, sedimentary rocks, and Upper Cretaceous or younger volcanic rocks of Armstrong (1949) within the Fort St. James and Fort Fraser map areas (Duffell, 1959). The Ootsa Lake Group was subsequently subdivided into rhyolite and andesite units within the Nechako River map area by Tipper (1955, 1963). Diakow and Mihalynuk (1987) refined the stratigraphy within the Whitesail Lake map area to include a sequence of basalt to rhyodacite flows and tuff.

Recent mapping, as part of the Nechako NATMAP Project (Fig. 1), has identified granitic to monzogranitic plutons associated with felsic and lesser intermediate to mafic units within the Ootsa Lake Group (Wetherup and Struik, 1996; Anderson and Snyder, 1998; Anderson et al., 1999). Distinguishing units within the Ootsa Lake Group from similar Cretaceous volcanic rocks has proven difficult (e.g. Anderson et al., 1999), as has making the distinction between mafic rocks of the Eocene Endako Group and the Neogene Chilcotin Group rocks within the map areas (e.g. Haskin et al., 1998; Resnick et al., 1999). Efforts to determine the internal stratigraphy of units within the Ootsa Lake Group are hampered by limited exposure which rarely reveals relationships between units and the integral, discontinuous nature of subunits (e.g. as thin and/or localized flows).

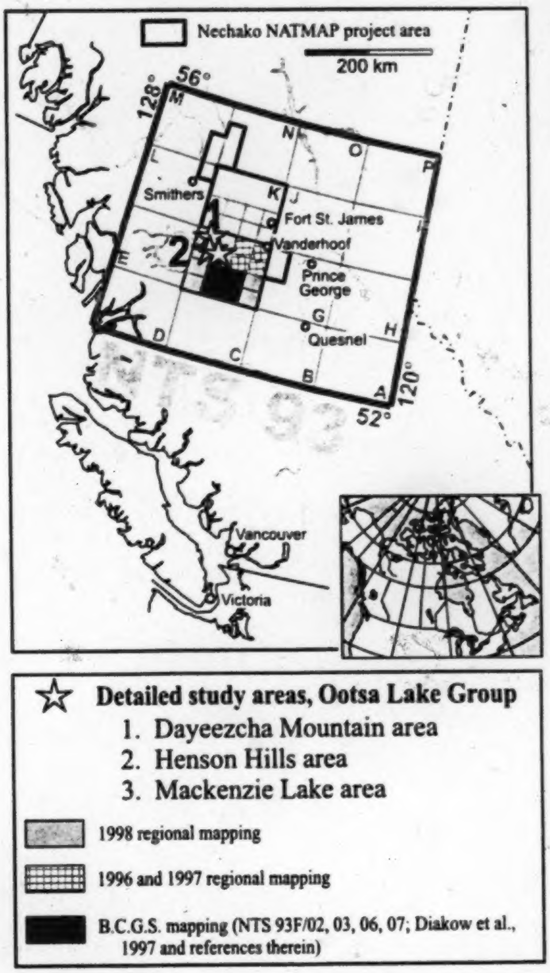
Nechako NATMAP project area
200 km
56°
128°
M
N
O
P
L
K
J
I
Smithers
Fort St. James
Vanderhoof
Prince George
1
2
E
D
C
B
A
G
H
Quesnel
120°
52°
Vancouver
Victoria
☆ Detailed study areas, Ootsa Lake Group
1. Dayeezcha Mountain area
2. Henson Hills area
3. Mackenzie Lake area
1998 regional mapping
1996 and 1997 regional mapping
B.C.G.S. mapping (NTS 93F/02, 03, 06, 07; Diakow et al., 1997 and references therein)

***Figure 1.** Location of study areas within Nechako NATMAP bedrock mapping area.*

Regional K-Ar age dates for the Ootsa Lake Group range from 54.0 to 47.6 Ma within the Fort Fraser and Nechako River map areas and from 55.6 to 47.4 Ma within the neighbouring Whitesail Lake (NTS 93 E) and Smithers (NTS 93 L) map areas (Fig. 2). Age dating within the Whitesail Range determined a significantly more restricted period of volcanism at 50 ± 1 Ma based on six age dates with only one anomalous date of 47.4 ± 2.7 Ma (Diakow and Koyanagi, 1988; Drobe, 1991). Similarly, recent Ar-Ar dating within the Hallett Lake map area (93 F/15) has identified a more restricted age range of Ootsa Lake Group volcanism ca. 53–51 Ma based on eight age dates (M. Villeneuve, unpub. data *in* Anderson et al., 1998).

The Ootsa Lake Group regionally has been characterized as a subalkaline to mildly alkaline and calc-alkaline series of rocks (Souther, 1977; 2 samples). Compositions in northeastern Nechako River map area are similar but show an additional bimodal and high potassium geochemical character (Anderson et al., 1998; 12 samples); rhyolite is silicic, enriched in the large ion lithophile elements and has rare-earth element (REE) patterns characterized by negative europium anomalies and light REE fractionation relative to heavy REEs.

Drobe (1991) concluded that the Ootsa Lake Group in the Whitesail Lake map area was likely formed from melting and mixing of lower crustal material with melts fluxed from the mantle, and further modified by fractionation. The model may not describe the Eocene magma generation within the Nechako River and Fort Fraser map areas because of the dissimilar nature of the volcanic rocks in the two areas. In addition, the genetic relationship of the Ootsa Lake Group magmatism with the local and preceding Late Cretaceous volcanic magmatism, nearby coeval Newman volcanism, coeval plutonic rocks, the subsequent Endako volcanism, and the regional Eocene extensional event (e.g. Souther, 1991; Struik, 1993; Wetherup and Struik, 1996; Wetherup, 1997) remains unclear.

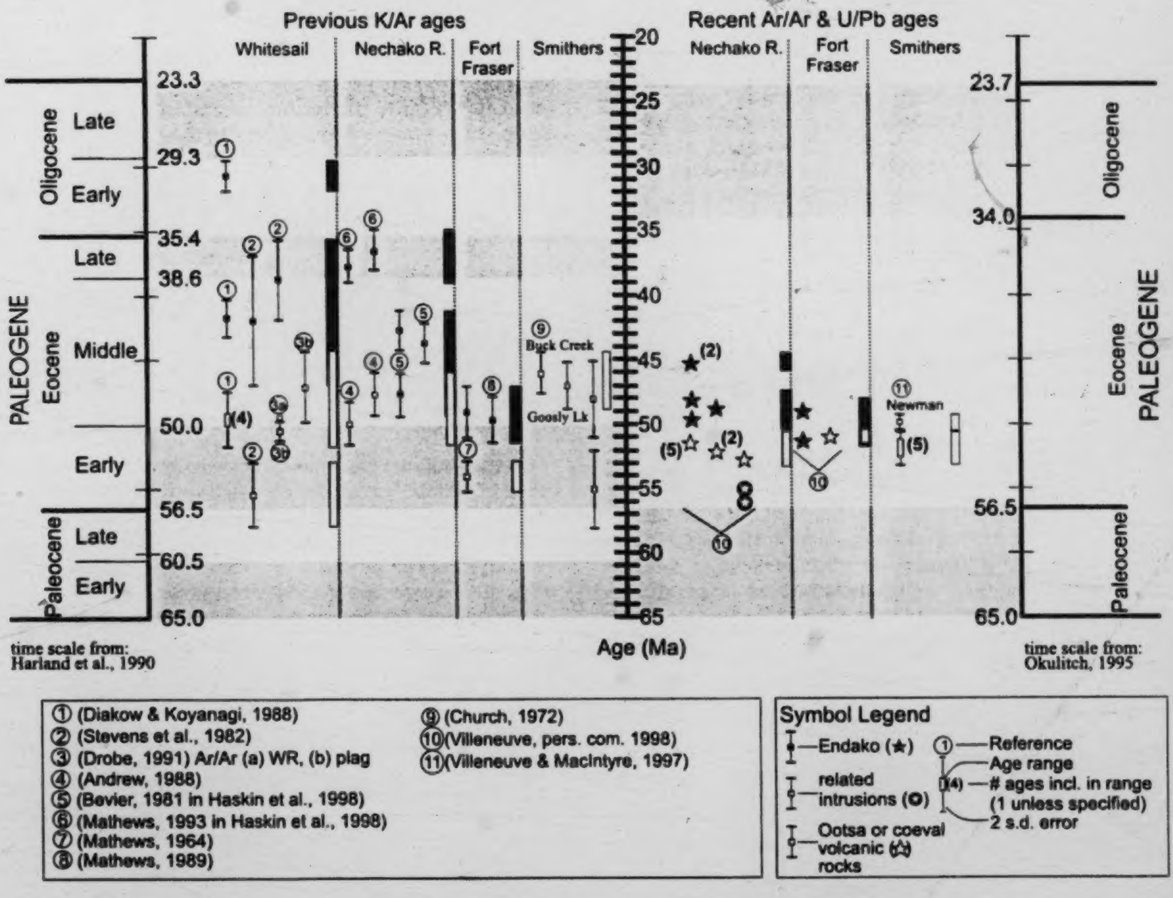

Figure 2. Regional age compilation for the Ootsa Lake and Endako groups and coeval intrusive rocks.

PHYSIOGRAPHY, ACCESS, AND FIELD METHODS

The study area is typical of the Interior Plateau, characterized by low-relief physiography, entirely below the treeline. Parts of the study area are accessible by provincial and municipal roads, but access is primarily via the regional network of logging roads and boat access from numerous lakes within the study area.

Thirty-six traverses were completed during June–August 1998 by the senior author to outcrops of Eocene rocks. Standard geological field mapping procedures were augmented by the use of global positioning systems to locate sites to within 50–100 m and the use of an Exploranium KT-9 Kappameter to obtain magnetic susceptibility measurements of units for correlation with potential geophysical data (Struik and MacMillan, 1996).

This report describes the composition and stratigraphy of the Ootsa Lake Group rocks observed regionally and within three study areas in the Nechako River map area. The following three areas of detailed study (Fig. 3) were chosen because they contained relatively extensive and continuous outcrop of units within the Ootsa Lake Group: 1) the Dayeezcha Mountain area in central-eastern part of Takysie Lake (NTS 93 F/13) and western Knapp Lake map areas (NTS 93 F/14), 2) Henson Hills area in north-central and eastern section of the Marilla map area (NTS 93 F/12), and 3) the Mackenzie Lake area, west-central portion of Cheslatta Lake map area (NTS 93 F/11). Samples were collected for additional studies at these sites and throughout the southern Fort Fraser and northern Nechako River map areas to provide regional coverage. Additional samples were collected from associated, presumably coeval, high-level plutons (e.g. Anderson and Snyder, 1998; Anderson et al., 1998; Barnes and Anderson, 1999; Sellwood et al., 1999).

Petrographical study, age dating, major and trace geochemical analyses, and isotopic tracer (Sr, Nd, Pb) studies are planned for subsets of the samples. Geochronological studies will involve U-Pb (on zircon) and/or Ar-Ar (on biotite) age dating to examine the timing, potential correlation, and duration of magmatic activity. A subset of samples collected for geochemistry will be analyzed for tracer isotopes, to investigate the role of crustal contamination in the origin of the Ootsa Lake Group. A suite of samples from the Newman volcanics (e.g. Villeneuve and MacIntyre (1997) and references therein) were also collected to compare their geochemical and isotopic compositions with the Ootsa Lake Group samples.

GEOLOGY

The Ootsa Lake Group consists of a heterogenous assemblage of felsic and less common intermediate volcanic flow and volcaniclastic rocks. The most abundant rock types described below characterize the regional distribution of the unit and the three study areas, Dayeezcha Mountain, Henson Hills, and Mackenzie Lake areas (Fig. 3), which themselves are distinguished stratigraphically.

Regional setting and composition of the Ootsa Lake Group

The regional geology of the northern Nechako River and southern Fort Fraser map areas is described by Struik et al. (1997), Wetherup (1997, 1998), and Anderson et al. (1998, 1999). The Ootsa Lake Group within the area is predominantly composed of rhyolite flows and domes, crystal and lithic-crystal tuff, pyroclastic and autoclastic breccia, and minor dacite and andesite flows. Approximately half of the Ootsa Lake Group consists of flows; subequal abundances of tuff and breccia are subordinate.

The predominant rock type is a generally red to white to grey, locally purple or green, flow-laminated rhyolite, which occurs as flows or less common domes and is widespread throughout the northern Nechako River map area. Outcrop-scale features include minor, locally rotated, rhyolite clasts (Fig. 4), primary flow folding, minor vesicles, perlitic or spherulitic textures, and minor lithophysae. Textures vary abruptly; for example, a unit may change from a flow-laminated rhyolite to rhyolite autobreccia within a few metres. Monolithic breccia containing flow-laminated clasts are generally found associated with rhyolite flows and domes. Generally the rocks are aphyric or sparsely plagioclase-phyric, and biotite, alkali feldspar, quartz, and/or rare hornblende are minor phenocryst phases.

Flow-layered or more massive rhyolite and rhyodacite flows also exhibit many of the same features in addition to microspherulites (Fig. 5) and locally abundant lithophysae. Flows are porphyritic (Fig. 6) to rarely aphyric. Several exposures of buff, flow-laminated rocks have black, glassy, perlitic flow bases (Fig. 7) which suggest the presence of shallow water at the time of extrusion.

Pyroclastic breccias are predominately unwelded to densely welded ignimbrite deposits, usually crystal rich, commonly containing lithic fragments and lesser portions of medium- to dark-grey pumiceous lapilli in a white to buff rhyolite, locally darker and glassy. Lithic fragments are angular, predominantly aphyric rhyolite and range in size from 1 cm to (more rarely) 40 cm. Black glass fragments are abundant in one locality. Autoclastic breccias are commonly moderately silicified and composed of flow-laminated rhyolite clasts (1–8 cm) in a slightly glassy, sparsely phyric matrix.

Rhyolite hyaloclastite is found on the west flank of Uncha Mountain (Fig. 8; *see also* Barnes and Anderson, 1999) and east of the Henson Hills area. Clasts are dark maroon to grey or black, glassy angular fragments of rhyolite, rarely exhibit a perlitic texture, and occur within a white to pale yellow rhyolitic matrix. Clast size varies from several centimetres up to 2 m at one locality. The most widespread type of breccia is a lapillistone with angular tuffaceous or flow-laminated rhyolite clasts in a glassy grey or tuffaceous rhyolitic matrix.

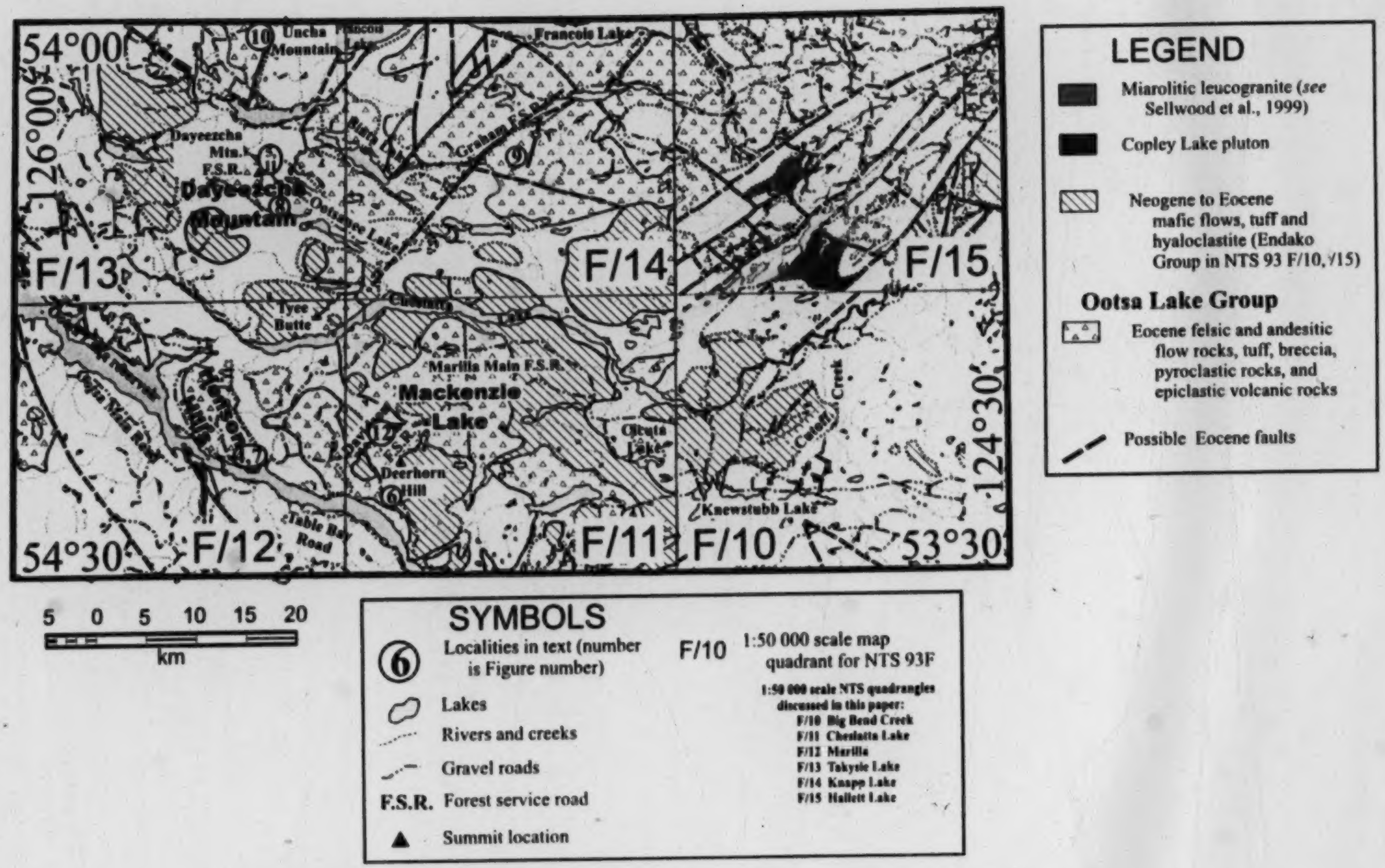
54°00
126°00
Uncha Mountain
Francois Lake
Dayeezcha Mtn. F.S.R.
Dayeezcha Mountain
Ootsanee Lake
Graham F.S.R.
F/13
F/14
F/15
Tyee Butte
Cheslatta Lake
Marilla Main F.S.R.
Mackenzie Lake
Henson Hills
Ootsa Main Road
Deerhorn Hill
Table Bay Road
Chedakuz Creek
Knewstubb Lake
124°30
54°30
F/12
F/11
F/10
53°30
10
11
8
9
12
6
7
5 0 5 10 15 20
km
LEGEND
Miarolitic leucogranite (see Sellwood et al., 1999)
Copley Lake pluton
Neogene to Eocene mafic flows, tuff and hyaloclastite (Endako Group in NTS 93 F/10, F/15)
Ootsa Lake Group
Eocene felsic and andesitic flow rocks, tuff, breccia, pyroclastic rocks, and epiclastic volcanic rocks
Possible Eocene faults
SYMBOLS
⑥ Localities in text (number is Figure number)
Lakes
Rivers and creeks
Gravel roads
F.S.R. Forest service road
▲ Summit location
F/10 1:50 000 scale map quadrant for NTS 93F
1:50 000 scale NTS quadrangles discussed in this paper:
F/10 Big Bend Creek
F/11 Cheslatta Lake
F/12 Marilla
F/13 Takysie Lake
F/14 Knapp Lake
F/15 Hallett Lake

***Figure 3.** Location of study areas mentioned in text (from Williams, 1997; Anderson et al., 1998; Barnes and Anderson, 1999; Sellwood et al., 1999; and R.G. Anderson, unpub. data, 1998).*

Similar units with a tuffaceous rhyolitic matrix and a more heterolithic clast assemblage are found in the Knapp Lake and Marilla map areas (93 F/14 and 93 F/12). Other distinctive types of breccia found regionally characterize the particular study areas described below.

Rhyolitic crystal tuff is generally 'punky' (i.e. friable, and commonly altered to clay) and may contain biotite, alkali feldspar, quartz, and/or plagioclase crystals. Tuff is generally unwelded to locally partly welded. Lithic crystal tuff resembles the crystal tuff, but contains sparse to abundant andesite or rhyolite clasts. Uncommonly, the lithic crystal tuff exhibits bedding, likely indicating reworking (Fig. 9), and in two localities was found to contain wood fragments. North of the Ootsa Lake reservoir, an erosional contact found between a crystal tuff and an underlying lithic breccia (Fig. 10) may represent an intraformational unconformity. At one locality, the bedded tuff appears to conformably underlie a green vesicular andesite flow with amethyst-calcite amygdules. The andesite member is interpreted to be the basal member of the Ootsa Lake Group within the study area (e.g. Anderson et al., 1999).

Distinct rhyolite ash-lignite interbeds are found at the Fraser Lake railway outcrop (Struik et al., 1997), Cheslatta Falls and Nautley Creek quarry localities (*see* Haskin et al., 1998 for location and details), and near Burns Lake (L. Struik, pers. comm., August 1998). The interbeds are commonly found immediately underlying basaltic andesite flows of the Endako Group and mark the top of the Ootsa Lake Group in these areas.

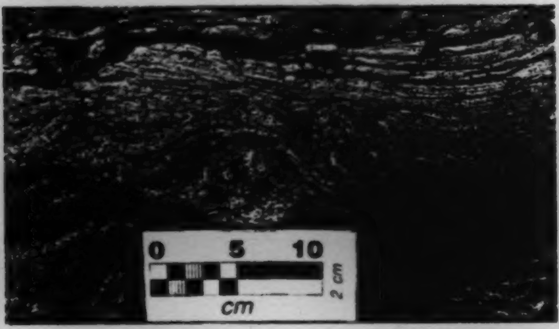

Figure 4. Flow-laminated rhyolite with rotated clasts on Marilla main forest service road, north of Ootsa Lake reservoir.

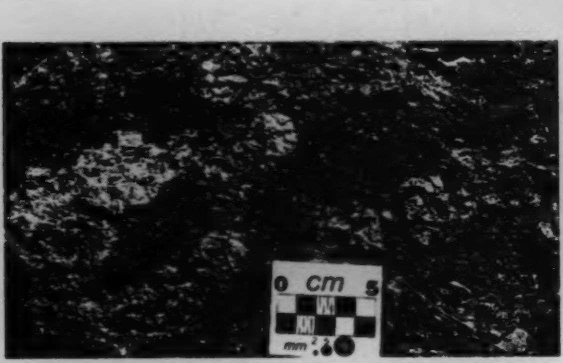

Figure 5. Spherulites in rhyolite flow north of Dayeezcha Mountain.

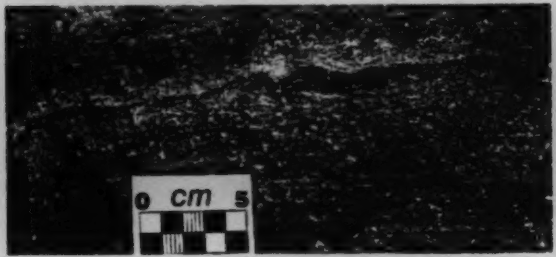

Figure 6. Flow-layered crystal-rich rhyolite near Deerhorn Hill.

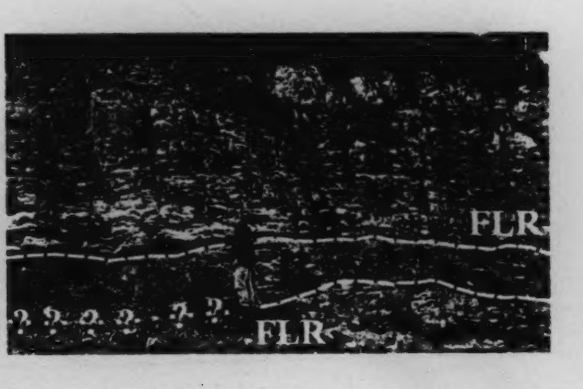

Figure 7. Flow-laminated rhyolite with black glassy perlitic flow base (to right of person) intercalated with flow-laminated rhyolite (FLR). Person is approximate 1.8 m high.

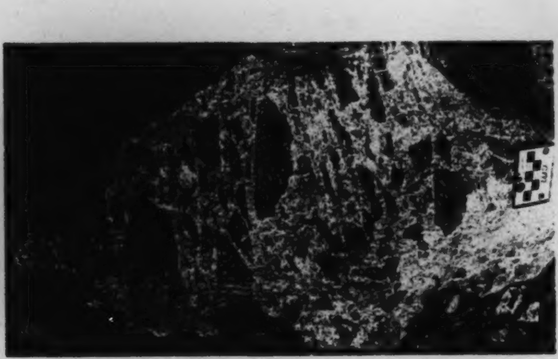

Figure 8. Rhyolite hyaloclastite on Uncha Mountain.

Dayeezcha Mountain area

Dayeezcha Mountain is a distinctive landmark and rises to an elevation of more than about 1170 m (3800 feet). It is underlain by a glassy, biotite-plagioclase-bearing, dacitic crystal ignimbrite containing partly welded clasts of flow-laminated rhyolite and tuffaceous rhyolite. Locally pyroclastic rocks include welded ignimbrite (Fig. 11), silicified green ash, tuffaceous rhyolite lapillistone, rhyolitic tuff, and crystal tuff.

Rhyolitic to dacitic flows interlayered with pyroclastic breccia and tuff occur in the immediate environs. Individual flows are 5–20 m thick. Flows contain spherulites, microspherulites, and/or lithophysae and common quartz, plagioclase, alkali feldspar, and biotite phenocrysts.

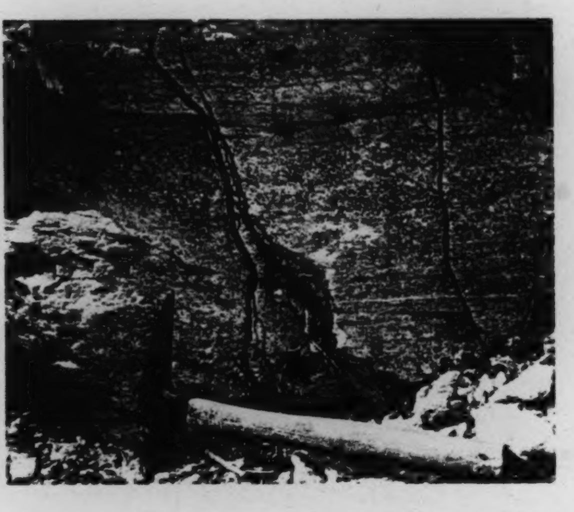

Figure 9. Bedded rhyolite crystal lithic tuff indicating likely reworking on Graham forest service road.

Outcrops distal from Dayeezcha Mountain are predominantly white and red or light grey, flow-laminated rhyolite with local spherulites, vesicles, primary folding of flow laminae, and associated autoclastic breccia. Minor lithic tuff and flow-layered rhyolitic biotite-quartz-plagioclase porphyry flows are also distal from Dayeezcha Mountain.

Henson Hills area

Ootsa Lake Group rocks outcrop extensively in Henson Hills and are in fault contact with Lower to Middle Jurassic sedimentary rocks to the east and possibly unconformably overlain by a series of (hornblende-)plagioclase-phyric andesite, basalt breccia, and vesicular basalt flows to the west. From east to west across Henson Hills, a sequence of tuff, pyroclastic breccia, and flows occurs. Rhyolitic biotite-alkali feldspar-quartz porphyry crystal tuff is conformably overlain by a series of pyroclastic breccia units.

The pyroclastic breccia varies in content from rhyolite tuff clasts in a glassy matrix, and minor crystal ash layers, to a partly welded, rhyolite breccia with glassy, dark maroon to grey biotite rhyolite which locally contains green tuffaceous clasts. The nature of the contact between breccia and the flows is uncertain.

Flow units comprise flow-laminated rhyolite, some with black glassy flow bases up to 1 m thick. Some flows display primary folding. They are generally aphyric or contain sparse biotite, plagioclase, and/or quartz phenocrysts. Minor flow-layered, massive rhyolite and rhyodacite flows north of flow-laminated rhyolite contain vesicles, primary folding, sparse plagioclase and rare quartz and biotite phenocrysts, and rhyolitic clasts with minor perlitic textures.

A crystal-rich, rhyolitic ignimbrite which contains abundant coarse-grained biotite, quartz, and plagioclase phenocrysts underlies an area of 1.3 km^2 and at least 80 m of vertical exposure. The ignimbrite typically contains light grey, aphyric, tuffaceous rhyolite clasts but to the north becomes glassy and includes cleaved biotite andesite clasts. The unit may represent the site of an eruptive centre.

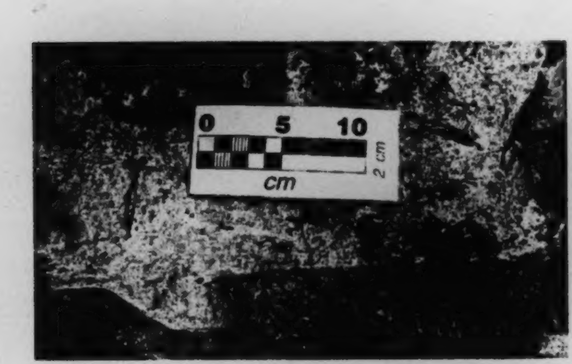

Figure 10. Erosional contact between crystal rhyolite tuff and underlying lithic breccia at locality between Dayeezcha Mountain and Ootsanee Lake.

Figure 11. Pyroclastic welded breccia with chilled rims on clast shown on Dayeezcha Mountain Road.

Mackenzie Lake area

Rocks of the Ootsa Lake Group within the Mackenzie Lake area are in fault contact with Jurassic Hazelton Group volcanic rocks. They may be locally overlain by Eocene or younger hornblende-bearing andesite flows, likely of middle to late Eocene age, and Neogene basalt hyaloclastite and pyroxene-olivine basalt. The Ootsa Lake Group assemblage within this area is typical: abundant flow-laminated rhyolite, flow-layered or massive rhyolite flows, crystal and lithic-crystal tuff, and tuffaceous rhyolite breccia. The last overlies flow-laminated rhyolite. A welded ignimbrite with eutaxitic texture (Fig. 12), which overlies a reversely graded sequence of green heterolithic tuff, characterizes the study area. Pyroclastic breccia is rare or absent in the area. At two localities, the green amygdaloidal andesite unit with minor amethyst-filled vesicles (Fig. 13) underlies glassy flow-layered and flow-laminated rhyolite.

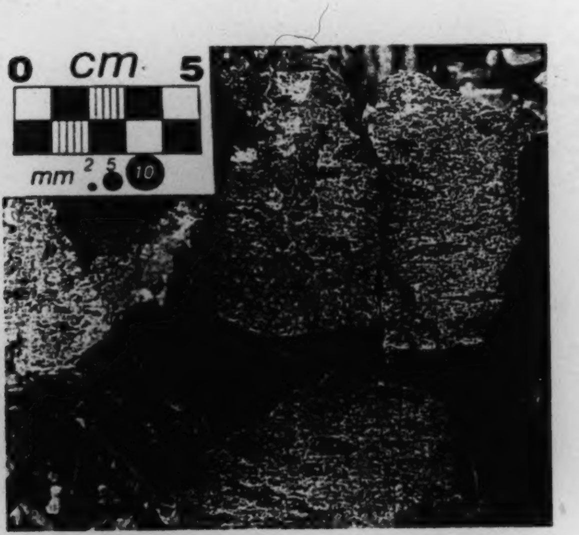

Figure 12. Eutaxitic texture in welded ignimbrite on Davidson forest service road.

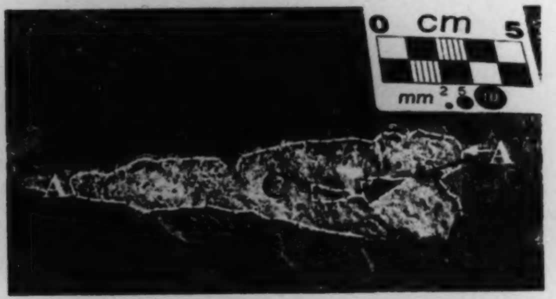

Figure 13. Amethyst-bearing (A) and calcite-bearing (C) amygdules in hand sample of basal andesite unit from Graham forest service road. Dashed line marks contact between outer amethyst and inner calcite fillings.

Plutonic rocks

Seriate or equigranular and miarolitic plutonic rocks and aphanitic to porphyritic hypabyssal intrusions make up at least three varieties of undated, commonly fault-bounded, felsic to bimodal intrusions which are co-spatial with the Ootsa Lake Group, and locally so strongly resemble the volcanic rocks in mineralogy and geochemical composition they are considered potentially cogenetic (Anderson and Snyder, 1998; Anderson et al., 1998; Barnes and Anderson, 1999; Sellwood et al., 1999). The most extensive and perhaps deepest level is the medium-grained, seriate, bimodal Copley Lake pluton which comprises biotite monzogranite, uncommon andesitic hornblende-plagioclase porphyry, and a variety of minor felsic porphyritic and intrusive breccia phases.

Possibly higher level but smaller plutons include leucocratic, fine- to medium-grained, equigranular granite to syenite with characteristic miarolitic cavities and associated porphyritic phases. The mineralogy and texture of the porphyry strongly resembles that of the nearby Ootsa Lake Group country rocks (Sellwood et al., 1999).

At Uncha Mountain, Tertiary faulting and associated small-scale deformation was important in the localization of synkinematic, high-level, aphanitic porphyry and miarolitic granite intrusions and hydrothermal alteration (Barnes and Anderson, 1999).

STRUCTURE

Flow-laminated rhyolite units throughout the study areas have dip magnitudes which range from 3–90°. Field evidence for synvolcanic faulting or fault control of volcanism is less obvious than that responsible for localizing younger Endako Group flows within the Big Bend Creek map area (NTS 93 F/10; Anderson et al., 1998) or higher level, cogenetic intrusions as at Uncha Mountain (Barnes and Anderson, 1999) and Hallett Lake map area (Anderson and Snyder, 1998; Anderson et al., 1998; Sellwood et al., 1999).

CONCLUSIONS

The Ootsa Lake Group within the northern Nechako River and southern Fort Fraser map areas mainly consists of felsic flows with tuff, pyroclastic breccia, and minor intermediate to mafic flows. Cospatial intrusions include aphanitic or porphyritic rhyolite, miarolitic leucogranite, and seriate biotite monzogranite.

The local development of thin lignite beds, black glassy quenched flow bases and reworking of some lithic rhyolite tuff suggest the presence of shallow water at the time of eruption and deposition.

The assemblage is distinct from that identified in the Whitesail Lake map area by Diakow and Koyanagi (1988) and Drobe (1991) which consisted of a series of generally more intermediate to mafic flows and tuff. Drobe (1991) suggested that the paucity of pyroclastic and epiclastic breccia in the Whitesail Range indicated little topographic relief existed during volcanism and that eruptions occurred onto a plateau. The differences in rock type and composition may be attributable to a different eruptive style, timing, structural setting, and/or magmatic source(s).

Further study will focus on establishing the relative timing of Ootsa Lake Group volcanism and related plutonism, and on obtaining and interpreting petrographic, geochronological, geochemical, and tracer isotope data to constrain the petrogenesis of the Eocene felsic magmatism. These data will enable comparison with other coeval volcanic rocks to better understand the distribution and nature of Eocene magmatism and its tectonic setting in central British Columbia.

ACKNOWLEDGMENTS

We would like to thank Bert Struik for his leadership and continued effort in the co-ordination of the Nechako NATMAP Project. Thanks to Bert and "Alpha" crew for conducting tours of potential sample sites, directing us to potential sites, and, in some cases, collecting samples for this study. We would like to acknowledge Don MacIntyre for enabling sample collection of potential equivalents to the Ootsa Lake Group rocks in the Babine Lake area and conducting a tour of the Newman volcanics to collect samples for isotopic comparison with the Ootsa Lake Group. We appreciate the time and energy Mike Villeneuve and Larry Heaman expended in order to visit the field this summer, for their valuable advice, and support of this study. Mike generously gave us access to his unpublished data on Ootsa Lake Group samples. We would like to thank Jonah Resnick, Elspeth Barnes, Lori Snyder, Amber McCoy, Tina Pint, and Stephen Sellwood, who provided invaluable support and assistance in identifying potential sample sites and completing the fieldwork for this study. Thank you to Steve Williams and Bev Vanlier who helped in the digital preparation of the maps and manuscript. This manuscript has benefited from suggestions by Howard Tipper who reviewed an earlier version.

REFERENCES

Anderson, R.G. and Snyder, L.D.
1998: Jurassic to Tertiary volcanic, sedimentary and intrusive rocks in the Hallett Lake area, central British Columbia; *in* Current Research 1998-A; Geological Survey of Canada, p. 135–144.

Anderson, R.G., Snyder, L.D., Resnick, J., Grainger, N.C., and Barnes, E.M.
1999: Bedrock geology of the Knapp Lake map area, central British Columbia; *in* Current Research 1999-A; Geological Survey of Canada.

Anderson, R.G., Snyder, L.D., Wetherup, S., Struik, L.C., Villeneuve, M.E., and Haskin, M.
1998: Mesozoic to Tertiary volcanism and plutonism in southern Nechako NATMAP area: part 1: influence of Eocene tectonics and magmatism on the Mesozoic arc and orogenic collapse: new developments in the Nechako River map area; *in* New Geological Constraints on Mesozoic to Tertiary Metallogenesis and on Mineral Exploration in Central British Columbia: Nechako NATMAP Project, (ed.) L.C. Struik and D.G. MacIntyre; Geological Association of Canada, Cordilleran Section, Short Course Notes, March 27, 1998, 26 p.

Andrew, K.P.E.
1988: Geology and genesis of the Wolf precious metal epithermal prospect and the Capoose base and precious metal porphyry-style prospect, Capoose Lake area, central British Columbia; M.Sc. thesis, University of British Columbia, Vancouver, British Columbia, 334 p.

Armstrong, J.E.
1949: Fort St. James map-area, Cassiar and Coast Districts, British Columbia; Geological Survey of Canada, Memoir 252, 210 p.

Barnes, E.M. and Anderson, R.G.
1999: Bedrock geology of the Uncha Mountain area, northwestern Nechako River map area, central British Columbia; *in* Current Research 1999-A; Geological Survey of Canada.

Bellefontaine, K.A., Legun, A., Massey, N., and Desjardins, P.
1995: Digital geological compilation of northeast B.C. – southern half (NTS 83D, E, 93F, G, H, I, J, K, N, O, P); British Columbia Ministry of Energy, Mines and Petroleum Resources, Open File 1995-24, scale 1:250 000.

Church, B.N.
1972: Geology of the Buck Creek area; *in* Geology, Exploration and Mining in British Columbia; British Columbia Ministry of Energy, Mines and Petroleum Resources, p. 353–363.

Diakow, L.J. and Koyanagi, V.
1988: Stratigraphy and mineral occurrences of Chikamin Mountain and Whitesail Reach map areas; *in* Geological Fieldwork 1987; British Columbia Ministry of Energy, Mines and Petroleum Resources, Paper 1988-1, p. 155–168.

Diakow, L.J. and Mihalynuk, M.
1987: Geology of Whitesail Reach and Triotsa Lake areas; *in* Geological Fieldwork 1986; British Columbia Ministry of Energy, Mines and Petroleum Resources, Paper 1987-1, p. 171–179.

Diakow, L.J., Webster, I.C.L., Richards, T.A., and Tipper, H.W.
1997: Geology of the Fawnie and Nechako Ranges, southern Nechako Plateau, central British Columbia (93F/2, 3, 6, 7); *in* Interior Plateau Geoscience Project: Summary of Geological, Geochemical and Geophysical Studies, (ed.) L.J. Diakow and J.M. Newell; British Columbia Geological Survey Branch, Open File 1996-2 and Geological Survey of Canada, Open File 3448, p. 7–30.

Drobe, J.R.
1991: Petrology and petrogenesis of the Ootsa Lake Group in the Whitesail Range, west-central British Columbia; M.Sc. thesis, Queen's University, Kingston, Ontario, 200 p.

Duffell, S.
1959: Whitesail Lake map-area, British Columbia; Geological Survey of Canada, Memoir 299, 119 p.

Harland, W.B., Armstrong, R.L., Cox, A.V., Craig, L.E., Smith, A.G., and Smith, D.G.
1990: A Geological Time Scale 1989; Cambridge University Press, Cambridge, United Kingdom, 279 p.

Haskin, M.L., Snyder, L.D., and Anderson, R.G.
1998: Tertiary Endako Group volcanic and sedimentary rocks at four sites in the Nechako River and Fort Fraser map areas, central British Columbia; *in* Current Research 1998-A; Geological Survey of Canada, p. 155–164.

Kimura, E.T., Bysouth, G.D., Cyr, J., Buckley, P., Peters, J., Boyce, R., and Nilsson, J.
1980: Geology of parts of southeast Fort Fraser and Northern Nechako River map areas, central British Columbia; Placer Dome Incorporated, Internal Report and Maps, Vancouver, British Columbia.

Mathews, W.H.
1964: Potassium-argon age determinations of Cenozoic volcanic rocks from British Columbia; Geological Society of America Bulletin, v. 75, p. 465–468.
1989: Neogene Chilcotin basalts in south-central British Columbia: geology, ages and geomorphic history; Canadian Journal of Earth Sciences, v. 26, p. 969–982.

Okulitch, A.V.
1995: Geological Time Scale, 1995; Geological Survey of Canada, Open File 3040 (National Earth Science Series, Geological Atlas), 1 sheet.

Resnick, J., Anderson, R.G., Russell, J.K., Edwards, B.R., and Grainger, N.C.
1999: Neogene basaltic flow rocks, xenoliths, and related diabase, northern Nechako River map area, central British Columbia; *in* Current Research 1999-A; Geological Survey of Canada.

Sellwood, S.M., Snyder, L.D., and Anderson, R.G.
1999: Geology of two high-level Tertiary granite plutons, northern Nechako River map area, central British Columbia; *in* Current Research 1999-A; Geological Survey of Canada.

Souther, J.G.
1977: Volcanism and tectonic environments in the Canadian Cordillera - a second look; *in* Volcanic Regimes in Canada, (ed.) W.R.A. Baragar, L.C. Coleman, and J.M. Hall; Geological Association of Canada, Special Paper 16, p. 3–24.
1991: Chapter 15, Volcanic Regimes; *in* Geology of the Cordilleran Orogen in Canada, (ed.) H. Gabrielse and C.J. Yorath; Geological Survey of Canada, Geology of Canada, no. 4, p. 457–490 (*also* Geological Society of America, The Geology of North America, no. G-2).

Stevens, R.D., Delabio, R.N., and Lachance, G.R.
1982: Age determinations and geological studies, K-Ar isotope ages; *in* Report 15; Geological Survey of Canada, Paper 81-2, p. 8–9.

Struik, L.C.
1993: Intersecting intracontinental Tertiary transform fault systems in the North American Cordillera; Canadian Journal of Earth Sciences, v. 30, p. 1262–1274.
1998: Bedrock geology, Fraser Lake map, British Columbia (93 K/SE); Geological Survey of Canada, Open File 3559, 1 coloured map, scale 1:100 000.

Struik, L.C. and McMillan, W.J.
1996: Nechako Project overview, central British Columbia; *in* Current Research 1996-A; Geological Survey of Canada, p. 57–62.

Struik, L.C. and Whalen, J.B.
1998: Bedrock geology, Endako map area, central British Columbia (93 K/3); Geological Survey of Canada, Open File 3630, 1 coloured map, scale 1:50 000.

Struik, L.C., Whalen, J.B., Letwin, J.M., and L'Heureux, R.
1997: General geology of southeast Fort Fraser map area, central British Columbia; *in* Current Research 1997-A; Geological Survey of Canada, p. 65–75.

Tipper, H.W.
1955: Nechako River, British Columbia; Geological Survey of Canada, Paper 54-11, scale 1:253 440.
1963: Nechako River map-area, British Columbia; Geological Survey of Canada, Memoir 324, 59 p.

Villeneuve, M.E. and MacIntyre, D.G.
1997: Laser ^{40}Ar/^{39}Ar ages of the Babine porphyries and Newman volcanics, Fulton Lake map area, west-central British Columbia; *in* Radiogenic Age and Isotope Studies: Report 10; Geological Survey of Canada, Current Research 1997-F, p. 131–139.

Wetherup, S.
1997: Geology of the Nulki Hills and surrounding area (NTS 93F/9 and F/16), central British Columbia; in Current Research 1997-A; Geological Survey of Canada, p. 125–132.
1998: Bedrock geology of the Nulki Hills (93F/9 and 16) map area, British Columbia; Geological Survey of Canada, Open File 3631, scale 1:100 000.

Wetherup, S. and Struik, L.C.
1996: Vanderhoof Metamorphic Complex and surrounding rocks, central British Columbia; *in* Current Research 1996-A; Geological Survey of Canada, p. 63–70.

Whalen, J.B., Struik, L.C., and Hrudey, M.
1998: Bedrock geology of the Endako map area, central British Columbia; *in* Current Research 1998-A; Geological Survey of Canada, p. 113–123.

Wheeler, J.O. and McFeely, P.
1991: Tectonic Assemblage Map of the Canadian Cordillera and Adjacent Parts of the United States of America; Geological Survey of Canada, Map 1712A, scale 1:2 000 000.

Williams, S.P.
1997: Geological compilation of the Nechako River (93F) map area, British Columbia; Geological Survey of Canada, Open File 3429, scale 1:250 000.

Geological Survey of Canada Project 950036-04

4

CHAPTER 4

Conclusions

The Nechako plateau in central British Columbia contains igneous rocks of Jurassic to Miocene age. The geochemical character of these rocks reflects their magmatic origin and tectonic setting. Study of these rocks can provide insight into the tectonic events that mark the geological history of this area. Despite the presence of several significant metal deposits in this area, few regional geological studies were completed prior to 1995.

The geochronological, geochemical and tracer isotope results presented here for igneous rocks from the Middle Jurassic, Late Cretaceous, Eocene and Oligo-Miocene periods provide new constraints on the timing of these suites and new insights into the different tectonic settings in which they were emplaced or erupted.

The Hallett Lake monzogranite is correlated with the Middle Jurassic Stag Lake plutonic suite on the basis of a U-Pb age determination of 169.0 ± 2.9 Ma, reported in Chapter 2, and the lithological similarity between these rocks. These Middle Jurassic plutons can be chemically distinguished from lithologically similar Eocene plutons by their volcanic arc rather than within plate affinity, their lower potassic content, lower level of LIL and LREE enrichment, less marked negative Eu anomaly and more primitive isotopic signature as compared to the Eocene plutons. The primitive isotopic signature of the Middle Jurassic plutons, $^{87}Sr/^{86}Sr_i \cong 0.7039$ and εNd_i from 3 to 7, and subduction-related geochemical character are consistent with the derivation of these rocks from an active arc beneath the accreted Stikine terrane.

By contrast the Cretaceous Tip Top Hill volcanics, with a U-Pb age date of 74.2 ± 0.3 Ma reported here, are geochemically similar to the Eocene Ootsa Lake Group volcanics and can not be distinguished on the basis of the limited data reported in Chapter 2. Further geochemical and tracer isotope study of these rocks is recommended. This age does indicate that the occurrence of Cretaceous volcanism is significantly more widespread in the Fort Fraser map area than previously understood. The relationship between plate motions and arc activity during the Cretaceous appear to be complex and while volcanism within central British Columbia during this interval may be related to continental arc magmatism, the spatial and temporal distribution of igneous activity can not be entirely explained by a simplistic arc model.

Ootsa Lake Group volcanism as determined by four U-Pb and seven $^{40}Ar/^{39}Ar$ age dates, reported in Chapter 3, was regionally continuous from 53 to 47 Ma. Local intervals of volcanism may be much more restricted. Within the northwestern portion of the Nechako River map area (NTS 93F) Ootsa Lake Group volcanism is constrained to 47 to 49 Ma. Related plutonic activity appears to be more episodic with dated events between 57 and 55 Ma, 51.5 and 49.5 Ma, and 49 to 47 Ma. There appears to be a good temporal correlation between magmatic events within the Nechako plateau and the relative plate motions of the Kula and North American plates (Engebretson et al 1985; Stock and Molnar 1988). This suggests that extension was important in the evolution of Eocene magmatism.

Geochemical and tracer isotope results, presented in Chapter 3, reveal the chemical similarity between the Newman volcanics, Ootsa Lake and Endako Groups. The data supports a similar magmatic origin for these rocks from an enriched upper mantle source with $^{87}Sr/^{86}Sr$ values of 0.7037 to 0.7046 and εNd of +2 to +5.5. The presence of this enriched component is indicated by tracer isotopic analyses of spinel lherzolite xenoliths within the Nechako plateau (Chapter 2) and Quesnel terrane to the east and south (Smith 1986). Isotopic variations from this range may be the result of contamination with other enriched mantle components or crustal material. The compositional range of these rocks can be produced by fractionation from a basaltic andesite source and there is little evidence to support magma mixing. Magma production was probably initiated by the subduction of the Kula plate to the west. Extension across the Nechako plateau was responsible for localizing magmatism. These rocks display a transitional volcanic arc to within plate character and are interpreted to reflect a transitional tectonic setting from a subduction to an extension dominated distal arc.

On the basis of these conclusions, a revised stratigraphy is presented in Chapter 3 which includes previously separate Eocene igneous units, the Endako Group, Newman volcanics, Buck Creek Formation, Goosly Lake Formation and Burns Lake Formation, within the Ootsa Lake Group to emphasize their geochemical and isotopic similarity. A new formation, the Henson Hills Formation, is designated to differentiate the dominantly felsic rocks within the Ootsa Lake Group from other more intermediate to mafic units.

^{40}Ar/^{39}Ar age dates, reported in Chapter 2, indicate Chilcotin Group volcanic activity occurred within the Nechako River map area at 11.3, 13.1 and 13.4 Ma. These data combined with compiled data indicate regionally continuous Chilcotin Group volcanic activity between 6 and 16 Ma. Earlier volcanism, between 18 and 23 Ma, 25 and 30 Ma, appears to be mostly restricted to the Nechako plateau, while later volcanism, 6 Ma and younger, is confined to the Chilcotin plateau to the south.

Tracer isotopic analyses from lherzolite xenoliths, presented in Chapter 2, demonstrate isotopic heterogeneity exists within the mantle and indicates the presence of at least one enriched mantle component. The tracer isotope results from the Chilcotin Group basalts within the Nechako River map area are primitive (^{87}Sr/^{86}Sr = 0.7036; εNd =+3.7 to +4.4) and support the interpretation of an asthenosphere source for these lavas (Suh 1999; Resnick 1999). These isotope results agree with analyses of type locality Chilcotin Group basalts to the south (Bevier 1983; Smith 1986) and support the interpretation of a back arc tectonic setting (Bevier 1983).

The geological history of this area can be summarized as follows. A Middle Jurassic volcanic arc continued to evolve within the central Stikine terrane following accretion of the Intermontane Superterrane onto the North American margin and reflects the predominantly juvenile nature of the subsurface at this time. Potassic calc-alkaline magmatism was generated in a continental arc tectonic setting during the Late Cretaceous and Eocene, related to the subduction of the Kula plate. However, the timing and distribution of magmatism during these periods can not be entirely explained by a simplistic arc model. Eocene magmatism was localized by extension and marked a shift from subduction towards extension dominated tectonism. Oligo-Miocene magmatism occurred in a back arc setting.

References

Bevier, M.L. 1983. Implications of Chemical and Isotopic Composition for Petrogenesis of Chilcotin Group Basalts, British Columbia. Journal of Petrology. 24; 207-226.

Engebretson, D.C., Cox, A. and Gordon, R.G. 1985. Relative motions between oceanic and continental plates in the Pacific basin. Geological Society of America. Special Paper 206. 59 p.

Resnick, J. 1999. Neogene magmatism from the northern Nechako and Summit Lake map areas, British Columbia: implications for the petrology of the lithosphere. Unpublished BSc thesis. University of British Columbia. Vancouver, British Columbia. 105p.

Smith, A.D. 1986. Isotopic and geochemical studies of Terrane I, South-Central British Columbia. Unpublished PhD thesis. University of Alberta. Edmonton, Alberta. 195 p.

Stock, J. and Molnar,P. 1988. Uncertainties and implications of the late Cretaceous and Tertiary position of North America relative to the Farallon, Kula and Pacific plates. Tectonics. 7; 1339-1384.

Suh, C. 1999. Petrology, chemistry and geothermometry of ultramafic xenoliths from the North Nechako River area, British Columbia, and the nature of the underlying mantle. Unpublished BSc thesis. University of British Columbia. Vancouver, British Columbia. 81 p.

Appendix I: Analytical Methods

All isotopic work was carried out at the Radiogenic Isotopic Facility in the Department of Earth and Atmospheric Sciences at the University of Alberta.

Sm/Nd and Rb/Sr isotope geochemistry

All weathering surfaces were removed from whole rock samples selected for analysis. Samples were then wrapped in multiple plastic bags and chipped to centimeter square fragments using a sledge hammer. A ring mill was used to reduce the material to ~35 microns. Separate powder splits were prepared using both a tungsten carbide and steel ring mill for geochemical analyses at the Geological Survey of Canada. Powders prepared in the tunsten carbide ring mill were also used for tracer isotope geochemistry at the University of Alberta. Sample powders were weighed into precleaned PFA Teflon vessels. Mixed enriched tracer solutions of ^{150}Nd - ^{149}Sm and ^{84}Sr – ^{87}Rb were weighed and used to totally spike the sample. Vapour-distilled 24N HF and 16 HNO_3 were added to the sample and spike solution at a ratio of 5:2. The teflon vessles were then sealed and placed on a hot plate at 150^{oC} for seven days (Nd only or combined) or twenty-four hours (Sr only) to dissolve the sample. Samples were removed and evaporated to dryness. 10 mL of 6N HCl was added to the flouride residues and the teflon vessels were resealed and heated at 100^{oC} for twenty-four hours to convert the samples to chloride solutes. Samples were removed, dried and dissolved in a loading solution of 6 mL of 0.75N HCl (Nd only or combined) or 3 mL mixed oxalic and HCl solution prior to column chemistry. Samples were centrifuged prior to loading. Rb, Sr and the rare earths were seperated using BioRad AG50W-X8 200 to 400 mesh H^+ cation exchange resin in PFA Teflon columns. Sr and Rb seperates were redissolved in approximately 1.5 mL of a mixed oxalic and HCl solution and passed through a second set of cation exchange columns, containing the same type of resin as for the initial separation, to further purify the sample. Sm and Nd were separated using columns containing BioBeads SX-8 Di-(2-ethylhexyl phosphate) coated 200 to 400 mesh resin. Column blanks are <400 pg for Nd, Sm, Sr and <100 pg for Rb. Samples were converted to nitrates before analysis. Rb and Sr were loaded on single rhenium filament beads using millipore, phosphoric acid and Ta gel. Sm and Nd were loaded using nitric acid onto double rhenium filament beads. Sm and Rb were analyzed on a Micromass 30 thermal ionization mass spectrometer. Sr and Nd were analyzed on a Finigan Mat VG 354 thermal ionization mass spectrometer. Measured ratios were normalized to ^{86}Sr/^{88}Sr = 0.1194 and ^{146}Nd/^{144}Nd = 0.7219. Replicate analyses of standards run during this study produced results of ^{87}Sr/^{86}Sr = 0.710275 ± 7 for the NBS 987 Sr standard (n=27). The La Jolla standard used during analyses of the Endako Group samples was measured as ^{143}Nd/^{144}Nd = 0.511833 ± 11 (n=4) and the Shin Etsu Nd standard used during analysis of all other samples was measured as ^{143}Nd/^{144}Nd = 0.512095 ± 4 (n=18). For all samples initial isotopic values were calculated using Ar-Ar or U-Pb results from the same or proximal sample and an average Miocene Ar-Ar age of 12.7 Ma was used for the one Chilcotin sample lacking a direct age determination. Decay constants used were $\lambda(^{147}\mathrm{Sm}) = 6.54 \times 10^{-12}$/yr and $\lambda(^{87}\mathrm{Rb}) = 1.42 \times$ 10-11/yr (Lugmair and Marti 1978; Neumann and Huster 1974; Davis et al. 1977). Values of $^{143}\mathrm{Nd}/^{144}\mathrm{Nd}_{CHUR} = 0.512638$, $^{147}\mathrm{Sm}/^{144}\mathrm{Nd}_{CHUR} = 0.1967$, $^{143}\mathrm{Nd}/^{144}\mathrm{Nd}_{DM} = 0.513163$, $^{147}\mathrm{Sm}/^{144}\mathrm{Nd}_{DM} = 0.2137$ were used to calculate initial εNd and depleted mantle model ages as $\varepsilon\mathrm{Nd} = (^{143}\mathrm{Nd}/^{144}\mathrm{Nd}_{(T)}/^{143}\mathrm{Nd}/^{144}\mathrm{Nd}_{CHUR(T)} - 1)\times 10^4$ and $T_{DM} = \ln[(^{143}\mathrm{Nd}/^{144}\mathrm{Nd} - ^{143}\mathrm{Nd}/^{144}\mathrm{Nd}_{DM})/(^{147}\mathrm{Sm}/^{144}\mathrm{Nd} - ^{147}\mathrm{Sm}/^{144}\mathrm{Nd}_{DM}) + 1]/\lambda$ where $^{143}\mathrm{Nd}/^{144}\mathrm{Nd}_{(T)} = ^{143}\mathrm{Nd}/^{144}\mathrm{Nd} - ^{147}\mathrm{Sm}/^{144}\mathrm{Nd}(e^{-\lambda t} - 1)$.

U/Pb isotope geochemistry

Samples were crushed using a Jaw crusher and a Bico disk mill. Sample material was then passed over a Wilfley table. Heavy material from the Wilfley table was seived to <70 microns and passed through a Frantz Isodynamic magnetic separator at a low current. Non magnetic material was further seperated using heavy liquids (Methylene iodide) and higher current and side tilt on the magnetic seperator. From this material, zircons were selected for analysis by handpicking under a microscope. Certain fractions were air abraded in an effort to obtain more concordant analyses using the method of Krogh (1982). Selected zircons were washed in warm 4N HNO_3, rinsed in millipore water and held in an ultrasonic bath for one minute. The grains were rinsed with millipore water several times and then several times with acetone. The zircons were transferred to a piece of aluminum foil, weighed and then placed into a precleaned teflon bomb. Bombs were cleaned four times for two days each time in an oven at 215^{oC} using 15 drops of 48% HF and 3 drops of 7N HNO_3 for the first, third and fourth cleaning and 20 drops of 6.2 N HCl for the second cleaning. Acid was discarded and bombs were rinsed with millipore following each cleaning. Each bomb containing zircons was removed to a fume hood and spiked with an appropriate quantity of a mixed ^{205}Pb-^{235}U spike. 15 drops of 48% HF and 3 drops of 7N HNO_3 were added to each bomb. The bombs were loaded into a metal carousel and placed into an oven at 215^{oC} for four days to dissolve the samples. The sample solutions were evaporated, 5-6 drops of 3.1N HCl was added to each bomb and then returned to the oven at 215^{oC} for twenty four hours to convert the flouride residue to a chloride solute. Micro-columns containing an anion exchange resin were used to separate Pb and U. Columns were cleaned three times with each of millipore water and 6.2N HCl. Columns were equilibrized with 3.1N HCl. Sample was loaded in 3.1 N HCl and a rinsed with more 3.1 N HCl to remove Zr and Hf from the columns. Both Pb and U were eluted into a precleaned PMP beaker using 6.2 N HCl and millipore water, respectively. 2 drops of phosphoric acid was added to the Pb and U seperates before drying. The Pb and U seperates were loaded together onto a single rhenium filament bead using silica gel and phosphoric acid. U and Pb isotopic ratios were measured either on a VG 354 or a Sector 54 thermal ionization mass spectrometer. Both mass spectrometers were operated in single-collector mode using either a Faraday cup or Daly photomultiplier detector. All data obtained using the Daly collector were corrected by a factor of 0.13%/amu and 0.15%/amu (VG 354) and 0.056%/amu and 0.024%/amu (Sector 54) for Pb and U, respectively. All isotopic ratios were corrected for mass discrimination based on repeated analyses of the NIST SRM981 Pb and U500 standards. Mass discrimination corrections of 0.09%/amu and 0.16%/amu (VG354) and 0.15%/amu and 0.14%/amu (Sector 54) were applied to Pb and U, respectively. Procedural blanks for U and Pb were measured as 5 ± 20% pg and 6 ± 50% pg by repeated analyses during the course of this study. Decay constants used were $\lambda(^{238}U) = 1.55125 \times 10^{-10}$/yr and $\lambda(^{235}U) = 9.8485 \times 10^{-10}$/yr and an atomic ratio of $^{238}U/^{235}U=137.88$ as recommended by Steiger and Jäger (1977) (Jaffrey et al. 1971; Cowan and Adler 1976). Data was calculated using in-house software. Errors were calculated by propagating all known sources of uncertainty.

References

Cowan, G.A. and Adler, H.H. 1976. The variability of the natural abundance of ^{235}U. Geochimica et Cosmochimica Acta. 40; 1487-1490.

Davis, D.W., Gray, J., Cumming, G.L., Baadsgaard, H. 1977. Determination of the ^{87}Rb constant. Geochimica et Cosmochimica Acta. 41; 1745-1749.

Jaffey, A.H., Flynn, K.F., Glendenin, L.F., Bentley, W.C., and Essling, A.M. 1971. Precision measurements of half-lives and specific activities or ^{235}U and ^{238}U. Physics Review. 4;1889-1906.

Krogh, T.E. 1982. Improved accuracy of U-Pb zircon ages by the creation of more concordant systems using an air abrasion technique. Geochimica et Cosmochimica Acta. 37; 485-494.

Lugmair, G.W. and Marti, K. 1978. Lunar initial ^{143}Nd/^{144}Nd: Differential evolution of the lunar crust and mantle. Earth and Planetary Science Letters. 35; 273-284.

Neumann, W. and Huster, H. 1974. The half-life of ^{87}Rb measured as a difference between the isotopes ^{87}Rb and ^{85}Rb. Z. Physik. 270; 121-127.

Steiger, R.H. and Jäger, E. 1977. Subcomission on Geochronology: Concention on the use of decay constants in geo- and cosmochronology. Earth and Planetary Science Letters. 36: 359-362.